

Woods Hole Oceanographic Institution

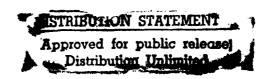


Abstracts of Manuscripts Submitted in 1991 for Publication

Technical Report WHOI-92-19







WHOI-92-19

Research In Progress

Abstracts of Manuscripts Submitted in 1991 for Publication

Woods Hole Oceanographic Institution
Woods Hole, Massachusetts

Editor: Alora K. Paul

Approved for Distribution:

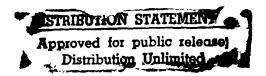
Robert B. Gagosian
Associate Director for Research

DTIC QUALITY INSTITUTE 5

When citing this report, it should be referenced as:

Woods Hole Oceanographic Institution Technical Report No. WHOI-92-19

Accesion	n For	
NTIS DTIC Unanno Justifica	TAB unced	
By Distribu	***********	
A	vailability	Codes
Dist	Avail at Spec	
A-1		



PREFACE

This volume contains the abstracts of manuscripts submitted for publication during calendar year 1991 by the staff and students of the Woods Hole Oceanographic Institution. We identify the journal of those manuscripts which are in press or have been published. The volume is intended to be informative, but not a bibliography.

The abstracts are listed by title in the Table of Contents and are grouped into one of our five departments, marine policy center, coastal research center, or the student category. An author index is presented in the back to facilitate locating specific papers.

Acknowledgements

Special thanks to Suzanne B. Volkmann, Research Associate; Staff Assistants Shirley Bowman, Applied Ocean Physics and Engineering; Ethel LeFave, Biology; Molly Lumping, Chemistry; Pamela Foster, Geology & Geophysics; Debbie Taylor, Physical Oceanography; Ellen Gately, Marine Policy Center; Olimpia McCall, Coastal Research Center; Pamela Goulart, Education; and Maureen O'Donnell, Library Assistant.

TABLE OF CONTENTS

DEPARTMENT OF APPLIED OCEAN PHYSICS AND ENGINEERING

Multisensor Visualization for Underwater Archaeology W. Kenneth Stewart	OPE-1
Frequency Dependence of Sound Backscattering from Live Individual Zooplankton D. Chu, T. K. Stanton and P. H. Wiebe	OPE-1
Mechanical Design Methods of Improving Manipulator Performance Nathan Ulrich and Vijay Kumar	OPE-1
Remote Control of a Telerobotic Underwater Vehicle via Satellite Dana R. Yoerger, Robert Weiman and Tagore Somers	OPE-1
Adaptive Sliding Control of an Experimental Underwater Vehicle Dana R. Yoerger and Jean-Jacques E. Slotine	OPE-2
Visualization Resources and Strategies for Remote Subsea Exploration W. Kenneth Stewart	OPE-2
Frequency Downshift in Narrow-Banded Surface Waves Under the Influence of Wind Tetsu Hara and Chiang C. Mei	OPE-2
A Three-Frequency Scatterometer Technique for the Measurement of Ocean Wave Spectra Dale L. Schuler, William C. Keller and William J. Plant	OPE-3
The Physical Oceanography of the Amazon Outflow W. Rockwell Geyer, Robert C. Beardsley, Julio Candela, Belmiro Castro, Richard V. Legeckis Steven J. Lentz, Richard Limeburner, Luis B. Miranda, and John H. Trowbridge	
Error Analysis of an Acoustic Current Meter D. Andrew Trivett, Eugene A. Terray and Albert J. Williams III	OPE-3
Fiber Optic Telemetry in JASON, the ROV Bob Elder	OPE-4
Evidence for Energetic Mode One Internal Waves Observed with 4000 km Acoustic Antennae Wayne R. Blanding, John L. Spiesberger and Arthur Miller	OPE-4
Comment on "Wind Wave Directionality Effects on the Radar Imaging of Ocean Swell" by F. J. Ocampo-Torres and I. S. Robinson William J. Plant	OPE-4
Transputer-Based Distributed Processing for Underwater Robotic Vehicle Control David A. Mindell and Dana R. Yoerger	OPE-5
High-Resolution Optical and Acoustic Remote Sensing for Underwater Exploration W. Kenneth Stewart	OPE-5
Remote-Sensing Issues for Intelligent Underwater Systems W. Kenneth Stewart	OPE-5
The Variance of the Normalized Radar Cross Section of the Sea William J. Plant	OPE-5
The Accuracy of GOES Satellite Clocks Kenneth R. Peal	AOPE-6

Design Optimization of an Electric Underwater Manipulator Nathan Ulrich and Dana R. Yoerger
Comment on the Full-Wave Controversy William J. Plant
Identification of Low Order Dynamic Models for Deeply-Towed Underwater Vehicle Systems Franz S. Hover and Dana R. Yoerger
Thrust Mechanics in Flapping Foils and Optimal Fish Propulsion George S. Triantafyllou, Michael S. Triantafyllou and Mark A. Grosenbaugh AOPE-7
Spatial Diversity Processing for Underwater Acoustic Telemetry Josko A. Catipovic and Lee E. Freitag
Compact Digital Signal Processing Enhances Acoustic Data Telemetry Josko Catipovic, Daniel F. Frye and Dave Porta
Oscillating Flows Over Periodic Ripples of Finite Slope Tetsu Hara, Chiang C. Mei and K. T. Shum
On Simple Representation of Mixing in a Stress-Driven Stratified Flow J. H. Trowbridge
Basin Scale Ocean Monitoring with Acoustic Thermometers John L. Spiesberger and Kurt Metzger
On Ripple Dynamics V. Linear Propagation of Cylindrical Waves on Liquids With and Without a Surface Dilatational Viscoelastic Response Erik J. Bock
Time Domain Analysis of Normal Mode, Parabolic, and Ray Solutions of the Wave Equation Linda Boden, James B. Bowlin and John L. Spiesberger
Study of Dominant Performance Characteristics in Robot Transmissions Hagen Schempf and Dana R. Yoerger
In Situ Processing of Boundary Layer Flow Measurements for Data Compression Albert J. Williams, 3rd and Thomas Gross
Sound Scattering by Rough Elongated Elastic Objects II. Fluctuations of Scattered Field T.K. Stanton and D. Chu
Determination of Geoacoustic Parameters of the Ocean Bottom - Data Requirements Subramaniam D. Rajan
Waveform Inversion to Obtain the Geoacoustic Properties of Sediment in Deep Water Subramaniam D. Rajan
A Fast Hydrographic Profiling System Albert M. Bradley, Alan R. Duester and Stephen P. Liberatore
Surface Support for a Free-Fall Hydrographic Profiler Albert M. Bradley, Alan R. Duester and Stephen Liberatore
Design Methods of Improving Robot Manipulator Performance Nath Ulrich and Vijay Kumar
Diffraction from the Juncture of a Pressure Release and Locally Reacting Half-Planes Peter H. Dahl and George V. Frisk AOPE-19

ARGO/JASON: A remotely Operated Survey and Sampling System for Full-Ocean Depth Robert D. Ballard, Dana R. Yoerger, W. Kenneth Stewart and Andrew Bowen AOPE-12
Seasonal Variations of the Sediment Compressional Wave Speed Profile in the Gulf of Mexico Subramaniam D. Rajan and George V. Frisk
Three Dimensional Ray Acoustics in a Realistic Ocean J. F. Lynch, A. E. Newhall, C. S. Chiu and J. H. Miller
On the Determination of Modal Attenuation Coefficients and Compressional Wave Attenuation Profiles in a Range Dependent Environment in Nantucket Sound Subramaniam D. Rajan, James F. Lynch and George V. Frisk
Reconciliation of Theories of Synthetic Aperture Radar Imagery of Ocean Waves William J. Plant
A Long-Term Evaluation of New Mooring Components and Underwater Telemetry Techniques A. Bocconcelli, H. O. Berteaux, Daniel E. Frye and B. Prindle
A Multiple Charge Deep Deployed Explosive Source for High Resolution Seismic Refraction Experiments in the Deep Ocean Donald E. Koelsch, G. M. Purdy, and James E. Broda
Wind Effects on the Nonlinear Evolution of Slowly Varying Gravity-Capillary Waves Tetsu Hara and Chiang C. Mei
Larval Habitat Choice in Still Water and Flume Flows in the Opportunistic Bivalve Mulinia Lateralis Judith P. Grassle, Paul V. R. Snelgrove and Cheryl Ann Butman
Maximum Likelihood and Lower Bounds in System Identification with Non-Gaussian Inputs Ofir Shalvi and Ehud Weinstein
Non-Selective Settlement of Mercenaria Mercenaria (Linné) Larvae in Short-Term, Still-Water, Laboratory Experiments Guy Bachelet, Cheryl Ann Butman, Christine M. Webb, Victoria R. Starczak, and Paul V. R. Snelgrove
Status of Krill Target Strength Kenneth G. Foote, Dezhang Chu, and Timothy K. Stanton
Underwater Acoustic Local Area Network For ROV And Instrument Communications Josko Catipovic, Lee Freitag and Steven Merriam
Acoustic Wave Scattering From An Object In A Shallow Water Waveguide-A General Formulation Dajun Tang and George V. Frisk
A Telemetry Theory For Ocean Acoustic Tomography: Real Time Monitoring John L. Spiesberger and James B. Bowlin
Spectral Parameterization Of Scattering From A Random Bottom Dajun Tang and George V. Frisk
Determination of Compressional Wave and Shear Wave Speed Profiles in Sea Ice by Crosshole Tomography - Theory and Experiment Subramaniam D. Rajan, George V. Frisk, James A. Doutt, and Cynthia J. Sellers AOPE-18

DEPARTMENT OF BIOLOGY

Separation of Coding Sequences from Structural DNA in the Dinoflagellate Crypthecodinium cohnii D. M. Anderson, A. Grabher, and M. Herzog
Paralytic Shellfish Poisoning on Georges Bank: In Situ Growth or Advection of Established Dinoflagellate Populations? Donald M. Anderson and Bruce A. Keafer
Lacunal allocation and gas transport capacity in the Salt Marsh Grass, Spartina alterniflora Andrea L. Arenovski and Brian L. Howes
Heterotrophic Flagellates of Planktonic Communities Their Characteristics and Methods of Study UG. Berninger, D. A. Caron, R. W. Sanders and B. J. Finlay
Grazing and Utilization of Chroococcoid Cyanobacteria and Heterotrophic Bacteria by Protozoa in Laboratory Cultures and a Coastal Plankton Community David A. Caron, Ee Lin Lim, Geraldine Miceli, John B. Waterbury and Frederica W. Valois B-2
Planktonic Protozoa and the Microbial Food Web: New Awareness and Perspective for Zooplankton Research David A. Caron, Robert W. Sanders and Diane K. Stoecker
Local and Regional Regulation of Species-Area Relations: A Patch-Occupancy Model Hal Caswell and Joel E. Cohen
Sequence and Chemical Structure of the Hexapeptide Chromophore of the Aequorea Green-Fluorescent Protein Chris W. Cody, Douglas C. Prasher, William M. Westler, Franklyn G. Prendergast and William W. Ward
Characterization and Site Description of Solemya borealis, a Newly Discovered Animal-Bacteria Symbiosis Noellette Conway, Brian Howes, Judith McDowell Capuzzo, Ruth Turner and Colleen Cavanaugh B-3
Effects of Constant and Intermittent Food Supply on Life History Parameters in a Marine Copepod Cabell S. Davis and Philip Alatalo
Micropatchiness, Turbulence, and Recruitment in Plankton Cabell S. Davis, Glenn R. Flierl, P. H. Wiebe and P. J. S. Franks
The Video Plankton Recorder (VPR): Design and Initial Results C. S. Davis, S. M. Gallager, M. S. Berman, L. R. Haury and J. R. Strickler
Microaggregations of Oceanic Zooplankton Observed by Towed Video Microscopy Cabell S. Davis, Scott M. Gallager, and Andrew R. Solow
Aquatic Ecosystems: High Pressure Habitats Edward F. DeLong
Exploring Marine Microbial Diversity via Molecular Phylogenetic Analysis Edward F. DeLong
Novel Archaea in Coastal Marine Bacterioplankton Edward F. DeLong
Arrangement and External Morphology of Sensilla on the Dorsal Surface of Three Genera of Hyperiid Amphipods Phronima, Lycaea, and Vibilia Carol E. Diebel

Aspects of Iron and Nitrogen Nutrition in the Red Tide Dinoflagellate Gymnodinium sanguineum. I. Effects of Iron Depletion and Nitrogen Source on Biochemical Composition
G. J. Doucette and P. J. Harrison
Aspects of Iron and Nitrogen Nutrition in the Red Tide Dinoflagellate Gymnodinium sanguineum. II. Effects of Iron Depletion and Nitrogen Source on Iron and Nitrogen Uptake G. J. Doucette and P. J. Harrison
Iron Control of the Vibrio fischeri Luminescence System in Escherichia coli. P. V. Dunlap
Organization and Regulation of Bacterial Luminescence Genes P. V. Dunlap
Growth of the Marine Luminous Bacterium Vibrio fischeri On 3':5'-Cyclic AMP: Correlation with a Periplasmic 3':5'-Cyclic AMP Phosphodiesterase Paul V. Dunlap, Ulrich Mueller, Teresita A. Lisa and Kelly S. Lundberg
Endogenously-mediated, Pretranslational Suppression of Cytochrome P450IA Expression in PCB-Contaminated Flounder A. A. Elskus, R. J. Pruell and J. J. Stegeman
The West Falmouth Oil Spill: Fate of Fuel Oil Compounds 20 Years Later John W. Farrington, John M. Teal, Bruce W. Tripp and Curtis Phinney
Effects of Tributlytin Chloride in Vitro on the Hepatic Microsomal Monooxygenase System in the Fish Stenotomus chrysops K. Fent and J. J. Stegeman
Inhibition of Cytochrome P450 Forms by Tributyltin in Fish Karl Fent and John J. Stegeman
Hydrodynamic Disturbances Produced by Small Zooplankton: A Case Study for Veliger Larvae of Bivalve Molluscs Scott M. Gallager
Locomotory Energetics and Buoyancy Control in Larvae of a Bivalve Mollusc Scott M. Gallager
Efficient Grazing and Utilization of the Marine Cyanobacterium Synechococcus sp. by Larvae of a Bivalve Mollusc
Scott M. Gallager, John B. Waterbury, and Diane K. Stoecker
Large Oceanic Diatoms: Potential Role in New Primary Production Joel C. Goldman
Phagotrophy and NH ₄ + Regeneration in a Three-Member Microbial Food Loop J. C. Goldman and M. R. Dennett
The Ah Receptor in Marine Animals: Phylogenetic Distribution and Relationship to Cytochrome P4501A Inducibility Mark E. Hahn, Alan Poland, Ed Glover and John J. Stegeman
Phylogenetic Distribution of the Ah Receptor in Non-Mammalian Species: Implications for Dioxin Toxicity and Ah Receptor Evolution Mark E. Hahn and John J. Stegeman
Preparation and Initial Characterization of Crystals of the Photoprotein Aequorin from Aequorea victoria L. I. Hannick, D. C. Prasher, L. W. Schultz, J. R. Deschamps, and K. B. Ward
- - $-$ -

Observations on the Swimming and Buoyancy of Cymbulia peroni (Gastropoda: Thecosomata) Made from a Submersible G. R. Harbison	B-13
Ultrastructure of the Feeding Apparatus and Myonemal System of the Heterotrophic Dinoflagellate Protoperidinium spinulosum Schiller Dean M. Jacobson and D. M. Anderson	B-13
The Microbial Turnover of Carbon in the Deep Sea Holger W. Jannasch	B-14
Microbiology of Deep-Sea Hydrothermal Vents Holger W. Jannasch	B-14
The Chemosynthetic Production of Potentially Useful Biomass by Sulfide Oxidizing Bacteria Holger W. Jannasch, Craig C. Taylor and Linda R. Hare	B-14
Particle Retention Efficiency of Salps Patricia Kremer and Laurence P. Madin	B-14
Methanopyrus kandleri Gen. and Sp. Nov. Represents A Novel Group of Hyperthermophilic Methanogens, Growing at 110°C Margit Kurr, Robert Huber, Helmut König, Holger W. Jannasch, Hans Fricke, Antonio Trincone, Jakob K. Kristjansson and Karl O. Stetter	
Deep-Sea and Benthopelagic Medusae: Recent Observations from Submersibles and a Remotely Operated Vehicle R. J. Larson, G. I. Matsumoto, L. P. Madin and L. M. Lewis	B-15
Physiological Responses of Phytoflagellates to Dissolved Organic Substrate Additions. 1. Dominant Role of Heterotrophic Nutrition in Poterioochromonas malhamensis (Cryptophyceae) Alan J. Lewitus and David A. Caron	B-15
Physiological Responses to Phytoflagellates to Dissolved Organic Substrate Additions. 2. Dominant Role of Autotrophic Nutrition in Pyrenomonas salina (Cryptophyceae) Alan J. Lewitus and David A. Caron	B-15
Effects of Light Intensity and Glycerol Addition on the Organization of the Photosynthetic Apparatus in the Facultative Heterotroph, Pyrenomonas salina (Cryptophyceae) Alan J. Lewitus, David A. Caron and Kenneth R. Miller	B-16
Acoustic Elements in the Sexual Behavior of African Cichlid Fishes Phillip S. Lobel	B-16
Four New Electric fishes (Pisces, Mormyridae) from an Isolated Lake in the African Congo P. S. Lobel, W. Harder and E. K. V. Kalko	B-16
Feeding, Metabolism and Growth of Cyclosalpa bakeri in the Subarctic Pacific L. P. Madin and J. E. Purcell	B-17
Physiological, Biochemical and Genetic Control of Bacterial Bioluminescence E. A. Meighen and P. V. Dunlap	B-17
Pattern Similarity in Shared Codas from Sperm Whales (Physeter catodon) Karen E. Moore, William A. Watkins and Peter Tyack	B-17
Evolutionary Origins of Bacterial Bioluminescence Dennis J. O'Kane and Douglas C. Prasher	B-18

Pyrodictium abyssi Sp. Nov. Represents a Novel Heterotrophic Marine Archaeal Hyperthermophile Growing at 110°C	
Ursula Pley, Jutta Schipka, Agata Gambacorta, Holger W. Jannasch, Hans Fricke, Reinhard Rachel and Karl O. Stetter	
Primary Structure of the Aequorea victoria Green-Fluorescent Protein Douglas C. Prasher, Virginia K. Eckenrode, William W. Ward, Frank G. Prendergast and Milton J. Cormier	B-18
Interactions Between Cetaceans and Gill Net and Trap Fisheries in the Northwest Atlantic Andrew J. Read	B-18
Massive Fluxes of Rhizosolenid Diatoms: A Common Occurrence? C. Sancetta, T. Villareal and P. Falkowski	B-19
Class Aplacophora Amélie H. Scheltema	B-19
Passive Dispersal of Planktonic Larvae and the Biogeography of Tropical Sublittoral Invertebrate Species	
Rudolf S. Scheltema	B-19
Denitrification in nitrate contaminated groundwater: Occurrence in steep vertical geochemical gradients	
Richard L. Smith, Brian L. Howes and John H. Duff	B-20
In Situ Measurement of Methane Oxidation in Groundwater Using Natural Gradient Tracer Tests Richard L. Smith, Brian L. Howes and Stephen P. Garabedian	B-20
The Role of Food Patches in Maintaining High Deep-Sea Diversity: Field Experiments Using Hydrodynamically Unbiased Colonization Trays P. V. R. Snelgrove, J. F. Grassle and R. F. Petrecca	B-21
Cytochrome P450 Forms in Fish John J. Stegeman	B-21
Nomenclature for Hydrocarbon Inducible Cytochrome P450 in Fish	
John J. Stegeman	B-21
Environmental and Hormonal Regulation of Cytochrome P450 1A Forms in Fish Liver John J. Stegeman, Pamela J. Kloepper-Sams and Adria A. Elskus	B-22
Immunohistochemical Localization of Environmentally Induced Cytochrome P450IA1 in Multiple Organs of the Marine Teleost Stenotomus chrysops (Scup)	
John J. Stegeman, Roxanna M. Smolowitz, and Mark E. Hahn	B-22
Video Systems for In Situ Studies of Zooplankton J. Rudi Strickler, Peter C. Schulze, Bo I. Bergström, Mark S. Berman, Percy Donaghay, Scott Gallager, James F. Haney, Bruce R. Hargraves, Uwe Kils, Gustav-A. Paffenhöfer, Sumner Richman, Henry A. Vanderploeg, Wolfgang Welsch, David Wethey, and Jeannette Yen	ı
Cytochrome P4501A in Hepatic Lesions of a Teleost Fish (Fundulus heteroclitus) Collected from a Polycyclic Aromatic Hydrocarbon-Contaminated Site P. A. Van Veld, W. K. Vogelbein, R. Smolowitz, B. R. Woodin, and J. J. Stegeman	B-23
Buoyancy Properties of the Giant Diatom Ethmodiscus	
Tracy A. Villareal	B-23
Marine Nitrogen-Fixing Diatom-Cyanobacteria Symbioses	B-24

Tracy A. Villareal	B-24
The Cyanobacteria: Isolation, Purification and Identification J. B. Waterbury	B-24
Sperm Whales Tagged with Transponders and Tracked Underwater by Sonar William A. Watkins, Mary Ann Daher, Kurt M. Fristrup, Terrance J. Howald, and Giuseppe Notarbartolo di Sciara	
Evidence for Rapid Speciation Following a Founder Event in the Laboratory James R. Weinberg, Victoria R. Starczak and Daniele Jörg	B-25
Differential Transport of Sewage-Derived Nitrogen and Phosphorus Through a Coastal Watershed Peter K. Weiskel and Brian L. Howes	B-25
Quantifying Dissolved Nitrogen Flux Through a Coastal Watershed Peter K. Weiskel and Brian L. Howes	B-25
Chemosynthetic Microbial Activity at Mid-Atlantic Ridge Hydrothermal Vent Sites Carl O. Wirsen, Holger W. Jannasch and Stephen J. Molyneaux	B-26
Physiological Studies on a Hyperthermophilic Archaeum from a Guaymas Basin Hydrothermal Vent Carl O. Wirsen, Toshihiro Hoaki, Tadashi Maruyama and Holger W. Jannasch	B-26

DEPARTMENT OF CHEMISTRY

BIOGEOCHEMISTRY

Carbon and Nitrogen Export During the JGOFS North Atlantic Bloom Experiment Estimated from ²³⁴ Th: ²⁵⁸ U Disequilibria Ken O. Buesseler, Michael P. Bacon, J. Kirk Cochran, and Hugh D. Livingston
The Measurement of Sediment Irrigation Rates: A Comparison of the Br ⁻ Tracer and ²²² Rn/ ²²⁶ Ra Disequilibrium Techniques W. R. Martin and G. T. Banta
Isotopic Signatures (14C, 13C, 15N) as Tracers of Sources and Cycling of Soluble and Particulate Organic Matter in the Santa Monica Basin, CA P. M. Williams, K. J. Robertson, A. Soutar, S. M. Griffin, and E. R. M. Druffel
ORGANIC GEOCHEMISTRY
Seasonal and Depth-Related Changes in the Source of Sinking Particles in the North Atlantic Mark A. Altabet, Werner G. Deuser, Susumu Honjo, and Christian Stienen
Optical Absorption Spectra of Waters from the Orinoco Outflow: Terrestrial Input of Colored Organic Matter to the Caribbean
N. V. Blough, O. C. Zafiriou, and J. Bonilla
The ¹⁴ C Activity of Dissolved Organic Carbon Fractions in the North Central Pacific and Sargasso
Sea Oligotro _l ·hic Gyres James E. Bauer, Peter M. Williams, and Ellen R. M. Druffel
Do Upper-Ocean Sediment Traps Provide an Accurate Record of Particle Flux? Ken O. Buesseler
Application of a Generalized Scavenging Model to Thorium Isotope and Particle Data at Equatorial and High Latitude Sites in the Pacific Ocean Simon L. Clegg, M. P. Bacon, and M. Whitfield
The Importance of Isotopic Measurements in Marine Organic Geochemistry Ellen R. M. Druffel and Peter M. Williams
Sedimentary and Geochemical Expressions of Oxic and Anoxic Conditions on the Peru Shelf Kay-Christian Emeis, Jean K. Whelan, and Martha Tarafa
Scaling of Marine Microlayer Film Surface Pressure-Area Isotherms Using Chemical Attributes Nelson M. Frew and Robert K. Nelson
Isolation of Marine Microlayer Surfactants for Ex-Situ Study of Their Surface Physical and Chemical
Properties Nelson M. Frew and Robert K. Nelson
Hydrothermal Scavenging at the Mid-Atlantic Ridge: Radionuclide Distributions C. R. German, A. P. Fleer, M. P. Bacon, and J. M. Edmond
The Pigments of Prochlorococcus marinus: The Presence of Divinyl-Chlorophyll-a and -b in a Marine Prochlorophyte
Ralf Goericke and Daniel J. Repeta
Investigation of the Electrostatic Properties of Humic Substances by Fluorescence Quenching Sarah A. Green, Francois M. M. Morel, and Neil V. Blough
Mass Spectrometric Identification of the Radical Adducts of a Fluorescamine-Derivatized Nitroxide David J. Kieber, Carl G. Johnson, and Neil V. Blough

Novel Pyropheophorbide Steryl Esters in Black Sea Sediments Linda L. King and Daniel J. Repeta
Organic Geochemistry as a Tool to Study Upwelling Systems: Recent Results from the Peru and Namibian Shelves Daniel J. Repeta, Mark A. McCaffrey, and John W. Farrington
GEOCHEMISTRY—INORGANIC, ISOTOPIC
Lead-210 Balance and Implications for Particle Transport on the Continental Shelf, Middle Atlantic Bight
Michael P. Bacon, Rebecca A. Belastock, and Michael H. Bothner
In-Situ Produced Cosmogenic ³ He in Antarctic Glacial Deposits: 1. Constraining Exposure Ages of Quartz Sandstone Boulders with ³ He Edward J. Brook and Mark D. Kurz
In-Situ Produced Cosmogenic ³ He in Antarctic Glacial Deposits: 2. Chronology of Taylor Glacier Advances in Arena Valley
Edward J. Brook, Mark D. Kurz, George H. Denton, and Robert P. Ackert
Mass Spectrometric ¹⁴ C and U-Th Measurements in Coral G. S. Burr, R. L. Edwards, D. J. Donahue, E. R. M. Druffel, and F. W. Taylor
A Lithium Isotope Study of Hot Springs and Metabasalts from Mid-Ocean Ridge Hydrothermal Systems Lui-Heung Chan, John M. Edmond, and Geoffrey Thompson
Lithium Isotopic Composition of Submarine Basalts L. H. Chan, J. M. Edmond, G. Thompson, and K. Gillis
A Model Function of the Global Bomb-Tritium Distribution in Precipitation, 1960–1986 Scott C. Doney, David M. Glover, and William J. Jenkins
A Tritium Budget for the North Atlantic Scott C. Doney, William J. Jenkins, and H. G. Ostlund
Radiocarbon in Seawater and Organisms from the Pacific Coast of Baja, California Ellen R. M. Druffel and Peter M. Williams
Seasonal Changes in the Isotopic Compositions and Sinking Fluxes of Euthecosomatous Pteropods in the Sargasso Sea
V. J. Fabry and W. G. Deuser
Glacial to Interglacial Changes in Surface Nitrate Utilization in the Indian Sector of the Southern Ocean as Recorded by Sediment δ ¹⁵ N Roger Francois and Mark A. Altabet
A Geochemical Study of Metalliferous Sediment from the TAG Hydrothermal Mound, 26°08'N, MAR C. R. German, R. Mills, J. Blusztajn, A. P. Fleer, M. P. Bacon, N. C. Higgs, H. Elderfield, and J. Thomson
Comparative Mineralogy and Geochemistry of Gold-Bearing Sulfide Deposits on the Mid-Ocean Ridges Mark Hannington, Peter Herzig, Steven Scott, Geoff Thompson, and Peter Rona
Gold-Rich Seafloor Gossans in the Troodos Ophiolite and on the Mid-Atlantic Ridge Peter M. Herzig, Mark D. Hannington, Steven D. Scott, George Maliotis, Peter A. Rona, and Geoffrey Thompson C-1:

An Isotopic Study of Dated Alkali Basalts from Sao Miguel, Azores: Implications for the Origin of the Azores Hot Spot Mark D. Kurz, Richard B. Moore, David P. Kammer, and Armine Guiesserian	C-12
Isotope Geochemistry of the Bouvet Mantle Plume Mark D. Kurz, Anton le Roez, and Henry J. B. Dick	
New Age Data for Mid-Atlantic Ridge Hydrothermal Sites: TAG and Snakepit Chronology Revisited Claude Lalou, Jean Louis Reyss, Evelyne Brichet, Maurice Arnold, Geoffrey Thompson, Yves Fou- quet, and Peter A. Rona	
Benthic Organic Carbon Degradation and Biogenic Silica Dissolution in the Central Equatorial Pacific W. R. Martin, M. Bender, M. Leinen, and J. Orchardo	C-14
Variability of the δ ¹³ C of Dissolved Inorganic Carbon at a Site in the North Pacific Ocean Ann P. McNichol and Ellen R. M. Druffel	C-14
Inflow of Chernobyl 90 SR to the Black Sea from the Dnepr River Gennady G. Polikarpov, Hugh D. Livingston, Ludmilla G. Kulebakina, Ken O. Buesseler, Nikolai A. Stokozov, and Susan A. Casso	
The Geochemistry of Re and Os in Recent Sediments from the Black Sea G. Ravizza, K. K. Turekian, and B. J. Hay	C-15
The Geochemistry of Rare Earth Elements in the Seasonally Anoxic Water Column and Pore Waters of Chesapeake Bay E. R. Sholkovitz, T. J. Shaw, and D. L. Schneider	C-15
Metamorphic and Hydrothermal Processes: Basalt-Seawater Interactions Geoffrey Thompson	C-16
MARINE CHEMISTRY	
Rapid Biogeochemical Coupling Between Surface and Deep Ocean Waters via Particles V. L. Asper, W. G. Deuser, G. A. Knauer, and S. E. Lohrenz	C-16
Seasonal Cycles of Manganese and Cadmium in Galapagos Coral M. L. Delaney, L. J. Linn, and E. R. M. Druffel	C-16
Photochemical Free Radical Production Rates in the Eastern Caribbean Brian Dister and Oliver C. Zafiriou	C-17
Photochemical Oxygen Activation: Superoxide Radical Detection and Production Rates in the Eastern Caribbean Edward Micinski, Lary A. Ball, and Oliver C. Zafiriou	C-17
Some Practical Aspects of Measuring DOC—Sampling Artifacts and Analytical Problems with Marine Samples Edward T. Peltzer and Peter G. Brewer	C-18
INSTRUMENTS AND METHODS	
Recovery of Sub-Milligram Quantities of Carbon Dioxide from Gas Streams by Molecular Sieve for Subsequent Determination of Isotopic Natural Abundances (13C and 14C) James E. Bauer, Peter M. Williams, and Ellen R. M. Druffel	C-18
Determination of Thorium Isotopes in Seawater by Non-Destructive and Radiochemical Procedures Ken O. Buesseler, J. Kirk Cochran, Michael P. Bacon, Hugh D. Livingston, Susan A. Casso David Hirschberg, Mary C. Hartman, and Alan P. Fleer	

Procedure for Calibration of a Coulometric System Used for Total Inorganic Carbon Measurements in Seawater	
Catherine Goyet and Sally D. Hacker	C-19
Development of a Fiber Optic Sensor for Measurements of pCO ₂ in Sea Water: Design Criteria and Sea Trials	
Catherine Goyet, David R. Walt, and Peter G. Brewer	C-19
A Fast and Sensitive ICP-MS Assay for the Determination of ²³⁰ Th in Marine Sediments Timothy J. Shaw and Roger Francois	C-19
Multiple Indicator Fiber Optic Sensor for High Resolution pCO ₂ Measurements in Seawater David R. Walt, G. Gabor, and Catherine Goyet	C-20

DEPARTMENT OF GEOLOGY AND GEOPHYSICS

ACCELERATOR MASS SPECTROMETRY
Illumination of a Black Box: Analysis of Gas Composition During Graphite Target Preparation A. P. McNichol, A. R. Gagnon, G. A. Jones and E. A. Osborne
GEOLOGY
The Geologic Image of Bransfield Trough, an Incipient Oceanic Basin on the Antarctic Continental Margin
Juan Acosta, P. Herranz, J. L. Sanz and Elazar Uchupi
Calcareous Nannofossil Stratigraphy of the Neogene Formations of Eastern Jamaica Marie Pierre Aubry
Toward a Revised Paleogene Geochronology William A. Berggren, Dennis V. Kent, John D. Obradovich and Carl C. Swisher III
Mapping the Seismic Structure of the Upper Oceanic Crust: Implications from DSDP Site 504B, Panama Basin
John A. Collins, Thomas M. Brocher and G. Michael Purdy GG-2
Hypsometry of Divergent and Translational Continental Margins of Southern Africa K. O. Emery, J. M. Bremner and J. Rogers
Deglacial Meltwater Discharge, North Atlantic Deep Circulation and Abrupt Climate Change Lloyd D. Keigwin, Glenn A. Jones, Scott J. Lehman and Edward A. Boyle
Hundreds of Small Volcanoes on the Median Valley Floor of the Mid-Atlantic Ridge at 24-30°N Deborah K. Smith and Johnson R. Cann
Seamount Abundances and Size Distributions, and Their Geographic Variations Deborah K. Smith
Massive Submarine Rockslide in the Rift Valley Wall of the Mid-Atlantic Ridge Brian E. Tucholke
The Renavigation of Sea Beam Bathymetric Data Between 9°N and 10°N on the East Pacific Rise W. S. D. Wilcock, Douglas R. Toomey, G. M. Purdy and Sean C. Solomon
GEOPHYSICS
Vertical Seismic Profile at Site 765 and Seismic Reflectors in the ARGO Abyssal Plain S. T. Bolmer, R. T. Buffler, H. Hoskins, R. A. Stephen and S. A. Swift
Scientific Use of Submarine Telecommunications Cables R. Butler, A. D. Chave, C. S. Cox, C. E. Helsley, J. A. Hildebrand, L. J. Lanzerotti, G. M. Purdy, T. E. Pyle and A. Schultz
Geophysical Constraints on the State of Stress along the Marquesas Fracture Zone Gail L. Christeson and Marcia K. McNutt
Structure of the Northern Symmetric Segment of the Juan de Fuca Ridge G. L. Christeson, G. M. Purdy and K. M. Rohr
Seismo/Acoustic Propagation Through Rough Seafloors Martin E. Dougherty and Ralph A. Stephen
A Global and Regional Stochastic Analysis of Near-Ridge Abyssal Hill Morphology John A. Goff

Quantitative Comparison of Bathymetric Survey Systems John A. Goff and Martin C. Kleinrock
Image of the Moho Across the Continent-Ocean Transition, U.S. East Coast W. S. Holbrook, E. C. Reiter, G. M. Purdy and M. N. Toksöz
Deep Velocity Structure of Rifted Continental Crust, U.S. Mid-Atlantic Margin, from EDGE Wide-
Angle Reflection/Refraction Data W. S. Holbrook, G. M. Purdy, J. A. Collins, R. E. Sheridan, D. L. Musser, L. Glover III, M. Talwani, J. I. Ewing, R. Hawman and S. Smithson
Using the F-Test for Eigenvalue Decomposition Problems to find the Statistically 'Optimal' Solution R. S. Jacobson and P. R. Shaw
Capabilities of Some Systems Used to Survey the Deep-Sea Floor Martin C. Kleinrock
Depth to Basement and Geoid Expression of the Kane Fracture Zone: A Comparison R. Dietmar Müller, David T. Sandwell, Brian E. Tucholke, John G. Sclater and Peter R. Shaw GG-9
A Relationship Between Spreading Rate and the Seismic Structure of Mid-Ocean Ridges G. M. Purdy, L. S. L. Kong, G. L. Christeson and S. C. Solomon
Isolation of Source and Receiver Statics and Scale Factors in Waveform Inversion of Marine Refraction Data Peter R. Shaw
The Role of Seamount Volcanism in Crustal Construction at the Mid-Atlantic Ridge (24°-30°N) Deborah K. Smith and Johnson R. Cann
Finite Difference Modelling of Shear Waves R. A. Stephen
Canonical Seafloor Models and the Finite Difference Method for Low-Angle Acoustic Backscatter Ralph A. Stephen and Martin E. Dougherty
ONR Seafloor Natural Laboratories on Slow- and Fast-Spreading Mid-Ocean Ridges B. E. Tucholke, K. C. Macdonald and P. J. Fox
Plio-Pleistocene Slope Construction off Western Nova Scotia, Canada Elazar Uchupi and Stephen A. Swift
Geohistory of the Angola Basin Region and Construction of the Continental Rise Elazar Uchupi
Electromagnetic Induction by a Finite Electric Dipole Source Over a Two-Dimensional Earth Martyn J. Unsworth, Bryan J. Travis and Alan D. Chave
The Rayleigh-Taylor Instability of an Embedded Layer of Low-Viscosity Fluid William S. D. Wilcock and J. A. Whitehead
HYDRODYNAMICS
Nonlinear Diffusion of the Tidal Signal in Frictionally-Dominated Embayments Carl T. Friedrichs and Ole S. Madsen
PALEOCEANOGRAPHY
Late Paleogene Calcareous Nannoplankton Evolution: A Tale of Climatic Deterioration M. P. Aubry

Reconstruction of Caribbean Climate Change over the Past 10,500 Years David A. Hodell, Jason H. Curtis, Glenn A. Jones, Antonia Higuera-Gundy, Mark Brenner, Michael W. Binford and Kathleen T. Dorsey
High Resolution Record of the North Atlantic Drift 14 -8 KYR BP: Implications for Climate, Circulation and Ice Sheet Melting Scott J. Lehman and Lloyd D. Keigwin
Increased Seasonal Upwelling in the Subtropical South Atlantic Over the Past 700,000 yrs: Evidence From Deep-Living Planktonic Foraminifera G. P. Lohmann
The Eocene-Oligocene Transition: An Overview Donald R. Prothero and William A. Berggren
Using 230 Th in Marine Sediments to Reconstruct the Late Quaternary History of Sea Level Niall C. Slowey and William B. Curry
PALEONTOLOGY
Neogene Planktonic Foraminiferal Biostratigraphy of Eastern Jamaica W. A. Berggren
Nephrolithus frequens GORKA (1957) and its morphotypes Thomas Ehrendorfer
Growth and Chemistry of Globorotalia truncatulinoides-Probes of the Past Thermocline: Part III. Shell Crust G. P. Lohmann
Paleogene Benthic Foraminifers from the Southern Indian Ocean (Kerguelen Plateau): Biostratigraphy and Paleoecology Andreas Mackensen and William A. Berggren
Biostratigraphy and Isotope Stratigraphy of Upper Eocene Microtektites at Site 612: How Many Impacts? Kenneth G. Miller, W. A. Berggren, Jijun Zhang and Amanda A. Palmer-Julson
Cenozoic Deep-Sea Benthic Foraminifera: A Tale of Three Turnovers Kenneth G. Miller, Miriam E. Katz and W. A. Berggren
Extinction Selectivity and Ecology in Planktonic Foraminifera Richard D. Norris
Wall Texture Classification of Planktonic Foraminifera Genera in the Lower Danian Richard K. Olsson, Christoph Hemleben, William A. Berggren and Chengjie Liu
PETROLOGY
Open System Melting and the Temporal and Spatial Variation of Peridotite and Basalt Compositions at the Atlantis II Fracture Zone Kevin T. M. Johnson and Henry J. B. Dick
SEDIMENTOLOGY
Sediment Trap Intercomparison Experiment in the Panama Basin, 1979 Susumu Honjo, Derek W. Spencer and Wilford D. Gardner

DEPARTMENT OF PHYSICAL OCEANOGRAPHY

OCEAN CIRCULATION & LOW FREQUENCY VARIABILITY
Formation of Taylor Caps Over a Tall Isolated Seamount in a Stratified Ocean David C. Chapman and Dale B. Haidvogel
Variation of the Western Equatorial Pacific Ocean, 1986-1988 Thierry Delcroix, Gérard Eldin, Marie-Hélène Radenac, John Toole and Eric Firing PO-
Advection and Diffusion Estimates in a Thermohaline Staircase Region Joyce M. Federiuk and Raymond W. Schmitt
Downstream Development of the Gulf Stream from 68° to 55°W Melinda M. Hall and Nicholas P. Fofonoff
On the Transport of the Gulf Stream Between Cape Hatteras and the Grand Banks Nelson G. Hogg
A Two-Layer Model for the Wind and Buoyancy Forced Circulation Rui Xin Huang
Intermediate Water Formation in a 5 × 3 box Model Rui Xin Huang
Multiple States in a Box Model of an Ice-Covered Ocean Rui Xin Huang
Subduction Rate Defined as an Integral Quantity Rui Xin Huang
Temporal and Spatial Variability of Volume Transport of the in Kuroshio in the East China Sea Hiroshi Ichikawa and Robert C. Beardsley
Thermohaline Catastrophe in a Simple Four Box Model of the Ocean Climate Terrence M. Joyce
Lagrangian Flow Observations in the East China, Yellow and Japan Seas Richard Limeburner, Kuh Kim, Robert C. Beardsley and Julio Candela PO-
A Note on the Inter-gyre Mass Exchange due to Migrating Wind Zhengyu Liu
A Note on the Feedback of the Rhines-Young Pool on the Ventilated Thermocline Zhengyu Liu, Joseph Pedlosky, David Marshall and Torsten Warncke PO-
Variety of Convective Flow Patterns Induced by the Surface Thermal Forcing of a Box Model James R. Luyten and Henry M. Stommel
Recirculating Components to the Deep Boundary Current of the Northern North Atlantic Michael S. McCartney
Diurnal Tides Near the Yermak Plateau Laurie Padman, Albert J. Plueddemann, Robin D. Muench and Rob Pinkel PO-
On the Baroclinic Structure of the Abyssal Circulation Joseph Pedlosky
Gulf Stream Meanders Over Steep Topography at Cape Hatteras

Internal Wave Observations From the Arctic Environmental Drifting Buoy Albert J. Plueddemann	O-7
Interannual Variability in the Mid- and Low-Latitude Western North Pacific Bo Qiu and Terrence M. Joyce	'O-8
Mean Flow and Variability in the Kuroshio Extension From Geosat Altimetry Data Bo Qiu, Kathryn A. Kelly and Terrence M. Joyce	'O-8
Velocity and Eddy Kinetic Energy of the Gulf Stream System From 700 m SOFAR Floats Subsampled to Simulate Pop-Up Floats Philip L. Richardson	
Direct Observations of Nutrient Fluxes at 24°N in the Pacific Ocean Paul E. Robbins and Harry L. Bryden	
Correction to "Evidence for Wind-Driven Current Fluctuations in the Eastern North Atlantic" by R. M. Samelson Roger M. Samelson P	PO-9
Fluid Exchange Across a Meandering Jet Roger M. Samelson	D-10
Effects of Horizontal Resolution on a Limited-Area Model of the Gulf Stream System William J. Schmitz, Jr. and J. Dana Thompson) -10
Mesoscale Ocean Currents William J. Schmitz, Jr	0-11
On the Sverdrup Circulation for the Atlantic Along 24N William J. Schmitz, Jr., J. Dana Thompson and James R. Luyten	0-11
A Diagnostic Study of the Wind- and Buoyancy-Driven North Atlantic Circulation Michael A. Spall	0-11
Cooling Spirals and Recirculation in the Subtropical Gyres Michael A. Spall) -12
Rossby Wave Radiation in the Cape Verde Frontal Zone Michael A. Spall	D-12
A Conjectural Regulating Mechanism for Determining the Thermohaline Structure of the Oceanic Mixed Layer Henry M. Stommel	∩-19
The Average T-S Relation of a Stochastically Forced Box Model Henry M. Stommel and William R. Young	
The Double Silica Maximum in the North Pacific Lynne D. Talley and Terrence M. Joyce	O-13
An Eastern Atlantic Section From Iceland Southward across the Equator Mizuki Tsuchiya, Lynne D. Talley and Michael S. McCartney	O-13
Deep Currents in the Arabian Sea in 1987 Bruce A. Warren and Gregory C. Johnson	O-14
Circulation and Water Mass Balance in the Brazil Basin Huai-Min Zhang and Nelson G. Hogg	∩.14

THEORETICAL AND LABORATORY MODELS

Some Global Conservation Laws in Quasigeostrophic Flows with Piecewise Constant Potential Vorticity	
George I. Bell and Larry J. Pratt	PO-14
Conduit Solitary Waves in a Visco-Elastic Medium Roger H. J. Grimshaw, Karl R. Helfrich and Jack A. Whitehead	PO-15
Internal Solitary Wave Breaking and Run-up on a Uniform Slope Karl R. Helfrich	PO-15
On the Absolute Velocity of the Geostrophic Circulation Grigory Isayev	PO-15
The Role of Dissipation Mechanisms in the Nonlinear Dynamics of Unstable Baroclinic Waves Patrice Klein and Joseph Pedlosky	PO-16
Baroclinic Instability Localized by Dissipation Joseph Pedlosky	PO-16
COASTAL CIRCULATION & DYNAMICS	
Colliding Water Masses over the Continental Slope East of Virginia James Churchill, Edward R. Levine, Donald N. Connors and Peter C. Cornillon	PO-16
The Role of Stratification in the Formation and Maintenance of Shelfbreak Fronts Glen Gawarkiewicz and David C. Chapman	PO-17
Large Scale Penetration of Gulf Stream Water onto the Continental Shelf North of Cape Hatteras Glen Gawarkiewicz, Thomas M. Church, George W. Luther, III, Timothy G. Ferdelman an Michael Caruso	
Continental Shelf Response to Forcing by Deep-Sea Internal Waves Roger H. J. Grimshaw and David C. Chapman	PO-17
Comparison of Velocity Estimates From AVHRR in the Coastal Transition Zone Kathryn A. Kelly and P. Ted Strub	PO-18
The Surface Boundary Layer in Coastal Upwelling Regions Steven J. Lentz	PO-18
Wind-Forced Variability of the Deep Eastern North Pacific: Theory and Relationship to Seafloon	•
Pressure and Abyssal Currents P. P. Niiler, J. Filloux, W. T. Liu, Roger M. Samelson, J. D. Paduan and C. A. Paulson	PO-18
Supercritical Marine Layer Flow Along a Smoothly-Varying Coastline Roger M. Samelson	PO-19
INSTRUMENTATION & EXPERIMENTAL METHODOLOGY	
Separation of Tidal and Subtidal Currents in Ship-Mounted Acoustic Doppler Current Profiler (ADCP) Observations	
Julio Candela, Robert C. Beardsley and Richard Limeburner	PO-19
Recent Developments in Ocean Data Telemetry at Woods Hole Oceanographic Institution Daniel E. Frye and W. Brechner Owens	PO-20
Sea Water Battery for Long Lived Upper Ocean Systems	PO-20

A Three Meter Discus Buoy with IMET Meteorological Sensors D. S. Hosom, R. A. Weller, K. E. Prada and R. P. Trask
Implementation of a Titanium Strain Gauge Pressure Transducer for CTD Applications Robert Millard, Gary Bond and John Toole
A Note on the Response Characteristics of the VACM Compass Sarah K. Patch, Edward P. Dever, Robert C. Beardsley and Steven J. Lentz PO-21
AIR-SEA INTERACTION
Analysis of Surface Fluxes in the Marine Atmospheric Boundary Layer in the Vicinity of Rapidly Intensifying Cyclones Gennaro H. Crescenti and Robert A. Weller
The Heat Budget in the North Atlantic Subtropical Frontal Zone Daniel L. Rudnick and Robert A. Weller
TECHNICAL REPORTS
Cruise Summaries of OCEANUS Cruises 205, Leg 8 and 216 Terrence M. Joyce, Marvel C. Stalcup, R. Lorraine Barbour, Jane A. Dunworth and David M. Schubert

MARINE POLICY CENTER

Soviet Arctic Marine Transportation 1990 Lawson W. Brigham
The Influence of Japanese Industrial Targeting and Trade Policy on the Markets for Marine Electronic Instruments
James M. Broadus
Marine Electronic Instrumentation: An Industrial Perspective James M. Broadus
The Sea Environment: Good News, Bad News James M. Broadus
World Trends in Ocean Industry James M. Broadus
Industrial Organization and Competitive Dynamics in Marine Electronic Instrumentation James M. Broadus, Porter Hoagland and Hauke L. Kite-Powell
The Oceans and Environmental Security James M. Broadus and Raphael V. Vartanov
Moult Staggering in the American Lobster: A Statistical Analysis Diane F. Cowan, Jelle Atema and Andrew R. Solow
Integrated Environmental Management and Land-Based Pollution in the East Asian Seas Mark E. Eiswerth
Electronic Instrumentation and Coastal Resources Management in the 1990's Arthur G. Gaines, Jr
Electronic Instrumentation and Environmental Security Arthur G. Gaines, Jr
The Narrow River: Laboratory for Science and Management Arthur G. Gaines, Jr
Scientific Research and the Galápagos Marine Resources Reserve: Synopsis of a Workshop April 20-24, 1987, Guayaquil, Ecuador
Arthur G. Gaines, Jr. and Hernán Moreano Andrade
Auks at Sea [Review] J. Christopher Haney MPC-5
The Plight of Cranes: A Case Study for Conserving Biodiversity J. Christopher Haney and Mark E. Eiswerth
Testing for Resource Use and Selection by Marine Birds J. Christopher Haney and Andrew R. Solow
Rare, Local, Little Known and Declining Breeders. A Closer Lock: Aleutian Tern J. Christopher Haney, Jon M. Andrew, and David S. Lee
An Observation of Fea's Petrel Pterodroma feae (Procellariiformes: Procellariidae) Off the Southeastern United States, with Comments on the Taxonomy and Conservation of Soft-Plumaged and Related Petrels in the Atlantic Ocean J. Christopher Haney, Craig A. Faanes, and W. R. P. Bourne

Geometry of Visual Recruitment by Seabirds to Ephemeral Foraging Flocks J. Christopher Haney, Kurt M. Fristrup, and David S. Lee	PC-6
Problems in the Meso-Scale Interpretation of Satellite Chlorophyll Data Eric W. Henderson and John H. Steele	PC-7
Advanced Marine Technologies and Historic Shipwreck Management Porter Hoagland	PC-7
The Advanced Marine Electronics Instrumentation Industry and the European Market: Government Policies and International Competitives *Porter Hoagland and Hauke L. Kite-Powell	PC-7
European Advanced Marine Electronic Instrumentation: A U.S. Perspective Porter Hoagland and Hauke L. Kite-Powell	PC-8
Legal and Political Issues of the Antarctic Legal Regime Christopher C. Joyner	PC-8
Differentiating Use and Nonuse Values for Coastal Pond Water Quality Improvement Yoshiaki Kaoru	PC-9
Valuing Marine Recreation by the Nested Random Utility Model: Functional Structure, Party	
Composition and Heterogeneity Yoshiaki Kaoru	PC-9
An Overview of Technology Transfer and Intellectual Property Management Between Marine Science Research Institutions and the Commercial Sector Hauke L. Kite-Powell and Porter Hoagland	PC-9
Is There a Global Warming Problem? Andrew R. Solow	C-10
Model-Checking in Non-Stationary Poisson Processes Andrew R. Solow	C-10
Decision-Making and the Value of Information Under Uncertainty Andrew R. Solow and James M. Broadus	C-10
Mapping Water Quality by Local Scoring Andrew R. Solow and Arthur G. Gaines	C-10
On the Measurement of Biological Diversity Andrew R. Solow, Stephen Polasky and James M. Broadus	C-10
The Statistical Analysis of Whistle Exchanges in Dolphins Andrew R. Solow, Peter Tyack, and Laela Sayigh	C-10
Can Ecological Theory Cross the Land-Sea Boundary? John H. Steele	C-11
Marine Ecosystem Dynamics: Comparison of Scales John H. Steele	'C-11
Marine Functional Diversity John H. Steele	'C-11
The Role of Predation in Plankton Models John H. Steele and Eric W. Henderson MP.	C-11

Innovation in Environmental Policy T. H. Tietenberg, Ed	MPC-12
Paleoshorelines and the Prehistory of Barbuda, West Indies David R. Watters, Jack Donahue and Robert Stuckenrath	MPC-12
Recent Development in Legal Protection of Historic Shipwrecks in P.R. China Hongye Zhao	MPC-12



GRADUATE STUDENTS

Geothermal Heat Flux from Hydrothermal Plumes on the Juan De Fuca Ridge Karen G. Bemis
Observations of Wave-Mean Flow Interaction in the Pacific Equatorial Undercurrent Esther C. Brady
Implementation and Evaluation of a Dual-Sensor Time-Adaptive Em Algorithm for Signal Enhancement John R. Buck
The Marine Geochemistry of Rhenium, Iridium and Platinum Debra Colodner
Mantle Convection, Melt Migration and the Generation of Basalts at Mid-Ocean Ridges Matthew J. Cordery
A Study of North Atlantic Ventilation using Transient Tracers Scott C. Doney
Acoustic Scattering from Elastic Ice: A Finite Difference Solution J. Robert Fricke
Human Factors Engineering in Sonar Visual Displays Lawrence Francis Galvin
Near-Equatorial Deep Circulation in the Indian and Pacific Oceans Gregory C. Johnson
Predictions and Observations of Seafloor Infrasonic noise generated by Sea Surface Orbital Motion Timothy E. Lindstrom
Mass, Heat, Oxygen and Nutrient Fluxes at 30°S and their Implications for the Pacific-Indian through Flow and the Global Heat Budget Alison M. MacDonald
Vacuolation, Proliferation and Neoplasia in the Liver of Boston Harbor Winter Flounder Michael J. Moore
Global Positioning System Measurement of Crustal Deformation in Central California Mark H. Hunter
Developmental Changes in the Structure and Function of Lobster Hhemocyanin Kirby S. Olson
Global Isotopic Signatures of Oceanic Island Basalts Lynn A. Oschmann
Surface-Referenced Current Meter Measurements Markku Junani Santala
Upper Ocean Dynamics during the LOTUS and TROPIC HEAT Experiments Rebecca R. Schudlich
The Modern and Glacial Thermoclines along the Bahama Banks Niall C. Slowey
Acoustic Wave Scattering from a Random Ocean Bottom Dajun Tang

Diffuse Flow from Hydrothermal Vents D. Andrew Trivett	GS-14
Propulsion Optimization for ABE, an Autonomous Underwater Vehicle (AUV) Thomas J. Woodford	GS-14
The Structure and Transport of the Brazil Current between 27° and 36° South Jan C. Zemba	GS-14
Circulations and Water Mass Balances in the Brazil Basin Huai-Min Zhang	GS-15
Flow Over Finite Isolated Topography LuAnne Thompson	GS-16

DEPARTMENT OF APPLIED OCEAN PHYSICS & ENGINEERING Albert J. Williams III, Chairman	

MULTISENSOR VISUALIZATION FOR UNDERWATER ARCHAEOLOGY

W. Kenneth Stewart

It has become a truism within the marine science community that the surface of the moon, and now of other celestial bodies, has been better explored than the ocean floor of our own planet. Perhaps less than a tenth of one percent of this vast undersea domain has ever been seen by human eyes. In contrast with remote sensing through the atmosphere, the relatively opaque and inhospitable medium presents formidable challenges to those who seek to probe its depths. Impenetrable to most forms of electromagnetic radiation, the ocean yields a picture of the seafloor mainly through acoustic and optical means.

Whether using sound or light, the fundamental trade-off is range for resolution. Low-frequency acoustic systems survey a swath tens of kilometers wide, but can only resolve features larger than several tens of meters; higher frequency sonars have better resolution, but coverage is limited. Cameras and other optical systems see greater detail, but image yet smaller areas. Special problems with both methods include attenuation, scattering noise, and distortion. These are compounded by the difficulty in measuring position underwater and deployment costs that rise sharply with depth.

Published in: IEEE Computer Graphics and Applications, March: 13-18, 1991.

Supported by: ONR contract N00014-88-K-2022, ONT and Sea Grant Program.

WHOI Contribution No. 7606.

FREQUENCY DEPENDENCE OF SOUND BACKSCATTERING FROM LIVE INDIVIDUAL ZOOPLANKTON

D. Chu, T. K. Stanton and P. H. Wiebe

This article presents an experimental investigation illustrating the strong frequency dependence of the backscatter from individual zooplankton for fixed shape and orientation. A broadband laboratory chirp sonar was used to investigate the frequency characteristics of the backscattering by two individual live decapod shrimp(Palaemonetes vulgaris). The measurements illustrate that for fixed shape and orientation, the backscattering amplitude varies dramatically with frequency with as low as 30-dB-deep nulls at certain frequencies (30 dB corresponds to a factor of 1000 in an echo integration value). The overall echo level and frequency characteristics vary from ping to ping as the animal changes shape and

orientation. The fluid bent cylinder model [T.K. Stanton (1989), J. Acoust. Soc. Am. 86: 691-705] describes the single-realization normal incidence data reasonably well, especially the frequencies at which the peaks and nulls occur. Our theoretical analysis only involved physical parameters that were either directly measured or taken from the literature where physical parameters involving similar animals are published. As expected, once the data are averaged across a number of pings, the nulls are "filled in" and the backscatter versus frequency curve becomes smoother. These data are useful for predicting volume scattering strengths observed in the field by taking averages with respect to shape and orientation.

In Press: Journal of the International Council for the Exploration of the Sea.

Supported by: Postdoctoral Fellowship, ONR N00014-89-J-1729 and N00014-87-K-007.

WHOI Contribution No. 7611.

MECHANICAL DESIGN METHODS OF IMPROVING MANIPULATOR PERFORMANCE

Nathan Ulrich and Vijay Kumar

Robot manipulator performance can be substantially improved by intelligent mechanical design. This paper presents several design methods for enhancing manipulator performance, especially in unconventional applications. These include a passive, mechanical, and energy-conservative gravity compensation method, a remote actuation technique, and the use of tension-element reducers. The energy consumption of a robot designed following these techniques is found to be a fraction of one of conventional construction.

Submitted to: 1991 International Conference on Advanced Robotics.

Supported by: DARPA grant N00014-88-K-0630, AFOSR grants 88-0244 and 88-0296, Army/DAAL 03-89-C-0031PRI, NSF grants CISE/CDA 88-22719 and IRI 80-06770.

WHOI Contribution No. 7617.

REMOTE CONTROL OF A TELEROBOTIC UNDERWATER VEHICLE VIA SATELLITE

Dana R. Yoerger, Robert Weiman and Tagore Somers

This paper describes remote operation of a telerobotic underwater vehicle system. As part of an educational effort called the JASON Project, students from a network of downlink sites across North America piloted the vehicle in the course of an archaeological expedition in Lake Ontario. The vehicle, control system, telecommunications, and remote control station technology are described, and operational results reported.

Submitted to: 1991 IEEE National Telesystems Conference.

Supported by: JASON Partners and Office of Chief Naval Research.

WHOI Contribution No. 7618.

ADAPTIVE SLIDING CONTROL OF AN EXPERIMENTAL UNDERWATER VEHICLE

Dana R. Yoerger and Jean-Jacques E. Slotine

This paper shows that adaptive extensions of sliding control are effective for precise control of underwater vehicles through experiments with an actual vehicle. Adaptive sliding control permits direct nonlinear control system design, including on-line parameter estimation. The paper details experimental results obtained from a tethered underwater vehicle equipped with precision broadband acoustic navigation system and 3 DOF attitude instrumentation controlled through a real-time network of transputers. Simulation and experimental trials show on-line determination of vehicle parameters such as mass and nonlinear drag.

Submitted to: 1991 IEEE International Conference on Robotics and Automation.

Supported by: ONR contract N00014-86-C-0038, N00014-88-K-2022 and ONR grant N00014-87-J-1111.

WHOI Contribution No. 7619.

VISUALIZATION RESOURCES AND STRATEGIES FOR REMOTE SUBSEA EXPLORATION

W. Kenneth Stewart

Common resources and strategies are described for graphics and imaging applications in remote subsea exploration. What is meant by resources are the hardware, software, and human assets that constitute sea-going and shore-based systems; strategies encompass the architectural, engineering, and practical aspects of making such a visualization environment operational and productive. Emphasis is placed on current applications within the oceanographic community for search/survey/mapping (towed, unmanned

systems), remotely operated vehicles and submersibles (man-in-the-loop systems), and autonomous underwater robots (intelligent systems). For these applications, a common goal is the acquisition and processing of underwater remote-sensor data to create a model of the subseaterrain. Visualization tools offer an important means of conveying the information contained in such a model.

Dominant requirements within this context are the management, processing, and presentation of high-bandwidth, multisensor data including optical and acoustic imagery, laser and sonar bathymetry, and other physical data sets. Specific visualization tools are used for image processing, volumetric modeling, terrain visualization, real-time operator displays, mapping and geographic information systems, as well as for scientific and engineering research and development. An overview and selected examples reflect a sampling of state-of-the-art approaches within the oceanographic community.

Published in: Scientific Visualization of Physical Phenomena, N.M. Patrikalakis, ed. Springer-Verlag, Tokyo, :85-109, 1991.

Supported by: JASON Foundation for Education. WHOI Contribution No. 7620.

FREQUENCY DOWNSHIFT IN NARROW-BANDED SURFACE WAVES UNDER THE INFLUENCE OF WIND

Tetsu Hara and Chiang C. Mei

It is well known that the spectral peak of wind-induced gravity waves on the sea surface tends to shift to lower frequencies as the fetch increases. In past theories the nonlinear dynamics subsequent to Benjamin-Feir instability has been found to initiate the downshift in narrow-band waves in the absence of wind. However these weakly nonlinear theories all predict the downshift to be only the first phase of an almost cyclic process. Limited by the length of a wave tank, existing experiments are usually made with relatively steep waves which often break. Although there is a theory on how breaking adds dissipation to stop the reversal of the initial trend of downshift, the details of breaking must be crudely characterized by semi-empirical hypotheses.

Since the direct role of wind itself must be relevant to the entire development of wind wave spectrum, we examine here the effect of wind on the nonlinear evolution of unstable sidebands in narrow-banded waves. We assume that the waves do not break and consider the case where the nonlinear effects that initiate the downshift, energy input by wind and damping by internal dissipation

all occur on the same time scale. This means that not only the waves must be mild but the wind stress intensity must also lie within a certain narrow range. With these limitations we couple the air flow above the waves with Dysthe's extension of the cubic Schr'odinger equation, and examine the initial as well as the long-time evolution of a mechanically generated wave train. For a variety of wind intensities, downshift is indeed found to be enhanced and rendered long lasting.

Published in: Journal of Fluid Mechanics, 230:429-477, 1991.

Supported by: ONR Physical Oceanography
Program under Accelerated Initiative on Surface
Wave Dynamics and NSF grant MSME 8813121.

WHOI Contribution No. 7621.

A THREE-FREQUENCY SCATTEROMETER TECHNIQUE FOR THE MEASUREMENT OF OCEAN WAVE SPECTRA

Dale L. Schuler, William C. Keller and William J. Plant

A new microwave technique for the measurement of directional ocean wave spectra has been compared with wave gauge output during extensive field testing. Prototype scatterometers have been built at L-band, and later, because of its suitability for aircraft use, at K_u -band. Both systems have been tested during field-trials at a pier site on the Outer Banks of North Carolina. The new method evolved from efforts to apply frequency agility techniques to dual-frequency scattering from the ocean. The purpose of such efforts was to reduce the incoherent clutter background that limited signal detectibility in such scatterometers. Re-examination of composite surface scattering theory indicated that a specialized form of frequency-agile signals might transform the formerly detrimental clutter background into a signal proportional to the ocean wave spectrum itself. The performance of the microwave spectrometer would then only be limited by system thermal noise.

Submitted to: IEEE Journal of Oceanic Engineering. WHOI Contribution No. 7622.

THE PHYSICAL OCEANOGRAPHY OF THE AMAZON OUTFLOW

W. Rockwell Geyer, Robert C. Beardsley, Julio Candela, Belmiro Castro, Richard V. Legeckis, Steven J. Lentz, Richard Limeburner, Luis B. Miranda, and John H. Trowbridge

The Amazon shelf is an unusually energetic region. The Amazon River discharges between 80,000 and 250,000 m³ s⁻¹ of fresh water onto the shelf at the equator (Oltman, 1968; Muller-Karger et al., 1989). The resulting surface plume of brackish water extends hundreds of kilometers seaward and northwestward along the coast (e.g., Gibbs, 1970; Milliman et al., 1975; Curtin, 1986a). The North Brazil Current sweeps the waters over the outer shelf and slope northwestward at speeds reaching 1-2 m s⁻¹ (Flagg et al., 1986; Richardson and Reverdin, 1987). Previous current measurements on the shelf indicate across-shelf tidal velocities in excess of 1 m s⁻¹ (Gibbs, 1982; Curtin, 1986b), and the persistent trade winds impose a cross-shelf wind stress as large as 1 dyn cm⁻² (Picaut et al., 1985). The Amazon River discharge, the North Brazil Current transport, and the trade winds all exhibit strong seasonal cycles (Figure 1). The limited set of previous measurements on the Amazon shelf provide only a crude characterization of the physical environment; little is known about the structure and variability of water properties and currents, and even less about the dynamics of the shelf regime. Furthermore, there has not been a sufficient observational basis for evaluating theoretical models of the Amazon shelf (e.g., Ou, 1989) or for guiding model development.

Published in: Oceanography, 4(1):8-14, 1991.

Supported by: NSF OCE 89-12917.

WHOI Contribution No. 7623.

ERROR ANALYSIS OF AN ACOUSTIC CURRENT METER

D. Andrew Trivett, Eugene A. Terray and Albert J. Williams III

Accuracy of the Benthic acoustic stress sensor (BASS) and the proposed modular acoustic velocity sensor (MAVS) is evaluated in this paper. A simple model of the hydrodynamic sources of error for acoustic current meters is presented and compared with the measured performance of BASS in a tow-tank and in field deployments. The sources of error addressed in this paper include those due to ideal flow around the sensor cage,

wake effects from the support structure and transducers, vortex shedding from the cage, and electronic zero-point offsets. Electronic error dominates at velocities less than 5-10 cm/s, while flow disturbance dominates at higher speeds.

Published in: IEEE Journal of Oceanic Engineering, 16(4):329-337, 1991.

Supported by: NSF grant OCE-89-17448 and NSF grant OCE-87-16937.

WHOI Contribution No. 7626.

FIBER OPTIC TELEMETRY IN JASON, THE ROV

Bob Elder

The Deep Submergence Laboratory (DSL) of the Woods Hole Oceanographic Institution's Department of Applied Ocean Physics and Engineering has developed a deep ocean ROV called JASON. The system has 4 real time video channels and a 125 Mbit per second digital data link providing 8 high speed channels and 20 RS-232 channels. The high data rates not only enhance the acquisition of sonar and sensor data, but also improve the vehicle's performance in real time closed loop control.

This paper gives an overview of both the digital and video telemetry systems in block diagram form. Each system element will be discussed, including design trade offs. Other elements discussed will be surprises encountered in bringing the vehicle to its full 20,000 ft. depth capability, the accumulation of 500 hours of bottom time, and a brief look at what our design goals are for the next few years.

Submitted to: Proceedings of ROV Conference, 1991.

Supported by: ONR contracts N00014-86-C-0038 and N00014-87-J-1111.

WHOI Contribution No. 7657.

EVIDENCE FOR ENERGETIC MODE ONE INTERNAL WAVES OBSERVED WITH 4000 KM ACOUSTIC ANTENNAE

Wayne R. Blanding, John L. Spiesberger and Arthur Miller

In January to May 1988, changes in acoustic travel time (133 Hz, 60 ms resolution) were measured between an acoustic source mounted on the Oahu slope and seven bottom-mounted receivers at 3000 to 4000 km distance in the northeast Pacific. Spectra of travel time change exhibit peaks whose periods vary between 12 and 24 hours (intertidal periods) and whose amplitudes

vary from about 1 to 14 ms. The larger peaks in the travel time spectra have amplitudes as large as those due to the barotropic tides. Intertidal oscillations in travel time are consistent with mode one internal wave packets whose phase crests are aligned nearly parallel to the acoustic sections. When phase crests differ significantly from parallel alignment, their acoustic signature vanishes. Our measures of change in travel time attenuate signals associated with waves whose vertical mode number is two or greater. Thus, each acoustic section exhibits sensitivity to waves in both the horizontal and vertical directions akin to an antenna. Vertical displacements of the mode one packets are about one to two meters. Their energy is 10 to 100 times that expected in Garrett-Munk spectra for internal waves. The signal-to-noise ratio of mode one waves is smaller in point measurements than in these acoustic travel time measurements because the acoustic technique attenuates the effects from waves with higher vertical mode number.

Submitted to: Journal of Geophysical Research.

Supported by: ONR contract N00014-86-C-0358 and ONT contract N00014-89-C-0179.

WHOI Contribution No. 7658.

COMMENT ON "WIND WAVE DIRECTIONALITY EFFECTS ON THE RADAR IMAGING OF OCEAN SWELL" BY F. J. OCAMPO-TORRES AND I. S. ROBINSON

William J. Plant

In a recent paper, Ocampo-Torres and Robinson [1990] (hereinafter referred to as OR) attempt to demonstrate that the tilt modulation transfer function relating modulations of microwave received power to long ocean waves is a more significant source of modulation than had been previously suspected, especially for azimuthally-travelling long waves. They argue that because of the sensitivity of the normalized radar cross section of the sea, σ_o , to facet tilting both in and normal to the plane of incidence, tilt modulation is very sensitive to wind direction and may be quite important even when long surface waves travel perpendicular to the radar look direction. Unfortunately, OR have made a fundamental error in the specification of the short wave variance spectrum which renders most of their arguments incorrect and invalidates their conclusions.

Published in: Journal of Geophysical Research, 96(C10):18,527-18,529, 1991.

Supported by: ONR grant N00014-89-J-1897.

WHOI Contribution No. 7659.

TRANSPUTER-BASED DISTRIBUTED PROCESSING FOR UNDERWATER ROBOTIC VEHICLE CONTROL

David A. Mindell and Dana R. Yoerger

High-precision, closed-loop control of underwater robotic vehicles presents unique computing requirements. This paper outlines a vehicle computer design philosophy based on transputers, microprocessors specially designed for parallel processing. Distributed processing can be seen as a subset of parallel processing, and transputers can be adapted to serve as high-performance distributed controllers for underwater vehicles, both tethered and autonomous. Two transputer-based designs are presented, Hylas, a tethered research vehicle, and ABE, an autonomous survey system. Data is presented to show the low-latency and high update-rate of vehicle controllers that can be achieved with transputers as distributed controllers.

Submitted to: 1991 American Control Conference.

Supported by: NSF grant OCE-8820227, ONR contracts N00014-86-C-0038, N00014-88-K-2022 and ONR grant N00014-87-J-1111.

WHOI Contribution No. 7660.

HIGH-RESOLUTION OPTICAL AND ACOUSTIC REMOTE SENSING FOR UNDERWATER EXPLORATION

W. Kenneth Stewart

It has become a truism within the marine science community that the surface of the moon, and now of other celestial bodies, has been better explored than the ocean floor of our own planet. Perhaps less than a tenth of one percent of this vast undersea domain has ever been seen by human eyes. In contrast with remote sensing through the atmosphere, the relatively opaque and inhospitable medium presents formidable challenges to those who seek to probe its depths. Impenetrable to most forms of electromagnetic radiation, the ocean yields a picture of the seafloor mainly through acoustic and optical means.

Published in: Oceanus, 34(1), 1991. WHOI Contribution No. 7664.

REMOTE-SENSING ISSUES FOR INTELLIGENT UNDERWATER SYSTEMS

W. Kenneth Stewart

In contrast with remote sensing through the

atmosphere, the relatively opaque and inhospitable ocean medium presents unique and formidable challenges. Impenetrable to most forms of electromagnetic radiation, the sea yields a glimpse of its hidden structure mainly through acoustic and optical means. For certain applications, though, an autonomous underwater system may benefit from a perception of its environment in terms of magnetics, gravity, chemical signature, or other sensing modalities. This paper offers an introduction for researchers unfamiliar with issues in remote sensing underwater. Application areas include machine perception for intelligent underwater systems, large-scale seafloor mapping, survey, and environmental characterization.

F blished in: Proceedings of the 1991 IEEE
Computer Society Conference on Computer
Vision and Pattern Recognition, Hawaii, June.
IEEE Computer Society Press, Los Alamitos,
:230-235, 1991.

WHOI Contribution No. 7665.

THE VARIANCE OF THE NORMALIZED RADAR CROSS SECTION OF THE SEA

William J. Plant

The dependence of the normalized radar cross section of the sea, $\overline{\sigma}_0$, on illuminated area and integration time is investigated. We show that the standard expression for this dependence cannot account for the correlation of power received from different points on the surface which is exhibited by microwave backscatter from the sea. An alternate expression is derived which does account for these correlations. We show that knowledge of the ocean wave spectrum and modulation transfer function along with the determination of three fundamental parameters, facet variance, the velocity spread of a facet, and correlation area, are necessary to specify the dependence of cross section variance on illuminated area and integration time. The correlation time is not a fundamental parameter but depends on illuminated area. An expression for that dependence is derived here. Issues of system noise and the relationship of received power variance to cross section variance are also addressed. We relate these calculations to the critical problem of determining confidence intervals for $\overline{\sigma}_0$ measurements at high spatial resolution.

Published in: Journal of Geophysical Research, 96(C11):20,643-20,654, 1991.

Supported by: ONR grant N00014-89-J-1897.

WHOI Contribution No. 7682.

THE ACCURACY OF GOES SATELLITE CLOCKS

Kenneth R. Peal

Clocks that receive and decode time signals from the GOES satellites are commonly used to provide accurate time reference for the recording of a wide variety of data types in academic research. These satellite clocks must be used with adequate knowledge of their operation. When corrections for satellite position are not made, comparison data presented in this paper show that errors of up to several milliseconds will result. However, with care and the application of proper corrections it is shown that accuracies of 100 to 200 microseconds are achievable.

Published in: Marine Geophysical Researches, 13:349-352, 1991.

Supported by: NSF grant OCE-8917628. WHOI Contribution No. 7686.

DESIGN OPTIMIZATION OF AN ELECTRIC UNDERWATER MANIPULATOR

Nathan Ulrich and Dana R. Yoerger

The next generation of underwater vehicles will require advanced manipulation capability. Current undersea manipulators have difficulty with many intervention tasks-including servicing complicated man-made underwater structures, performing delicate scientific sampling, and operating from hovering vehicles-and are large. heavy, and wasteful of power. We believe that intelligent mechanical design can solve these problems. Our experience with the JASON system has shown that a subsea manipulator designed to have excellent control properties is useful for a variety of demanding tasks. We are currently refining the principles demonstrated in the JASON design, while significantly reducing size, weight, mechanical complexity, and power consumption but increasing payload and dexterity.

Submitted to: Mechanical Design.

Supported by: NRL grant N00014-88-K-2022, and ONR grant N00014-90-J-1912.

WHOI Contribution No. 7688.

COMMENT ON THE FULL-WAVE CONTROVERSY

William J. Plant

Thorsos and Winebrenner [1991] compare the formally averaged predictions of Bahar's full-wave

theory, with and without Bahar's simplifying assumptions, with their numerical evaluation of full-wave theory, with their numerical calculations from an exact integral equation, and with analytical results from small-perturbation theory and the (first-order) Kirchoff approximation. They show that for small heights and slopes and for moderate incidence angles the formally-averaged full-wave theory without Bahar's simplifying assumptions agrees with their numerical evaluation of full-wave theory and with the Kirchoff approximation but not with perturbation theory. On the other hand, numerical results from the exact integral equation agree with perturbation theory in the cases they examine. Thus for these cases they conclude that perturbation theory is valid, that the Kirchoff approximation is not accurate, and the full-wave theory fails. By making Bahar's simplifying assumptions, namely, that correlations between surface heights and slopes may be neglected and that slopes at two different points are perfectly correlated, they find that full wave theory agrees with small perturbation theory where it should. In his rebuttal, Bahar (1991) reviews full-wave theory and its relationship to Rice's [1951] original small-perturbation theory, points out what he says is a divergence of higher-order perturbation theory for small heights and slopes, and takes exception to the tapering function used by Thorsos and Winebrenner in their numerical calculations. In this brief comment, I would like to try to clarify the central issue in this controversy while, hopefully, bringing an alternate viewpoint to bear on some side issues.

Published in: Journal of Geophysical Research, 96(C9):17,105-17,106, 1991.

Supported by: ONR grant N00014-89-J-1897.

WHOI Contribution No. 7702.

IDENTIFICATION OF LOW ORDER DYNAMIC MODELS FOR DEEPLY-TOWED UNDERWATER VEHICLE SYSTEMS

Franz S. Hover and Dana R. Yoerger

The horizontal dynamics of deeply-towed underwater vehicle systems can be effectively modeled by nonlinear partial differential equations. However, high resolution numerical solutions are of limited use in controller design, where methods for systems of very high or infinite order are not well developed. This paper examines the possibility of finding low-order dynamic models in differential equation form, in order to present a more tractable control problem. A learning model method is used, and the identification process is novel in that a verified high-order model provides the primary

data set. This approach allows a priori characterization of system responses in regimes or scenarios for which no experimental data exist. The performances of the reduced-order forms are verified through comparison of model output with actual sea data obtained during recent deepwater tests.

In Press: International Journal of Offshore and Polar Engineering, 2(2), 1992.

Supported by: ONR contract N00014-85-G-0084 and NSF contract OCE-8511431.

WHOI Contribution No. 7703.

THRUST MECHANICS IN FLAPPING FOILS AND OPTIMAL FISH PROPULSION

George S. Triantafyllou, Michael S. Triantafyllou and Mark A. Grosenbaugh

It is shown that thrust in oscillating foils is produced optimally when synchronized with the most unstable frequency of the wake forming behind the foil. Data from the fish and cetaceans establish that optimal fish propulsion is achieved in the same manner. The basic conclusion is that the non-dimensional number formed by dividing the product of the tail beat frequency times the amplitude of tail oscillation, with the forward velocity (Strouhal number) must be in range of 0.25 to 0.35.

Submitted to: Journal of Experimental Biology.

Supported by: MIT Sea Grant grants
NA86AA-D-SG089 and NA90AA-D-SG424;
Draper Laboratories contract DL-H-404182 and
ONR contract N00014-90-J-1312.

WHOI Contribution No. 7717.

SPATIAL DIVERSITY PROCESSING FOR UNDERWATER ACOUSTIC TELEMETRY

Josko A. Catipovic and Lee E. Freitag

A large increase in the reliability of shipboard or stationary underwater acoustic telemetry systems is achievable by using spatially distributed receivers with aperture sizes from 0.35 to 20 m. Output from each receiver is assigned a quality measure based on the estimated error rate, and the data, weighted by the quality measure, is combined and decoded. The quality measure is derived from a Viterbi error-correction decoder operating on each receiver and is shown to perform reliably in a variety of non-Gaussian noise and jamming environments and reduce to the traditional optimal

diversity system in a Gaussian environment. The dynamics of the quality estimator allow operation in the presence of high-power impulsive interference by exploiting the signal and noise differential travel times to individual sensors.

The spatial coherence structure of the shallow-water acoustic channel shows relatively low signal coherence at separations as short as 0.35 m. Increasing receiver spacing beyond 5 m offers additional benefits in the presence of impulsive noise and larger scale inhomogeneities in the acoustic field.

A number of data transmission experiments were carried out in Woods Hole Harbor to demonstrate system performance in realistic underwater environments where the acoustic telemetry system is expected to operate. Diversity combining, even with only two receivers, can lower uncoded error rates by up to several orders of magnitude while providing immunity to transducer jamming or failure. The performance improvement is achieved at no increase in bandwidth or transmitted power.

Published in: IEEE Journal of Oceanic Engineering, 16(1):86-97, 1991.

Supported by: ONR U.R.I.P. contract N00014-86-K-0751.

WHOI Contribution No. 7718.

COMPACT DIGITAL SIGNAL PROCESSING ENHANCES ACOUSTIC DATA TELEMETRY

Josko Catipovic, Daniel F. Frye and Dave Porta

Acoustic data telemetry has been used ever since it was discovered that the ocean could support signal transmission. Past applications have ranged from low-baud-rate command and control systems for ocean equipment such as sea floor valves and backup acoustic blowout preventer (BOP) control in the offshore industry to acoustic releases for oceanographic moorings. These systems typically operate at tens-of-bits per second. A few higher rate systems have been developed, but these have shown high sensitivity to ocean channel features such as multipath and doppler, and are generally useful only for vertical transmission from sea bottom instruments to surface ships.

Published in: Sea Technology, 31(5):10-15, 1990.

Supported by: ONR U.R.I.P. contract N00014-86-K-0751.

WHOI Contribution No. 7719.

OSCILLATING FLOWS OVER PERIODIC RIPPLES OF FINITE SLOPE

Tetsu Hara, Chiang C. Mei and K. T. Shum

The analysis of a laminar oscillating flow over a wavy surface is an important first step towards understanding the complicated dynamics over sand ripples along sea coasts. In a previous paper (Hara & Mei 1990) we have presented an asymptotic theory for a large Reynolds number and have predicted oscillating vortices high above the ripples when the ambient oscillation amplitude is comparable to the ripple wavelength. Here we present a numerically accurate solution of the Navier-Stokes equations in power series of the ripple slope. The solution is assumed to be periodic in time. When the Reynolds number is high enough so that the viscous Stokes boundary layer is relatively thin, the existence of oscillating vortices in the outer layer is confirmed. Results for smaller Reynolds numbers are also included in which the Stokes and the outer layers merge. Compared with an oscillating flow over a flat plate, the rate of energy dissipation is found to increase by as much as 40% due to the existence of ripples.

In Press: Physics of Fluids A.

Supported by: ONR contracts N00014-83-K-0550, N00014-89-J-3128 and NSF grant MSME-8813121.

WHOI Contribution No. 7720.

ON SIMPLE REPRESENTATION OF MIXING IN A STRESS-DRIVEN STRATIFIED FLOW

J. H. Trowbridge

The deepening and structure of a stably stratified flow driven by a surface stress are examined by means of a conceptual model in which local mixing does not occur if the gradient Richardson number Ri is greater than the critical value $Ri_c \simeq 1/4$ that indicates onset of shear instability, and local mixing occurs instantaneously, through a simple exchange of fluid volumes, if Ri is less than Ric. The model leads to a mathematical formulation in which turbulent mixing is a gradient transport process just strong enough to maintain Ri at the critical value Ric throughout the boundary layer. Although unrealistic just beneath the stressed surface, self-similar solutions based on this formulation plausibly describe the outer part of the boundary layer and the rate at which the layer deepens, provided that appropriately defined bulk Richardson and Reynolds numbers are sufficiently

large. A comparison of model computations with existing laboratory measurements and turbulence closure simulations supports the conceptual model as an approximate representation of the processes controlling the deepening of the boundary layer and the qualitative structure in the outer part of the flow.

Submitted to: Journal of Geophysical Research.

Supported by: ONR contracts N00014-89-J-1067 and N00014-89-J-1074.

WHOI Contribution No. 7721.

BASIN SCALE OCEAN MONITORING WITH ACOUSTIC THERMOMETERS

John L. Spiesberger and Kurt Metzger

The upper two meters of ocean have more thermal capacity than the entire atmosphere. Hence, it is important to measure the large scale (> 500 km) thermal field in the ocean to understand weather and climate. Satellites provide important global temperature measurements of the upper several millimeters of the ocean (Apel, 1987). In-situ temperature measurements taken at points have revealed important climatic changes in the ocean (Roemmich and Wunsch, 1984; Levitus, 1989; Roemmich, 1990). However, climatic variations of the ocean's thermal field are generally not well described or understood despite more than a century of observation. For example, available data are insufficient for determining whether the upper 100 m of the north Pacific are warmer or colder from one month to the next at large scales (Wyrtki and Uhrich, 1982). Over the past eight years we have adapted a technique called ocean acoustic tomography, originated by Munk and Wunsch (1979), to measure the large scale thermal field in the north Pacific basin with a temporal resolution as short as one week (Spiesberger and Metzger, 1991a). We believe that these acoustic measurements will be an important component of long term monitoring programs designed to understand the ocean's role in climatic change.

Submitted to: The Oceanography Society Journal.

Supported by: ONR contract N00014-86-C-0358 and ONT contract N00014-90-C-098.

WHOI Contribution No. 7722.

ON RIPPLE DYNAMICS V. LINEAR PROPAGATION OF CYLINDRICAL WAVES ON LIQUIDS WITH AND WITHOUT A SURFACE DILATATIONAL VISCOELASTIC RESPONSE

Erik J. Bock

The propagation of continuous-wave

cylindrical ripples as observed in the laboratory is the subject of this paper. The first explicit formulation of the linearized Navier-Stokes in cylindrical coordinates for waves in the presence of a surface dilatational viscoelastic response is derived. Observations of wave slope as measured by a laboratory laser slope gauge are reported; they are described accurately by the theoretically predicted Hankel functions of the second kind. The study uses n-decane as the liquid on which the waves propagate. Three surfaces are tested: they are pure n-decane, n-decane with a surface film of polydimethylsiloxane (PDMS) and a film of a fluorinated surfactant (FC740). The observed dispersion relation is shown to be in excellent agreement with theory and indicate values of surface dilatational elasticity equal to -0.048 ± .098 mN/m, .477 ± .012 mN/m, and 1.72 ± .300 mN/m for the cases of pure n-decane, n-decane with PDMS, and n-decane with FC740, respectively.

In Press: Journal of Colloid and Interface Science.

Supported by: ONR grant N00014-90-J-1717.

WHOI Contribution No. 7726.

TIME DOMAIN ANALYSIS OF NORMAL MODE, PARABOLIC, AND RAY SOLUTIONS OF THE WAVE EQUATION

Linda Boden, James B. Bowlin and John L. Spiesberger

Estimation of sound speed and temperature fields from tomographic data requires knowledge of the accuracy of the forward model. For this reason, time domain results using three models derived from the acoustic wave equation are compared here. The models chosen for the analysis are normal modes (NM) and the parabolic equation (PE) and ray approximations. (The NM and PE time series are obtained via Fourier synthesis). The analysis is done using a depth-dependent sound speed profile where only refracted and surface-reflected/refracted energy is allowed to propagate. Because the NM representation is theoretically exact in this environment, it is used as the comparative base. Travel time sequences generated using the PE and ray approximations are compared to those generated using NM. For the angular aperture analyzed (± 9 to ± 16.5 degrees), phase errors in the PE approximation limit reliable predictions of travel time to distances of about 1000 km. However, the ray approximation is found to be adequate for estimating arrival times at ranges out to 4000 km for frequencies of 100 Hz and above.

Published in: Journal of the Acoustical Society of America, 90(2), Pt. 1:954-958, 1991.

Supported by: ONR contracts N00014-86-C-0358 and N00014-90-C-098.

WHOI Contribution No. 7728.

STUDY OF DOMINANT PERFORMANCE CHARACTERISTICS IN ROBOT TRANSMISSIONS

Hagen Schempf and Dana R. Yoerger

Six different transmission types suitable for robotic manipulators were compared in an experimental and theoretical study. Single degree of freedom mechanisms based on the different transmissions were evaluated in terms of force control performance, achievable bandwidth, and stability properties in hard contact tasks. Transmission types considered were (1) cable reducer, (2) harmonic drive, (3) cycloidal disk reducer, (4) cycloidal cam reducer, (5) ball reducer, and (6) planetary/cycloidal gear head. Open loop torque following error, attenuation and phase lag, and closed loop bandwidth and stability margin were found to be severely dominated by levels of inertia, stiffness distribution and variability, stiction, coulomb and viscous friction, and ripple torque. These aspects were quantified and shown to vary widely among all transmissions tested. The degree of nonlinearity of each transmission affected its open and closed loop behavior directly, and limited the effectiveness of compensation schemes. Simple transmission models based on carefully measured transmission characteristics are shown to predict stability margins and achievable force-control bandwidths in hard contact to within a 5% to 15% error margin.

In Press: ASME Journal of Mechanisms, Transmissions and Automation in Design.

Supported by: ONR contracts N00014-86-C-0038 and N00014-88-K-2022.

WHOI Contribution No. 7739.

IN SITU PROCESSING OF BOUNDARY LAYER FLOW MEASUREMENTS FOR DATA COMPRESSION

Albert J. Williams, 3rd and Thomas Gross

Boundary layers are turbulent so simple velocity means do not provide sufficient information to characterize the flow. Higher moment averages must be used such as Reynolds stress turbulent kinetic energy, and vector averaged flux of scaler constituents. However, in long deployments, internally recording instruments cannot store the quantity of data these computations need so in situ processing is

required. BASS, an acoustic current meter array, has recorded 2 Hz samples, averaged to thirty minute means of velocity and vector flow component products for up to seven months with two megabytes of storage. Half-hour means of velocity and higher moments are sufficiently long to invoke stationarity for turbulent boundary layer eddies in the sea so the Reynolds decomposition can be used, further compressing the data to simple means and means to products of fluctuations. However, spectral information is lost for periods shorter than one hour. To extend the spectrum of velocity to higher frequency, two minute averages of velocity from one sensor are included with the thirty minute means.

Published in: Oceans '91, 2:973-975, 1991.

Supported by: ONR grant N00014-89-J-1058.

WHOI Contribution No. 7742.

SOUND SCATTERING BY ROUGH ELONGATED ELASTIC OBJECTS II. FLUCTUATIONS OF SCATTERED FIELD

T.K. Stanton and D. Chu

Sonar echoes from unresolved features of rough objects tend to interfere with each other. Because of these interferences, properties of the echoes such as its envelope level will vary from realization to realization of stochastically rough objects. In this article, the nature of the fluctuations of the backscattered echo envelope of rough solid elastic elongated objects is investigated. A general formulation is initially presented after which specific formulas are derived and numerically evaluated for straight finite length cylinders. The study uses both the modal-series-and Sommerfeld-Watson-transformation-based deformed cylinder solutions presented in the first part of this series (T.K. Stanton, J. Acoust. Soc. Am., submitted). The fluctuations of the backscattered echo envelope are related to the Rice probability density function (PDF) and shown to depend upon σ/a and \mathcal{L}/L in the Rayleigh scattering region $(ka \ll 1)$ and $k\sigma$ and \mathcal{L}/L in the geometric region $(ka \gg 1)$, where σ is the rms roughness, a the radius of the cylinder, \mathcal{L} the correlation length of the roughness, L the length of the cylinder, and k the acoustic wave number in the surrounding fluid. There are similarities shown between these fluctuations in the geometric region and those from rough planar interfaces. In addition, analytical expressions and numerical examples show that the fluctuation or "incoherent" component of the scattered field is random only in amplitude- its phase approaches a constant value, in phase with the mean scattered field, which

needed to be taken into account in the formulation. Finally, applications of the theory developed in this article to backscatter data involving live marine organisms (shrimp) are discussed.

Submitted to: Journal of the Acoustical Society of America.

Supported by: ONR grants N00014-89-J-1729 and N00014-90-J-1804.

WHOI Contribution No. 7743.

DETERMINATION OF GEOACOUSTIC PARAMETERS OF THE OCEAN BOTTOM - DATA REQUIREMENTS

Subramaniam D. Rajan

An important problem in ocean acoustics is the determination of the acoustic parameters of the ocean bottom sediment layers. A variety of inverse methods have been proposed in the literature for obtaining these quantities from measurements of the acoustic field in the water column using either narrowband or broadband sources. Broadly these algorithms can be classified as direct and perturbative methods. The measured pressure field or quantities derived from it are generally the input data to such inversion algorithms. Here we consider various quantities that can be used as data in perturbative methods and investigate which of these will yield accurate estimates of the unknown parameters. We do this by studying various issues like Frechet differentiability, resolution of estimates and others. This is done separately for shallow water and deep water experiments. For narrowband shallow water experiments it is shown that a full wave method which use the complex pressure field as data is nonlinear, the nonlinearity increasing with frequency and waveguide thickness. Methods which use modal eigenvalues as input data are weakly nonlinear and can successfully yield estimates with acceptable resolution if the experiment is performed over a number of frequencies. In the case of deep water experiments, the experimental configuration can be so arranged as to gate out surface reverberation and this results in making methods based on full wave inversion weakly nonlinear. Similar conclusions are arrived at for broadband experiments. In shallow water, methods based on group velocity or phase velocity dispersion data are weakly nonlinear and therefore preferable to full wave methods which are strongly nonlinear. Again in the case of a deep water broadband experiment the full wave method can be used if by suitable modifications to the experiment the surface reverberations can be gated out.

Submitted to: Journal of the Acoustical Society of America.

Supported by: ONR contract N00014-89-K-0055. WHOI Contribution No. 7744.

WAVEFORM INVERSION TO OBTAIN THE GEOACOUSTIC PROPERTIES OF SEDIMENT IN DEEP WATER

Subramaniam D. Rajan

The geoacoustic properties of ocean sediments in deep water environments are important parameters necessary to predict low frequency acoustic fields in the water column. We present a full wave method for obtaining the geoacoustic parameters from the acoustic field measured as a function of range with a CW source. By assuming horizontal stratification, the unknown geoacoustic parameters are reduced to functions of one variable i.e. depth. The problem of estimating the geoacoustic properties of the ocean floor is then cast as a parameter estimation problem in which a cost function $\phi(\mathbf{p})$, where \mathbf{p} is a vector containing the unknown parameters, is minimized. This problem is then solved using nonlinear optimization algorithm. This algorithm requires the determination of the derivative $\frac{\partial \phi}{\partial \mathbf{p}}$. For a fluid bottom model we present an efficient algorithm for obtaining these partial derivatives. We present examples of inversion carried out using noise free and noisy synthetic data. These inversions are carried out using the complex pressure field and the magnitude of the field as data. For the noise free case both approaches yield estimates close to the true value. In the case of noisy data inversions carried out using magnitude of the pressure field as data did not perform as well as inversions where the complex field is used. However, in both cases the algorithm is stable. We further study the effect of modelling errors on the estimates and show that even small errors in range and source/receiver location lead to significant errors in the estimates. The effect of modelling the sediment as a fluid on the estimation of its geoacoustic properties is studied. In the case where the sediment shear speed is much smaller than compressional wave speed, the fluid approximation has no significant effect on the estimate of the compressional wave speeds. On the other hand, if the shear speed is such that considerable conversion exists, the fluid bottom model leads to a poor estimate of the compressional wave speed. In both cases the estimates of compressional wave attenuation and density is significantly affected by the fluid approximation. Finally we apply this method to data obtained in a field experiment and obtain an estimate of the compressional wave speed in the sediment layers. This result is compared with the model obtained by iteration of forward models

Submitted to: Journal of the Acoustical Society of America.

Supported by: ONR contract N00014-89-K-0055. WHOI Contribution No. 7745.

A FAST HYDROGRAPHIC PROFILING SYSTEM

Albert M. Bradley, Alan R. Duester and Stephen P. Liberatore

The Fast Hydrographic Profiler (FHP) is a fast free-fall hydrographic profiling system developed at Woods Hole Oceanographic for large scale synoptic ocean surveys where the cost of ship station time is significant. It is capable of doing a high accuracy conductivity-temperature-depth section to 5000 meters in only 45 minutes of ship time on station. The instrument travels at approximately 5 meters per second on both descent and ascent. On ascent. it homes toward an acoustic beacon near the ship to minimize the pickup time. A unique suite of support equipment allows rapid, convenient and safe handling. A specialized radio controlled line tug and small A-frame are used to lift the FHP from the water within minutes of surfacing. The data is read out through a simple serial interface during the battering recharge interval. The on-deck turn around time is about 30 minutes which permits very close station spacing.

The entire system can be broken down for air shipment and can be operated by a team of two or three people.

Published in: Oceans '91, Honolulu, Hawaii, 3:1246-1252, 1991.

Supported by: NSF grants OCE-8310168 and OCE-8612101.

WHOI Contribution No. 7750.

SURFACE SUPPORT FOR A FREE-FALL HYDROGRAPHIC PROFILER

Albert M. Bradley, Alan R. Duester and Stephen Liberatore

High-speed, free-falling profilers present problems in recovery. Because they are streamlined for fast operation, they provide little in the way of conventional handholds to grab onto. We have developed a practical, safe, and fast method for recovering these vehicles. This method is applicable in other recovery scenarios.

Published in: Oceans '91, Honolulu, Hawaii, 3:1253-1258, 1991.

Supported by: NSF grants OCE-8310168 and OCE-8612101.

WHOI Contribution No. 7751.

DESIGN METHODS OF IMPROVING ROBOT MANIPULATOR PERFORMANCE

Nathan Ulrich and Vijay Kumar

Although industrial robot mechanisms are relatively mature, few manipulator arms are available for use outside of the factory. This paper presents several techniques of improving the performance of robot manipulators designed for use in unstructured or hazardous environments. These methods include a means of passive, mechanical, and energy-conservative gravity compensation, a remote actuation technique, and the use of tension-element transmission and speed reduction. In comparison with a conventional arm, an arm incorporating these techniques moves faster, handles a larger payload, and responds better to external forces. In addition, simulation results show that it consumes less than one-tenth the energy.

Submitted to: ASME Design Automation Conference.

Supported by: DARPA grant N00014-88-K-0630; AFOSR grants 88-244, 88-0269; Army/DAAL 03-89-C-0031PRI; NSF grant CISE/CDA 88-22719; IRI 89-06770; and Dupont Corporation.

WHOI Contribution No. 7756.

DIFFRACTION FROM THE JUNCTURE OF A PRESSURE RELEASE AND LOCALLY REACTING HALF-PLANES

Peter H. Dahl and George V. Frisk

Solutions to two coupled half-plane problems are derived. In the first, an exact solution to the canonical problem of acoustic plane wave diffraction from a pressure release (zero impedance) surface coupled to a perfectly rigid (infinite impedance) surface is given using the Wiener-Hopf method. The solution is expressed in terms of an angular spectrum of plane waves. In the second, the rigid surface is replaced by one characterized by a locally reacting finite impedance. Here an approximate kernel to the Wiener-Hopf functional equation is used which leads to a complete and readily interpretable solution. The solution is expressed in terms of the canonical angular spectrum for the first problem multiplied by a function that depends on material parameters of the locally reacting surface. Polar plots of the farfield amplitude level for the diffracted field are presented.

Published in: Journal of the Acoustical Society of America, 90:1093-1100, 1991.

Supported by: ONR contract N00014-89-K-0055. WHOI Contribution No. 7758.

ARGO/JASON: A REMOTELY OPERATED SURVEY AND SAMPLING SYSTEM FOR FULL-OCEAN DEPTH

Robert D. Ballard, Dana R. Yoerger, W. Kenneth Stewart and Andrew Bowen

The ARGO/JASON system is an integrated system that performs survey and sampling to depths of 6000 meters. This paper summarizes the capabilities of the system and includes descriptions of three vehicles: the deep-towed imaging sled ARGO, the ROV JASON, and the sidescan sonar DSL-120.

Published in: Oceans '91, Honolulu, Hawaii, 1:81-75, 1991.

Supported by: ONR contracts N00014-84-C-0070, N00014-82-C-0743, N00014-85-C-0410, N00014-86-C-0038 and N00014-90-J-1912.

WHOI Contribution No. 7762.

SEASONAL VARIATIONS OF THE SEDIMENT COMPRESSIONAL WAVE SPEED PROFILE IN THE GULF OF MEXICO

Subramaniam D. Rajan and George V. Frisk

The seasonal variation of the sediment compressional wave speed profile due to temperature variability in the water column is investigated for shallow water regions, where large temperature fluctuations can occur during the course of a year. For example, in the Gulf of Mexico, field observations indicate that the annual fluctuation of the ocean bottom temperature is approximately sinusoidal with a peak-to-trough value of about 15 degrees Centigrade. The heat flow across the water/sediment interface results in the variation of the pore water temperature with season. It is shown that the compressional wave speed varies approximately linearly with pore water temperature, an effect which is, to first order, independent of both the porosity and given sediment type. Further, the velocity ratio (ratio of sound speeds in the water and the sediment at the water/sediment interface) is shown to be independent of temperature but dependent on sediment type. The effect of variations in water column temperature on sediment compressional wave speed is demonstrated by inversions of two data sets. The data were obtained at the same location in the Gulf of Mexico but at different seasons. Finally, we study the importance of these

variations by considering their effect on a) the prediction of the pressure field in the water column and b) the errors introduced in source localization by matched-field processing.

Published in: Journal of the Acoustical Society of America, 91(1):127-135, 1992.

Supported by: ONR contract N00014-89-K-0055.

WHOI Contribution No. 7765.

THREE DIMENSIONAL RAY ACOUSTICS IN A REALISTIC OCEAN

J. F. Lynch, A. E. Newhall, C. S. Chiu and J. H. Miller

Ray theory is a well established and insightful way of describing the propagation of energy through a medium, and has been very useful in its application to underwater acoustic propagation, which is our interest here. Until recent years only two-dimensional raytracing codes, which assume that the refraction and scattering of sound out of plane by ocean features are negligibly small, existed for ocean acoustic applications. The earliest ocean acoustic raytrace codes were not only restricted to two dimensions, but were range independent as well, i.e. they considered only the vertical inhomogeneity of the water column and treated the bottom as flat. This was convenient, since the Snells law invariant and the cyclic property of the rays made raytracing and eigenray analysis fast and efficient. Moreover, the largest soundspeed gradients in the ocean are in the vertical, so that for many situations treating only the vertical inhomogeneity using range independent ray theory was adequate. As our detailed knowledge of the lateral inhomogeneity of the ocean increased, as computers became faster with larger memories, and as the demand from both the naval and oceanographic communities for more accurate propagation calculations became more intense, a second generation of "range dependent" ray codes came into being. The demands of these codes on both the computer and the user is much greater than the range independent ones. Calculationally, since the Snells law "invariant" is now range dependent, and the rays are no longer cyclic, one has to expend much more effort in tracing rays. To find eigenrays, one has to maintain elaborate ray history files so that, e.g., one interpolates rays with the same history when using "shooting" methods to find eigenrays. Moreover, one has to supply properly sampled and interpolated environmental information to the raytrace, which is perhaps more taxing to the user in terms of providing the proper environmental inputs and interpolation scheme, than it is to the computer in terms of memory or speed of

calculation. A graphic example of this can be seen in the range dependent, ray trace program MPP ("Multiple Profile Program") often used in tomographic applications^[1]. The user must specifically connect the oceanographic features (the range dependent sound velocity profiles) for the interpolator based on knowledge of the continuity or discontinuity of such features. This requires a more intelligent user, and takes raytraces away from the realm of "turnkey" operations.

In Press: Coupled Ocean Prediction and Acoustics Models, A.R. Robinson and D. Lee, eds.

Supported by: ONR contract N00014-88-K-0363. WHOI Contribution No. 7774.

ON THE DETERMINATION OF MODAL ATTENUATION COEFFICIENTS AND COMPRESSIONAL WAVE ATTENUATION PROFILES IN A RANGE DEPENDENT ENVIRONMENT IN NANTUCKET SOUND

Subramaniam D. Rajan, James F. Lynch and George V. Frisk

Techniques for determining modal attenuation coefficients and the compressional wave attenuation profile of the bottom in shallow water are presented. The input data consist of spatially well sampled measurements of the pressure field versus range due to a monochromatic point source which can be provided by either real or synthetic aperture arrays. Several methods are described for obtaining modal attenuation coefficients from the pressure field or its Hankel transform. The modal attenuation coefficients are related to the bottom attenuation profile through an integral equation which is solved using linear inverse theory. The methods are demonstrated using both noise free and noisy synthetic data. The results of inverting experimental data from Nantucket Sound at 140 Hz and 220 Hz are presented, including the resolution and variance estimates of the bottom attenuation profiles inferred. Separation of the contributions of other attenuating mechanisms which can be confused with compressional wave attenuation (shear, rough surface scattering) is also discussed.

Published in: IEEE Journal of Oceanic Engineering, 17(1):118-128, 1992.

Supported by: ONR contract N00014-89-K-0055.

WHOI Contribution No. 7782.

RECONCILIATION OF THEORIES OF SYNTHETIC APERTURE RADAR IMAGERY OF OCEAN WAVES

William J. Plant

Several theories of synthetic aperture radar (SAR) imagery of ocean waves, especially those dealing with the focusing issue, are examined. We show that the "time-dependent" theories of Lyzenga (1988) and of Kasilingham and Shemdin (1988) and the "velocity bunching" theory of Br'uning, Alpers and Shroter (1991) are identical for short integration times but may diverge on the focussing issue for long integration times. The reason for the divergence is simply that "velocity bunching" theory assumes that integration times are short compared to ocean wave periods. The inference is that for short integration times, the phase speed of the ocean wave plays a secondary role to that of orbital velocity and acceleration in determining the optimum focus setting but becomes dominant as integration times are increased. For the case of zero focus adjustment, these focus-dependent theories are shown to reduce to those of Plant and Keller (1983) and of Hasselmann, et al. (1985). Thus several of the apparently differing theories of SAR imagery of the ocean are reconciled and shown to be a single consistent theory.

Submitted to: Journal of Geophysical Research.

Supported by: ONR grant N00014-89-J-3224.

WHOI Contribution No. 7788.

A LONG-TERM EVALUATION OF NEW MOORING COMPONENTS AND UNDERWATER TELEMETRY TECHNIQUES

A. Bocconcelli, H. O. Berteaux, Daniel E. Frye and B. Prindle

An Engineering Surface Oceanographic Mooring (ESOM) program was initiated in 1989 by the Woods Hole Oceanographic Institution for the purpose of evaluating the long term, in situ performance of new moored array materials and sensors.

For logistic and practical reasons, a site 12 miles southwest of Bermuda, with a water depth of 3000 m. was selected to deploy the mooring. Following well established design practice the upper part of the mooring down to a depth of 1900 m. was made of plastic jacketed, steel armored wire ropes and cables. Groups of test samples were attached at different depths to the main mooring line. The lower part of the mooring was made of

compliant plaited nylon rope. The mooring was deployed in March 1989. It was recovered and reset, with a vertical acoustic telemetry prototype system, in April 1990. The at sea phase of the program ended in November 1990 when the termination of a test cable failed and the mooring broke loose. The entire mooring was recovered and all of its samples and components were carefully inspected and tested. In addition to the novel acoustic link, mooring components tested included new wire ropes, new electromechanical cables and their terminations, low drag fairings, fishbite resistant jackets, and a new type of surface buoy. This paper describes the experimental mooring and the results obtained after 18 months of exposure.

Published in: Proceedings of MTS '91 Conference, :848-857, 1991.

Supported by: ONR contract N00014-90-J-1719.

WHOI Contribution No. 7821.

A MULTIPLE CHARGE DEEP DEPLOYED EXPLOSIVE SOURCE FOR HIGH RESOLUTION SEISMIC REFRACTION EXPERIMENTS IN THE DEEP OCEAN

Donald E. Koelsch, G. M. Purdy, and James E. Broda

A Near Ocean Bottom Explosive Launcher (NOBEL) has been developed at the Woods Hole Oceanographic Institution that detonates forty-seven electrically fired 5 to 10 pound Pentolite charges near the ocean floor. During a fourteen day period in January 1991 aboard the R.V. Atlantis II, ten successful near bottom seismic refraction experiments were conducted. During this experiment 360 individual charges were detonated 10 meters above the ocean floor in water depths of 2500-2600 meters.

The control electronics consists of six barrel control modules (BCM). Each module controls the release and firing of eight explosive charges using a single board low power computer programmed in BASIC. Communication from the surface to NOBEL is through an armored coaxial cable. The protocol is half duplex ASCII using a 20 ma. current loop.

Because of the inherent dangers of using electrically detonated explosives, safety is a prime consideration with reliability a very close second. Particular attention has been paid to single point failures in the electronics which could cause pre-detonation. Pressure activated switches are used to connect the detonators to the circuit only after NOBEL has been lowered to a safe depth. Software and mechanical lock out systems are used to prevent detonations at critical times.

This equipment establishes a method of measuring structure velocity in the upper most crust with a resolution (using 40 to 50 Hz energy) that is not attainable any other way.

Published in: Proceedings on Ocean Cooperative MTS Conference, New Orleans, :255-258, 1991.

Supported by: NSF contract OCE-8917750.

WHOI Contribution No. 7822.

WIND EFFECTS ON THE NONLINEAR EVOLUTION OF SLOWLY VARYING GRAVITY-CAPILLARY WAVES

Tetsu Hara and Chiang C. Mei

A train of uniform two-dimensional gravity waves in deep water is known to be unstable to certain sideband disturbances. If the time of propagation is sufficiently long for the fourth order terms to be important, the sidebands may grow at unequal rates, resulting in a downward shift of peak frequency. But this shift is only a temporary phase of a recurrent evolution process. Recent work by us (Hara & Mei 1991) have shown that wind and dissipation can help maintain this downshift at large time. In this paper we examine a similar two-dimensional problem for capillary-gravity waves. The basic flow in air and water is assumed to be steady, horizontally uniform and turbulent, the wave-induced flow in both media is assumed to be laminar. Evolution equations are deduced with wind and dissipation included in such a way that their influence is comparable to the asymmetric spectral evolution. After finding the initial growth rates of unstable sidebands, the non-linear development of modulational instability is examined by integrating the evolution equations numerically. Computed results show that persistent downshift of frequency can happen for relatively long waves, but upshift for very short waves.

Submitted to: Philosophical Transactions of the Royal Society, London.

Supported by: ONR Physical Oceanography
Program under Accelerated Initiative on Surface
Wave Dynamics and NSF grant MSME 8813121.

WHOI Contribution No. 7826.

LARVAL HABITAT CHOICE IN STILL WATER AND FLUME FLOWS IN THE OPPORTUNISTIC BIVALVE MULINIA LATERALIS

Judith P. Grassle, Paul V. R. Snelgrove and Cheryl Ann Butman

Competent pediveligers of the coot clam Mulinia lateralis (Say) clearly preferred an

organically rich mud over abiotic glass beads in 24-hour flume-flow experiments, and often demonstrated the same choice in still-water experiments. We hypothesize that pediveligers with characteristic helical swimming paths above the bottom can exercise habitat choice in both still water and flow, but that the limited swimming ambits of physiologically older pediveligers require near-bottom flows to move the larvae between sediment patches so that they can exercise habitat choice. Although M. lateralis larvae are planktotrophic, their ability to delay metamorphosis in the absence of a preferred sediment cue is limited to about five days, a shorter time than the lecithotrophic larvae of the opportunistic polychaete species, Capitella spp. I and II. Field distributions of all three opportunistic species may result, at least in part, from active habitat selection for high-organic sediments by settling larvae.

Submitted to: 26th European Marine Biology Symposium.

Supported by: NSF grants OCE-8812651 and OCE-8813584, WHOI/MIT Joint Program.

WHOI Contribution No. 7834.

MAXIMUM LIKELIHOOD AND LOWER BOUNDS IN SYSTEM IDENTIFICATION WITH NON-GAUSSIAN INPUTS

Ofir Shalvi and Ehud Weinstein

We consider the problem of estimating the parameters of an unknown linear system driven by a sequence of independent identically distributed (i.i.d.) random variables whose probability density function (p.d.f.) may be non-Gaussian. We assume a general system structure that may contain causal and non-causal poles and zeros. The parameters characterizing the input p.d.f. may also be unknown. We derive an asymptotic expression for the Cramer-Rao lower bound (CRLB) under the assumption that the number of data samples observed at the system output is large compared with the total number of unknown parameters, and show that it is the highest (worst) in the Gaussian case, indicating that the estimation accuracy can only be improved when the input p.d.f. is non-Gaussian. We further show that the asymptotic error variance in estimating the system parameters is unaffected by lack of knowledge of the p.d.f. parameters, and vice versa. We develop a computationally efficient scheme for finding the Maximum Likelihood (ML) estimate of the unknown system and p.d.f. parameters, and indicate the relation to the blind deconvolution/equalization problem.

Submitted to: IEEE Transactions on Information Theory.

Supported by: Office of Naval Research grant N00014-90-J-1109.

WHOI Contribution No. 7839.

NON-SELECTIVE SETTLEMENT OF MERCENARIA MERCENARIA (LINNÉ) LARVAE IN SHORT-TERM, STILL-WATER, LABORATORY EXPERIMENTS

Guy Bachelet, Cheryl Ann Butman, Christine M. Webb, Victoria R. Starczak, and Paul V. R. Snelgrove

Sediment selection by settling larvae of the hard clam Mercenaria mercenaria (Linné) was determined in 4-h, still-water, laboratory experiments where larvae were given a choice between two highly contrasting sediment treatments: a natural, organic-rich mud, and an abiotic, glass-bead mixture with a grain-size distribution similar to the mud. The experiments were designed to evaluate the effects of intrinsic (larval age) and extrinsic (sea water temperature) factors on sediment selectivity. These specific effects were tested because results of initial experiments designed to replicate those of Butman et al., where M. mercenaria larvae had selected beads over mud in still water but not in flow, showed no significant selection. In the present study, only five of the 23 experiments conducted showed significant selection and, in all cases, for mud over beads. Larval age and water temperature had no significant effect on the outcome. In the earliest of these experiments we discovered a problem with larval preservation in mud samples (dissolution of the larval shell due to low pH) that may have resulted in underestimates of the number of larvae settled in mud in Butman et al., thus confounding interpretation of those results. The conclusions of Butman et al. are therefore modified based on results of the experiments presented here: settling M. mercenaria larvae do not select between two extreme sediment treatments in 4-h, still-water, laboratory experiments. In addition, competency tests used here failed to establish a consistent, predictable, precipitous rise in competency for a given batch of M. mercenaria larvae. This may be due to natural, large variation in physiological development within a given larval pool such that a small proportion of competent larvae are available each day over an extended period. Furthermore, the between-experiment variability in selectivity and some results of the competency tests suggest that the duration of these experiments may be too short to document definitive, initial larval settlement. Occasional selection would then reflect continual redistribution of larvae prior to final settlement and metamorphosis.

In Press: Journal of Experimental Marine Biology and Ecology.

Supported by: Minerals Management Service contract 14-12-0001-30262; NSF grants OCE-85000875 and OCE-8812651, NATO Fellowship; support from French Centre National de la Recherche Scientifique (CNRS); and WHOI.

WHOI Contribution No. 7842.

STATUS OF KRILL TARGET STRENGTH

Kenneth G. Foote, Dezhang Chu, and Timothy K. Stanton

Empirical estimates for the target strength of krill are extracted from the literature. These are confined to measurements on aggregations of live euphausiids, which should avoid a frequent cause of bias in single- animal measurements, namely thresholding. Theoretical estimates for the target strength are derived from the deformed-cylinder scattering model assuming specific sets of physical and orientational parameters, for which there is an empirical basis. The theoretical estimates show a non- monotonic dependence of target strength on both animal size and transmit frequency, notwithstanding admitted shortcomings. Some recent single- animal measurements of target strength for live euphausiids and euphausiidrelated specimens, made under high signal-to-noise-ratio conditions, are consistent with the general pattern. Several specific recommendations are made for future, improved determinations of krill target strength. Based on the comparisons, general prediction curves for the target strength are presented that are applicable to a wide range of lengths, acoustic frequencies, and orientation parameters.

Submitted to: Journal of the International Council of the Exploration of the Sea.

Supported by: Office of Naval Research grant N00014-89-J-1720 and Naval Underwater Systems Center contract N66604-91-C-5401.

WHOI Contribution No. 7890.

UNDERWATER ACOUSTIC LOCAL AREA NETWORK FOR ROV AND INSTRUMENT COMMUNICATIONS

Josko Catipovic, Lee Freitag and Steven Merriam

An underwater Acoustic Local Area Network (ALAN) for real-time data communications with

ocean-bottom oceanographic instruments and underwater vehicles is presented. The network is centered around one or several central moorings which function as node controllers for the underwater communications network. Each node can communicate with numerous underwater modems. It is equipped with an acoustic cellular communications controller and a satellite, packet RF or commercial cellular telephone for above-surface communications. The underwater acoustic modems are low-power acoustic transceivers with network and communication capabilities similar to RF cellular telephones. They are interfacable to underwater vehicles or instrumentation packages. The ALAN allows real-time two-way communications with a control of underwater devices within a 5-10 km range of at least one surface station. Power budgets allow 1 year deployments.

The system has undergone a 6 month deep-water deployment near Bermuda and has been tested in Monterey Canyon, CA. This paper presents system design details, including the acoustic telemetry protocols, electromechanical implementations of various subsystems, maintenance/deployment methods, and performance results from previous and current deployments. Current and future system application and research/development issues are summarized.

Published in: Proceedings of the AUVS Conference, Washington, DC, 1991.

Supported by: Mellon Foundation under WHOI project.

WHOI Contribution No. 7899.

ACOUSTIC WAVE SCATTERING FROM AN OBJECT IN A SHALLOW WATER WAVEGUIDE-A GENERAL FORMULATION

Dajun Tang and George V. Frisk

A general theoretical formalism for acoustic wave scattering from an object with arbitrary shape in a range-independent waveguide is developed. The formulation is expressed in terms of normal mode scattering coefficients, i.e., the coupling coefficients between a given incident mode and scattered modes associated with the incident mode. Thus the acoustic energy conversion between normal modes due to scattering is explicitly included. Since at long ranges from the scatterer only a few propagating modes exist, therefore by determining those complex modal amplitudes, the total field can be easily calculated through linear superposition of the propagating modes. Finally, the conservation of energy flux in this system is demonstrated.

Submitted to: Journal of the Acoustical Society of America.

Supported by: ONR contract N00014-86-C-0038.

WHOI Contribution No. 7900.

A TELEMETRY THEORY FOR OCEAN ACOUSTIC TOMOGRAPHY: REAL TIME MONITORING

John L. Spiesberger and James B. Bowlin

A new telemetry theory is described which will make it possible to monitor ocean temperatures in real time using acoustic tomography. The system incorporates autonomous sources mounted on subsurface moorings and receivers that are either cabled to shore or suspended from surface units which drift. The telemetry theory predicts that the corruption of acoustic travel times, due to wander of the source's mooring, can be largely eliminated in real time by shifting the start times of the tomographic transmissions in special ways. Corrections to source wander can be obtained without expending battery energy over and above that used in conventional tomography experiments. Standard techniques can be used to correct clock errors at the source in real time.

Submitted to: Journal of Atmospheric and Oceanic Technology.

Supported by: ONT contract N00014-90-C-0098. WHOI Contribution No. 7901.

SPECTRAL PARAMETERIZATION OF SCATTERING FROM A RANDOM BOTTOM

Dajun Tang and George V. Frisk

This paper concerns the development of a concept in bottom scattering theory, in which a key ingredient is the introduction of a set of parameters, called the Scattering Correlation Coefficient (SCC), to characterize low frequency sound scattering from random ocean bottoms. The conventional parameter used to characterize bottom scattering is the scattering cross section, which is not suitable either when scattering from small grazing angles is concerned or when sub-bottom structures take part in the scattering process, which is often the case for low frequency sound scattering problems. In this paper the SCC is defined in the wavenumber domain, so it does not have the ambiguity that the scattering cross section has.

Submitted to: Journal of the Acoustical Society of America.

Supported by: ONR contract N00014-86-C-0038.

WHOI Contribution No. 7920.

DETERMINATION OF COMPRESSIONAL WAVE AND SHEAR WAVE SPEED PROFILES IN SEA ICE BY CROSSHOLE TOMOGRAPHY – THEORY AND EXPERIMENT

Subramaniam D. Rajan, George V. Frisk, James A. Doutt, and Cynthia J. Sellers

Acoustic propagation in the Arctic ocean is strongly influenced by the ice cover. Sea ice is a heterogeneous material whose acoustic properties are functions of time and space. Field data of the acoustic properties such as the wave speeds and their attenuations are sparse. Because of this, sea ice has been modelled either as a pressure release surface or as a rigid reflector. Here we present the results of a crosshole tomography experiment conducted in multi-year ice with the objective of determining the spatial structure of the compressional wave speeds from travel time measurements made with high frequency pulses. The results of the experiment indicate that the compressional wave speed can be obtained from such a crosshole experiment with good resolution. The source used in the experiment generated both compressional and shear waves in the ice and shear (SV) arrivals were observed in the data allowing estimates of shear wave speeds to be obtained. The compressional and shear wave speed contour maps indicate that the spatial variations of the wave speeds are complex with regions of low speed. High brine volume is a likely cause for the low speed observed in the material. The occurrence of regions with salinity values as high as ten parts per thousand has been observed in multi-year ice by other investigators as well. Resolution and variance studies performed on the estimates are also presented. We also present estimates of material properties such as Poisson's ratio, salinity, elastic and shear moduli obtained from the estimates of compressional and shear wave speeds.

By measuring the amplitude of the transmitted and received signals along specific paths, estimates of the attenuation coefficients at different depth intervals were obtained. Spatial variability observed in the estimates is believed to be due to scattering by inhomogeneities in the material.

Submitted to: Journal of Geophysical Research.

Supported by: ONR grant N00014-90-J-1517.

WHOI Contribution No. 7921.

DEPARTMENT OF BIOLOGY
Peter H. Wiebe, Chairman

SEPARATION OF CODING SEQUENCES FROM STRUCTURAL DNA IN THE DINOFLAGELLATE CRYPTHECODINIUM COHNII

D. M. Anderson, A. Grabher, and M. Herzog

Mild restriction endonuclease digestion of intact nuclei isolated from the dinoflagellate Crypthecodinium cohnii released low molecular weight fragments of DNA, but left considerable quantities of high molecular weight DNA uncut. Epifluorescent microscope examination of DAPI-stained nuclei before and after the digestions showed that the chromosomes and nucleii remained intact throughout the incubations. Digestions of extracted, purified genomic DNA produced predominantly low molecular weight fragments. Southern blots of the two types of digestions (isolated nuclei, purified genomic DNA) were screened with 3 different cloned DNA probes: 1) heterologous dinoflagellate ribosomal DNA; 2) a single C. cohnii cDNA; and 3) a total C. cohnii cDNA library. The first two single gene probes hybridized mainly to distinct fragments of low molecular weight material cleaved from the isolated nuclei with relatively little labelling of the larger fragments of uncut DNA, despite its high abundance. The same distinct low molecular weight bands were observed in blots of the purified genomic DNA. As expected, when the entire cDNA library was used as a probe of the two types of digestions, the hybridization signal was a broad smear including both low and high molecular weight DNA, with several dense bands visible as well. Taken together, data from all three probes support the view that the main body of the dinoflagellate chromosome is bulk or "silent" DNA that is genetically inactive, whereas actively transcribed coding sequences are accessible to mild restriction nuclease digestion due to their location at the periphery of the chromosome, presumably on protruding filaments. The functional roles of these two classes of chromatin may thus be determined in part by their spatial organization. The differential accessibility to restriction enzymes makes it possible to design a cloning strategy that is optimized by dinoflagellate coding sequences.

In Press: Molecular Marine Biology and Biotechnology.

Supported by: NSF Grants OCE89-15043; and OCE89-11226.

WHOI Contribution No. 7710.

PARALYTIC SHELLFISH POISONING ON GEORGES BANK: IN SITU GROWTH OR ADVECTION OF ESTABLISHED DINOFLAGELLATE POPULATIONS?

Donald M. Anderson and Bruce A. Keafer

Evidence is presented that the alongshore progression of paralytic shellfish poisoning (PSP) in the southern Gulf of Maine in 1990 was due to the southward movement of a buoyant plume of lower salinity water and its associated population of the dinoflagellate Alexandrium tamarense, originating in the Androscoggin and Kennebec River outflow. The movement of this plume into and across Massachusetts Bay is documented by hydrographic cruise transects and by moored observations of salinity and temperature. These data are consistent with the hypothesized link between shellfish PSP toxicity in offshore waters of Georges Bank and the long distance transport of the buoyant plume. These results also suggest a pathway by which human contaminants in riverine flows can travel across large distances to impact the rich offshore fisheries of the Gulf of Maine.

Supported by: NOAA; Office of Sea Grant Award NA90-AA-D-SG480, R/B-100; and ONR Grant N00014-89-J-1111.

WHOI Contribution No. 7642.

LACUNAL ALLOCATION AND GAS TRANSPORT CAPACITY IN THE SALT MARSH GRASS, SPARTINA ALTERNIFLORA

Andrea L. Arenovski and Brian L. Howes

Lacunal allocation as the fraction of the total cross sectional area of leaves, stem bases, rhizomes, and roots was determined in both tall and short growth forms of *Spartina alterniflora* collected from natural monospecific stands. The results indicate that in both growth forms lacunal allocation is greater in stem bases and rhizomes than in leaves and roots and that tall form plants allocate more of their stem and rhizome to lacunae than short form plants.

Measurements made in natural stands of Spartina alterniflora suggest that total lacunal area of the stem base increases with increasing stem diameter and that stem diameter increases with increasing plant height and above-ground biomass. However, the fraction of cross section allocated to lacunae was relatively constant and increased only with the formation of a central lacuna.

Experimental manipulations of surface and subsurface water exchange were carried out to test the influence of flooding regime on aerenchyma

formation. No significant differences in lacunal allocation were detected between plants grown in flooded (reduced) and drained (oxidized) sediments in either laboratory or field experiments. While aerenchyma formation in Spartina alterniflora may be an adaptation to soil waterlogging/anoxia, our results suggest that lacunal formation is maximized as a normal part of development with allocation constrained structurally by the size of plants in highly organic New England and Mid-Atlantic marshes.

The cross sectional area of aerenchyma for gas transport was found to be related to the growth of Spartina alterniflora, with stands of short form Spartina alterniflora exhibiting a lower specific gas transport capacity (lacunal area per unit below ground biomass) than tall form plants despite having a similar below-ground biomass supported by a 10 fold higher culm density. The increased specific gas transport capacity in tall vs. short plants may provide a new mechanism to explain the better aeration, higher nutrient uptake rates and lower frequency of anaerobic respiration in roots of tall vs. short Spartina alterniflora.

In Press: Oecologia.

Supported by: NSF Grants BSR87-17701; and BSR85-07356.

WHOI Contribution No. 7755.

HETEROTROPHIC FLAGELLATES OF PLANKTONIC COMMUNITIES THEIR CHARACTERISTICS AND METHODS OF STUDY

U.-G. Berninger, D. A. Caron, R. W. Sanders and B. J. Finlay

Heterotrophic flagellates are an integral and important component of the plankton communities of aquatic ecosystems. Abundances of heterotrophic flagellates in most natural plankton assemblages range from 10² - 10⁵ cells per ml. Recent advances in the methods to count flagellates and examine their trophic activities have established that they are significant consumers of bacterial, cyanobacterial and microalgal biomass in these environments. Their grazing activities are the primary factor controlling bacterial densities. Flagellate herbivory can significantly affect the abundances of photosynthetic prokaryotes and eukaryotes. Collectively, the trophic behavior of these protozoa dictates the fate of a substantial portion of primary and secondary productivity in planktonic ecosystems.

Published in: Biology of Free-living Heterotrophic Flagellates. D. J. Patterson and J. Larsen, eds. Clarendon Press, Oxford, :39-56, 1991. Supported by: NSF Grants BSR89-19447, OCE89-01005; and the German Academic Exchange Service.

WHOI Contribution No. 7766.

GRAZING AND UTILIZATION OF CHROOCOCCOID CYANOBACTERIA AND HETEROTROPHIC BACTERIA BY PROTOZOA IN LABORATORY CULTURES AND A COASTAL PLANKTON COMMUNITY

David A. Caron, Ee Lin Lim, Geraldine Miceli, John B. Waterbury and Frederica W. Valois

Field and laboratory experiments were conducted to compare the rates of ingestion of planktonic protozoa for chroococcoid cyanobacteria and heterotrophic bacteria, and the fate of this ingested biomass. Laboratory experiments tested the ability of cyanobacteria and bacteria to support the growth of three species of bacterivorous protozoa. Two species of heterotrophic bacteria supported faster growth rates and higher cell yields of the protozoa than three strains of cyanobacteria. When mixtures of bacteria and cyanobacteria were offered, however, all protozoa grew as rapidly as when bacteria were offered alone. One protozoan showed a marked feeding selectivity against one strain of cyanobacteria when offered mixtures of bacteria and cyanobacteria. Grazing rate measurements performed in Vineyard Sound, Massachusetts, revealed removal rates as high as 54% of the cyanobacterial assemblage d-1 and 75% of the heterotrophic bacterial assemblage d⁻¹ Nanoplanktonic protists (organisms $<20 \mu m$) were the major consumers of both cyanobacterial and bacterial biomass in this environment on five sampling dates. Based on measurements of the ingestion rates of nanoplanktonic consumers and the carbon content of cyanobacteria and heterotrophic bacteria, we conclude that cyanobacterial biomass in this coastal environment at times reaches 30% of the total prokaryote biomass consumed by the nanoplankton. During times of peak abundance of chroococcoid cyanobacteria, this biomass is an important source of organic carbon for planktonic protozoa feeding on bacteria-sized particles.

Published in: Marine Ecology Progress Series, 76:205-217, 1991.

Supported by: NSF Grants OCE86-00510, OCE89-01005, and BSR86-07386; WHOI Education Program; Five Colleges Coastal Marine Science Program; Smith C. Dana Internship Grant; and Schumann Foundation.

WHOI Contribution No. 7705.

PLANKTONIC PROTOZOA AND THE MICROBIAL FOOD WEB: NEW AWARENESS AND PERSPECTIVE FOR ZOOPLANKTON RESEARCH

David A. Caron, Robert W. Sanders and Diane K. Stoecker

The realization that protozoa play an important, and perhaps pivotal role in the energetics of plankton communities is predicted on data amassed over the last few decades which indicate that heterotrophic and phototrophic picoplankton (predominantly bacteria and cyanobacteria in the size range $0.2 - 2.0 \mu m$) constitute a very significant fraction of the total energy flowing through freshwater and saltwater ecosystems. As the primary consumers of much (and probably most) of this biomass, protozoa are a vital trophic link between small primary and secondary producers and higher organisms, and, in partnership with the bacteria, carry out much of the remineralization in aquatic environments. This chapter presents a brief synopsis of the status of protozoan ecology in modern zooplankton research. and perspectives for future work on this taxon.

Supported by: ONR Grant N00014-89-J-1075; and NSF Grant OCE89-01005.

WHOI Contribution No. 7957.

LOCAL AND REGIONAL REGULATION OF SPECIES-AREA RELATIONS: A PATCH-OCCUPANCY MODEL

Hal Caswell and Joel E. Cohen

A simple patch-occupancy model leads to quite realistic-looking log-log species-area curves at small sample sizes, eventually becoming asymptotic to the regional species pool as the sample becomes large enough to include all the species. In communities without competition, the slope of the species-area curve is an increasing function of the ratio of the disturbance rate to the colonization rate. The intercept is a decreasing function of this same ratio. In the absence of competition, local diversity is directly proportional to the regional species pool.

When competitive saturation is added to the model, local diversity is independent of the regional species pool, provided that the disturbance rate is sufficiently low. Even in the presence of strong competitive saturation, extremely low rates of disturbance can obscure the effects of competition. Thus empirical studies describing local diversity as a function of the regional species pool must be interpreted with aution, because the absence of competition has effects that are indistinguishable

from strong competitive saturation in the presence of modest levels of disturbance.

In Press: Ecological Diversity, R. E. Ricklefs and D. Schluter, eds.

Supported by: NSF Grants OCE85-16177, BSR87-04936 and BSR87-05047; and John Simon Guggenheim Foundation.

WHOI Contribution No. 7641.

SEQUENCE AND CHEMICAL STRUCTURE OF THE HEXAPEPTIDE CHROMOPHORE OF THE AEQUOREA GREEN-FLUORESCENT PROTEIN

Chris W. Cody, Douglas C. Prasher, William M. Westler, Franklyn G. Prendergast and William W. Ward

The green-fluorescent proteins (GFP) are a unique class of proteins involved in bioluminescence of many cnidaria. The GFPs serve as energy-transfer acceptors, receiving energy from either a luciferase-oxyluciferin complex or a Ca²+-activated photoprotein, depending on the organism. Upon mechanical stimulation of the organism, GFP emits green light spectrally identical to its fluorescence emission. These highly fluorescent proteins are unique due to the nature of the covalently attached chromophore, which is composed of modified amino acid residues within the polypeptide. This report describes the characterization of the Aequorea victoria GFP chromophore which is released as a hexapeptide upon digestion of the protein with papain. The chromophore is formed upon cyclization of the residues Ser-dehydroTyr-Gly with the polypeptide. The chromophore structure proposed here differs from that described by Shimomura (FEBS Letters 104:220, 1979) in a number of ways.

Supported by: WHOI; and American Cancer Society Grant NP-640.

WHOI Contribution No. 7945.

CHARACTERIZATION AND SITE DESCRIPTION OF SOLEMYA BOREALIS, A NEWLY DISCOVERED ANIMAL-BACTERIA SYMBIOSIS

Noellette Conway, Brian Howes, Judith McDowell Capuzzo, Ruth Turner and Colleen Cavanaugh

Solemya borealis was collected from reducing sediments in Buzzards Bay, Cape Cod, Massachusetts and examined for the presence of symbiotic, chemoautotrophic bacteria. In addition, sediment cores collected at the same site were

analyzed to provide a detailed description of the S. borealis habitat. Here we present microscopic enzymatic biochemical, and stable isotope data which suggests that S. borealis, like the related species Solemya velum (Say) and Solemya reidi (Bernard), contains high concentrations of symbiotic chemoautotrophic bacteria in gill bacteriocytes which play a significant role in nutrition. Transmission electron microscopy revealed the presence of rod-shaped cells which resemble Gram-negative bacteria within gill epithelial cells. Ribulose-1,5-biohosphate carboxylase activity in cell-free extracts of S. borealis gill tissue was comparable with that found in other animal-bacteria symbioses. Very negative δ^{34} S ratios (-32.6°/ $_{\infty}$ to -15.7°/ $_{\infty}$) suggest the utilization of porewater sulfides as a sulfur source, and possibly an energy source, for the symbionts. Carbon and nitrogen stable isotope ratios were extremely negative $(\delta^{13}C = -32^{\circ}/_{\infty} \text{ to } -34.6^{\circ}/_{\infty})$ $\delta^{15}N = -9.7^{\circ}/_{\infty}$ to $-8.6^{\circ}/_{\infty}$) similar to those of other bivalve-chemoautotroph symbioses. High concentrations of cis-vaccenic acid, a fatty acid previously found in other invertebrate-chemoautotroph symbioses, were found in all the major lipid classes of the gills of S. borealis. The stable isotope ratios and lipid composition of S. borealis suggest that most of this animal's nutritional requirements are supplied by the bacterial endosymbionts. High levels of taurine in the free amino acid pool of S. borealis suggest the existence of unusual amino acid metabolic pathways which may be the result of endosymbiont activity. The S. borealis specimens were found in relatively shallow water sediments dominated by silts and clays. The sediments contain high concentrations of organic carbon and nitrogen, exhibit limited oxygen penetration, and have high rates of ammonium and sulfide input from the anaerobic microbial community.

In Press: Marine Biology.

Supported by: WHOI Ocean Ventures Fund; Camp, Dresser, McKee; and NSF Grants BSR87-17701 and DCB87-18799.

WHOI Contribution No. 7687.

EFFECTS OF CONSTANT AND INTERMITTENT FOOD SUPPLY ON LIFE HISTORY PARAMETERS IN A MARINE COPEPOD

Cabell S. Davis and Philip Alatalo

A laboratory experimental study was conducted to determine the effects of long and short- term food limitation on birth, growth, and death rates in *Centropages typicus* (Copepoda, Calanoida), a species previously reported to be

sensitive to a patch food resource. Life history parameters were measured in cohorts over their entire life span at a range of constant food treatments (0.2-7 μ g Chl a/1) and at two pulsed treatments providing low and high food (0.5-2.0 μ g Chl a/1) at periods of ~ 0.5 and 1.0 d. A flow-through culture system minimized biochemical and grazing-induced changes in food supply and allowed precise control and automated measurement of food levels. Results show that C. typicus can integrate daily fluctuations in food supply at amplitudes comparable to observed field patchiness levels ($\pm 50\%$). Furthermore, this suggests that laboratory experiments on food limitation in zooplankton, nearly all of which are done using batch cultures, are likely to yield accurate results if food levels are maintained daily to within 50% of the mean; the latter may be difficult without a flow through system, however, since grazing alone can cause order-of-magnitude changes in food levels over 1 d.

Growth in length and width of C. typicus was exponential and thus did not conform to current growth rules for copepods. Age-specific fecundity varied with food level but was relatively constant throughout adult life, yielding a high maximum total fecundity. Grazing and carnivory experiments revealed that both nauplii and adults of C. typicus can ingest very large prey (30-80% of their body length), but carnivory did not add significantly to the diet. Comparison of critical food concentrations with cross-shelf gradients in chlorophyll a on Georges Bank suggests that the largely neritic C. typicus is severely food-limited off the shelf and is nearly always food satiated in the center of the bank. Field production rates calculated for C. typicus based on the experimental results indicate that this species is a major contributor to total fall copepod production on the shelf.

Supported by: NSF Grant OCE87-00562.

WHOI Contribution No. 7754.

MICROPATCHINESS, TURBULENCE, AND RECRUITMENT IN PLANKTON

Cabell S. Davis, Glenn R. Flierl, P. H. Wiebe and P. J. S. Franks

A series of theoretical models are presented which examine the relative importance of microscale patchiness and turbulence to growth and recruitment in planktonic consumers. The analyses apply over scales from centimeters to meters (e.g. from copepods to fish larvae), and we assume food-limited conditions, since, otherwise, patchiness would not affect growth. A model of individual growth response to fluctuating food is

developed which shows that growth is approximately exponential and is linearly related to food concentration. A random walk model reveals that the swimming process can be approximated as a simple diffusion term which, when included in the exponential growth model, leads to accumulation of consumers in high growth (= prey) areas. This diffusive migration of consumers up the prey gradient is rapid; for example, half-maximum growth is reached in <2 hours for fish larvae swimming in a 10 m wavelength patch of copepod nauplii. Enhancement of the net growth by this process is substantial; larval fish growth rates increase by 25% when 10 m prey patches appear at 5 hour intervals and by >100% for steady patches. Physical turbulence, at intermediate levels, causes patch dissipation and reduced growth, whereas, at higher levels, it causes growth to be restored to original, low-turbulence values due to increased encounter velocities. Variations in population growth rate due to turbulence and micropatchiness, even when small (<10%), can cause large fluctuations in recruitment by affecting duration of pre-recruit life.

Published in: Journal of Marine Research, 49(1):109-151, 1991.

Supported by: NSF Grant OCE87-00562; and ONR Grant N00014-89-J-1358.

WHOI Contribution No. 7613.

THE VIDEO PLANKTON RECORDER (VPR): DESIGN AND INITIAL RESULTS

C. S. Davis, S. M. Gallager, M. S. Berman, L. R. Haury and J. R. Strickler

A Video Plankton Recorder (VPR) is being developed to quantify abundance of plankton on scales from microns to kilometers and identify them to a major taxa (eg., copepods, chaetognaths) in near real-time at towing speeds of 0.5-5.0 m/s. The VPR consists of three primary components: a video camera/strobe unit, a plankton recorder box, and an image processing system. Four video cameras are synchronized at 60 fields/s to a red strobe light positioned 1 m away. The field of view of each camera is adjustable between 0.5-10 cm (10-300 μ m resolution, respectively) with corresponding depths of field of 4.0-20 cm ($\pm 3\%$). Imaged volumes are concentric with their center located 0.5 m between cameras and strobe. The long working distance together with the red strobe filter are used to minimize avoidance problems. Each strobe pulse is about lus allowing clear stop-action pictures of plankton and seston. For calibration, a Longhurst-Hardy Plankton Recorder-type box is placed immediately

behind the imaged volume to collect organisms on gauze for comparison with video images. Plankton abundance is calculated from the video by counting number per field and dividing by the field volume. Outlines of video images are determined in real time by an image processor and transferred to a host computer where morphometric indices are computed and organisms are sorted to major taxa using discriminant analysis. Images from initial dockside tests reveal details of external and internal morphology of plankton not previously observed in situ.

Supported by: NSF Grant OCE90-12657.

WHOI Contribution No. 7781.

MICROAGGREGATIONS OF OCEANIC ZOOPLANKTON OBSERVED BY TOWED VIDEO MICROSCOPY

Cabell S. Davis, Scott M. Gallager, and Andrew R. Solow

Laboratory and modeling studies have suggested that oceanic plankton are distributed in micropatches (millimeters to a few meters) which enhance predator-prey encounter rates thus impacting population and ecosystem dynamics. Field data on these small scales has been difficult to obtain, however, due to technological limitations. Towed video microscopy was used to unobtrusively determine distributions of oceanic plankton over a continuum of scales from microns to kilometers. Spatial variance spectra based on individual taxa revealed patchiness at scales less than 1.0 meter. Observations were made of delicate forms including gelatinous species (Doliolum sp. with buds), marine snow, copepods with egg clusters (Pseudocalanus sp.), marine sarcodines (Acantharia sp.), cyanobacterium colonies (Trichodesminum sp)., and dinoflagellates (Ceratium sp.). Observable features of individuals included body size and vertical orientation, external parasites, and internal structures such as egg masses and gut size. The video observations provide new insights into basic plankton ecology by allowing for quantitative assessment of individual plankton in their natural undisturbed state.

Supported by: NSF Grant OCE90-12657.

WHOI Contribution No. 7928.

AQUATIC ECOSYSTEMS: HIGH PRESSURE HABITATS

Edward F. DeLong

Though the biosphere comprises only a small fraction of the earth's total volume, it encompasses

numerous diverse habitats. As a consequence of natural selection, organisms have specifically adapted to variable conditions of temperature, pH, nutrient availability, or osmolarity found in these environments. Arid deserts, acidic streams, freezing polar regions, boiling hot springs, oligotrophic seas and hypersaline lakes each contain their own unique biota. Procaryotes, due to their phylogenetic depth and physiological diversity, grow and survive in all of these diverse, and seemingly harsh, habitats. Sometimes they are the sole inhabitants.

Elevated hydrostatic pressure is a unique and conspicuous feature of deep-earth and deep-sea environments. Pressure exerts profound effects on phase equilibria, chemical equilibria, and chemical kinetics, and therefore also has a marked influence on biological processes. Pressure, in conjunction with temperature, largely defines the physical conditions which allow microbial growth and survival. The unique properties of microorganisms that have evolved in high-pressure habitats reflect their specific adaptations to the physical variable of pressure.

Supported by: ONR Grant N00014-90-J-1917. WHOI Contribution No. 7661.

EXPLORING MARINE MICROBIAL DIVERSITY VIA MOLECULAR PHYLOGENETIC ANALYSIS

Edward F. DeLong

Biological diversity in metazoan taxa is characteristically morphological, distributional or behavioral in nature. In contrast, microbial diversity is found at more fundamental levels: physiological, biochemical or genetic variability typify protistan and procaryotic biodiversity. Morphological criteria traditionally used for identifying some protists do not present a complete picture of their evolutionary diversity. Additionally, many microbial species which resist cultivation cannot be readily characterized using standard physiological or biochemical criteria. Newly emerging molecular phylogenetic techniques provide a more direct and applicable approach for documenting naturally-occurring genetic diversity in microbial populations. We are currently using these techniques to explore biological diversity in aggregate-associated marine microbial assemblages. These studies are providing new insights into the nature of marine microbial consortia, including the discovery of novel eubacterial and archaebacterial lineages.

Supported by: ONR Grant N00014-90-J-1917. WHOI Contribution No. 7855.

NOVEL ARCHAEA IN COASTAL MARINE BACTERIOPLANKTON

Edward F. DeLong

Novel Archaea were detected in spatially and temporally distinct bacterioplankton populations of North America. Two groups, different from any other known Archaea, were identified. The unsuspected presence of these Archaea in oxic marine surface waters suggests they may represent new physiological types, which reside and compete with their eubacterial picoplankton counterparts.

Supported by: ONR Grant N00014-90-J-1917. WHOI Contribution No. 7904.

ARRANGEMENT AND EXTERNAL MORPHOLOGY OF SENSILLA ON THE DORSAL SURFACE OF THREE GENERA OF HYPERIID AMPHIPODS PHRONIMA, LYCAEA, AND VIBILIA

Carol E. Diebel

Phronima, Lycaea, and Vibilia are three different genera of hyperiid amphipods that differ greatly in external morphology, ecology and possibly phyletic history. These three genera have four distinct morphological types of sensilla arranged in bilaterally symmetrical, serially homologous sets on successive body segments of these three genera. Vibilia has all four morphological types and the greatest density of sensilla. Phronima has two morphological types but the fewest number of sensilla. Lycaea has only one hair type that is distributed on every segment. One sensilla type ("fluted hair" on Vibilia) has not been previously reported. The probable functions of these sensory hairs is discussed in relation to other crustacean sensilla. This information is relevant to the behavior, ecology, systematics and evolution of hyperiid amphipods.

In Press: Journal of Crustacean Biology.

Supported by: WHOI Education Department, Lerner Gray Fund - American Museum of National History.

WHOI Contribution No. 7778.

ASPECTS OF IRON AND NITROGEN NUTRITION IN THE RED TIDE DINOFLAGELLATE GYMNODINIUM SANGUINEUM. I. EFFECTS OF IRON DEPLETION AND NITROGEN SOURCE ON BIOCHEMICAL COMPOSITION

G. J. Doucette and P. J. Harrison

Iron-stress-mediated effects on biochemical constituents of the red tide dinoflagellate Gymnodinium sanguineum Hirasaka were examined in 1988 by comparing Fe-replete and Fe-deplete batch cultures. The influence of nitrogen source (NO₃ or NH₄) on characteristics of Fe-deplete cells was also studied [i.e., Fe-deplete/NO₃-grown (=-Fe/NO₃) vs. Fe-deplete/NH₄-grown (=-Fe/NH₄)]. Common to both N sources were reductions of chlorophyll a and Fe quotas (per cell volume) by 75% and ca. 1.5 orders of magnitude, respectively, under Fe depletion. The Fe requirement of G. sanguineum exceeded those of certain neritic diatoms by one to two orders of magnitude. - Fe/NH₄ cells exhibited 30 to 50% greater N quotas and free amino acid:protein ratios than Fe-deplete cells grown on NO₃. In vivo fluorescence/chl a increased with Fe deficiency particularly in -Fe/NO₃ cultures, surpassing -Fe/NH₄ values by ca. two-fold. Effects of Fe depletion were consistent with this element's essential role in the biosynthesis of chl a and components of the photosynthetic electron transport (PET) system, and also in NO₃ utilization. Fe:N ratios were larger (1.5-fold) for iron-deficient NO3- grown than NH4-grown cells, likely reflecting the Fe content of NO₃ assimilatory enzymes [nitrate (NR) and nitrite (NiR) reductase] and of electron transport components needed to provide reductant, coupled with a diminished capacity of -Fe/NO₃ cells to acquire and assimilate nitrogen. Indicators of PET efficiency suggested that under iron stress, supply of Fe for NR and NiR is partly at the expense of iron-containing PET components. Utilization of nitrate by NO₃-grown cells was inhibited sufficiently by Fe depletion to yield symptoms bordering on N deficiency. In an ecological context, the most important effect mediated by nitrogen source may be the determination of critical Q_{Fe} (i.e., Fe required to just sustain maximal growth), thereby regulating the degree of growth limitation for a given subsaturating iron concentration.

Published in: Marine Biology, 110:165-173, 1991.

Supported by: Florence and John Schumann Foundation.

WHOI Contribution No. 7638.

ASPECTS OF IRON AND NITROGEN NUTRITION IN THE RED TIDE DINOFLAGELLATE GYMNODINIUM SANGUINEUM. II. EFFECTS OF IRON DEPLETION AND NITROGEN SOURCE ON IRON AND NITROGEN UPTAKE

G. J. Doucette and P. J. Harrison

Iron and nitrogen (NO₃ and NH₄) uptake by the red tide dinoflagellate Gymnodinium sanguineum Hirasaka were studied in 1988 in Fe-replete and Fe-deplete batch cultures. Saturated rates of Fe transport (ϱ , mol.liter cell vol⁻¹ h⁻¹) for cultures grown on NO₃ or NH₄ were measured following resuspension in either N source (i.e., NO₃ or NH₄). Enhanced Fe uptake capacity developed under Fe stress, and was manifested in all experiments except that involving a transition from NH₄ to NO₃ nutrition. Suppression appears to have resulted from a reduced ability of NH₄-grown cultures to utilize nitrogen in the form of NO₃, thereby causing cells to remain nutritionally stressed (with respect to N rather than Fe, however). Supporting evidence was provided by the complete initial inhibition of NO₃ uptake when Fe-deplete, NH₄-grown cells were given saturating iron additions. When NH4 was supplied continuously (i.e., no N source transition), NH₄-grown cells showed the greatest iron stress-mediated enhancement (i.e., Fe-replete vs. Fe-deplete) of Fe transport (2.5-fold) accompanied immediately by NH₄ uptake. Our findings are considered in relation to the potential consequences for this dinoflagellate of reduced iron bioavailability and available nitrogen source.

Published in: Marine Biology, 110:175-182, 1991.

Supported by: Florence and John Schumann Foundation.

WHOI Contribution No. 7639.

IRON CONTROL OF THE VIBRIO FISCHERI LUMINESCENCE SYSTEM IN ESCHERICHIA COLI.

P. V. Dunlap

Iron influences luminescence in Vibrio fischeri; cultures iron-restricted for growth rate induce luminescence at a lower optical density (OD) than faster growing, iron-replete cultures. An iron restriction effect analogous to that in V. fischeri (slower growth, induction of luminescence at a lower OD) was established using E. coli tonB and tonB+ strains transformed with recombinant plasmids containing the V. fischeri lux genes (luxR luxICDABEG) and grown in the presence and absence of the iron chelator ethylenediamine-di

(-hydroxyphenyl) acetic acid (EDDHA). This permitted the mechanism of iron control of luminescence to be examined. A fur mutant and its parent strain containing the intact lux genes exhibited no difference in the OD at induction of luminescence. Therefore, an iron-binding repressor protein apparently is not involved in iron control of luminescence. Furthermore, in the tonB and in tonB+ strains containing lux plasmids with Mu dI (lacZ) fusions in luxR, levels of β -galactosidase activity (expression from the luxRpromoter) and luciferase activity (expression from the luxICDABEG promoter) both increased by a similar amount (8-9 fold each for tonB, 2-3 fold each for tonB+) in the presence of EDDHA. Similar results were obtained with the luxR gene present on a complementing plasmid. The previously identified regulatory factors that control the lux system (autoinducer-LuxR protein, cyclic AMP-cAMP receptor protein) differentially control expression from the luxR and luxICDABEG promoters, increasing expression from one while decreasing expression from the other. Consequently, these results suggest that the effect of iron on the V. fischeri luminescence system is indirect.

Supported by: WHOI Independent Study Award.

WHOI Contribution No. 7895.

ORGANIZATION AND REGULATION OF BACTERIAL LUMINESCENCE GENES

P. V. Dunlap

Current status of the organization and regulation of the genes involved in bacterial bioluminescence (the lux genes) is summarized, with emphasis placed on the luminescence system of the marine luminous bacterium Vibrio fischeri. In this species, the lux genes occur on a contiguous portion of the chromosome in two transcriptional units, luxR and luxICDABEG, which are divergently transcribed from an intermediate regulatory region. Studies with the cloned V. fischeri lux genes in Escherichia coli have confirmed two forms of regulation, autoinduction, which is mediated by autoinducer and the LuxR protein, and control by cyclic AMP and cyclic AMP receptor protein. Physiological studies with V. fischeri have indicated that oxygen, glucose, and iron also control luminescence. Evidence from studies with lux::lacZ fusion mutants of V. fischeri links control by these physiological factors to a new form of regulation, a cell-density-dependent induction underlying autoinduction but that does not require autoinducer or LuxR protein. Additional proposed control at the genetic level

includes the involvement of LexA, HtpR, and Fnr. Regulation of the *lux* system of *V. fischeri* therefore is complex, involving several cellular and genetic regulatory factors.

Published in: Photochemistry Photobiology, 54(6):1157-1170, 1991.

Supported by: WHOI Independent Study Award. WHOI Contribution No. 7801.

GROWTH OF THE MARINE LUMINOUS BACTERIUM VIBRIO FISCHERI ON 3':5'-CYCLIC AMP: CORRELATION WITH A PERIPLASMIC 3':5'-CYCLIC AMP PHOSPHODIESTERASE

Paul V. Dunlap, Ulrich Mueller, Teresita A. Lisa and Kelly S. Lundberg

The marine luminous bacterium Vibrio fischeri, the species-specific light-organ symbiont of monocentrid (pinecone) fish, was found to grow on 3':5'-cyclic adenosine monophosphate (cAMP) as a sole source of carbon and energy, a capability not previously described in bacteria. In a minimal. chemically defined medium containing cAMP as the sole source of carbon and energy, V. fischeri cells grew slower than on glucose and ribose but as fast as on 5'-AMP. Expression of luminescence. which is dependent on cAMP in V. fischeri, was stimulated in cells grown on cAMP compared to cells grown on glucose or ribose. All tested strains of V. fischeri (MJ-1, B-61, ATCC 7744, MJ-A1, CG-A1) grew on cAMP, as did strains of two other marine luminous bacteria, V. logei and Photobacterium phosphoreum, and strains of the terrestrial enteric bacterium Serratia marcescens. Other tested species of marine luminous bacteria (P. leiognathi, Shewanella [Alteromonas] hanedai, V. harveyi, V. orientalis, V. splendidus) and terrestrial enteric bacteria (Escherichia coli, Salmonella typhimurium), which grew on 5'-AMP or ribose, did not grow on cAMP. Whole- cell assays and periplasmic extracts revealed that V. fischeri MJ-1 produced a periplasmic 3':5'-cAMP phosphodiesterase (cAMP phosphodiesterase) of a very high specific activity (9.0 μ moles phosphate released mg protein⁻¹ min⁻¹) and a narrow substrate specificity (3':5'-cAMP and 3':5'-cGMP attacked). The novel periplasmic location and unusually high activity of cAMP phosphodiesterase apparently account for the ability of this species to grow on cAMP. The periplasmic cAMP phosphodiesterase of V. fischeri might play a role in degrading cAMP free in seawater or in a cAMP-mediated aspect of the light organ symbiosis with monocentrid fish.

Supported by: NSF Grant DCB91-04653.

WHOI Contribution No. 7853.

ENDOGENOUSLY-MEDIATED, PRETRANSLATIONAL SUPPRESSION OF CYTOCHROME P450IA EXPRESSION IN PCB-CONTAMINATED FLOUNDER

A. A. Elskus, R. J. Pruell and J. J. Stegeman

Gonadally mature fish display strong sex-related differences in the content and activity of P450IA, the major polynuclear aromatic hydrocarbon-inducible P450 form in teleosts. Such differences appear related to plasma levels of the female sex steroid, estradiol (E2), however, neither the mechanism of estradiol suppression of P450IA, nor the capacity for hormonal regulation to overcome potent P450IA induction, are known. Gonadally mature flounder (Pseudopleuronectes americanus) were collected from Fox Island (FI), RI, a references site and New Bedford Harbor (NB), MA a site highly contaminated with polychlorinated biphenyls (PCBs). Differences in flounder P450IA expression were determined at the level of P450IA catalytic activity (measured as ethoxyresorufin O-deethylase, EROD), P450IA protein content (immunoquantitated) and P450IA-mRNA content (by Northern blot) as they relate to sex, reproductive status, and hepatic PCB content. Our results demonstrate that suppression of P450IA in gonadally mature female fish is likely due, at least in part, to elevated E2 titers, that such suppression occurs at a pretranslational level, and further, that endogenous regulation of P450IA expression can 'override' exogenous regulation by even high concentrations of potent P450IA inducers.

Supported by: EPA Cooperative Agreement CR-813155; and PHS Grant ES-04220.

WHOI Contribution No. 7740.

THE WEST FALMOUTH OIL SPILL: FATE OF FUEL OIL COMPOUNDS 20 YEARS LATER

John W. Farrington, John M. Teal, Bruce W. Tripp and Curtis Phinney

The barge FLORIDA spilled No. 2 fuel oil into Buzzards Bay, Massachusetts in September, 1969. Sediments from five of the original oiled stations were sampled in August, 1989 and analyzed for fuel oil hydrocarbons. Two subtidal and one intertidal marsh station had no evidence of fuel oil. One subtidal mud core had traces of biodegraded fuel oil at 10-15 cm. One marsh core contained 10-6 g/g dry weight of weathered and biodegraded fuel oil, aromatic hydrocarbons and cycloalkanes at 5-10 cm with lesser concentrations at 0-5 and

10-15 cm. Nearly twenty years later, substantive concentrations of fuel oil compounds remain in this marsh area.

Supported by: Minerals Management Service; and WHOI Coastal Research Center.

WHOI Contribution No. 7654.

EFFECTS OF TRIBUTLYTIN CHLORIDE IN VITRO ON THE HEPATIC MICROSOMAL MONOOXYGENASE SYSTEM IN THE FISH STENOTOMUS CHRYSOPS

K. Fent and J. J. Stegeman

Tributlytin (TBT) has been shown to be highly toxic to a number of aquatic species, but the mode(s) of action on a biochemical level remain(s) to be elucidated. Here we investigate the interaction in vitro of TBT with hepatic microsomal cytochrome P450 and associated enzyme activity in scup (Stenotomus chrysops). Hepatic microsomes from β naphthoflavone-induced scup were incubated in vitro with TBT and various components analyzed. TBT led to a time- and concentration-dependent decrease in total microsomal P450 content. This decrease was accompanied by the formation of cytochrome P420. A complete loss of P450 occurred with 1 mM TBT after 30 minutes incubation. Ethoxyresorufin-O-deethylase (EROD) activity was strongly inhibited by TBT in a concentration-dependent manner, with a complete inhibition at 0.3 mM TBT after 15 minutes incubation. Other components of the microsomal electron transport system were also investigated. Neither cytochrome b₅ content, nor NADPH-cytochrome c reductase activity were affected by TBT at concentrations up to 0.5 mM TBT. NADH-cytochrome c reductase activity, however, showed a concentration-dependent increase, with more than a doubling of activity at 0.5 mM TBT. This indicates that TBT has different effects on these reductases. In conclusion, TBT can strongly interact with hepatic microsomal P450 in fish leading to destruction of native enzyme and inhibition of enzyme activity.

Supported by: EAWAG and PHS Grant ES-04220. WHOI Contribution No. 7783.

INHIBITION OF CYTOCHROME P450 FORMS BY TRIBUTYLTIN IN FISH

Karl Fent and John J. Stegeman

The interaction of tributyltin chloride (TBT) in vivo with different forms of hepatic microsomal

cytochrome P450 and ethoxyresorufin O-deethylase (EROD) activity was studied in scup (Stenotomus chrysops). Fish were injected with single doses of 3.3, 8.1 and 16.3 mg/kg TBT. Hepatic microsomes were analyzed 24 h later for total cytochrome P450 content and three P450 forms by immunoblotting; scup P450E, the major polyaromatic hydrocarboninducible form (P4501A1), scup P450A, the major contributor to microsomal testosterone 6 β -hydroxylase activity, and scup P450B, that oxidizes testosterone at several different sites including the 15\alpha position. Spectrally determined conversion of P450 to its degraded form cytochrome P420 occurred at all TBT doses, the conversion being considerable only at the highest dose with more P420 (65%) than P450 (35%). EROD activity tended to be decreased by TBT in all doses, with a significant inhibition at 16.3 mg/kg. Immunoblot analysis with a monoclonal antibody to P450E (P4501A1) showed a decrease of P4501A protein content at all TBT doses, with a significant loss at 16.3 mg/kg, similar to EROD activity. Immunoblot analysis with polyclonal antibodies to P450A and P450B showed decreases in P450A and P450B protein content only at the highest dose, being significant for P450A only. Cytochrome bs content was unaffected in all doses. This study indicates important biochemical effects of TBT in fish liver, and suggest that exposure to TBT may alter the cytochrome P450 dependent metabolism, especially that of P4501A proteins. P4501A that is induced by various environmental pollutants appeared to be more strongly affected than other forms, which may indicate that TBT exposure can influence the environmental induction of this enzyme by other pollutants.

Supported by: EAWAG and PHS Grant ES-04220. WHOI Contribution No. 7850.

HYDRODYNAMIC DISTURBANCES PRODUCED BY SMALL ZOOPLANKTON: A CASE STUDY FOR VELIGER LARVAE OF BIVALVE MOLLUSCS

Scott M. Gallager

Zooplankton produce hydrodynamic disturbances during swimming and feeding that enlarge their perceptive volume. From the standpoint of both prey and predators, fluid disturbances increase the probability that an organism is detected, identified and reacted to within appropriate time and space scales. Morphology and kinematics dictate magnitude, symmetry and attenuation of disturbances in the fluid medium. Therefore, fluid disturbances may be species and age (size) specific.

Normal and high-speed video microscopy were used to study flow field generation by free swimming and tethered bivalve larvae. These organisms swim and feed using many highly coordinated and symmetrically distributed appendages (i.e., cilia). Larvae tethered in flow at various free stream velocities (Uo), simulating swimming activity, induced particle trajectories approximately parallel to the organism's dorso-ventral axis. Velocity (v) and acceleration (a) were symmetrical in the transverse plane and asymmetrical in the vertical plane. Greatest velocity magnitudes (ca. 7, 3, 6 mm s⁻¹) occurred dorsal to the velum and attenuated with source distance (r) as 1/r, $1/4^{1.8}$, $1/r^{2.9}$ at Uo= 0, 3.1 and 6.4 mm s⁻¹, respectively. For a larva in flow but with velum retracted, simulating sinking, velocity attenuated at 1/r^{0.9} towards the organism. Mean velocity gradients were on the order of 3, 8 and 10 s⁻¹ for swimming, sinking and hovering larvae, respectively. The high frequency (22 Hz) component of particle velocity past free swimming larvae was due to beat frequency of the velar cilia. This attenuated rapidly with r leaving only low frequency (3 Hz) disturbances 0.1 mm beyond the tips of the cilia.

Numerical simulations suggest that flow fields of larvae induce displacements of free neuromast-like organs at source distances up to 2 and 25 mm for swimming and hovering larvae, respectively, in the absence of turbulence. Comparisons of kinetic energy dissipation rate for turbulence in coastal waters with kinetic energy of laminar flow fields implied possible dominance of the flow field of hovering, but not swimming. larvae to at least three body diameters from the organism (ca. 1 mm). These differences in flow fields have important implications for larval survival. The perceptive volume of a hovering larva will be 40 fold greater than a swimming or sinking larva. However, a hovering larva is also more likely to be detected by a potential predator that uses mechanosensory organs to locate prey.

Supported by: NSF OCE89-11844. WHOI Contribution No. 7925.

LOCOMOTORY ENERGETICS AND BUOYANCY CONTROL IN LARVAE OF A BIVALVE MOLLUSC

Scott M. Gallager

To remain suspended in the water column, invertebrate larvae must maintain an effective neutral buoyancy. I describe here the mechanisms and energetic costs associated with controlling vertical position for a larva with a dense shell of calcium carbonate.

Empirical measurements of growth rate (shell length and total dry weight), proximate biochemical composition (protein, lipid and carbohydrate), swimming and falling velocities and larval density (isopycnic density gradients) were made over the planktonic development of the bivalve bankia gouldi (Bartsch). Oxygen consumption of individual larvae was estimated in relation to beat frequency of the velar cilia. Data were used to develop a simulation model that examined the relationship between larval buoyancy, fluid dynamics of energy dissipation during swimming activity and the ability to survive short episodes of nutrient deprivation.

The density of normally developing larvae increased hyperbolically attaining a maximum of 1.192 g.cm⁻¹ five days post fertilization. Three day periods of imposed starvation resulted in a 5 to 10% increase in larval density which was associated with catabolism of lipid. The relationship between larval respiration and beat frequency of the velar cilia suggested that the cost of swimming activity was 60 to 75% of total metabolism. Theoretical calculations of the power required to compensate for the combined forces opposing vertical movement (gravity and drag) also gave high values for the cost of transport. As a result, to maintain position in the water column, even small increases in larval density due to loss of lipid necessitated a large compensatory increase in metabolic output. Such feed-back enhancement of metabolism led to an exponential decrease in lipid content and less time larvae could survive short episodes of starvation than if lipid loss was calculated on a linear basis.

Growth and survival of larvae with dense shells appear in tenuous balance with anabolic and catabolic processes of lipid metabolism.

Supported by: NSF Grant OCE89-11844.

WHOI Contribution No. 7926.

EFFICIENT GRAZING AND UTILIZATION OF THE MARINE CYANOBACTERIUM SYNECHOCOCCUS SP. BY LARVAE OF A BIVALVE MOLLUSC

Scott M. Gallager, John B. Waterbury, and Diane K. Stoecker

Efficient grazing by marine bivalve larvae has been thought to be limited to particles larger than 4 μm in diameter, thereby eliminating photosynthetic and non-photosynthetic picoplankton as contributors to larval diets. Documentation of ingestion, carbon retention and growth of larvae of the bivalve Mercenaria mercenaria L. on Synechococcus sp. (WH7803, ≈1

μm) was facilitated using a variety of techniques: standard Coulter Counter grazing experiments with Synechococcus and Isochrysis aff.galbana (TISO), ¹⁴C- labelled cells in pulse/chase experiments and growth of larvae on diets of cell mixtures.

Clearance rates on Synechococcus ranged between 2 and 23 mul larva -1, h-1 depending on ambient cell concentration and larval age. Retention efficiency of cell carbon after gut evacuation was about 55% for both prey species. Growth on monocultures of Synechococcus at typical summer concentration in coastal waters $(1x10^5 \text{ cells ml}^{-1}, \approx 29 \mu \text{g C l}^{-1})$ was two-fold lower than on monocultures of Isochrysis at 1x104 cells ml⁻¹ (≈120 µg C1⁻¹). Larval growth was inhibited and atrophy of the digestive gland was observed when Synechococcus was offered at concentrations at or exceeding 8.6x10⁵ cells ml⁻¹. Larval growth was enhanced, however, in the presence of Synechococcus (5x10⁴ cells ml⁻¹) when Isochrysis was limiting.

During the diurnal study of Synechococcus population dynamics conducted by Waterbury et al. (1986) in Vineyard Sound, MA, the abundance of bivalve larvae was sufficient to account for 8-24% of the calculated grazing activity on Synechococcus. When nanoplankton are scarce, invertebrate larvae may exert considerable grazing pressure on Synechococcus and derive benefit from ingestion of these cyanobacteria.

Supported by: NSF Grant OCE89-11844, NOAA; Office of Sea Grant NA90-AA-D-SG480.

WHOI Contribution No. 7927.

LARGE OCEANIC DIATOMS: POTENTIAL ROLE IN NEW PRIMARY PRODUCTION

Joel C. Goldman

Very large phytoplankton species $> 50 \mu m$ in size, particularly diatoms, generally are found in background numbers throughout the euphotic zone of oceanic waters. Yet, when responding to episodic injections of new nutrients across the thermocline at the base of the euphotic zone these phototrophs may make a disproportionately large contribution to new primary production. To test this concept, we isolated a group of large diatoms from the Sargasso Sea and found that the specific growth rate of several of these species in culture was great enough at the $\approx 2\%$ light level in oligotrophic waters to meet the requirements of several hypothetical scenarios in which annual rates of new production from the sum of one or more episodic blooms were equal to contemporary estimates. Two of the fast-growing species, Stephanopyxis palmeriana, (Greville) Grunow and

Pseudoguinardia recta v von Stosch, formed giant flocculent masses while growing. Such masses could sink rapidly out of the euphotic zone or be a direct food source for invertebrates or fish higher up the food chain. Not only would a short, simple trophic system with low losses result, but the events would virtually be impossible to observe with conventional sampling.

In Press: Deep-Sea Research.

Supported by: NSF Grant OCE88-18619.

WHOI Contribution No. 7803.

PHAGOTROPHY AND NH₄ [†] REGENERATION IN A THREE-MEMBER MICROBIAL FOOD LOOP

J. C. Goldman and M. R. Dennett

In a series of batch experiments we compared the efficiency of nitrogen regeneration of a two- and three-member microbial food loop consisting of a mixed bacterial assemblage, a small (3-5 µm-sized) heterotrophic flagellate (Paraphysomonas sp.), and a large (7-12 µm-sized) heterotrophic flagellate (Paraphysomonas imperforata). In the two member system the nitrogen regeneration efficiency for NH₄ $^+$ (R_n) was 41% and the gross growth efficiency (GGE) was 57% during active grazing by the small flagellate on bacteria. Regeneration of NH₄ + continued during the stationary phase so that R-n was 75% after ≈ 6 days incubation. When the larger flagellate was introduced at the end of exponential growth of the smaller grazer in the three-member system, initially there was rapid regrowth of bacteria, tying up $\approx 15\%$ of the nitrogen originally in the bacteria. The larger flagellate grazed the smaller one with a gross growth efficiency of 55%. Total nitrogen regeneration efficiency through exponential growth of the larger flagellate was 73%. Because microbial food loops in natural waters are far more complicated and with more grazing steps than portrayed in this study, we would expect the bulk of nutrients within these systems to be recycled with little transfer to higher trophic levels.

In Press: Journal of Plankton Research.

Supported by: NSF Grants OCE85-11283 and OCE87-16026.

WHOI Contribution No. 7760

THE AH RECEPTOR IN MARINE ANIMALS: PHYLOGENETIC DISTRIBUTION AND RELATIONSHIP TO CYTOCHROME P4501A INDUCIBILITY

Mark E. Hahn, Alan Poland, Ed Glover and John J. Stegeman

In mammals, the induction of cytochrome P4501A forms by chlorinated dibenzo-p-dioxins, chlorinated dibenzofurans, and halogenated biphenyls is under control of a soluble protein known as the Ah (aromatic hydrocarbon) receptor. Little is known about the presence and properties of the Ah receptor in other vertebrate and invertebrate species. In these studies, we sought evidence for an Ah receptor in the liver or liver-equivalent of twenty-four species of marine animals, using the photoaffinity ligand 2-azido-3-[125I]iodo-7,8-dibromo-dibenzo-p-dioxin (N₃[¹²⁵I]Br₂DD). Specific labeling of cytosolic proteins by N₃[¹²⁵I]Br₂DD was observed in seven species of teleost and elasmobranch fish, in PLHC-1 fish hepatoma cells, and in beluga whales. No specifically labeled proteins were found in cytosol from two species of agnathan fish, nor in any of nine invertebrate species representing eight classes of four phyla. The presence or absence of specifically labeled polypeptides corresponds with the inducibility of cytochrome P450 1A and sensitivity to toxic effects of TCDD and related planar halogenated aromatic hydrocarbons in many of these groups. Thus, Ah receptor function may have arisen early in vertebrate evolution and has been conserved from elasmobranch and teleost fish through mammals.

In Press: Marine Environmental Research.

Supported by: PHS Grants ES-05479 and ES-04220; and the Donaldson Charitable Trust.

WHOI Contribution No. 7741.

PHYLOGENETIC DISTRIBUTION OF THE AH RECEPTOR IN NON-MAMMALIAN SPECIES: IMPLICATIONS FOR DIOXIN TOXICITY AND AH RECEPTOR EVOLUTION

Mark E. Hahn and John J. Stegeman

The mammalian Ah receptor (AhR) controls the expression of the CYP1A1 gene and may also mediate the toxic effects of chlorinated dioxins and related compounds. Little is known about the presence and characteristics of the AhR in non-mammalian species. Recent studies have identified an AhR in fish, consistent with their

sensitivity to dioxin toxicity. However, the AhR may be lacking in many species of marine invertebrates. Thus, invertebrate species may be less susceptible to dioxin effects, or may show different structure-activity relationships from those seen in vertebrates. The AhR may have evolved more than 450 million years ago in response to compounds present in the environment of early fishes, or to fulfill some physiologic role, as yet unidentified.

Supported by: Air Force Office of Scientific Research, Grant No. 6410-030.

WHOI Contribution No. 7918.

PREPARATION AND INITIAL CHARACTERIZATION OF CRYSTALS OF THE PHOTOPROTEIN AEQUORIN FROM AEQUOREA VICTORIA

L. I. Hannick, D. C. Prasher, L. W. Schultz, J. R. Deschamps, and K. B. Ward

Crystals of recombinant aequorin, the photoprotein from the jellyfish Aequorea victoria, have been grown from solutions containing sodium phosphate. The crystals grow as thin plates which diffract to beyond 2.2 Å resolution. The crystals are orthorhombic, space group P2₁2₁2₁; the axes are a=89.1(1), b=88.4(1) and c=52.7(1) Å. The asymmetric unit contains two molecules. Crystals exposed to calcium ion solutions emit a steady glow and slowly deteriorate, confirming that the crystals consists of a charged, competent photoprotein. This represents the first successful preparation of single crystals of a photoprotein suitable for diffraction analysis.

Supported by: ONR Grant N00014-90-J-1704. WHOI Contribution No. 7947.

OBSERVATIONS ON THE SWIMMING AND BUOYANCY OF CYMBULIA PERONI (GASTROPODA: THECOSOMATA) MADE FROM A SUBMERSIBLE

G. R. Harbison

The swimming and buoyancy of the gelatinous pteropod, Cymbulia peroni, was observed and videotaped from a submersible in the western Mediterranean. When not swimming, C. peroni hangs neutrally buoyant, with its parapodia outstretched and motionless. Two modes of swimming were observed, slow swimming, and rapid or "escape" swimming. Slow swimming predominated, at speeds ranging between 2 and 11 cm sec⁻¹. Most slow swimming was directed vertically up or down. Slow swimming is probably

used for vertical migration and the avoidance of turbulence. Turbulence frequently occurs both at epipelagic and mesopelagic depths in the Mediterranean. Escape swimming was more rapid, and speeds up to 40 cm sec⁻¹ were measured. Differences between slow and escape swimming appear to be quantitative rather than qualitative, in contrast to other cymbuliids. Cymbulia peroni is an active and vigorous swimmer, clearly capable of vertical migration, that probably attains speeds greater than the highest measured in this study. Its behavior in the field differs dramatically from its behavior in the laboratory.

In Press: Journal of the Marine Biological Association, United Kingdom.

Supported by: WHOI; ONR N00014-90-J-1819; and NOARL N00014-91-C-6007.

WHOI Contribution No. 7804.

ULTRASTRUCTURE OF THE FEEDING APPARATUS AND MYONEMAL SYSTEM OF THE HETEROTROPHIC DINOFLAGELLATE PROTOPERIDINIUM SPINULOSUM SCHILLER

Dean M. Jacobson and D. M. Anderson

The feeding veil or pallium of the thecate heterotrophic dinoflagellate Protoperidinium spinulosum is a highly vesiculated membranous sac bounded by arched, sometimes bifurcated microtubular ribbons. It originates from an internal microtubular basket, passes through a sphincter-like osmiophilic ring located inside the posterior flagellar pore, and emerges from the cell at that pore. A related species, Protoperidinium punctulatum, also possesses a microtubular basket/osmiophilic ring complex. Elongate electron-dense bodies within the basket resemble digestive secretory granules found in other protists. Granular, electron-lucent microbodies situated at the anterior end of the basket may also have a role in prey digestion. Dense membranous whorls observed within a P. spinulosum cell preparing to initiate feeding are presumed to represent a condensed storage site for pallium membranes. A narrow microtubule-strengthened pseudopodal appendage found in two non-feeding cells may constitute the tow filament which serves as the initial linkage between the dinoflagellate and its

The structures that constitute the pallium and pallium precursors, described here for the first time, are unlike those of other known protists, although some similarities with the dinoflagellate peduncle are evident. The existence of this unique system of organelles may have important ramifications in the search for evolutionary relationships among protists.

Published in: Journal of Phycology, 28:69-82, 1992.

Supported by: NSF Grants OCE84-00292 and OCE89-11226.

WHOI Contribution No. 7713.

THE MICROBIAL TURNOVER OF CARBON IN THE DEEP SEA

Holger W. Jannasch

The microbial turnover of inorganic and organic carbon in the deep-sea is limited by input of the source of energy, low temperatures and high hydrostatic pressures, in that order of effectiveness. In reference to surface water conditions, these limitations are partly compensated by special adaptations: oligotrophy, psychrophily and barophily. The pool of total organic carbon is largely consisting of unknown recalcitrant compounds, but also contains low molecular substrates readily available to microbial metabolism but below the threshold concentrations for effective uptake. The growth limiting input of photosynthetically produced organic carbon does not apply at certain areas of tectonic spreading activity where the availability of inorganic reduced substrates function as the source of energy for the microbial reduction of inorganic to organic carbon (chemosynthesis) in the presence of free oxygen. Estimated for the deep sea environment, this chemosynthetic production of organic carbon compares to 10% of the photosynthetic input.

Supported by: NSF Grant OCE89-22854; and ONR Grant N00014-91-J-1751.

WHOI Contribution No. 7893.

MICROBIOLOGY OF DEEP-SEA HYDROTHERMAL VENTS

Holger W. Jannasch

This overview (presented to the Australian Society of Microbiology at their annual meeting held at Launceston, Tasmania, July 1990) contains discussions of a brief history of the vent discovery, the microbial conversion of geothermal into biochemical energy, physiological diversity of vent microorganisms with emphasis on the new extremely thermophilic bacteria, the novel procaryotic/eucaryotic symbioses between chemosynthetic bacteria and certain new marine invertebrates, and some observations on biotechnological relevance.

Published in: Australian Microbiologist, 11:370-372, 1990.

Supported by: NSF Grant OCE89-22854; and ONR Contract N00014-88-K-0386.

WHOI Contribution No. 7556.

THE CHEMOSYNTHETIC PRODUCTION OF POTENTIALLY USEFUL BIOMASS BY SULFIDE OXIDIZING BACTERIA

Holger W. Jannasch, Craig C. Taylor and Linda R. Hare

The feasibility of using the microbial oxidation of hydrogen sulfide in a continuous system of running seawater has been studied. The generated biomass has been analyzed and applied as a food source in the aquaculture of blue mussels (Mytilis edulis).

Supported by: NSF Grant OCE89-22854.

WHOI Contribution No. 7879.

PARTICLE RETENTION EFFICIENCY OF SALPS

Patricia Kremer and Laurence P. Madin

Five species of salps retained plastic beads $\geq 2.5~\mu m$ diameter with high ($\geq 60\%$) efficiency, while 1.0 μm beads were retained with low ($\leq 15\%$) efficiency in all but one experiment.

In Press: Journal of Plankton Research.

Supported by: NSF Grant OCE88-18503.

WHOI Contribution No. 7698.

METHANOPYRUS KANDLERI GEN. AND SP. NOV. REPRESENTS A NOVEL GROUP OF HYPERTHERMOPHILIC METHANOGENS, GROWING AT 110°C

Margit Kurr, Robert Huber, Helmut König, Holger W. Jannasch, Hans Fricke, Antonio Trincone, Jakob K. Kristjansson and Karl O. Stetter

A novel group of hyperthermophilic rod-shaped motile methanogens was isolated from a hydrothermally heated deep-sea sediment (Guaymas Basin, Gulf of California) and from a shallow marine hydrothermal system (Kolbeinsey Ridge, Iceland). They grow between 84 and 110°C (opt: 98°C) and from 0.2% to 4% NaCl (opt: 2%) and pH 5.5 to 7 (opt: 6.5). The isolates are obligate chemolithoautotrophs using H₂S/CO₂ as energy and carbon sources. In the presence of sulfur, H₂S is formed and cells tend to lyse. The

cell wall consists of a new type of pseudomurein containing ornithine in addition to lysine and no N-acetyl-glucosamine. The pseudomurein layer is covered by an SDS-sensitive protein surface layer. The core lipid consists exclusively of phytanyl diether. The G+C content of the DNA is 60 mol%. By 16S rRNA comparisons the new organisms are not related to any of the 3 methanogenic lineages. Based on the physiological and molecular properties of the new isolates, we are providing here the first description of a new genus recently named by us Methanopyrus (the "methane fire"). The type species is Methanopyrus kandleri (type strain: AV19; DSM6324).

Published in: Archives of Microbiology, 156:239-247, 1991.

Supported by: NSF Grant OCE89-22854; and ONR Contract N00014-91-J-175.

WHOI Contribution No. 7615.

DEEP-SEA AND BENTHOPELAGIC MEDUSAE: RECENT OBSERVATIONS FROM SUBMERSIBLES AND A REMOTELY OPERATED VEHICLE

R. J. Larson, G. I. Matsumoto, L. P. Madin and L. M. Lewis

Recent direct observations in the western Atlantic and eastern Pacific show that benthic and benthopelagic medusae are more numerous and diverse in the deep-sea than previously believed. Some of these medusae are behaviorally and anatomically modified for living at the bottom. Others are facultative species that also live in midwater. Data obtained using submersibles and a remotely operated vehicle show that three genera can occur at densities of up to 80 medusae m⁻².

In Press: Bulletin of Marine Science.

Supported by: NSF Grants OCE77-22511, OCE84-00243, OCE85-16083, OCE87-01388, OCE87-46136; and NURC-FDU Subcontract No. 88-9 under NOAA Grant NA88AA-H-UR020.

WHOI Contribution No. 7833.

PHYSIOLOGICAL RESPONSES OF PHYTOFLAGELLATES TO DISSOLVED ORGANIC SUBSTRATE ADDITIONS. 1.

DOMINANT ROLE OF HETEROTROPHIC NUTRITION IN POTERIOOCHROMONAS MALHAMENSIS (CRYPTOPHYCEAE)

Alan J. Lewitus and David A. Caron

Algal heterotrophy is a potentially important consideration in the flow of carbon through aquatic

food webs. The physiological re-ponses to organic compound additions under various light intensities were examined with Poterioochromonas malhamensis, a freshwater chrysophyte with an exceptionally high heterotrophic capability. P. malhamensis demonstrated a much greater potential for heterotrophic growth than for photoautotrophic growth. When organic substrates (glucose, glycerol, or ethanol) were added to the culture medium, the growth rate of P. malhamensis significantly increased while the chlorophyll a content cell -1 decreased, even at light intensities saturating for photoautotrophic growth. After an initial decline in chlorophyll production caused by organic substrate uptake, chlorophyll a cell -1 increased and the uptake rate of organic substrates decreased, despite the persistence of a relatively high substrate concentration in the medium. The results are consistent with the production of substances(s) by P. malhamensis that conditioned the culture medium, leading to a relief of the inhibitory effect of organic substrates on chlorophyll production.

Published in: Plant and Cell Physiology, 32:671-680, 1991.

Supported by: NSF Grants BSR86-20443 and BSR89-19447; WHOI Education Program; and Ocean Ventures Fund.

WHOI Contribution No. 7768.

PHYSIOLOGICAL RESPONSES TO PHYTOFLAGELLATES TO DISSOLVED ORGANIC SUBSTRATE ADDITIONS. 2. DOMINANT ROLE OF AUTOTROPHIC NUTRITION IN PYRENOMONAS SALINA (CRYPTOPHYCEAE)

Alan J. Lewitus and David A. Caron

The enhancement of algal growth by organic substrate assimilation is a common laboratory observation, yet few studies have addressed the interaction of dissolved organic compounds and environmental factors for controlling the relative contribution of heterotrophy and autotrophy to the nutrition of these algae. The effects of light intensity and glycerol addition on the growth, cell volume, pigmentation, and carbon uptake of the facultative heterotroph, Pyrenomonas salina Santore, were examined. Glycerol addition to cultures growing at a limiting light intensity increased the growth rate, increased the average cell volume and cellular starch content, decreased the cellular phycoerythrin to chlorophyll a ratio, and had no effect on the CO₂ fixation rate cell Glycerol addition to cultures growing at a moderate light intensity that was saturating for photoautotrophic growth increased the average cell volume and cellular starch content but had no effect on the CO₂ fixation rate cell⁻¹. The results indicate that autotrophy was the major process for carbon acquisition during the growth of *P. salina*, but that carbon acquisition from glycerol catabolism also was used to partially support growth of the alga at the limiting light intensity. In addition, glycerol presumably was used to fulfill the energy and/or reductant requirements of the alga, and to increase the reserve carbohydrate (starch).

Published in: Plant and Cell Physiology, 32:791-801, 1991.

Supported by: NSF Grants BSR86-20443 and BSR89-19447; WHOI Education Program; and Ocean Ventures Fund.

WHOI Contribution No. 7769.

EFFECTS OF LIGHT INTENSITY AND GLYCEROL ADDITION ON THE ORGANIZATION OF THE PHOTOSYNTHETIC APPARATUS IN THE FACULTATIVE HETEROTROPH, PYRENOMONAS SALINA (CRYPTOPHYCEAE)

Alan J. Lewitus, David A. Caron and Kenneth R. Miller

The marine cryptophyte, Pyrenomonas salina Santore, is capable of autotrophic and heterotrophic nutrition. This study examines the physiological and ultrastructural changes that accompany the shift between these nutritional modes. The addition of glycerol to bath cultures of P. salina, grown at a light intensity limiting for photoautotrophic growth, increased its growth rate and induced specific biochemical and structural changes in its photosynthetic system. Results from extracted pigment analyses, thin-section electron microscopy, and freeze-fracture electron microscopy indicated that glycerol addition reduced the cell phycoerythrin content. phycoerythrin to chlorophyll a ratio, degree of thylakoid packing, number of thylakoids per cell, and PSII particle size. These properties were reduced to a similar extent in cells grown photoautotrophically under a light intensity saturating for growth. These results are consistent with the hypothesis that enhancement of heterotrophic potential occurs at the expense of light-harvesting ability in glycerol-grown P. salina.

Published in: Journal of Phycology, 27:578-587, 1991.

Supported by: NSF Grants BSR86-20443 and BSR89-19447; WHOI Education Program; and Ocean Ventures Fund.

WHOI Contribution No. 7767.

ACOUSTIC ELEMENTS IN THE SEXUAL BEHAVIOR OF AFRICAN CICHLID FISHES

Phillip S. Lobel

The runaway sexual selection model has been invoked as an explanation for the bower-building behavior of the African Rift-Lake cichlid, Copadichromis eucinostomus. The basic assumption is that female choice in this species is based upon bower size and that females cannot distinguish male size by other cues. This study shows, for the first time, that males of this cichlid species produce distinct sounds during courtship and mating. The dominant frequency of such sounds is correlated with male size. These results support other studies arguing a more parsimonious model of sexual selection in this species.

Supported by: World Wildlife Fund, Grant 6129. WHOI Contribution No. 7857.

FOUR NEW ELECTRICFISHES (PISCES, MORMYRIDAE) FROM AN ISOLATED LAKE IN THE AFRICAN CONGO

P. S. Lobel, W. Harder and E. K. V. Kalko

A collection of fishes from Lake Téllé, Republic of Congo, yielded eight electricfishes (Mormyridae); 4 of which are new species including one which represents a new genus. Brienomyrus mbute sp. nov. is most similar to B. niger (Günther 1866) but differs by having more dorsal fin rays, fewer lateral line scales, fewer scales around the caudal peduncle, the number of teeth and the mouth orientation. Marcusenius likoualaenis sp. nov. is most similar to M. paucisquamatus Taverne, Thys van den Audenaerde and Heymer 1977 but differs by having fewer dorsal and anal fin rays and more lateral line scales. Mormyrops monkutu sp. nov. is very similar to M. nigricans Boulenger 1899 but can be differentiated on the basis of body proportions and dorsal fin ray count. M. monkutu can be distinguished from other Mormyrops spp. by fin ray, scale and teeth counts. Metambumyrus telleensis gen. nov., sp. nov. is described from a single specimen. It is overtly different from other mormyrids by a combination of characters including its terminal mouth, deep body, relative fin lengths, wide distance between nostrils and lack of a globular swelling on the chin. Other species collected were: Gnathonemus longibarbis (Hilgendorf, 1888), Marcusenius leopoldianus (Boulenger, 1899), Petrocephalus catostoma haullevilles Boulenger, 1912 and Petrocephalus schoutedeni Poll, 1954.

Supported by: World Wildlife Fund, Grant 6129; National Geographic Society, Grant 3940-88; and New England Biolabs Foundation.

WHOI Contribution No. 7858.

FEEDING, METABOLISM AND GROWTH OF CYCLOSALPA BAKERI IN THE SUBARCTIC PACIFIC

L. P. Madin and J. E. Purcell

Populations of Cyclosalpa bakeri occurred during late summer at Station "P" in the Subarctic Pacific in 1987 and 1988. Salps were collected by divers for measurement of rates of feeding, metabolism, growth and reproduction. These parameters were used to create the first complete carbon and nitrogen budget for a pelagic tunicae. Egestion, ingestion and filtration rates were determined from chlorophyll and phaeopigment in the fecal material. Counts of diatoms in the guts indicated that pigment based rates underestimated filtration by about 50%. Salps ranging in size from 10 to 100 mm filtered from .05 to 10.0 1 h⁻¹. Respiration rate was 0.44 μ mol 0₂ mg C⁻¹ h⁻¹, and ammonium excretion was $0.034 \mu \text{mol NH}_4 + \text{mg C}^{-1} \text{ h}^{-1}$. Growth was measured on salps maintained in aquaria. A model growth curve based on size-specific rates of increase in length gave maximum growth rates of 2% h⁻¹, and predicted a generation time of 24 days. Solitary generation salps would produce approximately 170 aggregate produces one solitary. Budget for a 50 mm solitary salp indicate that daily rations of carbon and nitrogen were 61% and 54% of body C and N, respectively. Assimilation efficiency was 61% for C and 71% for N. Rates of filtration, metabolism and growth were lower than some other salp species, but comparable, on a weight basis, to many other herbivores.

Supported by: NSF Grants OCE86-00776 and OCE86-14201.

WHOI Contribution No. 7924.

PHYSIOLOGICAL, BIOCHEMICAL AND GENETIC CONTROL OF BACTERIAL BIOLUMINESCENCE

E. A. Meighen and P. V. Dunlap

Knowledge of the bioluminescence systems of marine and terrestrial bacteria has developed rapidly in the past ten years, due in large part to the cloning and sequencing of genes involved in luminescence (lux genes). This chapter assesses these developments, from biochemical and molecular genetic perspectives, to provide a

comparative description of the bioluminescence systems of bacteria. Emphasis is placed on the biochemistry of luciferase and the fatty acid reductase complex, the key enzymatic components of these systems, and on lux gene organization and the regulation of lux gene expression at the molecular and physiological levels. Comparative lux gene sequence analysis is presented to suggest evolutionary relationships among the luminous bacteria, and sequence-based approaches to the identification of luminous bacteria are also described in the context of their geographical distribution and habitat diversity.

Supported by: Medical Research Council for Canada; and WHOI.

WHOI Contribution No. 7794.

PATTERN SIMILARITY IN SHARED CODAS FROM SPERM WHALES (PHYSETER CATODON)

Karen E. Moore, William A. Watkins and Peter Tyack

Similarities in codas (short sequences of click patterns) from sperm whales (Physeter catodon) were investigated by comparing two coda patterns repeated by single whales with similar patterns produced as overlapping sequences by two whales. Underwater recordings from four cruises west of the Windward Islands in the Southeast Caribbean were analyzed. Over 700 spectrograms were made of at least 28 different coda patterns from 46 hrs of recording. Two of these codas, named "C" and "E" comprised more than 50% of the codas recorded. Codas C and E were called "shared" codas because they were produced by a number of different whales in the area, both as repeated sequences by individual whales, and as exchanges by two or more whales, occasionally in overlapping series. Differences in the timing of click intervals of pairs of overlapping shared codas (produced by two whales) were compared with click intervals of pairs of sequential shared codas produced by single whales. Two types of analysis were performed on the coda pairs: (1) comparison of absolute timing, and (2) comparison of relative timing, i.e. rhythmic patterns. These analyses indicated no greater temporal stereotypy for sequential than for overlapping shared codas, therefore providing no evidence for individually distinctive patterns in these shared codas (as has been suggested for other coda patterns).

Supported by: ONR Contract N00014-88-K-0273. WHOI Contribution No. 7699.

EVOLUTIONARY ORIGINS OF BACTERIAL BIOLUMINESCENCE

Dennis J. O'Kane and Douglas C. Prasher

In bacteria, most genes required for the bioluminescence phenotype are contained in lux operons. Sequence alignments of several lux gene products show the existence of at least two groups of paralogous products. The α - and β -subunits of bacterial luciferase and the non-fluorescent flavoprotein are paralogous, and two antennae proteins (lumazine protein and yellow fluorescence protein) are paralogous with riboflavin synthetase. Models describing the evolution of these paralogous proteins are suggested, as well as a postulate for the identity of the gene encoding a protobioluminescent luciferase.

Published in: Molecular Microbiology, 6(4):443-449, 1992.

Supported by: The University of Georgia (NIH Subcontract No. RR166-171/1867333).

WHOI Contribution No. 7922.

PYRODICTIUM ABYSSI SP. NOV. REPRESENTS A NOVEL HETEROTROPHIC MARINE ARCHAEAL HYPERTHERMOPHILE GROWING AT 110°C

Ursula Pley, Jutta Schipka, Agata Gambacorta, Holger W. Jannasch, Hans Fricke, Reinhard Rachel and Karl O. Stetter

Novel hyperthermophilic heterotrophic members of the Archaea domain were isolated from marine hot abyssal as well as from shallow vents off Mexico and Iceland, respectively. The isolates grew between 80 and 110°C with an optimum around 97°C. They fermented carbohydrates, proteins, cell homogenates, acetate and formate. Isovalerate, isobutyrate, butanol and CO₂ were detected as end products. Growth was stimulated by H₂. In the presence of So, H₂S was formed. Cells were disc-shaped and appeared entrapped within networks of fibers. Based on DNA/DNA homology and 16 S rRNA partial sequences, the new isolates represent a new species of Pyrodictium, which we name Pyrodictium abyssi. Type strain is isolate AV2 (DSM 6158).

Published in: Systematic Applied Microbiology, 14:245-253, 1991.

Supported by: NSF Grant OCE89-22854; and ONR N00014-91-J-1751.

WHOI Contribution No. 7593.

PRIMARY STRUCTURE OF THE AEQUOREA VICTORIA GREEN-FLUORESCENT PROTEIN

Douglas C. Prasher, Virginia K. Eckenrode, William W. Ward, Frank G. Prendergast and Milton J. Cormier

Many cnidarians utilize green-fluorescent proteins (GFP's) as energy-transfer acceptors in bioluminescence. GFP's fluoresce in vivo upon receiving energy from either a luciferaseoxyluciferin excited-state complex or a Ca2+ -activated photoprotein. These highly fluorescent proteins are unique due to the chemical nature of their chromophore, which is comprised of modified amino acid (aa) residues within the polypeptide. This report describes the cloning and sequencing of both cDNA and genomic clones of GFP from the cnidarian, Aequorea victoria. The gfp10 cDNA encodes a 238-aa-residue polypeptide with a calculated molecular weight of 26,888. Comparison of A. victoria GFP genomic clones show three different restriction enzyme patterns which suggests that at least three different genes are present in the A. victoria population at Friday Harbor, Washington. The gfp gene encoded by the λGFP2 genomic clone is comprised of at least three exons spread over 2.6 kb. The nucleotide sequences of the cDNA and the gene will aid in the elucidation of structure-function relationships in this unique class of proteins.

In Press: Gene.

Supported by: American Cancer Society, Grant NP-640.

WHOI Contribution No. 7877.

INTERACTIONS BETWEEN CETACEANS AND GILL NET AND TRAP FISHERIES IN THE NORTHWEST ATLANTIC

Andrew J. Read

In this paper, I review the gill net and trap fisheries of the Northwest Atlantic and their potential for cetacean entanglement. Ten major categories of passive fisheries are identified, five of which are known to take substantial numbers of cetaceans during the course of their operations. These five fisheries are: Atlantic Canada and Gulf of Maine groundfish gill nets, Atlantic Canada cod traps, Bay of Fundy and Gulf of Maine herring weirs, Atlantic Canada and Greenland salmon gill nets, and U.S. East Coast swordfish drift nets. The cetacean species most threatened by incidental mortality in commercial fisheries in this region are the harbour porpoise, *Phocoena phocoena*, which is

taken in large numbers and the endangered northern right whale, Eubalaena glacialis.

In Press Reports of the International Whaling Commission

Supported by: International Whaling Commission. WHOI Contribution No. 7714.

MASSIVE FLUXES OF RHIZOSOLENID DIATOMS: A COMMON OCCURPENCE?

C. Sancetta, T. Villareal and P. Falkowski

The relationship between vertical flux of material to the deep sea and rates of production in the surface water has become an important subject of study. Several workers have emphasized the potential nonlinearities in this relationship, including the possibility that stochastic events might be responsible for a large proportion of export below the euphoric zone. It has been suggested that large diatoms might play a role in such export production. We summarize data sets referring specifically to the Rhizosolenid diatoms including several not previously published, and show that mass sinking of Rhizosolenids may be a common occurrence. Considerations of Rhizosolenid ecology suggest that this may produce a large and rapid pulse of organic matter to the deep sea, a pulse occurring more rapidly than, and not linearly related to, the rates of surface water production.

Published in: Limnology and Oceanography, 36(7):1452-1456, 1991.

Supported by: WHOI Postdoctoral Fellowship. WHOI Contribution No. 7770.

CLASS APLACOPHORA

Amélie H. Scheltema

The aplacophoran Continental Shelf fauna of Bass Strait is one of the most diverse yet sampled. Described here are 8 families and 12 genera, which are comprised of 28 species and 376 specimens. Fifty-four percent of the specimens are in the subclass Chaetodermomorpha with 2 or 3 genera in 2 families; a single species forms 98 percent of all chaetoderms. The Neomeniomorpha are comprised of 7 or 8 families, 11 or 12 genera, and 24 species. Dominance is by one species of Pararrhopalidae, accounting for 30 percent of all neomenioids. Species at depths less than 125 m are restricted to the Continental Shelf. Three genera of neomenioids are endemic, but endemicity of species belonging to nonendemic genera has not been determined.

Also described are two neomenioid genera from the Great Barrier Reef shelf, one genus from Torres Strait, one from MacQuarie Island, and one from off northwest Australia. All but the northwestern and MacQuarie Island genera occur in Bass Strait as well.

A general description of aplacophorans is included: history; morphology and physiology including feeding and digestion, locomotion, excretion, circulation, nervous system, reproduction, and embryology; natural history; biogeography; methods of study; and classification and keys to families. Each family is illustrated.

Supported by: National Parks and Wildlife Service.

WHOI Contribution No. 7655.

PASSIVE DISPERSAL OF PLANKTONIC LARVAE AND THE BIOGEOGRAPHY OF TROPICAL SUBLITTORAL INVERTEBRATE SPECIES

Rudolf S. Scheltema

The widespread occurrence of planktonic larvae of benthic invertebrates in the major currents of the tropical Atlantic, Pacific and Indian Oceans supports the hypothesis that such larvae contribute not only to the initial colonization of oceanic islands to the distribution of benthic species along extensive tropical coastlines or across ocean basins but also to the genetic exchange among islands or even between islands and more distant continents. Evidence for the dispersal of teleplanic polychaete larvae of sublittoral species is offered as an example to support of the hypothesis of "long-distance" passive dispersal.

Major criticisms of passive-dispersal as a factor in determining the biogeography of species are: 1) The idea that most larvae generally have a fixed life-span too short to account for longdistance dispersal; both laboratory and field data show that this generalization is mistaken. Rather than fixed, the length of larval life for most species is extremely flexible. 2) The notion that teleplanic larvae lose their competence to metamorphose and therefore cannot importantly contribute to long-distance dispersal; existing evidence does not support this view, whenever tested under suitable conditions teleplanic larvae have been shown to retain the ability to metamorphose. 3) The claim that dispersal is a random process and therefore cannot explain the congruent non-random associations found among widely differing taxa over large geographic regions; major current systems provide quasi-permanent or seasonally re-occurring corridors for the transport of larvae. All passively advected larvae necessarily are dispersed over similar routes and such transport

will result in congruent distributions of widely different taxa. 4) The observations that many benthic species lacking a planktonic larval stage nevertheless have wide geographic ranges and that consequently there is little relationship between the mode of reproduction and the geographic range of species; most species having wide geographic distributions but lacking a planktonic larval stage are sessile forms that attach to hard substrates and consequently are pre-adapted for rafting. Rafting of infaunal sediment-dwelling invertebrates is not likely on a biogeographically relevant scale. Biogeographic evidence from the tropical Pacific Ocean further supports the hypothesis that passive dispersal has a continuing role for both the colonization and genetic exchange among the populations of widely distributed sublittoral invertebrate species.

Supported by: Woods Hole Oceanographic Institution.

WHOI Contribution No. 7827.

DENITRIFICATION IN NITRATE CONTAMINATED GROUNDWATER: OCCURRENCE IN STEEP VERTICAL GEOCHEMICAL GRADIENTS

Richard L. Smith, Brian L. Howes and John H. Duff

A relatively narrow vertical zone (5-6 m thick) of nitrate containing groundwater was identified using multilevel sampling devices in a sand and gravel aquifer on Cape Cod, MA, USA. The aguifer has been chronically contaminated by surface disposal of treated sewage 0.3 km upgradient from the study area. The NO₃ zone was anoxic and contained high concentrations of N_2O (16.5 μ M), suggesting that it was a zone of active denitrification. Denitrifying activity was confirmed with direct measurement using acetylene block incubations with aquifer core material; peak rates were 2.4 nmol N reduced (g sed)-1day-Concentrations of dissolved inorganic carbon and N₂ were close to atmospheric equilibrium in uncontaminated groundwater, but were more than 2 times higher within the contaminant plume. Excess CO₂ and N₂ suggested in situ formation with a a stoichiometry of C and N mineralized via denitrification of 0.8 (C/N). Denitrification within the aquifer resulted in an increase in the natural δ^{15} N of NO₃⁻ (from +13.6 to +42.0 $^{\circ}/_{\infty}$) and the N₂ produced, with an isotopic enrichment factor of -13.9 %. Verticle profiles of NH₊4 and δ^1 5N of NH₊4 indicated that dissimilatory reduction of NO_3 was also occurring, but mass balance calculations indicated that denitrification was the predominant process. These results demonstrate

that a combination approach using field mass balance, stable isotope analysis, and laboratory incubations yields useful insight to the significance of denitrification in aquifer sediments and that closely spaced vertical sampling is necessary to adequately quantify the processes controlling C and N transport and transformation within these environments.

Published in: Geochimica Cosmochimica Acta, 55:1815-1825, 1991.

Supported by: NSF Grant BSR88-17701; and USGS IPA No. 9-4386-29500.

WHOI Contribution No. 7504.

IN SITU MEASUREMENT OF METHANE OXIDATION IN GROUNDWATER USING NATURAL GRADIENT TRACER TESTS

Richard L. Smith, Brian L. Howes and Stephen P. Garabedian

Methane oxidation was measured in an unconfined sand and gravel aquifer (Cape Cod, MA) by using in situ natural-gradient tracer tests at both a pristine, oxygenated site and an anoxic sewage-contaminated site. The tracer sites were equiped with multi-level sampling devices to create target grids of sampling points; the injectate was prepared with groundwater from the tracer site to maintain the same geochemical conditions. Methane oxidation was calculated from breakthrough curves of methane relative to halide and inert gas (hexafluoroethane) tracers and was confirmed by the appearance of 13C-enriched carbon dioxide in experiments in which ¹³C-enriched methane was used as the tracer. A Vmax for methane oxidation could be colculated when the methane concentration was sufficiently high to result in zero-order kinetics throughout the entire transport interval. Methane breakthrough curves could be simulated by modifying a one-dimensional advection-dispersion transport model to include a Michaelis-Menton-based consumption term for methane oxidation. The K_m values for methane oxidation that gave the best match for the breakthrough curve peaks were 6.0 and 9.0 µM for the uncontaminated and contaminated sites, respectively. Natural-gradient tracer tests are a promising approach for assessing microbial processes and for testing in situ bioremediation potential in groundwater systems.

Published in: Applied and Environmental Microbiology, 57:1997-2004, 1991.

Supported by: USGS IPA No. 9-4386-29500; and NOAA Grant NA88AA-D-CZ01.

WHOI Contribution No. 7633.

THE ROLE OF FOOD PATCHES IN MAINTAINING HIGH DEEP-SEA DIVERSITY: FIELD EXPERIMENTS USING HYDRODYNAMICALLY UNBIASED COLONIZATION TRAYS

P. V. R. Snelgrove, J. F. Grassle and R. F. Petrecca

To test the hypothesis that deep-sea macrofaunal diversity is enhanced by specialization on small scale patches of food, colonization trays were deployed by a submersible at 900 m depth south of St. Croix. Trays were buried flush with the seafloor to minimize potential hydrodynamic bias that has generated criticism of previous deep-sea colonization studies. Treatments in trays included unenriched, prefrozen, natural sediment and similar sediment enriched with either the diatom Thalassiosira sp. or the seaweed Sargassum sp.. After 23 days, different macrofaunal responses were observed in each of the colonization "patches", and all differed from background fauna. Density comparisons and rarefaction analysis indicate that Thalassiosira sp. attracted high densities of several species of juvenile opportunists, and Sargassum sp. trays were colonized by fewer individuals of a more diverse fauna. Unenriched trays contained much lower densities than in either of the enrichments, though diversity appeared to be considerably higher. Faunal diversity in the ambient sediment was considerably higher than in either of the enrichment treatments, and ambient densities were considerably lower. Unenriched trays failed to attain ambient density levels. Results are consistent with a larval bottleneck hypothesis in which juveniles, rather than adults, specialize on and colonize specific patch types, thus avoiding competition and contributing to the high species diversity observed in the deep sea. This may be a fundamental difference between the highly diverse, deep-sea, macrofaunal assemblages and their much less diverse, shallow-water counterparts.

In Press: Limnology and Oceanography.

Supported by: NOAA Contract NA88AA-H-UR020, Subcontract 89-9.

WHOI Contribution No. 7407.

CYTOCHROME P450 FORMS IN FISH

John J. Stegeman

P450s play key roles in pharmacology, toxicology, carcinogenis and endocrinology. The need for understanding the functions and regulation of P450 in diverse species has not diminished, but increased, and more investigators

are recognizing that P450 functions critically in chemical-biological interactions and animal responses to man-made and natural organic chemicals. This review presents a capsule view of P450 forms in fish, dealing primarily with forms most likely involved in xenobiotic metabolism. Distinct forms of hepatic P450 have been purified or partially purified from several marine and freshwater species, including rainbow trout, scup, cod, perch and little skate. Catalytic activity with drug, carcinogen and endogenous substrates, and studies with antibodies to fish and mammalian P450s have indicated relationships between several of the fish liver P450 forms, and between fish and mammalian forms. Gene family 1: The single homologous relationship that has been established with certainty between P450 forms in fish and other vertebrates, and where the fish proteins have been studied in detail, is that involving 1A proteins (trout LM4b, trout DS-3, scup E, cod c, perch V, skate DBA-I). Gene family 2: Two fish forms now have been found to bear close immunological relationships to mammalian 2B proteins (trout LMC1 and scup B). Furthermore, the N-terminal amino acid sequence of the scup P450B is about 50% identical to the same region of rat 2B1/2. Gene family 3: Several lines of evidence including catalytic and immunological similarities indicate a relationship of teleost forms to members of subfamily 3A (trout LMC5, trout "con" and scup A). Demonstrated and suggested relationships of fish P450s are based primarily on catalytic and immunological similarities, rather than primary sequence, making classifications tenuous. Clearly, our understanding of toxicology and carcinogenesis in fish, for their own sake and as models, would benefit from greater detail on P450 diversity and structure.

In Press: Handbook of Experimental Pharmacology.

Supported by: PHS Grant ES-04220.

WHOI Contribution No. 7916.

NOMENCLATURE FOR HYDROCARBON INDUCIBLE CYTOCHROME P450 IN FISH

John J. Stegeman

A growing number of studies concerning organic chemical pollutant induction of cytochrome P450 mixed function oxidases in fish stimulates a need for common terminology. Similar names for proteins might be based on similarities in function, in regulation, and in their structure. Under the current guidelines for P450 proteins, classification is based on measured or inferred amino acid sequence. At present, a single teleost hydrocarbon-inducible P450 (rainbow trout) can

conclusively be termed 1A1; a second (scup P450E) can be so termed on the basis of partial sequence. The lack of primary sequence information makes it difficult to assign a specific identity to hydrocarbon-inducible P450s in other fish. Nevertheless, the sum of information on catalytic activities, induction and immunological cross-reactivities provides a weight of evidence sufficient to assume (but not prove) gene family (1) and subfamily (A) identities for hydrocarboninducible proteins in many species. Reference to these proteins as P4501A or (CYP1A) in fish species where sequence data are lacking is suggested as more appropriate than reference to them as P4501A1 (Or CYP1A1). Additional primary sequence data are required to further define orthologous relationships among P4501A genes in fish, and to determine whether 1A1 is a correct designation for a hydrocarbon-inducible P450 in many species.

Supported by: PHS Grant ES-04220.

WHOI Contribution No. 7887.

ENVIRONMENTAL AND HORMONAL REGULATION OF CYTOCHROME P450 1A FORMS IN FISH LIVER

John J. Stegeman, Pamela J. Kloepper-Sams and Adria A. Elskus

With demonstration that P4501A induction in fish can be closely linked to the degree of contamination by chemicals such as PCBs, induction is being tested as a marker for contamination in coastal waters, rivers and lakes around the world. Although the induction of P4501A proteins in fish has many similarities with that in mammals, there are also distinctions in how induction can be influenced by hormonal and environmental factors. These studies addressed the mechanisms by which estradiol and temperature acclimation influence the rate and magnitude of induction response in fish. Microsomal EROD activity was induced 10-fold by BNF in 16°C fish but only slightly in 6°C fish by four days after treatment. P4501A specific content measured by slot blot paralleled EROD activity, in fish at both temperatures. Although P4501A content changed little at 6°C, P4501A mRNA content was significantly elevated in these same fish, and declined only slowly. P4501A mRNA content rose and fell rapidly in 16°C animals, similar to results seen in earlier studies. The markedly different P4501A mRNA turnover and P4501A protein synthesis in cold vs. warm fish is the first indication that important effects of temperature on P4501A induction in fish can occur at post-transcriptional events. A second set of studies

determined whether suppressed levels of P450IA protein in gravid female flounder were related to altered levels or translation of P450IA mRNA. Gravid female fish had much lower levels of P4501A mRNA than either spent females or ripe males, a result which mirrored the relative P4501A protein content. These data suggest that E₂ in the plasma of gravid female fish can suppress P4501A expression at a pretranslational level.

Supported by: PHS Grant ES-04220.

WHOI Contribution No. 7876.

IMMUNOHISTOCHEMICAL LOCALIZATION OF ENVIRONMENTALLY INDUCED CYTOCHROME P450IA1 IN MULTIPLE ORGANS OF THE MARINE TELEOST STENOTOMUS CHRYSOPS (SCUP)

John J. Stegeman, Roxanna M. Smolowitz, and Mark E. Hahn

Differences in expression of cytochrome P450 forms and their functions in different organs and cell types could determine the response of those cells and organs to xenobiotics. Recently, we described the cellular localization of the hydrocarbon-inducible cytochrome P450E (P450IA1) induced in 10 organs or organ systems of the fish, Stenotomus chrysops (Scup) treated with 3,3',4,4'-tetrachlorobiphenyl (TCB) or with 2,3,7,8-tetrachlorodibenzofuran (TCDF) (Drug. Metab. Dispos. 19:113,1991). Here we describe the presence and localization of P450IA1 in organs of scup sampled directly from an environment contaminated by chlorinated biphenyls and dibenzofurans, the outer New Bedford Harbor of Massachusetts. Western blot analysis of microsomes from selected organs (liver, kidney, gill and heart), using monoclonal antibody 1-12-3, revealed induced levels of P450IA1 in each. The localization of P450IA1 in these and other organs was determined in sections prepared by standard histological methods and stained with MAb 1-12-3 and peroxidase-labeled second antibody. P450IA1 was detected in multiple cell types in liver, including hepatic, pancreatic and vascular tissue. Kidney and gut also showed prominent P450IA1 levels in epithelial structures and in vascular endothelial cells. Specific staining was detected in endothelial cells, but not other cell types, in heart. gill, spleen, testis, ovary, nose and brain. In heart, the staining was present in the endocardium of atrium and ventricle, and endothelium of the coronary vasculature and great vessels. The results demonstrate that P450IA proteins are induced by environmental chemicals in many organs of fish exposed in the wild, with patterns of cellular

localization like those seen in fish experimentally treated with known inducers. The strong staining of P450IA1 in endothelial cells in all organs examined supports experimental results indicating that endothelium is a major site of P450IA1 induction. Our results indicate further that immunohistochemistry is a useful method for detecting P450 induction as a biomarker for exposure.

Published in: Toxicology and Applied Pharmacology, 110:486-504, 1991.

Supported by: PHS Grants ES-04220 and CA-44306; EPA Cooperative Agreement CR181355; and the Donaldson Charitable Trust.

WHOI Contribution No. 7662.

VIDEO SYSTEMS FOR IN SITU STUDIES OF ZOOPLANKTON

J. Rudi Strickler, Peter C. Schulze, Bo I. Bergström, Mark S. Berman, Percy Donaghay, Scott Gallager, James F. Haney, Bruce R. Hargraves, Uwe Kils, Gustav -A. Paffenhöfer, Sumner Richman, Henry A. Vanderploeg, Wolfgang Welsch, David Wethey, and Jeannette Yen

A variety of survey instruments and systems designed for measuring the behavior of individual zooplankton have been built around video technology. Several video systems have already collected novel behavioral observations. If the survey tools under development achieve their potential they will dramatically exceed the spatial and temporal resolution of conventional sampling methods, and also collect taxonomic information that is not available from acoustic systems or the Optical Plankton Counter. Furthermore, if they are successful, these new survey devices will reduce the amount of human effort required for data processing. This paper (i) describes a variety of video systems for studying zooplankton in situ; (ii) discusses their common design considerations and technical challenges to further development; and (iii) compares the present and future capabilities of video devices with other methods of studying zooplankton in situ.

Supported by: NSF Grant OCE90-12657.

WHOI Contribution No. 7936.

CYTOCHROME P4501A IN HEPATIC LESIONS OF A TELEOST FISH (FUNDULUS HETEROCLITUS) COLLECTED FROM A POLYCYCLIC AROMATIC HYDROCARBON-CONTAMINATED SITE

P. A. Van Veld, W. K. Vogelbein, R. Smolowitz, B. R. Woodin, and J. J. Stegeman

The expression of cytochrome P4501A was examined in hepatic lesions of mummichog (Fundulus heteroclitus), a small, nonmigratory teleost fish collected from a site in the Elizabeth River VA heavily contaminated with polycyclic aromatic hydrocarbons (PAH) of creosote origin. Immunoblot ("Western" blot) analysis using monoclonal antibody (Mab 1-12-3) to P4501A of the marine fish Stenotomus chrysops indicated that cytochrome P4501A levels in hepatocellular carcinoma and in foci of cellular alteration were 20-85% lower than those of adjacent non-neoplastic tissue. P4501A-dependent monooxygenase activity, measured as ethoxyresorufin O-deethylase (EROD), exhibited a similar trend with EROD activity in lesions being 15-77% lower than activity in non-neoplastic tissue. Immunohistochemical examination of liver sections revealed general low intensity P4501A-associated staining in hepatocellular carcinoma, exocrine pancreatic tissue, bile ducts, and cholangiocellular proliferative lesions. Staining intensity of non-neoplastic hepatic parenchyma varied considerably and was focally distributed. In one case intense staining was observed in an altered hepatocellular focus (putative preneoplastic lesion). The results indicate important similarities in the expression of P4501A in neoplasms of fish and mammals and suggest an adaptive response of a wild population to carcinogen exposure.

Supported by: Donaldson Charitable Trust: and PHS Grant ES-04220.

WHOI Contribution No. 7917.

BUOYANCY PROPERTIES OF THE GIANT DIATOM ETHMODISCUS

Tracy A. Villareal

Net-collected Ethmodiscus spp. were examined to determine their potential for positive buoyancy in the southwestern North Atlantic Ocean in January and April, 1990. Ethmodiscus cells were capable of positive buoyancy with ascent rates averaging 1.4 m hr⁻¹ on individually measured cells, and 0.3 m hr⁻¹ using a homogeneous settling technique. Negatively buoyant living cells of Ethmodiscus were observed, and this observation

provides further evidence that depth-keeping and vertical migration mechanisms documented in the non-motile dinoflagellate *Pyrocystis* may also occur in diatoms.

In Press: Journal of Plankton Research, 14(3), 1991. Supported by: NSF Grants OCE87-10798 and OCE88-16584.

WHOI Contribution No. 7653.

MARINE NITROGEN-FIXING DIATOM-CYANOBACTERIA SYMBIOSES

Tracy A. Villareal

This review summarizes growth and nitrogen-fixation data on diatom cyanobacteria symbioses. These symbiotic associations between diatoms and filamentous cyanobacteria are frequently noted in tropical and subtropical waters, and direct evidence indicates that at least two associations are diazotrophic. Abundance data is limited, but Rhizosolenia-Richelia blooms are recorded from the central Pacific gyre at up to 10⁴ cells L-1. In situ growth rates of these associations are not known, but laboratory data on the Rhizosolenia-Richelia symbiosis suggests the host-symbiont association can reproduce at approximately 0.8-1.0 div day⁻¹. Growth kinetics in nitrogen-poor medium suggest that transfer of fixed nitrogen from host to symbiont occurs and that this process can support the host's growth under N- limiting conditions. Additional symbioses, particularly in Hemiaulus may be more widespread than previously realized due to the difficulty in identifying the symbiont in standard light microscopy. Few field measurements of N₂-fixation are available for these associations. Rhizosolenia-Richelia appears to be locally important in the central Pacific gyre. Hemiaulus spp. are a common and abundant diatom in oligotrophic seas, and if 80-100% of the cells are symbiotic as reported, then they represent an unquantified, and potentially substantial, source of nitrogen-fixation.

In Press: NATO ASI Workshop Proceedings.

Supported by: WHOI Postdoctoral Fellowship.

WHOI Contribution No. 7802.

NITROGEN-FIXATION BY THE CYANOBACTERIAL SYMBIONT OF THE DIATOM HEMIAULUS

Tracy A. Villareal

Nitrogen-fixation by cyanobacterial symbionts in the oceanic diatoms Hemiaulus membranaceous,

H. hauckii, and H. sinensis was documented in the Southwestern Atlantic Ocean. All Hemiaulus cells with diatom chlorophyll autofluorescence contained fluorescent symbionts undetectable in standard light microscopy. Average cell-specific ethylene reduction rates (2.3-5.3 Xl0⁻¹³ M ethylene cell hr⁻¹) were 2.2-5.2 times lower than calculated rates from Rhizosolenia-Richelia blooms in the central Pacific gyre and 26 times lower than results from Richela-containing Rhizosolenia cultures. Calculations suggest that this unquantified new nitrogen source is capable of significant nitrogen inputs into oligotrophic oceanic waters.

Published in: Marine Ecology Progress Series, 76(2):201-204, 1991.

Supported by: NSF Grant OCE90-12199; and WHOI Postdoctoral Fellowship.

WHOI Contribution No. 7773.

THE CYANOBACTERIA: ISOLATION, PURIFICATION AND IDENTIFICATION

J. B. Waterbury

This review describes the major groups of cyanobacteria, their phylogeny and their physiological properties that allow them to occupy a wide range of habitats. The techniques of isolation and purification are reviewed, including collection and treatment of samples, media and growth conditions and maintenance of pure cultures. The identification of cyanobacteria in pure culture is reviewed, including the description of 27 genera and "groups" belonging to five orders. Also included are keys to the orders and genera, and illustrations showing the morphological diversity and developmental patterns of cyanobacteria.

Supported by: NSF Grant OCE89-00588. WHOI Contribution No. 7725.

SPERM WHALES TAGGED WITH TRANSPONDERS AND TRACKED UNDERWATER BY SONAR

William A. Watkins, Mary Ann Daher, Kurt M. Fristrup, Terrance J. Howald, and Giuseppe Notarbartolo di Sciara

Two of three sperm whales tagged with sonar transponder tags were tracked underwater during a cruise from 16 to 30 October 1991 in the southeast Caribbean west of Dominica Island. More than 20 dives to depths greater than 500 m were followed, including dives to 1200 m and one possibly to 2000 m. The whales were individually tracked for

periods of 3 to 13.5 hours, and both whales were relocated together four days and eight days after tagging and were tracked together for 13 hours. Every track ended because tag signals became obscured at night by dense biological scatterers concentrated in offshore areas selected by the whales for diving. Both whales apparently were males of 15 and 11 m, each dominant in different groups, but when together the larger whale was dominant (chases and agonistic vocalizations). The whales did not react to the tags or the sounds associated with tracking (30, 32, and 36 kHz). Other whales, from calves of 4.5 m to large adults, ignored the tagging and the presence of the tags.

Supported by: Laurel Foundation and other private sources.

WHOI Contribution No. 7923.

EVIDENCE FOR RAPID SPECIATION FOLLOWING A FOUNDER EVENT IN THE LABORATORY

James R. Weinberg, Victoria R. Starczak and Daniele Jörg

Due to its long duration, the entire process of speciation can rarely be observed. Consequently, there is a proliferation of untested theory and controversy about which modes of speciation occur, their relative frequencies and their accompanying genetic changes. This is the first paper to document the formation of a new marine invertebrate species where the date of the founding event, the number of founders and ancestry is known. The new polychaete species was discovered 100 generations after a founder event by six individuals. When this "laboratory" species is crossed with field populations, the offspring do not survive to maturity. Furthermore, there is partial premating isolation involving aggressive pushing, biting and head swallowing. One chromosomal mutation was detected. These results demonstrate how drastic founder events can lead to rapid speciation. This new species should be valuable for examining genetic changes responsible for pre- and postmating reproductive isolation.

In Press: Evolution.

Supported by: WHOI; and National Geographic Society Grant 4334-90.

WHOI Contribution No. 7800.

DIFFERENTIAL TRANSPORT OF SEWAGE-DERIVED NITROGEN AND PHOSPHORUS THROUGH A COASTAL WATERSHED

Peter K. Weiskel and Brian L. Howes

Changes of land use in coastal watersheds to residential development with on-site sewage disposal represent a potential change in both the quantity and quality of nutrient inputs to coastal marine systems. Measurements of dissolved N and phosphate P in septic system effluent indicated initial concentrations 100-1000-fold greater than receiving coastal waters, with inorganic N/P ratios (17/1) similar to phytoplankton growth requirements. Transformations of organic and inorganic N and retention of inorganic P occurred in the initial meters of groundwater transport with substantial (≈ 70%) nitrification of effluent ammonium to nitrate and retention of phosphate by the soil ($\approx 60\%$). The degree of initial transformation and retention was directly related to unsaturated infiltration distance, and is consistent with the requirements of these processes for oxidizing conditions. At greater distances (10-100 m) over 99% of the total dissolved N occurred as nitrate, phosphate concentrations were reduced to background levels, and groundwater N/P ratios exceeded 2500/1. The greater the importance of high-N, low-P groundwater inputs to the nutrient balance of a coastal water body, the greater the potential for shifts in the nutrient which limits primary production.

Published in: Environmental Science and Technology, 26:352-362, 1992.

Supported by: EPA No. CX812866-01-3; NOAA,
Office of Sea Grant No. NA86-AA-D-SG090; and
Jessie B. Cox Foundation.

WHOI Contribution No. 7505.

QUANTIFYING DISSOLVED NITROGEN FLUX THROUGH A COASTAL WATERSHED

Peter K. Weiskel and Brian L. Howes

Available nitrogen loading models, commonly used to estimate subsurface fluxes of dissolved nitrogen to coastal waters, have not been quantitatively or systematically compared; nor have they generally been field-verified at regional scales. We employed three published loading models, a site-specific model based upon water use data, and both Darcian and non-Darcian field approaches to obtain estimates of steady state, dissolved nitrogen flux through a permeable Massachusetts watershed. The two field

approaches, based on independent data, yielded similar results. Results of the published loading models agreed closely with each other, but exceeded the mean of the field approaches (130 ± 12 mol N m⁻¹ aquifer width yr⁻¹ by 60%, on average. The Water Use loading model agreed closely with the field results (within 4%), largely because it did not require estimates of occupancy rate, which was found to be the major source of error to the published models. The observed, median concentration of total dissolved nitrogen (TDN) in groundwater increased from 1.9 to 313 μM during transport through the subbasin, confirming loading model predictions that >99% of the TDN flux is anthropogenic. In contrast to the watershed inputs, downgradient TDN was dominantly nitrate (98%), indicating near-complete nitrification during transport. Significant transverse horizontal and vertical variations were found in the groundwater TDN distribution at scales of meters and tenths of meters, respectively, consistent with a large number of discrete nitrogen sources at the ground surface, and low transverse macrodispersivities in the aquifer. Loading models, if properly verified by field measurements at the stream tube scale, hold promise for characterizing the effects of land use on subsurface nitrogen flux through coastal watersheds.

Published in: Water Resources Research, 21:2929-2939, 1991.

Supported by: EPA No. CX812886-01-3; NSF Grant BSR87-17701; and NOAA, Office of Sea Grant NA86-AA-D-SG090.

WHOI Contribution No. 7506.

CHEMOSYNTHETIC MICROBIAL ACTIVITY AT MID-ATLANTIC RIDGE HYDROTHERMAL VENT SITES

Carl O. Wirsen, Holger W. Jannasch and Stephen J. Molyneaux

Chemosynthetic activity of free living microbes at the Mid-Atlantic Ridge (MAR) vent sites at 23° and 26° N is generally higher than that measured at various East Pacific Rise (EPR) vent sites. It is carried out primarily by cells in warm water emissions, by loosely rock-attached flocculent material, by dense morphologically diverse bacterial mats covering the surfaces of polymetal sulfide deposits and by filamentous microbes on the carapaces of shrimp (Rimicarus exoculata), dominating the macrofauna at the MAR vent sites. The bacterial mats on polymetal sulfide surfaces contain unicellular and filamentous bacteria which appear to use as their chemolithotrophic electron or energy source either dissolved reduced minerals

from vent emissions, mainly sulfur compounds, or solid metal sulfide deposits, mainly pyrite. Thermophilic chemosynthetic activity was observed in carbon dioxide fixation experiments and in enrichments but no thermophilic aerobic sulfur oxidizers could be isolated. Both obligate and facultative chemoautotrophs growing at mesophilic temperatures were isolated from all chemosynthetically active surface scrapings. The obligate autotrophs could oxidize sterilized MAR natural sulfide deposits as well as technical pyrite at near neutral pH, in addition to dissolved reduced sulfur compounds. While the grazing by shrimp on the surface mats of MAR metal sulfide deposits has been observed and deemed important, the animals' primary occurrence in dense swarms near vent emissions suggests their feeding at these sites where conditions for chemosynthetic growth of their filamentous microbial epiflora are optimal. The data show that the transformation of geothermal energy at the massive polymetal sulfide deposits of the MAR sites follows a novel mechanism for the production of biomass as compared to the known, largely symbiotic system described for the EPR.

Supported by: NSF Grant OCE89-22854.

WHOI Contribution No. 7790.

PHYSIOLOGICAL STUDIES ON A HYPERTHERMOPHILIC ARCHAEUM FROM A GUAYMAS BASIN HYDROTHERMAL VENT

Carl O. Wirsen, Toshihiro Hoaki, Tadashi Maruyama and Holger W. Jannasch

A new hyperthermophilic archaeum (archaebacterium), isolated from a deep-sea vent field, is being characterized and compared to the sulfur-dependent genus *Desulfurococcus* with emphasis on nutritional requirements.

Supported by: NSF Grant OCE89-22854; and ONR Grant N00014-91-J-1751.

WHOI Contribution No. 7880.

SUBJECT HEADING INDEX Department of Biology 1991

ANIMAL BEHAVIOR
Cabell S. Davis, Glenn R. Flierl, P. H. Wiebe and P. J. S. Franks
Cabell S. Davis, Scott M. Gallager and Andrew R. SolowB-
Scott M. GallagerB-1
Scott M. GallagerB-1
Scott M. Gallager, John B. Waterbury and Diane K. StoeckerB-1
G. R. Harbison B-1
R. J. Larson, G. I. Matsumoto, L. P. Madin and L. M. Lewis
Phillip S. Lobel B-1
Karen E. Moore, William A. Watkins and Peter TyackB-1
J. Rudi Strickler, Peter C. Schulze, Bo I. Bergström, Mark S. Berman, Percy Donaghay, Scott Gallager James F. Haney, Bruce R. Hargreaves, Uwe Kils, Gustav - S. Paffenhöefer, Sumner Richman, Henry A. Vanderploeg, Wolfgang Welsch, David Wethey, and Jeunnette Yen
William A. Watkins, Mary Ann Daher, Kurt M. Fristrup, Terrance J. Howald and
Giuseppe Notarbartolo di Sciara
James R. Weinberg, Victoria R. Starczak and Daniel Jorg
BENTHIC ECOLOGY
Noellette Conway, Brian Howes, Judith McDowell Capuzzo, Ruth Turner and Colleen Cavanaugh B-
Scott M. GallagerB-1
Scott M. GallagerB-1
Scott M. Gallager, John B. Waterbury and Diane K. Stoecker
C. Sancetta, T. Villareal and P. Falkowski
James R. Weinberg, Victoria R. Starczak and Daniel Jörg
PFNTHOS
John W. Farrington, John M. Teal, Bruce W. Tripp and Curtis Phinney
Amélie H. ScheltemaB-1
Rudolf S. ScheltemaB-3
P. V. R. Snelgrove, J. F. Grassle and R. F. Petrecca
James R. Weinberg, Victoria R. Starczak and Daniel Jörg
BIOACOUSTICS
Scott M. Gallager B-1
Phillip S. Lobel B-1
Karen E. Moore, William A. Watkins and Peter Tyack
William A. Watkins, Mary Ann Daher, Kurt M. Fristrup, Terrance J. Howald and
Giuseppe Notarbartolo di SciaraB-2
BIOCHEMISTRY
Chris W. Cody, Douglas C. Prasher, William M. Westler, Franklyn G. Prendergast, and William W. Ward
Edward F. DeLongB.
A. A. Elskus, R. J. Pruell and J. J. Stegeman

P. V. R. Snelgrove, J. F. Grassle and R. F. Petrecca	B-21
John J. Stegeman, Pamela J. Kloepper-Sams and Adria A. Elskus	B-22
John J. Stegeman, R.oxanna M. Smolowitz and Mark E. Hahn	B-22
J. Rudi Strickler, Peter C. Schulze, Bo I. Bergström, Mark S. Berman, Percy Donaghay, Sco James F. Haney, Bruce R. Hargreaves, Uwe Kils, Gustav - S. Paffenhöefer, Sumner Ric Henry A. Vanderploeg, Wolfgang Welsch, David Wethey, and Jeannette Yen	ott Gallager, chman, B-23
Peter K. Weiskel and Brian L. Howes	B-25
Peter K. Weiskel and Brian L. Howes	B-25
BIOTECHNOLOGY	
Edward F. DeLong	B-6
Holger W. Jannasch, Craig C. Taylor and Linda R. Hare	B-14
COMMUNITY ECOLOGY	
UG. Berninger, D. A. Caron, R. W. Sanders and B. J. Finlay	B-2
David A. Caron, Ee Lin Lim, Geraldine Miceli, John B. Waterbury and Frederica W. Valois	
Hal Caswell and Joel E. Cohen	
Cabell S. Davis, Scott M. Gallager and Andrew R. Solow	
Cabell S. Davis, Scott M. Gallager, Mark S. Berman, Loren R. Haury and J. Rudi Strickler.	
John W. Farrington, John M. Teal, Bruce W. Tripp and Curtis Phinney	
C. Sancetta, T. Villareal and P. Falkowski	
J. Rudi Strickler, Peter C. Schulze, Bo I. Bergström, Mark S. Berman, Percy Donaghay, Sco James F. Haney, Bruce R. Hargreaves, Uwe Kils, Gustav - S. Paffenhöefer, Sumner Ric Henry A. Vande: ploeg, Wolfgang Welsch, David Wethey, and Jeannette Yen	
Tracy A. Villareal	
Peter K. Weiskel and Brian L. Howes	B-25
DESCRIPTIVE/FUNCTIONAL MORPHOLOGY	
Andrea L. Arenovski and Brian L. Howes	B-1
Carol E. Diebel	
Scott M. Gallager	
G. R. Harbison	
R. J. Larson, G. I. Matsumoto, L. P. Madin and L. M. Lewis	
P. S. Lobel, W. Harder and E. K. V. Kalko	
ECOSYSTEM STUDIES	
Andrea L. Arenovski and Brian L. Howes	R_1
UG. Berninger, D. A. Caron, R. W. Sanders and B. J. Finlay	
Cabell S. Davis and Philip Alatalo	
Cabell S. Davis, Glenn R. Flierl, P. H. Wiebe and P. J. S. Franks	
Cabell S. Davis, Scott M. Gallager and Andrew R. Solow	
Cabell S. Davis, Scott M. Gallager, Mark S. Berman, Loren R. Haury and J. Rudi Strickler.	
Edward F. DeLong	
Edward F. DeLong.	D-0
John W. Farrington, John M. Teal, Bruce W. Tripp and Curtis Phinney	De
Peter K. Weiskel and Brian L. Howes	
F MIN TO THE METERS OF THE PROPERTY OF THE PRO	B-9
reset n. weiskei and orian L. nowes	B-9
EVOLUTION	B-9

Edward F. DeLong	B-6
Edward F. DeLong	B-6
Mark E. Hahn, Alan Poland, Ed Glover and John J. Stegeman	B-12
Mark E. Hahn and John J. Stegeman	В-12
G. R. Harbison	B-13
Dennis J. O'Kane and Douglas C. Prasher	B-18
Rudolf S. Scheltema	В-19
James R. Weinberg, Victoria R. Starczak and Daniel Jörg	B-25
<u>FISHERIES</u>	
Donald M. Anderson and Bruce A. Keafer	B-1
Cabell S. Davis, Glenn R. Flierl, P. H. Wiebe and P. J. S. Franks	B-4
Cabell S. Davis, Scott M. Gallager, Mark S. Berman, Loren R. Haury and J. Rudi Strickler	B-5
Andrew J. Read	B-18
<u>FISHES</u>	
Cabell S. Davis, Glenn R. Flierl, P. H. Wiebe and P. J. S. Franks	B-4
A. A. Elskus, R. J. Pruell and J. J. Stegeman	B-9
John W. Farrington, John M. Teal, Bruce W. Tripp and Curtis Phinney	
K. Fent and J. Stegeman	B-9
Karl Fent and John J. Stegeman	B-9
Mark E. Hahn, Alan Poland, Ed Glover and John J. Stegeman	B-12
Mark E. Hahn and John J. Stegeman	B-12
Phillip S. Lobel	B-16
P. S. Lobel, W. Harder and E. K. V. Kalko	B-16
John J. Stegeman	B-21
John J. Stegeman	B-21
John J. Stegeman, Pamela J. Kloepper-Sams and Adria A. Elskus	B-22
John J. Stegeman, Rozanna M. Smolowitz and Mark E. Hahn	B-22
J. Rudi Strickler, Peter C. Schulze, Bo I. Bergström, Mark S. Berman, Percy Donaghay, Scott James F. Haney, Bruce R. Hargreaves, Uwe Kils, Gustav - S. Paffenhöefer, Sumner Rich Henry A. Vanderploeg, Wolfgang Welsch, David Wethey, and Jeannette Yen	Gallager, man, B-23
P. A. Van Veld, W. K. Vogelbein, R. Smolowitz, B. R. Woodin and J. J. Stegeman	B-23
GENETICS	
Edward F. DeLong	B-6
Paul V. Dunlap	B-8
E.A. Meighen and P. V. Dunlap	
Douglas C. Prasher, Virginia K. Eckenrode, William W. Ward, Frank G. Prendergast, and	· · · · · · · ·
Milton J. Cormier	
Rudolf S. Scheltema	
James R. Weinberg, Victoria R. Starczak and Daniel Jörg	B-25
INSTRUMENTATION	
Cabell S. Davis and Philip Alatalo	B-4
Cabell S. Davis, Scott M. Gallager and Andrew R. Solow	B-5
Cabell S. Davis, Scott M. Gallager, Mark S. Berman, Loren R. Haury and J. Rudi Strickler	B-5
P. V. R. Snelgrove, I. F. Grassle and R. F. Petrecca	B_21

Cabell S. Davis and Philip Alatalo. Cabell S. Davis, Scott M. Gallager and Andrew R. Solow. B-5 Scott M. Gallager. Scott M. Gallager. Scott M. Gallager. B-10 Scott M. Gallager, John B. Waterbury and Diane K. Stoecker. B-11 Rudolf S. Scheltema. B-12 MARINE MAMMALS Mark E. Hahn, Alan Poland, Ed Glover and John J. Stegeman. B-13 Mark E. Hahn, Alan Poland, Ed Glover and John J. Stegeman. B-14 Andrew J. Read. William A. Watkins, Mary Ann Daher, Kurt M. Fristrup, Terrance J. Howald and Giuseppe Notarbartolo di Sciara. B-24 MARINE POLLUTION A. A. Elskus, R. J. Pruell and J. J. Stegeman. B-9 K. Fent and J. J. Stegeman. B-9 K. Fent and John J. Stegeman. B-9 Mark E. Hahn, Alan Poland, Ed Glover and John J. Stegeman. B-12 Mark E. Hahn, Alan Poland, Ed Glover and John J. Stegeman. B-12 Mark E. Hahn, Alan Poland, Ed Glover and John J. Stegeman. B-12 Mark E. Hahn, Alan Poland, Ed Glover and John H. Duff. B-10 John J. Stegeman, Rozanna M. Smolowitz and Mark E. Hahn B-12 Mark E. Hahn and John J. Stegeman. B-14 Mark E. Hahn and John J. Stegeman. B-15 MATHE M. Weiskel and Brian L. Howes and John H. Duff. B-20 John J. Stegeman, Rozanna M. Smolowitz and Mark E. Hahn B-22 P. A. Van Veld, W. K. Vogelbein, R. Smolowitz, B. R. Woodin and J. J. Stegeman B-13 MATHEMATICAL ECOLOGY Hal Cawell and Joel E. Cohen. B-3 MICROBIAL ECOLOGY UG. Berninger, D. A. Caron, R. W. Sanders and B. J. Finlay. B-2	J. Rudi Strickler, Peter C. Schulze, Bo I. Bergstrom, Mark S. Berman, Percy Donaghay, Scott (James F. Haney, Bruce R. Hargreaves, Uwe Kils, Gustav - S. Paffenhöefer, Sumner Richm: Henry A. Vanderploeg, Wolfgang Welsch, David Wethey, and Jeannette Yen	iallager, an, B-23
Cabell S. Davis, Scott M. Gallager, Mark S. Berman, Loren R. Haury and J. Rudi Strickler Cabell S. Davis, Clenn R. Flierl, P. H. Wiebe and P. J. S. Franks B-4 Cabell S. Davis, Scott M. Gallager and Andrew R. Solow B-5 Scott M. Gallager B-10 P. V. R. Snelgrove, J. F. Grassle and R. F. Petrecca B-11 Rudolf S. Scheltema B-19 P. V. R. Snelgrove, J. F. Grassle and R. F. Petrecca B-21 LIFE HISTORY Cabell S. Davis and Philip Alatalo. B-4 Cabell S. Davis and Philip Alatalo. B-5 Scott M. Gallager B-10 Scott M	LARVAL FCOLOGY	
Cabell S. Davis, Glenn R. Flierl, P. H. Wiebe and P. J. S. Franks. Cabell S. Davis, Scott M. Gallager and Andrew R. Solow. B-5 Scott M. Gallager. B-10 Scott M. Gallager. B-10 Scott M. Gallager. B-11 Rudolf S. Scheltema. B-12 Rudolf S. Scheltema. B-19 P. V. R. Snelgrove, J. F. Grassle and R. F. Petrecca. B-12 LIFE HISTORY Cabell S. Davis and Philip Alatalo. Cabell S. Davis and Philip Alatalo. Cabell S. Davis and Philip Alatalo. B-4 Cabell S. Davis and Philip Alatalo. B-5 Scott M. Gallager. B-10 Scott M. Gallager. B-10 Scott M. Gallager. B-10 Scott M. Gallager. B-11 Rudolf S. Scheltema B-19 MARINE MAMMALS Mark E. Hahn, Alan Poland, Ed Glover and John J. Stegeman. B-12 Karen E. Moore, William A. Watkins and Peter Tyack. B-14 Andrew J. Read. B-15 MARINE POLLUTION A. A. Elskus, R. J. Pruell and J. J. Stegeman. B-24 MARINE POLLUTION A. A. Elskus, R. J. Pruell and J. J. Stegeman. B-9 John W. Farrington, John M. Teal, Bruce W. Tripp and Curtis Phinney. B-9 K. Fent and J. J. Stegeman. B-12 Richard L. Smith, Brian L. Howes and John H. Duff. B-20 John J. Stegeman, Rozanna M. Smolowitz and Mark E. Hahn. B-22 Peter K. Weiskel and Brian L. Howes B-25 MATHEMATICAL ECOLOGY Hal Caswell and Joel E. Cohen. Cabell S. Davis, Glenn R. Flierl, P. H. Wiebe and P. J. S. Franks MICROBIAL ECOLOGY UG. Berninger, D. A. Caron, R. W. Sanders and B. J. Finlay. B-24 MICROBIAL ECOLOGY UG. Berninger, D. A. Caron, R. W. Sanders and B. J. Finlay. B-25 MICROBIAL ECOLOGY UG. Berninger, D. A. Caron, R. W. Sanders and B. J. Finlay. B-26 MICROBIAL ECOLOGY UG. Berninger, D. A. Caron, R. W. Sanders and B. J. Finlay. B-26 MICROBIAL ECOLOGY UG. Berninger, D. A. Caron, R. W. Sanders and B. J. Finlay. B-26 MICROBIAL ECOLOGY UG. Berninger, D. A. Caron, R. W. Sanders and B. J. Finlay.		R_5
Cabell S. Davis, Scott M. Gallager and Andrew R. Solow B-5 Scott M. Gallager B-10 Scott M. Gallager B-10 Scott M. Gallager John B. Waterbury and Diane K. Stoecker B-11 Rudolf S. Scheltema B-19 P. V. R. Snelgrove, J. F. Grassle and R. F. Petrecca B-21 LIFE HISTORY Cabell S. Davis and Philip Alatalo. B-4 Cabell S. Davis, Scott M. Gallager and Andrew R. Solow B-5 Scott M. Gallager B-10 Sco		
Scott M. Gallager. Scott M. Gallager. B-10 Scott M. Gallager, John B. Waterbury and Diane K. Stoecker. B-11 Rudolf S. Scheltema B-19 P. V. R. Snelgrove, J. F. Grassle and R. F. Petrecca B-21 LIFE HISTORY Cabell S. Davis and Philip Alatalo. B-4 Cabell S. Davis and Philip Alatalo. B-5 Scott M. Gallager. B-10 Scott M. Gallager. B-11 Rudolf S. Scheltema B-19 MARINE MAMMALS Mark E. Hahn, Alan Poland, Ed Glover and John J. Stegeman B-12 Karen E. Moore, William A. Watkins and Peter Tyack. B-13 William A. Watkins, Mary Ann Daher, Kurt M. Fristrup, Terrance J. Howald and Giusseppe Notorbartolo di Sciara. MARINE POLLUTION A. A. Elskus, R. J. Pruell and J. J. Stegeman B-9 K. Fent and J. J. Stegeman B-9 K. Fent and J. J. Stegeman B-9 Mark E. Hahn, Alan Poland, Ed Glover and John J. Stegeman B-12 Richard L. Smith, Brian L. Howes and John H. Duff B-12 B-14 B-15 B-16 B-17 B-18 B-18 B-19 B-19 B-19 B-19 B-19 B-19 B-20 B-21 B-21 B-21 B-21 B-22 B-21 B-22 B-23 B-24 B-24 B-24 B-24 B-25 B-25 B-26 B-26 B-26 B-27 B-27 B-28 B-28 B-28 B-29 B-29 B-29 B-29 B-20 B-21 B-20 B-21 B-21 B-22 B-21 B-22 B-23 B-24 B-24 B-24 B-25 B-26 B-26 B-27 B-27 B-28 B-28 B-28 B-29 B-29 B-29 B-29 B-29 B-20 B-20 B-21 B-20 B-21 B-21 B-22 B-23 B-24 B-24 B-26 B-26 B-27 B-27 B-28 B-28 B-28 B-29 B-29 B-29 B-29 B-29 B-20 B-20 B-20 B-21 B-20 B-21 B-20 B-21 B-21 B-22 B-23 B-24 B-24 B-26 B-26 B-27 B-27 B-28 B-28 B-28 B-29 B-28 B-29 B-29 B-29 B-29 B-29 B-29 B-29 B-29	•	
Scott M. Gallager	-	
Scott M. Gallager, John B. Waterbury and Diane K. Stoecker. B-11 Rudolf S. Scheltema B-19 P. V. R. Snelgrove, J. F. Grassle and R. F. Petrecca. B-21 LIFE HISTORY Cabell S. Davis and Philip Alatalo. Cabell S. Davis, Scott M. Gallager and Andrew R. Solow B-5 Scott M. Gallager. B-10 Scott M. Gallager. B-10 Scott M. Gallager, John B. Waterbury and Diane K. Stoecker B-11 Rudolf S. Scheltema B-19 MARINE MAMMALS Mark E. Hahn, Alan Poland, Ed Glover and John J. Stegeman B-12 Karen E. Moore, William A. Watkins and Peter Tyack. B-13 Andrew J. Read. William A. Watkins, Mary Ann Daher, Kurt M. Fristrup, Terrance J. Howald and Giuseppe Notarbartolo di Sciara. B-24 MARINE POLLUTION A. A. Elskus, R. J. Pruell and J. J. Stegeman B-9 John W. Farrington, John M. Teal, Bruce W. Tripp and Curtis Phinney B-9 Karl Fent and John J. Stegeman B-9 Mark E. Hahn, Alan Poland, Ed Glover and John J. Stegeman B-12 Richard L. Smith, Brian L. Howes and John H. Duff B-10 John J. Stegeman, Rozanna M. Smolowitz and Mark E. Hahn B-12 P. A. Van Veld, W. K. Vogelbein, R. Smolowitz and Mark E. Hahn B-12 P. A. Van Veld, W. K. Vogelbein, R. Smolowitz, B. R. Woodin and J. J. Stegeman B-15 MATHEMATICAL ECOLOGY Hal Caswell and Brian L. Howes B-26 MATHEMATICAL ECOLOGY UG. Berninger, D. A. Caron, R. W. Sanders and B. J. Finlay B-26 MICROBIAL ECOLOGY UG. Berninger, D. A. Caron, R. W. Sanders and B. J. Finlay B-26 MICROBIAL ECOLOGY UG. Berninger, D. A. Caron, R. W. Sanders and B. J. Finlay	-	
Rudolf S. Scheltema	•	
P. V. R. Snelgrove, J. F. Grassle and R. F. Petrecca. LIFE HISTORY Cabell S. Davis and Philip Alatalo. B-4 Cabell S. Davis, Scott M. Gallager and Andrew R. Solow B-5 Scott M. Gallager B-10 Scott M. Gallager. B-11 Rudolf S. Scheltema B-19 MARINE MAMMALS Mark E. Hahn, Alan Poland, Ed Glover and John J. Stegeman Karene E. Moore, William A. Watkins and Peter Tyack B-17 Andrew J. Read. William A. Watkins, Mary Ann Daher, Kurt M. Fristrup, Terrance J. Howald and Giuseppe Notarbartolo di Sciara B-24 MARINE POLLUTION A. A. Elskus, R. J. Pruell and J. J. Stegeman B-9 K. Fent and J. J. Stegeman B-9 Karl Fent and John J. Stegeman B-9 Karl Fent and John J. Stegeman B-12 Mark E. Hahn, alan Poland, Ed Glover and John H. Duff. B-12 John J. Stegeman, Rosanna M. Smolowitz and Mark E. Hahn B-12 John J. Stegeman, Rosanna M. Smolowitz and Mark E. Hahn B-12 John J. Stegeman, Rosanna M. Smolowitz and Mark E. Hahn B-12 John J. Stegeman, Rosanna M. Smolowitz and Mark E. Hahn B-12 John J. Stegeman, Rosanna M. Smolowitz and Mark E. Hahn B-12 John J. Stegeman, Rosanna M. Smolowitz, B. R. Woodin and J. J. Stegeman B-14 Mart Hematical Ecology Hal Cawell and Joel E. Cohen Cabell S. Davis, Glenn R. Flierl, P. H. Wiebe and P. J. S. Franks B-14 MICROBIAL ECOLOGY UG. Berninger, D. A. Caron, R. W. Sanders and B. J. Finlay B-2 MICROBIAL ECOLOGY UG. Berninger, D. A. Caron, R. W. Sanders and B. J. Finlay B-2 MICROBIAL ECOLOGY		
LIFE HISTORY Cabell S. Davis, Scott M. Gallager and Andrew R. Solow		
Cabell S. Davis and Philip Alatalo. Cabell S. Davis, Scott M. Gallager and Andrew R. Solow. B-5 Scott M. Gallager. Scott M. Gallager. Scott M. Gallager. B-10 Scott M. Gallager. B-10 Scott M. Gallager, John B. Waterbury and Diane K. Stoecker B-11 Rudolf S. Scheltema. B-12 MARINE MAMMALS Mark E. Hahn, Alan Poland, Ed Glover and John J. Stegeman B-12 Andrew J. Read. William A. Watkins and Peter Tyack. B-18 William A. Watkins, Mary Ann Daher, Kurt M. Fristrup, Terrance J. Howald and Giuseppe Notarbartolo di Sciara. B-24 MARINE POLLUTION A. A. Elskus, R. J. Pruell and J. J. Stegeman. B-9 K. Fent and J. J. Stegeman. B-9 K. Fent and John J. Stegeman. B-9 Mark E. Hahn, Alan Poland, Ed Glover and John J. Stegeman. B-12 Mark E. Hahn, Alan Poland, Ed Glover and John J. Stegeman. B-12 B-13 Mark E. Hahn, Alan Poland, Ed Glover and John H. Duff. B-16 B-17 B-18 B-18 B-18 B-19 B-19 B-19 B-19 B-10 B-10 B-10 B-10 B-10 B-10 B-10 B-10	1. V. It. Oncegroot, V. I. Grassic and It. I. I threeta	15-21
Cabell S. Davis, Scott M. Gallager and Andrew R. Solow. Scott M. Gallager. B-10 Scott M. Gallager. B-10 Scott M. Gallager. B-11 Rudolf S. Scheltema. B-19 MARINE MAMMALS Mark E. Hahn, Alan Poland, Ed Glover and John J. Stegeman. B-12 Karen E. Moore, William A. Watkins and Peter Tyack. B-13 Mark E. Hahn, Alan Poland, Ed Glover and John J. Stegeman. B-14 William A. Watkins, Mary Ann Daher, Kurt M. Fristrup, Terrance J. Howald and Giuseppe Notarbartolo di Sciara. B-24 MARINE POLLUTION A. A. Elskus, R. J. Pruell and J. J. Stegeman. B-9 John W. Farrington, John M. Teal, Bruce W. Tripp and Curtis Phinney. B-9 Karl Fent and J. J. Stegeman. B-9 Karl Fent and John J. Stegeman. B-9 Mark E. Hahn, Alan Poland, Ed Glover and John J. Stegeman. B-12 Richard L. Smith, Brian L. Howes and John H. Duff. John J. Stegeman, Rozanna M. Smolowitz and Mark E. Hahn B-22 John J. Stegeman, Rozanna M. Smolowitz and Mark E. Hahn B-23 Peter K. Weiskel and Brian L. Howes. B-25 MATHEMATICAL ECOLOGY Hal Caswell and Joel E. Cohen. B-3 Cabell S. Davis, Glenn R. Flierl, P. H. Wiebe and P. J. S. Franks. B-4 MICROBIAL ECOLOGY UG. Berninger, D. A. Caron, R. W. Sanders and B. J. Finlay. B-5 MICROBIAL ECOLOGY UG. Berninger, D. A. Caron, R. W. Sanders and B. J. Finlay. B-6 B-12 B-14 B-16 B-17 B-18 B-18 B-19 B-19 B-10 B-10 B-10 B-11 B-12 B-13 B-14 B-15 B-16 B-17 B-18 B-19 B-19 B-10 B-10 B-10 B-10 B-10 B-10 B-11 B-12 B-12 B-13 B-14 B-15 B-16 B-17 B-18 B-19 B-19 B-19 B-10	LIFE HISTORY	
Scott M. Gallager. B-10 Scott M. Gallager. B-10 Scott M. Gallager, John B. Waterbury and Diane K. Stoecker B-11 Rudolf S. Scheltema B-19 MARINE MAMMALS Mark E. Hahn, Alan Poland, Ed Glover and John J. Stegeman B-12 Karen E. Moore, William A. Watkins and Peter Tyack. B-17 Andrew J. Read. B-18 William A. Watkins, Mary Ann Daher, Kurt M. Fristrup, Terrance J. Howald and Giuseppe Notarbardolo di Sciara. B-24 MARINE POLLUTION A. A. Elskus, R. J. Pruell and J. J. Stegeman. B-9 John W. Farrington, John M. Teal, Bruce W. Tripp and Curtis Phinney. B-9 K. Fent and J. J. Stegeman B-9 Mark E. Hahn, Alan Poland, Ed Glover and John J. Stegeman B-12 Mark E. Hahn, Alan Poland, Ed Glover and John J. Stegeman B-12 Richard L. Smith, Brian L. Howes and John H. Duff. B-20 John J. Stegeman, Rozanna M. Smolowitz and Mark E. Hahn B-22 Peter K. Weiskel and Brian L. Howes. B-25 MATHEMATICAL ECOLOGY Hal Caswell and Joel E. Cohen. B-3 Cabell S. Davis, Glenn R. Flierl, P. H. Wiebe and P. J. S. Franks. B-4 MICROBIAL ECOLOGY UG. Berninger, D. A. Caron, R. W. Sanders and B. J. Finlay. B-26 MICROBIAL ECOLOGY UG. Berninger, D. A. Caron, R. W. Sanders and B. J. Finlay. B-26 MICROBIAL ECOLOGY UG. Berninger, D. A. Caron, R. W. Sanders and B. J. Finlay. B-26 MICROBIAL ECOLOGY UG. Berninger, D. A. Caron, R. W. Sanders and B. J. Finlay. B-26 MICROBIAL ECOLOGY	Cabell S. Davis and Philip Alatalo	B-4
Scott M. Gallager. B-10 Scott M. Gallager, John B. Waterbury and Diane K. Stoecker B-11 Rudolf S. Scheltema B-19 MARINE MAMMALS Mark E. Hahn, Alan Poland, Ed Glover and John J. Stegeman B-12 Karen E. Moore, William A. Watkins and Peter Tyack B-18 William A. Watkins, Mary Ann Daher, Kurt M. Fristrup, Terrance J. Howald and Giuseppe Notarbartolo di Sciara B-24 MARINE POLLUTION A. A. Elskus, R. J. Pruell and J. J. Stegeman B-9 John W. Farrington, John M. Teal, Bruce W. Tripp and Curtis Phinney B-9 K. Fent and J. J. Stegeman B-9 Mark E. Hahn, Alan Poland, Ed Glover and John J. Stegeman B-12 Mark E. Hahn, Alan Poland, Ed Glover and John J. Stegeman B-12 Mark E. Hahn, Brian L. Howes and John H. Duff B-10 John J. Stegeman, Rozanna M. Smolowitz and Mark E. Hahn B-22 P. A. Van Veld, W. K. Vogelbein, R. Smolowitz, B. R. Woodin and J. J. Stegeman B-23 Peter K. Weiskel and Brian L. Howes B-25 MATHEMATICAL ECOLOGY Hal Caswell and Joel E. Cohen B-3 Cabell S. Davis, Glenn R. Flierl, P. H. Wiebe and P. J. S. Franks B-4 MICROBIAL ECOLOGY UG. Berninger, D. A. Caron, R. W. Sanders and B. J. Finlay B-2 MICROBIAL ECOLOGY UG. Berninger, D. A. Caron, R. W. Sanders and B. J. Finlay B-2 MICROBIAL ECOLOGY UG. Berninger, D. A. Caron, R. W. Sanders and B. J. Finlay B-2	Cabell S. Davis, Scott M. Gallager and Andrew R. Solow	B-5
Scott M. Gallager, John B. Waterbury and Diane K. Stoecker B-11 Rudolf S. Scheltema B-19 MARINE MAMMALS Mark E. Hahn, Alan Poland, Ed Glover and John J. Stegeman B-12 Andrew J. Read William A. Watkins and Peter Tyack B-18 William A. Watkins, Mary Ann Daher, Kurt M. Fristrup, Terrance J. Howald and Giuseppe Notarbartolo di Sciara B-24 MARINE POLLUTION A. A. Elskus, R. J. Pruell and J. J. Stegeman B-9 John W. Farrington, John M. Teal, Bruce W. Tripp and Curtis Phinney B-9 K. Fent and J. J. Stegeman B-9 Mark E. Hahn, Alan Poland, Ed Glover and John J. Stegeman B-12 Mark E. Hahn, Alan Poland, Ed Glover and John J. Stegeman B-12 Mark E. Hahn and John J. Stegeman B-12 Mark E. Hahn, Rozanna M. Smolowitz and Mark E. Hahn B-12 John J. Stegeman, Rozanna M. Smolowitz and Mark E. Hahn B-20 John J. Stegeman, Rozanna M. Smolowitz and Mark E. Hahn B-22 P. A. Van Veld, W. K. Vogelbein, R. Smolowitz, B. R. Woodin and J. J. Stegeman B-25 MATHEMATICAL ECOLOGY Hal Caswell and Brian L. Howes B-3 MICROBIAL ECOLOGY UG. Berninger, D. A. Caron, R. W. Sanders and B. J. Finlay B-2 MICROBIAL ECOLOGY UG. Berninger, D. A. Caron, R. W. Sanders and B. J. Finlay B-14 MICROBIAL ECOLOGY UG. Berninger, D. A. Caron, R. W. Sanders and B. J. Finlay	Scott M. Gallager	B-10
MARINE MAMMALS Mark E. Hahn, Alan Poland, Ed Glover and John J. Stegeman B-12 Karen E. Moore, William A. Watkins and Peter Tyack B-18 William A. Watkins, Mary Ann Daher, Kurt M. Fristrup, Terrance J. Howald and Giuseppe Notarbartolo di Sciara B-24 MARINE POLLUTION A. A. Elskus, R. J. Pruell and J. J. Stegeman John W. Farrington, John M. Teal, Bruce W. Tripp and Curtis Phinney B-9 KAF Fent and J. J. Stegeman B-9 Karl Fent and John J. Stegeman B-12 Mark E. Hahn, Alan Poland, Ed Glover and John J. Stegeman B-12 Mark E. Hahn, and John J. Stegeman B-12 Richard L. Smith, Brian L. Howes and John H. Duff B-20 John J. Stegeman, Rozanna M. Smolowitz and Mark E. Hahn B-22 P. A. Van Veld, W. K. Vogelbein, R. Smolowitz, B. R. Woodin and J. J. Stegeman B-23 Peter K. Weiskel and Brian L. Howes B-25 MATHEMATICAL ECOLOGY Hal Caswell and Joel E. Cohen Cabell S. Davis, Glenn R. Flierl, P. H. Wiebe and P. J. S. Franks B-4 MICROBIAL ECOLOGY UG. Berninger, D. A. Caron, R. W. Sanders and B. J. Finlay B-2 MICROBIAL ECOLOGY UG. Berninger, D. A. Caron, R. W. Sanders and B. J. Finlay B-2 B-12 B-12 B-13 B-14 B-16 B-17 B-19 B	Scott M. Gallager	B-10
MARINE MAMMALS Mark E. Hahn, Alan Poland, Ed Glover and John J. Stegeman	Scott M. Gallager, John B. Waterbury and Diane K. Stoecker	B-11
Mark E. Hahn, Alan Poland, Ed Glover and John J. Stegeman B-12 Karen E. Moore, William A. Watkins and Peter Tyack B-17 Andrew J. Read. B-18 William A. Watkins, Mary Ann Daher, Kurt M. Fristrup, Terrance J. Howald and Giuseppe Notarbartolo di Sciara. MARINE POLLUTION A. A. Elskus, R. J. Pruell and J. J. Stegeman. B-9 John W. Farrington, John M. Teal, Bruce W. Tripp and Curtis Phinney. B-9 K. Fent and J. J. Stegeman. B-9 Karl Fent and John J. Stegeman. B-12 Mark E. Hahn, Alan Poland, Ed Glover and John J. Stegeman. B-12 Mark E. Hahn and John J. Stegeman. B-12 Richard L. Smith, Brian L. Howes and John H. Duff. B-20 John J. Stegeman, Rozanna M. Smolowitz and Mark E. Hahn B-22 P. A. Van Veld, W. K. Vogelbein, R. Smolowitz, B. R. Woodin and J. J. Stegeman B-23 Peter K. Weiskel and Brian L. Howes. B-25 MATHEMATICAL ECOLOGY Hal Caswell and Joel E. Cohen. B-3 Cabell S. Davis, Glenn R. Flierl, P. H. Wiebe and P. J. S. Franks B-4 MICROBIAL ECOLOGY UG. Berninger, D. A. Caron, R. W. Sanders and B. J. Finlay. B-2 B-2 MICROBIAL ECOLOGY B-2 B-2 MICROBIAL ECOLOGY UG. Berninger, D. A. Caron, R. W. Sanders and B. J. Finlay. B-2 B-2 B-2 B-2 B-2 B-2 B-2 B-2 B-2 B-	Rudolf S. Scheltema	B-19
Mark E. Hahn, Alan Poland, Ed Glover and John J. Stegeman B-12 Karen E. Moore, William A. Watkins and Peter Tyack B-17 Andrew J. Read. B-18 William A. Watkins, Mary Ann Daher, Kurt M. Fristrup, Terrance J. Howald and Giuseppe Notarbartolo di Sciara. MARINE POLLUTION A. A. Elskus, R. J. Pruell and J. J. Stegeman. B-9 John W. Farrington, John M. Teal, Bruce W. Tripp and Curtis Phinney. B-9 K. Fent and J. J. Stegeman. B-9 Karl Fent and John J. Stegeman. B-12 Mark E. Hahn, Alan Poland, Ed Glover and John J. Stegeman. B-12 Mark E. Hahn and John J. Stegeman. B-12 Richard L. Smith, Brian L. Howes and John H. Duff. B-20 John J. Stegeman, Rozanna M. Smolowitz and Mark E. Hahn B-22 P. A. Van Veld, W. K. Vogelbein, R. Smolowitz, B. R. Woodin and J. J. Stegeman B-23 Peter K. Weiskel and Brian L. Howes. B-25 MATHEMATICAL ECOLOGY Hal Caswell and Joel E. Cohen. B-3 Cabell S. Davis, Glenn R. Flierl, P. H. Wiebe and P. J. S. Franks B-4 MICROBIAL ECOLOGY UG. Berninger, D. A. Caron, R. W. Sanders and B. J. Finlay. B-2 B-2 MICROBIAL ECOLOGY B-2 B-2 MICROBIAL ECOLOGY UG. Berninger, D. A. Caron, R. W. Sanders and B. J. Finlay. B-2 B-2 B-2 B-2 B-2 B-2 B-2 B-2 B-2 B-	AAA DINIT AAAAAAA C	
Karen E. Moore, William A. Watkins and Peter Tyack B-17 Andrew J. Read B-18 William A. Watkins, Mary Ann Daher, Kurt M. Fristrup, Terrance J. Howald and Giuseppe Notarbartolo di Sciara B-24 MARINE POLLUTION A. A. Elskus, R. J. Pruell and J. J. Stegeman B-9 John W. Farrington, John M. Teal, Bruce W. Tripp and Curtis Phinney B-9 K. Fent and J. J. Stegeman B-9 Karl Fent and John J. Stegeman B-9 Mark E. Hahn, Alan Poland, Ed Glover and John J. Stegeman B-12 Mark E. Hahn and John J. Stegeman B-12 Richard L. Smith, Brian L. Howes and John H. Duff B-20 John J. Stegeman, Rozanna M. Smolowitz and Mark E. Hahn B-20 John J. Stegeman, Rozanna M. Smolowitz and Mark E. Hahn B-22 P. A. Van Veld, W. K. Vogelbein, R. Smolowitz, B. R. Woodin and J. J. Stegeman B-23 Peter K. Weiskel and Brian L. Howes B-25 MATHEMATICAL ECOLOGY Hal Caswell and Joel E. Cohen B-3 Cabell S. Davis, Glenn R. Flierl, P. H. Wiebe and P. J. S. Franks B-4 MICROBIAL ECOLOGY UG. Berninger, D. A. Caron, R. W. Sanders and B. J. Finlay B-2		D
Andrew J. Read. William A. Watkins, Mary Ann Daher, Kurt M. Fristrup, Terrance J. Howald and Giuseppe Notarbartolo di Sciara. B-24 MARINE POLLUTION A. A. Elskus, R. J. Pruell and J. J. Stegeman. John W. Farrington, John M. Teal, Bruce W. Tripp and Curtis Phinney. E-9 K. Fent and J. J. Stegeman. B-9 K. Fent and John J. Stegeman. B-12 Mark E. Hahn, Alan Poland, Ed Glover and John J. Stegeman. B-12 Mark E. Hahn and John J. Stegeman. B-12 Mark E. Hahn and John J. Stegeman. B-13 B-14 Michard L. Smith, Brian L. Howes and John H. Duff. B-20 John J. Stegeman, Rozanna M. Smolowitz and Mark E. Hahn. B-22 P. A. Van Veld, W. K. Vogelbein, R. Smolowitz, B. R. Woodin and J. J. Stegeman. B-23 Peter K. Weiskel and Brian L. Howes. B-25 MATHEMATICAL ECOLOGY Hal Caswell and Joel E. Cohen. B-3 Cabell S. Davis, Glenn R. Flierl, P. H. Wiebe and P. J. S. Franks. B-4 MICROBIAL ECOLOGY UG. Berninger, D. A. Caron, R. W. Sanders and B. J. Finlay. B-2		
William A. Watkins, Mary Ann Daher, Kurt M. Fristrup, Terrance J. Howald and Giuseppe Notarbartolo di Sciara		
MARINE POLLUTION A. A. Elskus, R. J. Pruell and J. J. Stegeman. B-9 John W. Farrington, John M. Teal, Bruce W. Tripp and Curtis Phinney. B-9 K. Fent and J. J. Stegeman. B-9 Karl Fent and John J. Stegeman. B-12 Mark E. Hahn, Alan Poland, Ed Glover and John J. Stegeman. B-12 Mark E. Hahn and John J. Stegeman. B-12 Richard L. Smith, Brian L. Howes and John H. Duff. B-20 John J. Stegeman, Roxanna M. Smolowitz and Mark E. Hahn B-22 P. A. Van Veld, W. K. Vogelbein, R. Smolowitz, B. R. Woodin and J. J. Stegeman. B-23 Peter K. Weiskel and Brian L. Howes. B-25 MATHEMATICAL ECOLOGY Hal Caswell and Joel E. Cohen. B-3 Cabell S. Davis, Glenn R. Flierl, P. H. Wiebe and P. J. S. Franks. B-4 MICROBIAL ECOLOGY UG. Berninger, D. A. Caron, R. W. Sanders and B. J. Finlay. B-9 B-9 B-9 MICROBIAL ECOLOGY B-9 B-10 B	William A. Watkins, Mary Ann Daher, Kurt M. Fristrup, Terrance J. Howald and	
A. A. Elskus, R. J. Pruell and J. J. Stegeman. John W. Farrington, John M. Teal, Bruce W. Tripp and Curtis Phinney. B-9 K. Fent and J. J. Stegeman. B-9 Karl Fent and John J. Stegeman. B-9 Mark E. Hahn, Alan Poland, Ed Glover and John J. Stegeman. B-12 Mark E. Hahn and John J. Stegeman. B-12 Richard L. Smith, Brian L. Howes and John H. Duff. B-20 John J. Stegeman, Rozanna M. Smolowitz and Mark E. Hahn B-22 P. A. Van Veld, W. K. Vogelbein, R. Smolowitz, B. R. Woodin and J. J. Stegeman B-23 Peter K. Weiskel and Brian L. Howes B-25 Peter K. Weiskel and Brian L. Howes B-25 MATHEMATICAL ECOLOGY Hal Caswell and Joel E. Cohen. B-3 Cabell S. Davis, Glenn R. Flierl, P. H. Wiebe and P. J. S. Franks B-4 MICROBIAL ECOLOGY UG. Berninger, D. A. Caron, R. W. Sanders and B. J. Finlay. B-2		
John W. Farrington, John M. Teal, Bruce W. Tripp and Curtis Phinney. K. Fent and J. J. Stegeman. B-9 Karl Fent and John J. Stegeman. B-9 Mark E. Hahn, Alan Poland, Ed Glover and John J. Stegeman. B-12 Mark E. Hahn and John J. Stegeman. B-12 Richard L. Smith, Brian L. Howes and John H. Duff. B-20 John J. Stegeman, Rozanna M. Smolowitz and Mark E. Hahn. B-22 P. A. Van Veld, W. K. Vogelbein, R. Smolowitz, B. R. Woodin and J. J. Stegeman. B-23 Peter K. Weiskel and Brian L. Howes. B-25 Peter K. Weiskel and Brian L. Howes. B-25 MATHEMATICAL ECOLOGY Hal Caswell and Joel E. Cohen. Cabell S. Davis, Glenn R. Flierl, P. H. Wiebe and P. J. S. Franks. B-4 MICROBIAL ECOLOGY UG. Berninger, D. A. Caron, R. W. Sanders and B. J. Finlay. B-2		D o
K. Fent and J. J. Stegeman. B-9 Karl Fent and John J. Stegeman. B-9 Mark E. Hahn, Alan Poland, Ed Glover and John J. Stegeman. B-12 Mark E. Hahn and John J. Stegeman. B-12 Richard L. Smith, Brian L. Howes and John H. Duff. B-20 John J. Stegeman, Rozanna M. Smolowitz and Mark E. Hahn. B-22 P. A. Van Veld, W. K. Vogelbein, R. Smolowitz, B. R. Woodin and J. J. Stegeman. B-23 Peter K. Weiskel and Brian L. Howes. B-25 Peter K. Weiskel and Brian L. Howes. B-25 MATHEMATICAL ECOLOGY Hal Caswell and Joel E. Cohen. Cabell S. Davis, Glenn R. Flierl, P. H. Wiebe and P. J. S. Franks. B-4 MICROBIAL ECOLOGY UG. Berninger, D. A. Caron, R. W. Sanders and B. J. Finlay. B-2		
Karl Fent and John J. Stegeman. Mark E. Hahn, Alan Poland, Ed Glover and John J. Stegeman. B-12 Mark E. Hahn and John J. Stegeman. Richard L. Smith, Brian L. Howes and John H. Duff John J. Stegeman, Rozanna M. Smolowitz and Mark E. Hahn. P. A. Van Veld, W. K. Vogelbein, R. Smolowitz, B. R. Woodin and J. J. Stegeman. B-23 Peter K. Weiskel and Brian L. Howes. B-25 Peter K. Weiskel and Brian L. Howes. B-25 MATHEMATICAL ECOLOGY Hal Caswell and Joel E. Cohen. Cabell S. Davis, Glenn R. Flierl, P. H. Wiebe and P. J. S. Franks. B-4 MICROBIAL ECOLOGY UG. Berninger, D. A. Caron, R. W. Sanders and B. J. Finlay. B-2	•••	
Mark E. Hahn, Alan Poland, Ed Glover and John J. Stegeman. Mark E. Hahn and John J. Stegeman. Richard L. Smith, Brian L. Howes and John H. Duff. John J. Stegeman, Rozanna M. Smolowitz and Mark E. Hahn B-22 P. A. Van Veld, W. K. Vogelbein, R. Smolowitz, B. R. Woodin and J. J. Stegeman Peter K. Weiskel and Brian L. Howes. B-25 Peter K. Weiskel and Brian L. Howes. B-26 MATHEMATICAL ECOLOGY Hal Caswell and Joel E. Cohen. Cabell S. Davis, Glenn R. Flierl, P. H. Wiebe and P. J. S. Franks. B-4 MICROBIAL ECOLOGY UG. Berninger, D. A. Caron, R. W. Sanders and B. J. Finlay. B-2		
Mark E. Hahn and John J. Stegeman. Richard L. Smith, Brian L. Howes and John H. Duff	•	
Richard L. Smith, Brian L. Howes and John H. Duff	· · · · · · · · · · · · · · · · · · ·	
John J. Stegeman, Rozanna M. Smolowitz and Mark E. Hahn P. A. Van Veld, W. K. Vogelbein, R. Smolowitz, B. R. Woodin and J. J. Stegeman Peter K. Weiskel and Brian L. Howes Peter K. Weiskel and Brian L. Howes B-25 MATHEMATICAL ECOLOGY Hal Caswell and Joel E. Cohen Cabell S. Davis, Glenn R. Flierl, P. H. Wiebe and P. J. S. Franks B-4 MICROBIAL ECOLOGY UG. Berninger, D. A. Caron, R. W. Sanders and B. J. Finlay B-2		
P. A. Van Veld, W. K. Vogelbein, R. Smolowitz, B. R. Woodin and J. J. Stegeman. Peter K. Weiskel and Brian L. Howes. Peter K. Weiskel and Brian L. Howes. B-25 MATHEMATICAL ECOLOGY Hal Caswell and Joel E. Cohen. Cabell S. Davis, Glenn R. Flierl, P. H. Wiebe and P. J. S. Franks. B-4 MICROBIAL ECOLOGY UG. Berninger, D. A. Caron, R. W. Sanders and B. J. Finlay. B-2		
Peter K. Weiskel and Brian L. Howes. Peter K. Weiskel and Brian L. Howes. B-25 MATHEMATICAL ECOLOGY Hal Caswell and Joel E. Cohen. Cabell S. Davis, Glenn R. Flierl, P. H. Wiebe and P. J. S. Franks. B-4 MICROBIAL ECOLOGY UG. Berninger, D. A. Caron, R. W. Sanders and B. J. Finlay. B-25		
Peter K. Weiskel and Brian L. Howes. MATHEMATICAL ECOLOGY Hal Caswell and Joel E. Cohen. Cabell S. Davis, Glenn R. Flierl, P. H. Wiebe and P. J. S. Franks. B-4 MICROBIAL ECOLOGY UG. Berninger, D. A. Caron, R. W. Sanders and B. J. Finlay. B-2	•	
MATHEMATICAL ECOLOGY Hal Caswell and Joel E. Cohen		
Hal Caswell and Joel E. Cohen	Peter K. Weiskel and Brian L. Howes	B -25
Cabell S. Davis, Glenn R. Flierl, P. H. Wiebe and P. J. S. Franks MICROBIAL ECOLOGY UG. Berninger, D. A. Caron, R. W. Sanders and B. J. Finlay B-2	MATHEMATICAL ECOLOGY	
Cabell S. Davis, Glenn R. Flierl, P. H. Wiebe and P. J. S. Franks MICROBIAL ECOLOGY UG. Berninger, D. A. Caron, R. W. Sanders and B. J. Finlay B-2	Hal Caswell and Joel E. Cohen	B -3
UG. Berninger, D. A. Caron, R. W. Sanders and B. J. Finlay		
UG. Berninger, D. A. Caron, R. W. Sanders and B. J. Finlay	MICROBIAL ECOLOGY	
		R o
- Duviu A. Valvii, De Diii Diiii, Velluanie Micell, John D. Walerdufu ana fredetica W. Valais - H7	David A. Caron, Ee Lin Lim, Geraldine Miceli, John B. Waterbury and Frederica W. Valois	

David A. Caron, Robert W. Sanders and Diane K. Stoecker	В-3
Noellette Conway, Brian Howes, Judith McDowell Capuzzo, Ruth Turner and Colleen Cavanaugh	B-3
Cabell S. Davis, Scott M. Gallager and Andrew R. Solow	B-5
Edward F. DeLong	B-5
Edward F. DeLong	B-6
Edward F. DeLong	B-6
J. C. Goldman and M. R. Dennettt	. B-12
Holger W. Jannasch	. B-14
Holger W. Jannasch	. B-14
Margit Kurr, Robert Huber, Helmut König, Holger W. Jannasch, Hans Fricke, Antonio Trincone, Jakob K. Kristjansson and Karl O. Stetter	. B-14
Alan J. Lewitus, and David A. Caron	. B-15
Alan J. Lewitus, and David A. Caron	. B-15
Alan J. Lewitus, David A. Caron and Kenneth R. Miller	. B-16
Richard L. Smith, Brian L. Howes and John H. Duff	. B-20
Richard L. Smith, Brian L. Howes and Stephen P. Garabedian	.B-20
Tracy A. Villareal	. B-23
Tracy A. Villareal	. B-24
Tracy A. Villareal	. B-24
Peter K. Weiskel and Brian L. Howes	. B-25
Carl O. Wirsen, Toshihiro Hoaki, Tadashi Maruyama and Holger W. Jannasch	. B-26
Carl O. Wirsen, Holger W. Jannasch, Stephen J. Molyneaux	. B-2 6
MICROBIAL GENETICS	
Edward F. DeLong	B-6
P. V. Dunlap	
Paul V. Dunlap	
E.A. Meighen and P. V. Dunlap	
MICROBIOLOGY	
David A. Caron, Ee Lin Lim, Geraldi. e Miceli, John B. Waterbury and Frederica W. Valois	-
Edward F. DeLong	
Edward F. DeLong	B-6
Edward F. DeLong	
P. V. Dunlap	B-7
P. V. Dunlap	В-8
P. V. Dunlap, U. Mueller, T. A. Lisa and K. S. Lundberg	B-8
Holger W. Jannasch	. B-14
Holger W. Jannasch	. B-14
Holger W. Jannasch, Craig C. Taylor and Linda R. Hare	. B-14
Margit Kurr, Robert Huber, Helmut König, Holger W. Jonnasch, Hans Fricke, Antonio Trincone, Jakob K. Kristjansson and Karl O. Stetter	. B-14
E.A. Meighen and P. V. Dunlap	. B-17
Dennis J. O'Kane and Douglas C. Prasher	. B-18
Ursula Pley, Jutta Schipka, Agate Gambacorta, Holger W. Jannasch, Hans Fricke, Reinhard Rachel Karl O. Stetter	and . B-18
Richard L. Smith, Brian L. Howes and John H. Duff	. B-20
J. B. Waterbury	. B-24
Carl O. Wirsen, Toshihiro Hoaki, Tadashi Maruyama and Holger W. Jannasch	. B-26

	B-26
MODELLING	
Cabell S. Davis and Philip Alatalo	B-4
Cabell S. Davis, Glenn R. Flierl, P. H. Wiebe and P. J. S. Franks	B-4
Scott M. Gallager	B-10
Peter K. Weiskel and Brian L. Howes	B-25
Peter K. Weiskel and Brian L. Howes	B-25
MOLECULAR BIOLOGY	
D. M. Anderson, M. Herzog and A. Grabher	B-1
Chris W. Cody, Douglas C. Prasher, William M. Westler, Franklyn G. Prendergast, and William W. Ward	B-3
Edward F. DeLong	B-6
P. V. Dunlap	
Paul V. Dunlap	_
A. A. Elskus, R. J. Pruell and J. J. Stegeman	
Mark E. Hahn, Alan Poland, Ed Glover and John J. Stegeman	
E.A. Meighen and P. V. Dunlap	
Dennis J. O'Kane and Douglas C. Prasher.	
Douglas C. Prasher, Virginia K. Eckenrode, William W. Ward, Frank G. Prendergast, an	d
Milton J. Cormier	
PHYSIOLOGY No North Man Communi Project House And State Ma Donald Communi Public Towns And No. 10. 10. 10. 10. 10. 10. 10. 10. 10. 10	
Noellette Conway, Brian Howes, Judith McDowell Capuzzo, Ruth Turner and Colleen Ca	
Gregory J. Doucette and Paul J. Harrison	•
	В-7
P. V. Dunlap	B-7
P. V. Dunlap	B-7 B-8 B-8
P. V. Dunlap Paul V. Dunlap, Ulrich Mueller, Teresita A. Lisa and Kelly S. Lundberg	B-7 B-8 B-8 B-8
P. V. Dunlap	B-7 B-8 B-8 B-8 B-9
P. V. Dunlap Paul V. Dunlap, Ulrich Mueller, Teresita A. Lisa and Kelly S. Lundberg	B-7 B-8 B-8 B-8 B-9
P. V. Dunlap	B-7 B-8 B-8 B-9 B-10 B-10
P. V. Dunlap Paul V. Dunlap, Ulrich Mueller, Teresita A. Lisa and Kelly S. Lundberg. John W. Farrington, John M. Teal, Bruce W. Tripp and Curtis Phinney. Scott M. Gallager. Scott M. Gallager. Scott M. Gallager, John B. Waterbury and Diane K. Stoecker.	B-7 B-8 B-8 B-9 B-10 B-11
P. V. Dunlap Paul V. Dunlap, Ulrich Mueller, Teresita A. Lisa and Kelly S. Lundberg. John W. Farrington, John M. Teal, Bruce W. Tripp and Curtis Phinney. Scott M. Gallager. Scott M. Gallager. Scott M. Gallager, John B. Waterbury and Diane K. Stoecker. Dean M. Jacobson and D. M. Anderson.	B-7 B-8 B-8 B-9 B-10 B-11 B-13
P. V. Dunlap Paul V. Dunlap, Ulrich Mueller, Teresita A. Lisa and Kelly S. Lundberg. John W. Farrington, John M. Teal, Bruce W. Tripp and Curtis Phinney. Scott M. Gallager. Scott M. Gallager. Scott M. Gallager, John B. Waterbury and Diane K. Stoecker.	B-7 B-8 B-8 B-9 B-10 B-11 B-13
P. V. Dunlap Paul V. Dunlap, Ulrich Mueller, Teresita A. Lisa and Kelly S. Lundberg. John W. Farrington, John M. Teal, Bruce W. Tripp and Curtis Phinney. Scott M. Gallager. Scott M. Gallager. Scott M. Gallager, John B. Waterbury and Diane K. Stoecker. Dean M. Jacobson and D. M. Anderson.	B-7 B-8 B-8 B-9 B-10 B-11 B-13 B-15
P. V. Dunlap Paul V. Dunlap, Ulrich Mueller, Teresita A. Lisa and Kelly S. Lundberg. John W. Farrington, John M. Teal, Bruce W. Tripp and Curtis Phinney. Scott M. Gallager. Scott M. Gallager. Scott M. Gallager, John B. Waterbury and Diane K. Stoecker. Dean M. Jacobson and D. M. Anderson. Alan J. Lewitus, and David A. Caron.	B-7 B-8 B-8 B-9 B-10 B-11 B-13 B-15
P. V. Dunlap Paul V. Dunlap, Ulrich Mueller, Teresita A. Lisa and Kelly S. Lundberg. John W. Farrington, John M. Teal, Bruce W. Tripp and Curtis Phinney. Scott M. Gallager. Scott M. Gallager. Scott M. Gallager, John B. Waterbury and Diane K. Stoecker. Dean M. Jacobson and D. M. Anderson. Alan J. Lewitus, and David A. Caron. Alan J. Lewitus, and David A. Caron.	B-7 B-8 B-8 B-9 B-10 B-11 B-13 B-15 B-15
P. V. Dunlap Paul V. Dunlap, Ulrich Mueller, Teresita A. Lisa and Kelly S. Lundberg. John W. Farrington, John M. Teal, Bruce W. Tripp and Curtis Phinney. Scott M. Gallager. Scott M. Gallager. Scott M. Gallager, John B. Waterbury and Diane K. Stoecker. Dean M. Jacobson and D. M. Anderson. Alan J. Lewitus, and David A. Caron. Alan J. Lewitus, David A. Caron and Kenneth R. Miller.	B-7 B-8 B-8 B-9 B-10 B-11 B-13 B-15 B-15 B-16
P. V. Dunlap Paul V. Dunlap, Ulrich Mueller, Teresita A. Lisa and Kelly S. Lundberg. John W. Farrington, John M. Teal, Bruce W. Tripp and Curtis Phinney. Scott M. Gallager. Scott M. Gallager. Scott M. Gallager, John B. Waterbury and Diane K. Stoecker. Dean M. Jacobson and D. M. Anderson. Alan J. Lewitus, and David A. Caron. Alan J. Lewitus, and David A. Caron. Alan J. Lewitus, David A. Caron and Kenneth R. Miller. E. A. Meighen and P. V. Dunlap.	B-7 B-8 B-8 B-9 B-10 B-11 B-13 B-15 B-15 B-16 B-17
P. V. Dunlap Paul V. Dunlap, Ulrich Mueller, Teresita A. Lisa and Kelly S. Lundberg. John W. Farrington, John M. Teal, Bruce W. Tripp and Curtis Phinney. Scott M. Gallager Scott M. Gallager Scott M. Gallager, John B. Waterbury and Diane K. Stoecker Dean M. Jacobson and D. M. Anderson Alan J. Lewitus, and David A. Caron Alan J. Lewitus, and David A. Caron Alan J. Lewitus, David A. Caron and Kenneth R. Miller E. A. Meighen and P. V. Dunlap Tracy A. Villareal	B-7 B-8 B-8 B-9 B-10 B-11 B-13 B-15 B-15 B-16 B-17
P. V. Dunlap. Paul V. Dunlap, Ulrich Mueller, Teresita A. Lisa and Kelly S. Lundberg. John W. Farrington, John M. Teal, Bruce W. Tripp and Curtis Phinney. Scott M. Gallager. Scott M. Gallager. Scott M. Gallager, John B. Waterbury and Diane K. Stoecker. Dean M. Jacobson and D. M. Anderson. Alan J. Lewitus, and David A. Caron. Alan J. Lewitus, and David A. Caron. Alan J. Lewitus, David A. Caron and Kenneth R. Miller. E. A. Meighen and P. V. Dunlap. Tracy A. Villareal. Carl O. Wirsen, Toshihiro Hoaki, Tadashi Maruyama and Holger W. Jannasch.	B-7 B-8 B-8 B-9 B-10 B-11 B-13 B-15 B-15 B-16 B-17 B-24 B-26

Cabell S. Davis and Philip Alatalo	
Cabell S. Davis, Glenn R. Flierl, P. H. Wiebe and P. J. S. Franks	. B-4
Cabell S. Davis, Scott M. Gallager, Mark S. Berman, Loren R. Haury and J. Rudi Strickler	B-5
Gregory J. Doucette and Paul I. Harrison	B-7
Gregory J. Doucette and Paul J. Harrison	B-7
Scott M. Gallager, John B. Waterbury and Diane K. Stoecker	B-11
Joel C. Goldman	B-11
Dean M. Jacobson and D. M. Anderson	B-13
Alan J. Lewitus, and David A. Caron	B-15
Alan J. Lewitus, and David A. Caron	B-15
Alan J. Lewitus, David A. Caron and Kenneth R. Miller	B-16
C. Sancetta, T. Villareal and P. Falkowski	B-19
Tracy A. Villareal	B-23
Tracy A. Villareal	B-24
Tracy A. Villareal	B-24
J. B. Waterbury	B-24
PHYTOPLANKTON ECOLOGY	
Donald M. Anderson and Bruce A. Keafer	. B-1
UG. Berninger, D. A. Caron, R. W. Sanders and B. J. Finlay	B-2
Cabell S. Davis and Philip Alatalo	B-4
Cabell S. Davis, Glenn R. Flierl, P. H. Wiebe and P. J. S. Franks	B-4
Cabell S. Davis, Scott M. Gallager, Mark S. Berman, Loren R. Haury and J. Rudi Strickler	B-5
Cabell S. Davis, Scott M. Gallager and Andrew R. Solow	
	B-5
Cabell S. Davis, Scott M. Gallager and Andrew R. Solow	B-5 B-7
Cabell S. Davis, Scott M. Gallager and Andrew R. Solow	B-5 B-7 B-7
Cabell S. Davis, Scott M. Gallager and Andrew R. Solow	B-5 B-7 B-7 . B-11
Cabell S. Davis, Scott M. Gallager and Andrew R. Solow	B-5 B-7 B-7 . B-11
Cabell S. Davis, Scott M. Gallager and Andrew R. Solow Gregory J. Doucette and Paul J. Harrison Gregory J. Doucette and Paul J. Harrison Scott M. Gallager, John B. Waterbury and Diane K. Stoecker Joel C. Goldman	B-5 B-7 B-7 . B-11 . B-15
Cabell S. Davis, Scott M. Gallager and Andrew R. Solow. Gregory J. Doucette and Paul J. Harrison. Gregory J. Doucette and Paul J. Harrison. Scott M. Gallager, John B. Waterbury and Diane K. Stoecker. Joel C. Goldman. Alan J. Lewitus, and David A. Caron.	B-5 B-7 B-7 . B-11 . B-15 . B-15
Cabell S. Davis, Scott M. Gallager and Andrew R. Solow Gregory J. Doucette and Paul J. Harrison Gregory J. Doucette and Paul J. Harrison Scott M. Gallager, John B. Waterbury and Diane K. Stoecker Joel C. Goldman Alan J. Lewitus, and David A. Caron Alan J. Lewitus, and David A. Caron	B-5 B-7 B-7 . B-11 . B-11 . B-15 . B-15
Cabell S. Davis, Scott M. Gallager and Andrew R. Solow. Gregory J. Doucette and Paul J. Harrison. Gregory J. Doucette and Paul J. Harrison. Scott M. Gallager, John B. Waterbury and Diane K. Stoecker. Joel C. Goldman. Alan J. Lewitus, and David A. Caron. Alan J. Lewitus, and David A. Caron. Alan J. Lewitus, David A. Caron and Kenneth R. Miller.	B-5 B-7 B-7 . B-11 . B-15 . B-15 . B-16
Cabell S. Davis, Scott M. Gallager and Andrew R. Solow Gregory J. Doucette and Paul J. Harrison Gregory J. Doucette and Paul J. Harrison Scott M. Gallager, John B. Waterbury and Diane K. Stoecker Joel C. Goldman Alan J. Lewitus, and David A. Caron Alan J. Lewitus, and David A. Caron Alan J. Lewitus, David A. Caron and Kenneth R. Miller C. Sancetta, T. Villareal and P. Falkowski	B-5 B-7 B-11 . B-11 . B-15 . B-15 . B-16 . B-19
Cabell S. Davis, Scott M. Gallager and Andrew R. Solow Gregory J. Doucette and Paul J. Harrison Gregory J. Doucette and Paul J. Harrison Scott M. Gallager, John B. Waterbury and Diane K. Stoecker Joel C. Goldman Alan J. Lewitus, and David A. Caron Alan J. Lewitus, and David A. Caron Alan J. Lewitus, David A. Caron and Kenneth R. Miller C. Sancetta, T. Villareal and P. Falkowski Tracy A. Villareal	B-5 B-7 B-11 . B-11 . B-15 . B-16 . B-19 . B-23
Cabell S. Davis, Scott M. Gallager and Andrew R. Solow Gregory J. Doucette and Paul J. Harrison Gregory J. Doucette and Paul J. Harrison Scott M. Gallager, John B. Waterbury and Diane K. Stoecker Joel C. Goldman Alan J. Lewitus, and David A. Caron Alan J. Lewitus, and David A. Caron Alan J. Lewitus, David A. Caron and Kenneth R. Miller C. Sancetta, T. Villareal and P. Falkowski Tracy A. Villareal Tracy A. Villareal Tracy A. Villareal	B-5 B-7 B-11 . B-15 . B-15 . B-16 . B-19 . B-23 . B-24
Cabell S. Davis, Scott M. Gallager and Andrew R. Solow Gregory J. Doucette and Paul J. Harrison Gregory J. Doucette and Paul J. Harrison Scott M. Gallager, John B. Waterbury and Diane K. Stoecker Joel C. Goldman Alan J. Lewitus, and David A. Caron Alan J. Lewitus, and David A. Caron Alan J. Lewitus, David A. Caron and Kenneth R. Miller C. Sancetta, T. Villareal and P. Falkowski Tracy A. Villareal Tracy A. Villareal Tracy A. Villareal	B-5 B-7 B-7 . B-11 . B-15 . B-15 . B-16 . B-19 . B-23 . B-24
Cabell S. Davis, Scott M. Gallager and Andrew R. Solow Gregory J. Doucette and Paul J. Harrison Gregory J. Doucette and Paul J. Harrison Scott M. Gallager, John B. Waterbury and Diane K. Stoecker Joel C. Goldman Alan J. Lewitus, and David A. Caron Alan J. Lewitus, and David A. Caron Alan J. Lewitus, David A. Caron and Kenneth R. Miller C. Sancetta, T. Villareal and P. Falkowski Tracy A. Villareal Tracy A. Villareal Tracy A. Villareal	B-5 B-7 . B-7 . B-11 . B-15 . B-15 . B-16 . B-19 . B-23 . B-24
Cabell S. Davis, Scott M. Gallager and Andrew R. Solow Gregory J. Doucette and Paul J. Harrison. Gregory J. Doucette and Paul J. Harrison Scott M. Gallager, John B. Waterbury and Diane K. Stoecker Joel C. Goldman. Alan J. Lewitus, and David A. Caron Alan J. Lewitus, and David A. Caron Alan J. Lewitus, David A. Caron and Kenneth R. Miller C. Sancetta, T. Villareal and P. Falkowski Tracy A. Villareal	B-5 B-7 B-7 . B-11 . B-15 . B-16 . B-19 . B-23 . B-24
Cabell S. Davis, Scott M. Gallager and Andrew R. Solow Gregory J. Doucette and Paul J. Harrison. Gregory J. Doucette and Paul J. Harrison. Scott M. Gallager, John B. Waterbury and Diane K. Stoecker Joel C. Goldman. Alan J. Lewitus, and David A. Caron Alan J. Lewitus, and David A. Caron Alan J. Lewitus, David A. Caron and Kenneth R. Miller C. Sancetta, T. Villareal and P. Falkowski Tracy A. Villareal Tracy A. Villareal Tracy A. Villareal Tracy A. Villareal Tracy A. Villareal Tracy A. Villareal Tracy A. Villareal	B-5 B-7 B-7 . B-11 . B-15 . B-16 . B-19 . B-23 . B-24
Cabell S. Davis, Scott M. Gallager and Andrew R. Solow Gregory J. Doucette and Paul J. Harrison. Gregory J. Doucette and Paul J. Harrison Scott M. Gallager, John B. Waterbury and Diane K. Stoecker Joel C. Goldman. Alan J. Lewitus, and David A. Caron Alan J. Lewitus, and David A. Caron Alan J. Lewitus, David A. Caron and Kenneth R. Miller C. Sancetta, T. Villareal and P. Falkowski Tracy A. Villareal	B-5 B-7 . B-7 . B-11 . B-15 . B-15 . B-16 . B-19 . B-24 . B-24
Cabell S. Davis, Scott M. Gallager and Andrew R. Solow. Gregory J. Doucette and Paul J. Harrison. Gregory J. Doucette and Paul J. Harrison. Scott M. Gallager, John B. Waterbury and Diane K. Stoecker. Joel C. Goldman. Alan J. Lewitus, and David A. Caron. Alan J. Lewitus, and David A. Caron. Alan J. Lewitus, David A. Caron and Kenneth R. Miller. C. Sancetta, T. Villareal and P. Falkowski. Tracy A. Villareal. Tracy A. Villareal. Tracy A. Villareal. POPULATION ECOLOGY David A. Caron, Robert W. Sanders and Diane K. Stoecker. Cabell S. Davis and Philip Alatalo. Cabell S. Davis, Glenn R. Flierl, P. H. Wiebe and P. J. S. Franks. Cabell S. Davis, Scott M. Gallager, Mark S. Berman, Loren R. Haury and J. Rudi Strickler. Cabell S. Davis, Scott M. Gallager and Andrew R. Solow.	B-5 B-7 B-7 B-11 B-15 B-16 B-19 B-23 B-24 B-3 B-4 B-4 B-4 B-5
Cabell S. Davis, Scott M. Gallager and Andrew R. Solow. Gregory J. Doucette and Paul J. Harrison. Gregory J. Doucette and Paul J. Harrison. Scott M. Gallager, John B. Waterbury and Diane K. Stoecker. Joel C. Goldman. Alan J. Lewitus, and David A. Caron. Alan J. Lewitus, and David A. Caron and Kenneth R. Miller. C. Sancetta, T. Villareal and P. Falkowski. Tracy A. Villareal. Tracy A. Villareal. Tracy A. Villareal. Tracy A. Villareal. POPULATION ECOLOGY David A. Caron, Robert W. Sanders and Diane K. Stoecker. Cabell S. Davis and Philip Alatalo. Cabell S. Davis, Glenn R. Flierl, P. H. Wiebe and P. J. S. Franks. Cabell S. Davis, Scott M. Gallager, Mark S. Berman, Loren R. Haury and J. Rudi Strickler.	B-5 B-7 B-7 B-11 B-15 B-16 B-19 B-23 B-24 B-3 B-4 B-4 B-4 B-5
Cabell S. Davis, Scott M. Gallager and Andrew R. Solow. Gregory J. Doucette and Paul J. Harrison. Gregory J. Doucette and Paul J. Harrison. Scott M. Gallager, John B. Waterbury and Diane K. Stoecker. Joel C. Goldman. Alan J. Lewitus, and David A. Caron. Alan J. Lewitus, and David A. Caron. Alan J. Lewitus, David A. Caron and Kenneth R. Miller. C. Sancetta, T. Villareal and P. Falkowski. Tracy A. Villareal. Tracy A. Villareal. Tracy A. Villareal. POPULATION ECOLOGY David A. Caron, Robert W. Sanders and Diane K. Stoecker. Cabell S. Davis and Philip Alatalo. Cabell S. Davis, Glenn R. Flierl, P. H. Wiebe and P. J. S. Franks. Cabell S. Davis, Scott M. Gallager, Mark S. Berman, Loren R. Haury and J. Rudi Strickler. Cabell S. Davis, Scott M. Gallager and Andrew R. Solow.	B-5 B-7 B-7 B-11 B-15 B-15 B-16 B-19 B-24 B-24 B-3 B-4 B-4 B-5 B-6

RECRUITMENT

Cabell S. Davis, Glenn R. Flierl, P. H. Wiebe and P. J. S. Franks	4
Cabell S. Davis, Scott M. Gallager, Mark S. Berman, Loren R. Haury and J. Rudi Strickler	5
Cabell S. Davis, Scott M. Gallager and Andrew R. Solow B-	5
Scott M. GallagerB-10	0
Scott M. Gallager, John B. Waterbury and Diane K. Stoecker	1
Rudolf S. Scheltema B-19	9
P. V. R. Snelgrove, J. F. Grassle and R. F. Petrecca	1
J. Rudi Strickler, Peter C. Schulze, Bo I. Bergström, Mark S. Berman, Percy Donaghay, Scott Gallager, James F. Haney, Bruce R. Hargreaves, Uwe Kils, Gustav - S. Paffenhöefer, Sumner Richman, Henry A. Vanderploeg, Wolfgang Welsch, David Wethey, and Jeannette Yen	3
REMOTE SENSING	
Cabell S. Davis, Scott M. Gallager and Andrew R. Solow	5
William A. Watkins, Mary Ann Daher, Kurt M. Fristrup, Terrance J. Howald and Giuseppe Notarbartolo di Sciara	
<u>SYSTEMATICS</u>	
Edward F. DeLongB-	
Carol E. Diebel	
P. S. Lobel, W. Harder and E. K. V. Kalko	6
Amélie H. ScheltemaB-1	9
J. B. WaterburyB-2	4
James R. Weinberg, Victoria R. Starczak and Daniel Jörg	5
P. V. DunlapB-	7
TAYONOMY	
TAXONOMY	_
Cabell S. Davis, Scott M. Gallager, Mark S. Berman, Loren R. Haury and J. Rudi StricklerB-	
Cabell S. Davis, Scott M. Gallager, Mark S. Berman, Loren R. Haury and J. Rudi Strickler	5
Cabell S. Davis, Scott M. Gallager, Mark S. Berman, Loren R. Haury and J. Rudi Strickler	.5 .6
Cabell S. Davis, Scott M. Gallager, Mark S. Berman, Loren R. Haury and J. Rudi Strickler	.5 .6 .6
Cabell S. Davis, Scott M. Gallager, Mark S. Berman, Loren R. Haury and J. Rudi Strickler	.5 .6 .6
Cabell S. Davis, Scott M. Gallager, Mark S. Berman, Loren R. Haury and J. Rudi Strickler. Cabell S. Davis, Scott M. Gallager and Andrew R. Solow. B-Edward F. DeLong. Carol E. Diebel. P. V. Dunlap. B-P. S. Lobel, W. Harder and E. K. V. Kalko. B-1	.5 .6 .6 .7
Cabell S. Davis, Scott M. Gallager, Mark S. Berman, Loren R. Haury and J. Rudi Strickler	.5 .6 .6 .7
Cabell S. Davis, Scott M. Gallager, Mark S. Berman, Loren R. Haury and J. Rudi Strickler	.5 .6 .6 .7
Cabell S. Davis, Scott M. Gallager, Mark S. Berman, Loren R. Haury and J. Rudi Strickler	.5 .6 .6 .7 .16
Cabell S. Davis, Scott M. Gallager, Mark S. Berman, Loren R. Haury and J. Rudi Strickler	.5 .6 .6 .7 .16
Cabell S. Davis, Scott M. Gallager, Mark S. Berman, Loren R. Haury and J. Rudi Strickler. Cabell S. Davis, Scott M. Gallager and Andrew R. Solow. Edward F. DeLong. B-Carol E. Diebel. B-P. V. Dunlap. P. S. Lobel, W. Harder and E. K. V. Kalko. J. B. Waterbury. B-2 TOXICOLOGY Donald M. Anderson and Bruce A. Keafer. A. A. Elskus, R. J. Pruell and J. J. Stegeman. B-	.5 .6 .7 .16 .24
Cabell S. Davis, Scott M. Gallager, Mark S. Berman, Loren R. Haury and J. Rudi Strickler. Cabell S. Davis, Scott M. Gallager and Andrew R. Solow. Edward F. DeLong. Carol E. Diebel. B- P. V. Dunlap. B- P. S. Lobel, W. Harder and E. K. V. Kalko. J. B. Waterbury. B-2 TOXICOLOGY Donald M. Anderson and Bruce A. Keafer. A. A. Elskus, R. J. Pruell and J. J. Stegeman. B- John W. Farrington, John M. Teal, Bruce W. Tripp and Curtis Phinney. B-	.5 .6 .7 .6 .4 -1 .9
Cabell S. Davis, Scott M. Gallager, Mark S. Berman, Loren R. Haury and J. Rudi Strickler. B-Cabell S. Davis, Scott M. Gallager and Andrew R. Solow. Edward F. DeLong. B-Carol E. Diebel. P. V. Dunlap. B-P. S. Lobel, W. Harder and E. K. V. Kalko. J. B. Waterbury. B-2 TOXICOLOGY Donald M. Anderson and Bruce A. Keafer. A. A. Elskus, R. J. Pruell and J. J. Stegeman. B-John W. Farrington, John M. Teal, Bruce W. Tripp and Curtis Phinney. B-K. Fent and J. J. Stegeman. B-K. Fent and J. J. Stegeman. B-Carol E. Haury and J. Rudi Strickler. B-Carol E. Haury and	.5 .6 .7 .6 .4 -1 .9 .9
Cabell S. Davis, Scott M. Gallager, Mark S. Berman, Loren R. Haury and J. Rudi Strickler. B-Cabell S. Davis, Scott M. Gallager and Andrew R. Solow. B-Edward F. DeLong. B-Carol E. Diebel. B-P. V. Dunlap. B-P. S. Lobel, W. Harder and E. K. V. Kalko. J. B. Waterbury. B-2 TOXICOLOGY Donald M. Anderson and Bruce A. Keafer. A. A. Elskus, R. J. Pruell and J. J. Stegeman. John W. Farrington, John M. Teal, Bruce W. Tripp and Curtis Phinney. B-K. Fent and J. J. Stegeman. B-Karl Fent and John J. Stegeman. B-Karl Fent and John J. Stegeman. B-Karl Fent and John J. Stegeman. B-	.5 .6 .7 .6 .4 .1 .9 .9
Cabell S. Davis, Scott M. Gallager, Mark S. Berman, Loren R. Haury and J. Rudi Strickler. B-Cabell S. Davis, Scott M. Gallager and Andrew R. Solow. B-Edward F. DeLong. B-Carol E. Diebel. B-P. V. Dunlap. P. S. Lobel, W. Harder and E. K. V. Kalko. B-1 J. B. Waterbury. B-2 TOXICOLOGY Donald M. Anderson and Bruce A. Keafer. A. A. Elskus, R. J. Pruell and J. J. Stegeman. B-John W. Farrington, John M. Teal, Bruce W. Tripp and Curtis Phinney. B-K. Fent and J. J. Stegeman. B-Karl Fent and John J. Stegeman. B-Karl Fent and John J. Stegeman. B-Mark E. Hahn, Alan Poland, Ed Glover and John J. Stegeman. B-1	·5 ·6 ·6 ·7 ·6 ·4 ·9 ·9 ·9
Cabell S. Davis, Scott M. Gallager, Mark S. Berman, Loren R. Haury and J. Rudi Strickler. B-Cabell S. Davis, Scott M. Gallager and Andrew R. Solow. B-Edward F. DeLong. B-Carol E. Diebel. B-P. V. Dunlap. P. S. Lobel, W. Harder and E. K. V. Kalko. B-1 J. B. Waterbury. B-2 TOXICOLOGY Donald M. Anderson and Bruce A. Keafer. A. A. Elskus, R. J. Pruell and J. J. Stegeman. B-John W. Farrington, John M. Teal, Bruce W. Tripp and Curtis Phinney. B-K. Fent and J. J. Stegeman. B-Karl Fent and John J. Stegeman. B-Mark E. Hahn, Alan Poland, Ed Glover and John J. Stegeman. B-Mark E. Hahn and John J. Stegeman. B-1 Mark E. Hahn and John J. Stegeman. B-1	-5 -6 -6 -7 -6 -4 -1 -9 -9 -9 -9 -12 12
Cabell S. Davis, Scott M. Gallager, Mark S. Berman, Loren R. Haury and J. Rudi Strickler. B-Cabell S. Davis, Scott M. Gallager and Andrew R. Solow. B-Edward F. DeLong. B-Carol E. Diebel. P. V. Dunlap. P. S. Lobel, W. Harder and E. K. V. Kalko. J. B. Waterbury. B-2 TOXICOLOGY Donald M. Anderson and Bruce A. Keafer. A. A. Elskus, R. J. Pruell and J. J. Stegeman. B-John W. Farrington, John M. Teal, Bruce W. Tripp and Curtis Phinney. B-K. Fent and J. J. Stegeman. B-Karl Fent and John J. Stegeman. B-Mark E. Hahn, Alan Poland, Ed Glover and John J. Stegeman. B-1 Mark E. Hahn and John J. Stegeman. B-1 John J. Stegeman. B-1 John J. Stegeman. B-1	.5 .6 .7 .6 .4 .1 .9 .9 .9 .9 .12 .12
Cabell S. Davis, Scott M. Gallager, Mark S. Berman, Loren R. Haury and J. Rudi Strickler. B-Cabell S. Davis, Scott M. Gallager and Andrew R. Solow. B-Edward F. DeLong. B-Carol E. Diebel. B-P. V. Dunlap. P. S. Lobel, W. Harder and E. K. V. Kalko. B-1 J. B. Waterbury. B-2 TOXICOLOGY Donald M. Anderson and Bruce A. Keafer. A. A. Elskus, R. J. Pruell and J. J. Stegeman. B-John W. Farrington, John M. Teal, Bruce W. Tripp and Curtis Phinney. B-K. Fent and J. J. Stegeman. B-Karl Fent and John J. Stegeman. B-Mark E. Hahn, Alan Poland, Ed Glover and John J. Stegeman. B-Mark E. Hahn and John J. Stegeman. B-1 Mark E. Hahn and John J. Stegeman. B-1	-1 -9 -9 -9 12 12
Cabell S. Davis, Scott M. Gallager, Mark S. Berman, Loren R. Haury and J. Rudi Strickler. B-Cabell S. Davis, Scott M. Gallager and Andrew R. Solow. B-Edward F. DeLong. B-Carol E. Diebel. P. V. Dunlap. P. S. Lobel, W. Harder and E. K. V. Kalko. J. B. Waterbury. B-2 TOXICOLOGY Donald M. Anderson and Bruce A. Keafer. A. A. Elskus, R. J. Pruell and J. J. Stegeman. B-John W. Farrington, John M. Teal, Bruce W. Tripp and Curtis Phinney. B-K. Fent and J. J. Stegeman. B-Karl Fent and John J. Stegeman. B-Mark E. Hahn, Alan Poland, Ed Glover and John J. Stegeman. B-1 Mark E. Hahn and John J. Stegeman. B-1 John J. Stegeman. B-1 John J. Stegeman. B-1	.5 .6 .7 .6 .4 .1 .9 .9 .9 .9 .12 .12
Cabell S. Davis, Scott M. Gallager, Mark S. Berman, Loren R. Haury and J. Rudi Strickler. B-Cabell S. Davis, Scott M. Gallager and Andrew R. Solow. B-Edward F. DeLong. B-Carol E. Diebel. B-P. V. Dunlap. B-P. S. Lobel, W. Harder and E. K. V. Kalko. B-1 J. B. Waterbury. B-2 TOXICOLOGY Donald M. Anderson and Bruce A. Keafer. A. A. Elskus, R. J. Pruell and J. J. Stegeman. B-John W. Farrington, John M. Teal, Bruce W. Tripp and Curtis Phinney. B-K. Fent and J. J. Stegeman. B-Karl Fent and John J. Stegeman. B-Mark E. Hahn, Alan Poland, Ed Glover and John J. Stegeman. B-1 Mark E. Hahn and John J. Stegeman. B-1 John J. Stegeman. B-2 John J. Stegeman, Rozanna M. Smolowitz and Mark E. Hahn. B-2	-5 -6 -6 -7 -6 -24 -1 -9 -9 -9 -12 12 12 22
Cabell S. Davis, Scott M. Gallager, Mark S. Berman, Loren R. Haury and J. Rudi Strickler. B-Cabell S. Davis, Scott M. Gallager and Andrew R. Solow. B-Edward F. DeLong. B-Carol E. Diebel. B-P. V. Dunlap. B-P. S. Lobel, W. Harder and E. K. V. Kalko. B-1 J. B. Waterbury. B-2 TOXICOLOGY Donald M. Anderson and Bruce A. Keafer. A. A. Elskus, R. J. Pruell and J. J. Stegeman. B-A. A. Elskus, R. J. Pruell and J. J. Stegeman. B-K. Fent and J. J. Stegeman. B-K. Fent and J. J. Stegeman. B-Karl Fent and John J. Stegeman. B-Mark E. Hahn, Alan Poland, Ed Glover and John J. Stegeman. B-1 Mark E. Hahn and John J. Stegeman. B-1 John J. Stegeman, Rozanna M. Smolowitz and Mark E. Hahn. B-2 ZOOPLANKTON	-5 -6 -6 -7 -6 -2 -9 -9 -9 -9 -12 12 12 -4

Cabell S. Davis, Scott M. Gallager and Andrew R. Solow B-5
Carol E. DiebelB-6
Scott M. GallagerB-10
Scott M. GallagerB-10
Scott M. Gallager, John B. Waterbury and Diane K. Stoecker
G. R. Harbison
Patricia Kremer and Laurence P. MadinB-14
R. J. Larson, G. I. Matsumoto, L. P. Madin and L. M. Lewis
L. P. Madin and J. E. Purcell B-17
Rudolf S. Scheltema B-19
J. Rudi Strickler, Peter C. Schulze, Bo I. Bergström, Mark S. Berman, Percy Donaghay, Scott Gallager, James F. Haney, Bruce R. Hargreaves, Uwe Kils, Gustav - S. Paffenhöefer, Sumner Richman, Henry A. Vanderploeg, Wolfgang Welsch, David Wethey, and Jeannette YenB-23
ZOOPLANKTON ECOLOGY
UG. Berninger, D. A. Caron, R. W. Sanders and B. J. Finlay
David A. Caron, Ee Lin Lim, Geraldine Miceli, John B. Waterbury and Frederica W. Valois
David A. Caron, Robert W. Sanders and Diane K. Stoecker B-3
Cabell S. Davis and Philip AlataloB-4
Cabell S. Davis, Glenn R. Flierl, P. H. Wiebe and P. J. S. Franks
Cabell S. Davis, Scott M. Gallager, Mark S. Berman, Loren R. Haury and J. Rudi Strickler
Cabell S. Davis, Scott M. Gallager and Andrew R. Solow
Carol E. Diebel
Scott M. GallagerB-10
Scott M. GallagerB-10
Scott M. Gallager, John B. Waterbury and Diane K. Stoecker
G. R. HarbisonB-13
J. Rudi Strickler, Peter C. Schulze, Bo I. Bergström, Mark S. Berman, Percy Donaghay, Scott Gallager, James F. Haney, Bruce R. Hargreaves, Uwe Kils, Gustav - S. Paffenhöefer, Sumner Richman, Henry A. Vanderploeg, Wolfgang Welsch, David Wethey, and Jeannette YenB-23

DEPARTMENT OF CHEMISTRY

Frederick L. Sayles, Chairman

BIOGEOCHEMISTRY

CARBON AND NITROGEN EXPORT DURING THE JGOFS NORTH ATLANTIC BLOOM EXPERIMENT ESTIMATED FROM ²³⁴TH:²³⁸U **DISEQUILIBRIA**

Ken O. Buesseler, Michael P. Bacon, J. Kirk Cochran, and Hugh D. Livingston

The disequilibrium between the particlereactive tracer 234 Th ($t_{1/2} = 24.1$ days) and its soluble parent, ²³⁸U, was used to examine Th scavenging and export fluxes during the U.S. JGOFS North Atlantic Bloom Experiment (24 April to 30 May 1989) at ~47°N 20°W. Four profiles of dissolved and particulate ²³⁴Th in the upper 300 m and a non-steady state box model were used to quantify dissolved ²³⁴Th uptake and particle export rates. The highest export fluxes occurred during the first half of May. From POC/234Th and PON/234Th ratios, particulate organic C and N fluxes were calculated. Results were 5 to 41 mmol C/m²/day and 0.9 to 6.5 mmol N/m²/day from the 0 to 35 m layer. The ratio of POC export flux to primary production ranged from 0.05 to 0.42, peaking in the first half of May. The estimated fluxes agree with the observed losses of total C and N from the upper ocean during the bloom, but yield significantly higher fluxes than were measured by floating traps at 150 m and 300 m.

Submitted to: Deep-Sea Research.

Supported by: NSF Grants OCE90-16494 and OCE88-17836.

WHOI Contribution No. 7831.

THE MEASUREMENT OF SEDIMENT IRRIGATION RATES: A COMPARISON OF THE BR- TRACER AND 222RN/226RA **DISEQUILIBRIUM TECHNIQUES**

W. R. Martin and G. T. Banta

We have carried out a series of experiments designed to allow comparison of sediment irrigation rates determined simultaneously using two methods: the measurement of ²²²Rn/²²⁶Ra disequilibrium in pore waters, and the measurement of distributions of a tracer, Br-. which was added to the water overlying sediments at the start of incubation experiments. The experiments were carried out on fine-grained sediments from Buzzards Bay, MA. We made irrigation rate measurements on sediments in their

natural state, as well as on sediments that had been treated to alter macrofaunal abundance and diversity. The range of irrigation rates measured was similar for both tracers, and was similar to rates measured at the study site previously by Martin and Sayles (1987). Furthermore, the two tracers gave similar patterns of irrigation rate variability between cores and with depth below the sediment-water interface. On the other hand, comparisons of individual cores showed significant differences in the absolute rates measured using the different tracers; in particular, the ²²²Rn/²²⁶Ra disequilibrium method yielded more rapid irrigation rate estimates at depths exceeding 10 cm below the sediment-water interface. These differences could be due to the inherent limitations on the sensitivity of the methods, to artifacts in measurement procedures, to differences in the permeability of burrow walls to the two tracers (Rn and Br⁻), or to differences in the time-scales on which the two tracers record irrigation events. Irrigation rates determined by the Br tracer method were roughly correlated with the abundance of Nephtys incisa in the sediments, but were not related to abundances of the other numerically important deposit feeders, Nucula annulata and Mediomastus ambiseta.

In Press: Journal of Marine Research.

Supported by: NSF Grants OCE90-12473, OCE87-11962 and OCE86-15055; and EPA Grant CX-815451-01-0.

WHOI Contribution No. 7861.

ISOTOPIC SIGNATURES (14C, 13C, 15N) AS TRACERS OF SOURCES AND CYCLING OF SOLUBLE AND PARTICULATE ORGANIC MATTER IN THE SANTA MONICA BASIN, CA

P. M. Williams, K. J. Robertson, A. Soutar, S. M. Griffin, and E. R. M. Druffel

Measurements of Δ^{14} C, δ^{13} C and δ^{15} N are reported for dissolved (plus colloidal), suspended and sinking particulate, and total sedimentary organic matter in the Santa Monica Basin (mid-basin and shelf sites) on CaBS cruises 1, 3, 4, 7, 8 and 10. These isotopic signatures were indicative of the following processes occurring within the basin regime: (1) terrestrial inputs of organic matter to the sinking and suspended particulate organic matter were of the order of 10% of less, and as high as 25% for the sedimentary organic matter, (2) Δ^{14} C values of the uv-oxidizable dissolved organic matter below 5 m were similar to those measured in open ocean waters, while the Δ^{14} C values in the suspended, and, to a lesser degree, in the sinking organic

matter decreased markedly with depth. This latter decrease was primarily attributed to episodic resuspension of shelf and slope sedimentary organic matter, and secondarily to natural and/or anthropogenic petroleum inputs; and (3) the isotopic signatures of the uv-oxidizable dissolved organic matter, coupled with total dissolved carbon and amino acid and carbohydrate concentrations were strikingly similar in the deep basin and at an open-ocean site, suggesting a common history for the subsurface (>300 m) and deep water at both sites.

In addition, total mass and organic carbon and nitrogen fluxes from five particle trap deployments are described in detail. Mass fluxes increased with depth, especially on the shelf, suggesting that particle input from the basin slopes may reach the mid-basin site.

We conclude that there is minimal perturbation of all organic phases in the basin from terrestrial sources, and that the properties of the uv-oxidizable dissolved organic matter are not greatly influenced by particles of local origin.

In Press: Progress in Oceanography.

Supported by: NSF Grants OCE84-16632 and OCE87-16590

WHOI Contribution No. 7848.

ORGANIC GEOCHEMISTRY

SEASONAL AND DEPTH-RELATED CHANGES IN THE SOURCE OF SINKING PARTICLES IN THE NORTH ATLANTIC

Mark A. Altabet, Werner G. Deuser, Susumu Honjo, and Christian Stienen

Large, fast-sinking particles are important in the downward transport and redistribution of major biogeochemical species in the deep ocean. Using nitrogen isotope ratio, ¹⁵N/¹⁴N, as an in-situ tracer, we investigate the source and transformation of these particles in the North Atlantic ocean. We observe seasonal variations in $\delta^{15}N$ associated with seasonal changes in near-surface NO₃ concentration and particle flux; the nitrogen isotope variations are consistent with, but much larger than, previously observed variability. Our results show that the signal from these near-surface changes propagates rapidly into the deep ocean, but is modified depending on the phase of the seasonal production cycle. Surprisingly, we find that $\delta^{15}N$ value for sinking particles decrease with depth during low-flux periods—behaviour that may occur generally in the open ocean. The sinking particles must

therefore be either gaining light nitrogen or losing heavy nitrogen, an effect that we believe requires there to be another source of sinking particles, apart from recent surface production.

Published in: Nature, 354(6349):136-139, 1991.

Supported by: NSF Grant OCE87-17508.

WHOI Contribution No. 7648.

OPTICAL ABSORPTION SPECTRA OF WATERS FROM THE ORINOCO OUTFLOW: TERRESTRIAL INPUT OF COLORED ORGANIC MATTER TO THE CARIBBEAN

N. V. Blough, O. C. Zafiriou, and J. Bonilla

An extensive series of optical absorption spectra were recorded for waters in the eastern Caribbean Sea, the Gulf of Paria and the Orinoco River Estuary during the high flow period of the Orinoco River in the fall of 1988. Evidence of high levels of dissolved, colored organic matter (COM) was found throughout the eastern Caribbean, with these levels increasing substantially at stations nearer the Gulf of Paria and the Orinoco River. The dependence of the absorption at 300 nm (a₃₀₀) on salinity exhibited conservative mixing behavior for transects through the Gulf of Paria. In contrast, transects through the Orinoco Estuary revealed that a₃₀₀) remained approximately constant or slightly increased with increasing salinity up to 27°/m, after which it decreased linearly with increasing salinity. This nonconservative input of COM was not produced by COM release from suspended particulate matter at higher salinity, nor did it appear to originate from the sediment. Below 30%, the slopes of the log-linearized absorption spectra were independent of salinity (0.0140 nm⁻¹). At higher salinities, the slopes apparently increased, suggesting that the COM is modified. Based on specific absorption coefficients measured for COM isolated from this area, COM input by the Orinoco River is estimated to be $\sim 2.5 \times 10^{12}$ g C/yr, which represents about 1% of the total global transport of dissolved organic carbon in the ocean. This input is likely to influence substantially the carbon cycle, photochemical properties, and optical characteristics of the waters in this region.

In Press: Journal of Geophysical Research.

Supported by: ONR Grants N00014-87-K-007 and N00014-89-J-1260, and NSF Grant OCE87-00576.

WHOI Contribution No. 7616.

THE ¹⁴C ACTIVITY OF DISSOLVED ORGANIC CARBON FRACTIONS IN THE NORTH CENTRAL PACIFIC AND SARGASSO SEA OLIGOTROPHIC GYRES

James E. Bauer, Peter M. Williams, and Ellen R. M. Druffel

Dissolved organic carbon (DOC) in ocean waters constitutes one of the largest exchangeable pools of organic carbon (~1018 g) on earth, and is composed mostly of uncharacterized material. Bulk analyses (δ^{13} C and humic constituents) of DOC in the deep sea suggest that this material has a marine planktonic origin, yet little is known of the processes which contribute to changes in the magnitude and distribution of DOC in the ocean's interior. Earlier ¹⁴C measurements of DOC oxidizable by ultraviolet irradiation (DOC_{uv}) revealed apparent ages of about 6000 years in the deep waters of the oligotrophic north central Pacific (NCP) gyre. However, recent reports of a potentially larger pool of DOC as measured by high temperature catalytic combustion (DOC $_{htc}$) have led to speculation that this additional material may be "younger," more recently produced DOC which contributes significantly to overall oceanic organic carbon fluxes due to its suspected greater biological lability. Here we present the first Δ^{14} C (per mil deviation from 14 C activity of 19th century wood) values of the DOChte in profiles from the oligotrophic NCP and Sargasso Sea (SS) and compare them to the corresponding $DOC_{uv} \Delta^{14}C$ values. The $\Delta^{14}C$ values of the DOChtc and DOCuv fractions were remarkably similar, indicating that the bulk of the DOC in these regions of the world's oceans cycles on time scales of several thousands of years (apparent ages of ~6000 and ~4000 years BP in the deep NCP and SS, respectively). The observed ocean-ocean differences in Δ^{14} C values of DOC can, to a large extent, be accounted for by differences in the Δ^{14} C of the DOC sources to the deep basins and by deep water circulation patterns (transit times) between the SS and the NCP.

Submitted to: Nature.

Supported by: NSF Grants OCE87-16590 and OCE88-40531.

WHOI Contribution No. 7913.

DO UPPER-OCEAN SEDIMENT TRAPS PROVIDE AN ACCURATE RECORD OF PARTICLE FLUX?

Ken O. Buesseler

Sediment traps are widely used to measure the

vertical flux of particulate matter in the oceans. In the upper ocean, sediment traps have been used to determine the extent of which CO₂ fixed by primary producers is exported as particulate organic carbon. In addition, the observed decrease of particle flux with depth has been used to predict regeneration rates of organic matter and associated elements. Over seasonal or annual timescales, the import of limiting nutrients into the upper ocean (new production) should be balanced by particle export. Given the importance of accurately determining the sinking particle flux, it has been suggested that ²³⁴Th might be used to 'calibrate' shallow-trap fluxes. Here I present a re-evaluation of existing ²³⁴Th data which indicates that trap-derived and model-derived ²³⁴Th particle fluxes can differ by a factor of $\pm 3-10$, suggesting that shallow traps may not provide an accurate measure of particle fluxes.

Published in: Nature, 353(6343):420-423, 1991.

Supported by: NSF Grant OCE89-17836.

WHOI Contribution No. 7652.

APPLICATION OF A GENERALIZED SCAVENGING MODEL TO THORIUM ISOTOPE AND PARTICLE DATA AT EQUATORIAL AND HIGH LATITUDE SITES IN THE PACIFIC OCEAN

Simon L. Clegg, M. P. Bacon, and M. Whitfield

A generalized trace metal scavenging model has been applied to particle cycle and ²³⁴Th data at three equatorial Pacific sites, and to dissolved and particulate ²²⁸Th, ²³⁰Th and ²³⁴Th profiles at a single high latitude station. The one dimensional (and here steady-state) model consists of two particle classes-small (suspended) and large (sinking). It is driven by particle primary production and parameterized from particle and tracer concentration and flux data. The model has been used to determine, as functions of depth, (1) rates of particle remineralization; (2) aggregation and disaggregation of the small and large particle classes, respectively; and (3) adsorption and desorption rate constants of thorium. The results are insensitive to the assumed large particle sinking rate of 150 m d^{-1} . The profiles of all three tracers at Station 'P' are described satisfactorily by a single set of model parameters. The adsorption rate constant, normalized for the effect of particle concentration, is enhanced in the upper 100 m of the water column by a factor of two or greater at all sites. Values of this and the other major model parameters are consistent with earlier results for a variety of oceanic environments, suggesting that the gross observable features and

processes of scavenging are similar over large areas of the ocean.

In Press: Journal of Geophysical Research.
Supported by: NSF Grant OCE88-00620.

WHOI Contribution No. 7640.

THE IMPORTANCE OF ISOTOPIC MEASUREMENTS IN MARINE ORGANIC GEOCHEMISTRY

Ellen R. M. Druffel and Peter M. Williams

The largest exchangeable organic carbon reservoir on earth is in the form of dissolved organic matter (DOM) in seawater (~10¹⁸g C). Less than 10 percent of this DOM has been characterized either with regard to organic compound classes or specific organic molecules. Moreover, little is known about the sources of marine DOM. For instance, it remains a mystery whether or not an appreciable part of this DOM is of terrestrial origin, and if so, is it significantly altered with time? Isotopic signatures (Δ^{14} C, δ^{13} C, δ^{15} N) have proven powerful tracers in helping establish the sources and sinks of DOM and living and detrital particulate organic matter (POM) in the oceans and in assisting in determining the extent and direction of transformation processes between the soluble and particulate phases. In conjunction with chemical data (i.e., total DOM, oxygen, nutrients, total CO₂, alkalinity, salinity), isotopic measurements are essential for assessing the processes controlling organic matter distributions in the oceans. We present here some specific areas of research, prefaced by brief and selected reviews, into the cycling of organic matter in the marine environment. These are areas which, in our opinion, isotopic signatures will provide vital answers or clues.

In Press: Marine Chemistry as a Contribution to the Proceedings for the Marine Organic Geochemistry, Review and Future Challenges Workshop, Honolulu, January, 1990.

Supported by: NSF Grant OCE87-16590.

WHOI Contribution No. 7846.

SEDIMENTARY AND GEOCHEMICAL EXPRESSIONS OF OXIC AND ANOXIC CONDITIONS ON THE PERU SHELF

Kay-Christian Emeis, Jean K. Whelan, and Martha Tarafa

Sediments from drill hole transects across the Peru shelf and upper slope show that the extent and intensity of the oxygen-minimum zone has varied considerably from the early Pleistocene to the Present. Primary sedimentary features, such as laminations vs. bioturbation, and the hydrogen index of sedimentary organic matter appear to covary with the presence and intensity of the OMZ. Sediments deposited under anoxic bottomwater conditions are significantly more hydrogen-rich relative to bulk TOC. The molecular composition of pyrolytic hydrocarbons and heterocompounds, however, is surprisingly uniform, and is consistent with minimal oxic nor anoxic degradation once the organic matter reaches the sediment. The concept of better preservation of hydrogen-rich organic matter under anoxic conditions in the bottom water is reflected in the bulk parameter of pyrolyzable organicmatter content relative to TOC, but not in individual compound classes incorporated into kerogen. The most important control on the hydrogen-richness of organic matter appears to be sediment reworking and redeposition.

In Press: Continental Shelf Anoxia, R. Tyson and T. Person, eds., Geological Society of London Special Publication.

Supported by: NSF Grants OCE85-09859 and OCE87-17019.

WHOI Contribution No. 7670.

SCALING OF MARINE MICROLAYER FILM SURFACE PRESSURE-AREA ISOTHERMS USING CHEMICAL ATTRIBUTES

Nelson M. Frew and Robert K. Nelson

Heterogeneity in the chemical composition of sea-surface films due to variation in sources of surfactant materials and in physical dynamics during film formation may lead to spatial and temporal variability in interfacial physical properties. Alternatively, slick physical properties may be postulated to be largely averaged and therefore similar across a variety of oceanic regimes. In order to assess interslick variability in regimes of different productivity, surface pressure-area $(\pi - A)$ isotherms have been measured for a suite of microlayers sampled at inshore and offshore stations in the southern California Bight. Surface-active organics isolated from the microlayers by solid phase extraction were respread on clean seawater and the π -A isotherms determined. Several bulk chemical parameters, including dry weight, UV absorbance, carbon, nitrogen and lipid content, have been examined in an attempt to scale the isotherms; the latter are shown not to collapse to a single well-constrained envelope when compared on a specific area basis.

However, for several parameters there was a clear separation of the slicked microlayer isotherms into two distinct film types comprised primarily of inshore and offshore samples, respectively. Area scaling and virial equation modeling also clustered the isotherms into two groups with different elastic properties suggesting the presence of distinct 'end-member' components. Surfactants from an unslicked microlayer appeared to produce films which were much less elastic than those from slicked microlayers. The observed interslick variability in π -A characteristics was larger than the uncertainties inherent in the methodology and we conclude that the variability was related to significant differences in chemical composition of films. These compositional differences must be taken into account in order to correctly define interfacial boundary conditions in modeling of wind-wave interactions.

In Press: Journal of Geophysical Research, Special Microlayer Section.

Supported by: ONR Contract No. N00014-87-K-007 and Grant No. N00014-89-J-1080.

WHOI Contribution No. 7695.

ISOLATION OF MARINE MICROLAYER SURFACTANTS FOR EX-SITU STUDY OF THEIR SURFACE PHYSICAL AND CHEMICAL PROPERTIES

Nelson M. Frew and Robert K. Nelson

Surface-active organic matter from natural marine microlayers has been isolated by solid phase adsorption using reversed phase (C₁₈) cartridges. Surfactants collected from a suite of microlayer films in the California Bight and the Gulf of Maine and isolated by this technique were respread on clean seawater to reconstitute surface films, which exhibited surface pressure- area $(\pi-A)$ isotherms and static (Gibbs) surface elasticities closely approximating those measured for films formed by diffusion in the original fresh microlayer samples. The estimated mean recovery of microlayer dissolved organic carbon (DOC) was $20 \pm 5\%$. The select hydrophobic DOC fraction isolated was the dominant surfactant class responsible for microlayer film characteristics as measured quasi-statically, even though other relatively hydrophilic DOC fractions, which may have been enriched in the microlayer, were not absorbed and passed through the isolation procedure. This technique allows collection of marine microlaver films for systematic ex situ study and correlation of their surface physical and chemical properties. For the first time, the π -A isotherms for microlayer films can be expressed on a specific area basis and, in cases where molecular weights can be estimated, according to mean molecular area.

In Press: Journal of Geophysical Research, Special Microlayer Section.

Supported by: ONR Contract No. N00014-87-K-007 and Grant No. N00014-89-J-1080.

WHOI Contribution No. 7696.

HYDROTHERMAL SCAVENGING AT THE MID-ATLANTIC RIDGE: RADIONUCLIDE DISTRIBUTIONS

C. R. German, A. P. Fleer, M. P. Bacon, and J. M. Edmond

We have carried out a study of U-series radionuclide distributions in the neutrally-buoyant plume overlying the TAG hydrothermal vent field at 26°N, Mid-Atlantic Ridge. Limited uptake of U accompanies the formation of Fe-oxyhydroxide particulate material within the hydrothermal plume. The particulate U concentrations are too small for measurable dissolved U anomalies to be produced within the water column at plume height. However, such uptake, followed by deposition in the underlying sediments, could account for ~10% of the U-enrichment that has been reported previously for metalliferous ridge-crest sediments. Particulate ²³⁴Th, ²³⁰Th and ²³⁸Th activities in the TAG hydrothermal plume represent >65% of total Th activities typical of the deep ocean. Low dissolved Th activities coincide with the high particulate Th activities. indicating that hydrothermal scavenging strongly affects Th-isotope distributions in the water column close to hydrothermal vents. Much of the scavenging occurs during the initial formation of Fe-rich hydrothermal precipitates but some further scavenging continues as the material is dispersed, away from its source. Distributions of particulate ²¹⁰Pb and ²³¹Pa activities in the neutrally-buoyant plume are also extremely high $(7-12 \text{ dpm}/10^2 \ell \text{ and})$ 30-60 dpm/10⁶ ℓ , respectively). Like Th, ²¹⁰Pb and ²³¹Pa show evidence for scavenging within the hydrothermal plume. Total Th activities at plume height are ~50% higher than "background." This "focussing" of Th into the plume is consistent with the entrainment and re-emplacement at plume height of particulate material recycled from beneath the neutrally-buoyant plume.

Published in: Earth and Planetary Science Letters, 105:170-181, 1991.

Supported by: NSF Grant OCE88-00620.

WHOI Contribution No. 7651.

THE PIGMENTS OF PROCHLOROCOCCUS MARINUS: THE PRESENCE OF DIVINYL-CHLOROPHYLL-A AND -B IN A MARINE PROCHLOROPHYTE

Ralf Goericke and Daniel J. Repeta

The pigments of the recently isolated marine prochlorophyte Prochlorococcus marinus were characterized by modern chromatographic and spectroscopic analysis. The major photosynthetic pigment is 8-desethyl, 8-vinyl chlorophyll-a. Accessory pigments are 8-desethyl, 8-vinyl chlorophyll-b, zeaxanthin, α-carotene, an unknown carotenoid and possibly Mg 3,8 divinyl-pheoporphyrin-a₅. Chlorophyll-a is not present in this organism. P. marinus is the first wild type oxygenic phototroph that does not have chlorophyll-a as its major photosynthetic pigment and it is the only procaryote with ε -cyclic carotenoids (a-carotene). P. marinus demonstrates a range of biosynthetic abilities that will necessitate a re-evaluation of the evolution of chlorophyll and carotenoid biosynthesis in pro- and eucaryotic phototrophs.

In Press: Limnology & Oceanography.

Supported by: NSF Grant OCE88-14398.

WHOI Contribution No. 7799.

INVESTIGATION OF THE ELECTROSTATIC PROPERTIES OF HUMIC SUBSTANCES BY FLUORESCENCE QUENCHING

Sarah A. Green, Francois M. M. Morel, and Neil V. Blough

A fluorescence quenching technique was employed to explore the electrostatic properties of fulvic (FA) and humic (HA) acids. Cationic nitroxides were found to be up to 16 times more effective than neutral analogues in quenching the fluorescence of humic materials. This result is attributed to the enhanced coulombic attraction of cations to the anionic FA or HA surface, and is interpreted as an estimate of surface potential. Reduction of molecular charge at low pH and shielding of charge at high ionic strength produced diminished enhancements consistent with this interpretation. High molecular weight fractions of HA have a higher apparent surface potential than lower molecular weight fractions, indicating that larger humic molecules may have an enhanced ability to bind metal ions.

Published in: Environmental Science and Technology, 26(2):294-302, 1992.

Supported by: EPA Grant No. CR-815293.01, ONR Grant No. N00014-89-J-1260, and NSF Grant OCE89-17688.

WHOI Contribution No. 7734.

MASS SPECTROMETRIC IDENTIFICATION OF THE RADICAL ADDUCTS OF A FLUORESCAMINE-DERIVATIZED NITROXIDE

David J. Kieber, Carl G. Johnson, and Neil V. Blough

The radical adducts of fluorescamine-derivatized 3-aminomethyl-2,2,5,5-tetramethyl-1-pyrrolidinyloxy free radical are readily identified by mass spectrometry employing a solid source probe and electron impact ionization.

Published in: Free Radical Research Communications, 16(1):35-39, 1992.

Supported by: ONR Grants N00014-89-J-1260 and N00014-87-K-007.

WHOI Contribution No. 7646.

NOVEL PYROPHEOPHORBIDE STERYL ESTERS IN BLACK SEA SEDIMENTS

Linda L. King and Daniel J. Repeta

A series of non-polar chlorophyll degradation products (NPCs) with greater than 10 components has been isolated from Black Sea sediment and identified as pyropheophorbide steryl esters by visible and mass spectrometry. These compounds have been previously observed in seawater and sediment trap samples, and may be formed during grazing of phytoplankton by zooplanktonic herbivores. In Black Sea sediments, NPCs constitute 14% of the total phorbins determined spectroscopically at 660 nm, and 39% of the total chlorophyll degradation products measured by high pressure liquid chromatography. NPCs therefore constitute a significant sedimentary sink for chlorophyll. The distribution of sterols released by hydrolysis of NPCs most closely resembles sterols in suspended particulate matter collected from the euphotic zone and is quite different from the distribution of solvent-extractable sterols in sediments. Sterols extracted from sediments have high concentrations of 4-methylsterols and high stanol/stenol ratios. NPC-derived sterols have very low concentrations of 4-methylsterols and low stanol/stenol ratios. We suggest that these differences reflect an enhanced preservation of NPCs in sediments relative to free sterols and phorbins. As a result, the original production of

sterols in the euphotic zone may be more closely approximated by the distribution of NPC-derived sterols than by the distribution of free sterols in sediments.

Published in: Geochimica et Cosmochimica Acta, 55:2067-2074, 1991.

Supported by: NSF Grant OCE88-14398.

WHOI Contribution No. 7715.

ORGANIC GEOCHEMISTRY AS A TOOL TO STUDY UPWELLING SYSTEMS: RECENT RESULTS FROM THE PERU AND NAMIBIAN SHELVES

Daniel J. Repeta, Mark A. McCaffrey, and John W. Farrington

Organic geochemists are currently developing new, molecular-based tools for studying the historical record of coastal upwelling. Several hundred biomarkers, organic compounds with known biological sources, have been identified in sediments underlying the world's major upwelling systems. Studies completed over the last two decades show that the distribution of many biomarkers in sediments is heavily impacted by the oceanographic and ecological conditions that prevail at the time of sediment deposition. Therefore, these biomarkers have the potential to serve as useful paleoenvironmental indicators. In order to decipher the sedimentary record on the molecular level, a better understanding of early diagenesis, and the coupling between water column biology, chemistry, and biomarker distribution in sediments is needed. Upwelling environments provide excellent sites to conduct such studies. High sediment accumulation rates and good preservation of organic matter in sediments relative to other depositional environments permit high-resolution time-series studies. We summarize here some recent research on early diagenesis, the effect of dysaerobic conditions on biomarker preservation, and the impact of El Niño Southern Oscillation (ENSO) events on the organic geochemical record. We further suggest some specific areas of future research that could substantially enhance our understanding of upwelling environments.

In Press: Evolution of Upwelling Systems Since The Early Miocene.

Supported by: NSF Grants OCE88-14398 and OCE88-11409.

WHOI Contribution No. 7711.

GEOCHEMISTRY—INORGANIC, ISOTOPIC

LEAD-210 BALANCE AND IMPLICATIONS FOR PARTICLE TRANSPORT ON THE CONTINENTAL SHELF, MIDDLE ATLANTIC BIGHT

Michael P. Bacon, Rebecca A. Belastock, and Michael H. Bothner

Supply of ²¹⁰Pb to the continental shelf off the northeastern United States is dominated by the deposition from the atmosphere, the rate of which is reliably known from previously published work. Excess ²¹⁰Pb inventories in the shelf sediments show accumulations that are nearly in balance with the supply, even in areas of relict sands where it is believed that no net accumulation of sediment presently occurs. The ²¹⁰Pb distributions in Shelf and Slope Water indicate that the two-way fluid exchange at the shelf/slope front and the net transport in the alongshore flow make comparatively small contributions to the shelf ²¹⁰Pb budget. The near balance between supply and decay of ²¹⁰Pb on the shelf implies a limit to the particle export flux. It is concluded that the export of particulate organic carbon does not exceed 60 g/m²-y (~25% of primary production) and is probably lower. The hypothesis is advanced that fine particulate matter introduced to the continental shelf is detained in its transit of the shelf because of bioturbational trapping in the sediment due to benthic animals. Distributions of ²¹⁰Pb in suspended particulate matter and in the fine fraction of shelf sediments suggest that the average fine particle must undergo several cycles of deposition-bioturbation-resuspension-redeposition and requires a number of decades for its transit and ultimate export from the shelf. Thus only the most refractory organic matter is likely to be exported.

Submitted to: Continental Shelf Research.

Supported by: DOE Grant DE-FGO2-88ER60681.

WHOI Contribution No. 7869.

IN-SITU PRODUCED COSMOGENIC ³HE IN ANTARCTIC GLACIAL DEPOSITS: 1. CONSTRAINING EXPOSURE AGES OF QUARTZ SANDSTONE BOULDERS WITH ³HE

Edward J. Brook and Mark D. Kurz

In-situ produced cosmogenic ³He (³He_c) provides a new tool for constraining ages and histories of Quaternary geomorphic surfaces. Before this utility is fully realized, however, the

systematics and production rates of ³He_c must be well understood. Brook et al. (1992, this issue) use ³He data from sandstone and granite boulders in the Dry Valleys region of Antarctica to constrain the ages of an important moraine sequence formed by the Taylor Glacier. The data from this study also provide information about the systematics of ³He in quartz that has important implications for geochronology based on ³He_c.

In contrast to previous results from olivine and clinopyroxene, in vacuo crushing of quartz releases helium with high ${}^{3}\text{He}/{}^{4}\text{He ratios}$ (up to $148 \times R_a$). ³He concentrations and ³He/⁴He ratios in helium released by crushing roughly correlate with total ³He, suggesting a relationship with exposure age. The data indicate that in vacuo crushing cannot be used to determine the isotopic composition of trapped or magmatic helium in quartz, as is possible in volvine and clinopyroxene. However, because non-cosmogenic helium in quartz is dominantly radiogenic ${}^{3}\text{He}/{}^{4}\text{He} \sim 10^{-8}$), the correction for non-cosmogenic helium is small and contributes little to uncertainties in ³He_c.

Detailed analysis of seven size fractions (from 425 to 2000 microns) from two samples suggest significant ³He loss in older samples that is not predicted by existing measurements of the ³He diffusivity in quartz. There are several possible explanations for the discrepancy, including solar heating of rock surfaces, diffusion domains in quartz that are not related to grain size, changes in diffusion mechanisms at low temperatures. post-depositional alteration of small grains, or crystal damage related to exposure to cosmic rays. Nonetheless, ³He loss from these samples is not as extensive as suggested by the limited data of previous studies.

Submitted to: Quaternary Research. Supported by: NSF Grant DPP88-17406.

WHOI Contribution No. 7897.

IN-SITU PRODUCED COSMOGENIC ³HE IN ANTARCTIC GLACIAL DEPOSITS: 2. CHRONOLOGY OF TAYLOR GLACIER ADVANCES IN ARENA VALLEY

Edward J. Brook, Mark D. Kurz, George H. Denton, and Robert P. Ackert

In-situ produced cosmogenic nuclides provide a new technique for constraining exposure ages of geological surfaces, including glacial moraine boulders. New measurements of in-situ ³He in quartz sandstone boulders from Arena Valley, a small glacial valley in southern Victoria Land, Ant :rctica, provide chronological constraints for a sequence of boulder-belt moraines ("Taylor II-IVb" moraines) related to past expansions of

the Taylor Glacier and East Antarctic Ice Sheet. Using median ³He exposure ages as minimum estimates suggests ages of $115,000 \pm 36,000$ yr for "Taylor II", $207,000 \pm 64,000$ yr for "Taylor III", $365,000 \pm 181,000$ yr for "Taylor IVa," and 1.12 \pm 0.35 myr for "Taylor IVb." The ages for "Taylor II" and "Taylor III" are consistent with isotope stage 5 (\sim 100,000 yr) and stage 7 (\sim 200,000 yr) ages suggested by correlations with U-Th dated deposits in lower Taylor Valley. The ³He age for "Taylor IVb" is younger than a maximum age of 2 myr based on previous 40 Ar-39 Ar dating of volcanic ash in stratigraphically older sediments, and younger than an age of ~2 myr suggested by previous 10 Be data. For "Taylor IVa," in-situ cosmogenic nuclides provide the first direct chronological constraints.

Although the median exposure ages appear consistent with available geological data, each moraine has a broad distribution of ages. The scatter in the age distribution is potentially affected by a variety of factors, including erosion, prior exposure to cosmic rays, ³He loss, and radiogenic production of ³He. Nonetheless, for the Arena Valley moraine sequence, which has important ties to the history of the East Antarctic Ice Sheet, the exposure ages provide direct chronological constraints.

The data confirm previous interpretations of this moraine sequence, suggesting a thickening of the Taylor Glacier relative to the present ice surface of not more than about ~500 m since the early Pleistocene, indicating that the McMurdo Dome and the East Antarctic Ice Sheet have not been significantly larger than today in at least the past 2 myr. Inclusion of previously published ¹⁰Be data allows extension of this conclusion back to the late to middle Pliocene.

Submitted to: Quaternary Research. Supported by: NSF Grant DPP88-17406. WHOI Contribution No. 7898.

MASS SPECTROMETRIC 14C AND U-TH MEASUREMENTS IN CORAL

G. S. Burr, R. L. Edwards, D. J. Donahue, E. R. M. Druffel, and F. W. Taylor

This article describes U-Th and radiocarbon measurements in coral. Samples with U-Th dates in excess of 50 ky BP were chosen for study. Some bulk samples have measurable radiocarbon dates. which range from 30 ky BP to 43 ky BP. These can be explained by 0.5 to 2.5% contamination by modern carbon. This small amount of contamination may be undetectable with X-Ray powder diffraction patterns. A sample pretreatment for

radiocarbon analysis is described which removes the modern carbon by selective dissolution.

In Press: Radiocarbon.

Supported by: NSF Grant OCE89-15919.

WHOI Contribution No. 7863.

A LITHIUM ISOTOPE STUDY OF HOT SPRINGS AND METABASALTS FROM MID-OCEAN RIDGE HYDROTHERMAL SYSTEMS

Lui-Heung Chan, John M. Edmond, and Geoffrey Thompson

The Li isotopic compositions of seawater, and of fresh and altered basalts are distinct and therefore applicable to the study of the hydrothermal processes in the oceanic crust and the Li balance in the ocean. High-temperature fluids from seven vents on the East Pacific Rise (EPR) at 21°N and 11-13°N have δ^6 Li values ranging between $-6^{\circ}/_{\infty}$ and $-11^{\circ}/_{\infty}$, i.e., $3-7^{\circ}/_{\infty}$ heavier than fresh basalt values. No temporal change in the isotopic value was observed between 1981 and 1985. Metabasalts show both Li depletion and enrichment relative to fresh basalt. A Li-rich amphibolite was found to have a light Li isotopic value reflecting incorporation of Li initially mobilized from fresh basalt. From these observations we conclude that the Li isotopic composition of submarine hot springs is buffered by alteration minerals, much like the major element chemistry. δ^6 Li values of fluids from the Mid-A+lantic Ridge (MAR) (-6% to -8%) fall in the range of the EPR, indicating similar equilibrium controls at the two ridge systems. The lack of ⁷Li enrichment in the fluids from slower spreading ridges indicates that Li is not recycled from older weathered crust. Thus the difference between the ³He an ¹⁸⁷Sr/⁸⁶Sr based hydrothermal flux and the crustal transfer rate of Li cannot be reconciled by the inclusion of secondary Li from older cruse.

In Press: Journal of Geophysical Research.

Supported by: NSF Grant OCE89-17352 and OCE90-13150.

WHOI Contribution No. 7915.

LITHIUM ISOTOPIC COMPOSITION OF SUBMARINE BASALTS

L. H. Chan, J. M. Edmond, G. Thompson, and K. Gillis

We have measured the Li isotope composition of young, pristine basalts from active ocean ridge

crests, and of progressively older basalts along a dredging transect. The data significantly extend our limited knowledge of the isotopic abundance ratio of Li in geological material. Fresh mid-ocean ridge basalts have $\delta^6 \text{Li}$ values between -3.4 to -4.7°/∞ relative to the isotope standard L-SVEC. During low temperature weathering on the seafloor, the isotopic composition of the rock becomes increasingly heavier due to addition of seawater Li (δ^6 Li = 32.3°/ $_{\infty}$). The cldest (46 m.y.) and most altered rock studied has an isotopic composition of -14°/_∞. A linear relationship exists between δ^6 Li and the inverse of Li concentration, suggesting that Li in weathered basalts can be regarded as a two-component mixture of pristine basaltic Li and seawater-derived Li that has been incorporated in alteration minerals, most likely secondary clays such as smectite and phillipsite. The inferred Li isotopic composition of the alteration endmember indicates an apparent isotopic fractionation factor of 1.019 relative to the seawater source. Thus Li uptake by secondary minerals from the low temperature weathering process and, by analogy, incorporation in similar authigenic minerals in marine sediments provide a mechanism for preferential removal of the lighter Li isotope from ocean water. However, isotopic fractionation due to authigenic clay formation alone cannot accourt for the isotopic difference between seawater and its principal sources, unless the hydrothermal flux is comparable to the river flux. Alternatively, more important sinks of ⁶Li must exist if the steady state isotopic composition Li in ocean water were to be maintained.

In Press: Earth and Planetary Science Letters.

Supported by: NSF Grant OCE89-17352.

WHOI Contribution No. 7736.

A MODEL FUNCTION OF THE GLOBAL BOMB-TRITIUM DISTRIBUTION IN PRECIPITATION, 1960-1986

Scott C. Doney, David M. Flover, and William J. Jenkins

We have developed using the WMO/IAEA tritium data set, a global model function for predicting the annual mean concentration of decay-corrected bomb-tritium (TU81N) in precipitation over the time period 1960–1986. The model consists of two reference time histories or factors—calculated from a factor analysis of the zonally averaged global data set—and global maps of the two spatial coefficients associated with the factors. By combining the reference curves with the appropriate coefficient values taken from these maps, an estimate of the tritium time history for particular locations can be produced. The

predicted error for the integrated tritium concentration from the annual model is approximately 3-10% and, in a comparison with previous work (Weiss and Roether, 1980), provides a statistically better fit of the tritium data at most stations. We also discuss the seasonal cycle of tritium in precipitation and present estimates for the amplitude and phase for tritium using a simple seasonal model. At most of the WMO/IAEA monitoring stations, our four-parameter seasonal model accounts for greater than 80% of the variance in the monthly observations.

In Press: Journal of Geophysical Research.
Supported by: NSF Grant OCE86-13324.
WHOI Contribution No. 7691.

A TRITIUM BUDGET FOR THE NORTH ATLANTIC

Scott C. Doney, William J. Jenkins, and H. G. Ostlund

We develop a new model bomb-3H budget for the North Atlantic between 1950 and 1986. The model, which calculates the atmospheric and continental ³H delivery, as well as the advective ³H transports from the South Atlantic and Arctic, agrees within about 10% with the ³H inventories calculated from the 1972 GEOSECS and the 1981-1983 TTO observations. The decay-corrected ³H inventory for the North Atlantic increased by about 43% between the GEOSECS and TTO programs (1972 to 1981), and the inflow of high ³H polar water from the Arctic is found to be crucial for correctly simulating this increase. Key aspects of the model that differ from previous studies include the treatment of vapor/rain isotopic equilibrium, the continental vapor flux, and the downward flux of water vapor into the ocean. The sensitivity of the atmospheric ³H delivery to model parameters and to seasonal and inter-annual variability are explored.

Submitted to: Journal of Geophysical Research (Oceans).

Supported by: NSF Grant OCE89-11697.

WHOI Contribution No. 7870.

RADIOCARBON IN SEAWATER AND ORGANISMS FROM THE PACIFIC COAST OF BAJA, CALIFORNIA

Ellen R. M. Druffel and Peter M. Williams

Radiocarbon was measured in dissolved inorganic carbon (DIC) and living organisms collected off the west coast of Baja, California, in

October 1980. Samples from three locations were examined. $\Delta^{14}\mathrm{C}$ of DIC at the southernmost station was higher than those further north, which reflects reduced upwelling in the southern region. Crabs and anchovies had $\Delta^{14}\mathrm{C}$ values significantly lower than surface DIC $\Delta^{14}\mathrm{C}$, indicating the incorporation of 'older', sediment-derived carbon sources from their diets. Comparisons are made between our DIC $\Delta^{14}\mathrm{C}$ measurements and those obtained during other cruises and at a coastal site, from 1959 through 1987. Two distinct time histories of DIC $\Delta^{14}\mathrm{C}$ are apparent for the postbomb period: (1) a lower $\Delta^{14}\mathrm{C}$ curve for sites close to the coast influenced by enhanced coastal upwelling, and (2) a higher $\Delta^{14}\mathrm{C}$ curve for sites further offshore within the California Current.

Published in: Radiocarbon, 33(3):291-296, 1991.

Supported by: NSF Grants OCE79-17653 and OCE81-11954.

WHOI Contribution No. 7845.

SEASONAL CHANGES IN THE ISOTOPIC COMPOSITIONS AND SINKING FLUXES OF EUTHECOSOMATOUS PTEROPODS IN THE SARGASSO SEA

V. J. Fabry and W. G. Deuser

Seasonal variations in the oxygen and carbon isotopic compositions and fluxes of five euthecosomatous pteropods were determined from a 14-month series of sediment trap deployments in the Sargasso Sea. Medium and large shell sizes of Styliola subula, Clio pyramidata, Limacina inflata, Creseis acicula and Cuvierina columnella were collected throughout the sampling period. Comparisons of the δ^{18} O of shell samples with the vertical and temporal variations in the calculated δ^{18} O of aragonite in equilibrium with seawater suggest that these pteropods deposited the bulk of their shell mass at the following depths: S. subula and L. inflata at 50 m, C. pyramidata at 75 m, C. acicula in the upper 25 m and C. columnella at 50-75 m. Although several of these species undergo diel vertical migration of several hundred meters in this region, the estimated depths of calcification match the upper parts of the species' vertical ranges, where the mean populations occur only at night. In all species, changes in the $\delta^{18}O$ of shells were closely coupled to those of seawater, suggesting that most of the shell mass of these individuals was formed within several months. Flux-weighted, mean δ^{18} O values for the species reveal that seasonal variations in the sinking fluxes of shells would not affect the isotopic compositions of shell accumulations in Bermuda Rise sediments. Carbon and oxygen isotopes were positively

correlated in all species except C. columnella, which suggests that temperature may influence the δ^{13} C of the shells of these species.

In Press: Paleoceanography.

Supported by: NSF Grants OCE84-17909 and OCE87-16589.

WHOI Contribution No. 7832.

GLACIAL TO INTERGLACIAL CHANGES IN SURFACE NITRATE UTILIZATION IN THE INDIAN SECTOR OF THE SOUTHERN OCEAN AS RECORDED BY SEDIMENT δ^{15} N

Roger Francois and Mark A. Altabet

We present a new approach for paleoceanographic reconstruction of surface nutrient utilization in the Southern Ocean. It has been observed in the contemporary ocean that, due to preferential uptake of 14NO3 during photosynthesis, the $\delta^{15}N$ of planktonic organic matter increases with increasing nitrate depletion in surface waters. Our results demonstrate that the $\delta^{15}N$ signal produced in surface waters is reflected in the underlying sediments; core top $\delta^{15}N$ is inversely correlated with surface nitrate concentration along a transect across the Subtropical Convergence and the Polar Front in the South-East Indian Ocean. These results are consistent with a 4-box model showing that the nitrogen isotopic composition of sinking organic matter depends on % nitrate utilization in the euphotic zone. By comparing the $\delta^{15}N$ of surface sediments with that measured in the glacial sections of several cores, we infer changes in the intensity and latitudinal distribution of nitrate uptake in this region during the last glacial maximum. The results suggest that Subantarctic waters in the SE Indian sector became more nutrient depleted as they migrated northward. Increased nitrate depletion might have also occurred slightly south of the glacial Polar front. We use a 6-box model to explore the possible impact of this observation on atmospheric CO₂.

Submitted to: Paleoceanography.

Supported by: NSF Grant OCE91-15641.

WHOI Contribution No. 7881.

A GEOCHEMICAL STUDY OF METALLIFEROUS SEDIMENT FROM THE TAG HYDROTHERMAL MOUND, 26°08'N, MAR

C. R. German, R. Mills, J. Blusztajn, A. P. Fleer, M. P. Bacon, N. C. Higgs, H. Elderfield, and J. Thomson

Pb-isotope, natural radioisotope, and REE distributions have been employed to investigate metal-enriched sediments collected from close to the base of the TAG hydrothermal mound. 26°08'N, Mid-Atlantic Ridge. The core sampled a 7-cm thick horizon of Fe-rich, red-brown mud (20-40 wt.% Fe) overlying a horizon of carbonate ooze (5-7% CaCO₃) which also contains up to 32 wt.% Fe. On the basis of elemental compositions, two separate layers can be identified within the red-brown mud, from 0-3 cm and from 3-7 cm. The core position and XRD, Pb-isotope and elemental analyses all indicate that these two layers derive from local mass wasting of oxidized, originally sulphidic material from the TAG hydrothermal mound. High concentrations (11-19 ppm) of seawater-derived U are observed in both Fe-rich layers and we propose that these enrichments derive from uptake of U linked to the oxidation of sulphide phases before and/or after their deposition in the sediments. Metal concentrations in the CaCO₃-rich horizon (7-11 cm), although lower than in the upper part of the core, are significantly enriched over open ocean carbonate sediment concentrations. ²³⁰Th_{x4}/Fe, ²³¹Pa_{xs}/Fe and REE/Fe distributions indicate that the hydrothermal input to this layer is dominated by settling of suspended particulate material from the overlying hydrothermal plume. Thus, these more diluted CaCO3-rich sediments may record an important "missing" component in the flux of hydrothermal material to sediments of the Mid-Atlantic Ridge rift valley, away from the sulphide-derived mounds.

Submitted to: Journal of Geophysical Research.

Supported by: NSF Grant OCE88-00620.

WHOI Contribution No. 7919.

COMPARATIVE MINERALOGY AND GEOCHEMISTRY OF GOLD-BEARING SULFIDE DEPOSITS ON THE MID-OCEAN RIDGES

Mark Hannington, Peter Herzig, Steven Scott, Geoff Thompson, and Peter Rona

A comparative study of the mineralogy and geochemistry of sulfide deposits on mid-ocean

ridges in the N.E. Pacific and the Mid-Atlantic reveals common characteristics associated with gold enrichment. Average gold contents of 0.8 to 5 ppm Au occur in sulfides from Southern Explorer Ridge and Axial Seamount (N.E. Pacific) and from the TAG hydrothermal field and Snakepit vent field (Mid-Atlantic Ridge). Enrichment of gold in these deposits is consistently related to a phase of late-stage, low-temperature (<300°C) venting. Concentrations >1 ppm Au occur exclusively in pyritic assemblages and commonly with abundant Fe-poor sphalerite and a suite of complex Pb-Sb-As sulfosalts. Amorphous silica and locally barite or carbonate are important constituents of the gold-rich precipitates but do not contain gold themselves. High-temperature (350°C) black smoker assemblages, consisting dominantly of pyrite, chalcopyrite, pyrrhotite, isocubanite and abundant anhydrite are uniformly gold-poor (<0.2 ppm Au). To the extent that individual sulfides can be mechanically separated, chemical analyses by neutron activation indicate that gold is most abundant in sphalerite (up to 5.7 ppm Au) but also occurs in pyrite and marcasite. Samples of sphalerite with abundant inclusions of fine-grained sulfosalts locally contain up to 18 ppm Au, suggesting that the sulfosalts may be the repositories for gold. No free gold has been observed at 4,000 X magnification of polished specimens, indicating that the gold is present only as submicroscopic inclusions or as a chemical constituent within the sulfides. Samples from gold-rich deposits in the N.E. Pacific and Mid-Atlantic are compared with similar but relatively gold-poor sulfides from the Galapagos Rift and 13°N EPR, and with barren sulfides from 11°N EPR, 21°N EPR, the Endeavour Ridge, and the Southern Juan de Fuca Ridge. Trace element analyses of more than 170 samples show that gold enrichment in almost all of the deposits is associated with high concentrations of Ag, As, Sb, Pb, and Zn, and locally with high Cd, Hg, Tl, and Ga. In contrast, gold is typically depleted in samples with high Co, Se, and Mo. The close association of Au with Ag, As, Sb, and Pb may reflect the common behaviour of these metals as aqueous sulfur complexes $[e.g., Au(HS)_2^-]$ at low temperatures. Similar mineralogical and geochemical associations are observed in recent sulfide deposits from modern back-arcs and in the ancient geologic record.

Published in: Marine Geology, 101:217-248, 1991.

Supported by: NSF Grant OCE90-13150.

WHOI Contribution No. 7735.

GOLD-RICH SEAFLOOR GOSSANS IN THE TROODOS OPHIOLITE AND ON THE MID-ATLANTIC RIDGE

Peter M. Herzig, Mark D. Hannington, Steven D. Scott, George Maliotis, Peter A. Rona, and Geoffrey Thompson

Massive sulfide deposits in the late Cretaceous Troodos ophiolite complex on Cyprus are among the best known ancient analogs of sulfide mineralization at modern oceanic spreading centers (e.g., Spooner, 1980; Oudin et al., 1981; Oudin and Constantinou, 1984; Scott, 1985; Herzig, 1988, Herzig et al., 1988a; Richardson et al., 1987; Richards et al., 1989). Several of the sulfide deposits along the northern margin of the Troodos complex are spatially related to structural grabens associated with fossil seafloor spreading (Schiffman et al., 1987; Schiffman and Smith, 1988). Although their tectonic setting may be more similar to a supra-subduction zone rather than a mid-ocean ridge (e.g., Miyashiro, 1973; Robinson et al., 1983; Schmincke et al., 1983; Moores et al., 1984; Rautenschlein et al., 1985; Muenow et al., 1990), the bulk composition of the Cyprus massive sulfides and the style of mineralization closely resembles that of black smoker deposits currently forming on the mid-ocean ridges. The Cyprus sulfides are characterized by a predominance of pyrite, varying amounts of chalcopyrite, minor sphalerite, and rare marcasite and pyrrhotite. The gold contents of the deposits are not well documented, but several are known to have produced more than 1,000 kg Au at grades ranging from 0.3 to 2.0 ppm Au (Bear, 1963; Spooner, 1980; Mosier et al., 1983). Analyses of 11 grab samples of massive sulfide from 9 different deposits also indicate gold contents in the range 0.02 to 2.5 ppm Au (Herzig et al., 1988a).

In Press: Economic Geology.

Supported by: NSF Grant OCE90-13150.

WHOI Contribution No. 7737.

AN ISOTOPIC STUDY OF DATED ALKALI BASALTS FROM SAO MIGUEL, AZORES: IMPLICATIONS FOR THE ORIGIN OF THE AZORES HOT SPOT

Mark D. Kurz, Richard B. Moore, David P. Kammer, and Armine Gulesserian

We have measured Sr, Pb and He isotopic compositions in a suite of radiocarbon dated basaltic rocks from Sao Miguel, Azores. All the isotopic ratios from the eastern part of the island are more radiogenic than those from the western

part; new 87 Sr/ 86 Sr values between 0.7033 and 0.7055, and 206 Pb/ 204 Pb values between 19.2 and 20.6, extend the ranges reported by previous workers. Extremely low ³He/⁴He ratios, between 3.5 and 8 times atmospheric (Ra), for Sao Miguel are reported here for the first time. ³He/⁴He ratios found in lavas from the Nordeste complex and Furnas volcano are the lowest reported for any oceanic island volcanics. Radiometric age control indicates that the isotopic variations are not related to eruption age. The correlations among the isotopes of He, Sr, and Pb strongly suggest that the low ³He/⁴He ratios are related to the mantle source, as opposed to magma chamber or metasomatic decoupling processes. The data therefore document that low ³He/⁴He ratios characterize the mantle source of the Sao Miguel volcanics, and that the Azores hot spot has typically higher (Th+U)/He ratios than MORB, which implies that it is more degassed. Samples from Sete Cidades volcano, on the western end of the island, have the least radiogenic isotopic compositions and are tectonically related to the Terceira Rift. Most of the isotopic variability is observed within roughly 15 km, in the region between Sete Cidades and Agua de Pau, where the Terceira Rift bisects the island. The isotopic boundary suggests that there is a pronounced discontinuity in the underlying mantle, and the data are consistent with an ancient sediment contribution to the mantle source of the eastern Sao Miguel volcanics. The preferred explanation for the isotopic variability from west to east on Sao Miguel is that the Terceira Rift magmas tap more homogenized mantle, while those from the eastern side of the island are derived from a more enriched mantle.

Submitted to: Earth and Planetary Science Letters.

Supported by: NSF Grants EAR88-3783 and OCE88-17406.

WHOI Contribution No. 7671.

ISOTOPE GEOCHEMISTRY OF THE BOUVET MANTLE PLUME

Mark D. Kurz, Anton le Roex, and Henry J. B. Dick

We have measured the isotopes of helium and lead in a suite of dredged basalts from the Southwest Indian Ridge, the American-Antarctic Ridge, and the Mid-Atlantic Ridge near the Bouvet Triple Junction. The ³He/⁴He ratios range from 6.5 to 14.2 times atmospheric (R_a), which encompass the entirety of existing MORB data, and differ significantly from values obtained from depleted MORB. Based on a compilation of data from Atlantic, Indian and Pacific Oceans, we

suggest that a benchmark value for depleted MORB 3 He/ 4 He of $8.5 \pm 0.3 \times R_a$.

Several samples from the Speiss Ridge have extremely low helium concentrations, low ³He/⁴He ratios, and display internal isotopic disequilibrium between glass and vesicles. These basalt glasses are therefore unique among the sample suite in having been affected by post-eruptive accumulation of radiogenic ⁴He. Although these data do not reflect the mantle source, they can be used to calculate eruption ages for the basalts, which fall between 3 and 51 kyr for these samples, which are the first He-U ages for MORB.

Pb isotopic compositions from the dredged basalt glasses range from near depleted MORB to those of Bouvet island itself (206 Pb/204 Pb of 18.2 to 19.6). The results are consistent with a hot spot origin of Bouvet island, in that high ³He/⁴He and ²⁰⁶Pb/²⁰⁴Pb ratios are observed both on Bouvet island and the ridge segment closest to it. The American-Antarctic Ridge has lower He, Sr and Pb isotope ratios than those of the Southwest Indian Ridge, which suggests a lesser influence of the hot spot to this region. The dredge samples from near the triple junction have relatively low ³He/⁴He ratios (~7 R_a), which suggests that the hot spot is centered beneath Bouvet island rather than beneath the triple junction. The data from the ridge segment adjacent to Bouvet island, on the Southwest Indian Ridge, define a trend toward high He, Sr, and Pb isotope ratios, which could be explained by mixing processes.

One ridge segment, between the Islas Orcadas and Shaka Fracture Zones, at 7°E, has distinct isotopic compositions, requiring more than two mantle components. The highest ³He/⁴He ratios were obtained from this ridge segment (~14 R_a) and are associated with relatively unradiogenic Sr and Pb isotopic compositions. A single dredge from this ridge segment also defines most of the helium isotopic variability. The remarkable isotopic variability over short distances on the ridge may be related to the slow spreading rates, and the lack of steady state magma chambers which homogenize geochemically distinct magma batches at faster spreading ridges. Alternatively, there is a different scale of heterogeneity in the mantle beneath this region. In either case, the Bouvet mantle plume itself must be heterogeneous to explain the isotopic diversity found within the basalts.

Submitted to: Geochimica et Cosmochimica Acta.

Supported by: NSF Grant OCE88-16970.

WHOI Contribution No. 7697.

NEW AGE DATA FOR MID-ATLANTIC RIDGE HYDROTHERMAL SITES: TAG AND SNAKEPIT CHRONOLOGY REVISITED

Claude Lalou, Jean Louis Reyss, Evelyne Brichet, Maurice Arnold, Geoffrey Thompson, Yves Fouquet, and Peter A. Rona

Using ²¹⁰Pb/Pb, ²³⁰Th/²³⁴U and ¹⁴C dating the chronologies of TAG and Snakepit hydrothermal fields have been established. At the TAG field, a Mn-oxide record indicative of low temperature events, began at least 125,000 years and possibly 140,000 years ago with maximum intensities at 15,000, 7,000 and 4,000 years before present. High temperature events, giving rise to sulfide deposits, began about 100,000 years ago and have been intermittent to the present day. A presently active site has experienced intermittent pulses of activity every 4,000 to 6,000 years over the past 20,000 years. Decrease in activity is often marked by low temperature aragonite precipitation in chimney conduits at 4,000, 7,000 and 9,000 years ago. After a period of quiescence lasting about 4,000 years, this site was reactivated about 50 years ago.

The Snakepit field is much younger and no sulfides older than 4,000 years have been recovered. Relict sulfide deposits are dated between 2,000 and 4,000 years old indicating this site was active during a quiescent period at TAG.

Comparison with hydrothermal sites on the East Pacific Rise suggests that on slow spreading ridges the major fracture systems focussing on the hydrothermal discharge can be reactivated at intervals and new deposits precipitated on top of older ones, whilst on faster spreading ridges each pulse of activity is separated in space and time resulting in discrete deposits.

In Press: Journal of Geophysical Research.
Supported by: NSF Grant OCE90-13150.

WHOI Contribution No. 7716.

BENTHIC ORGANIC CARBON DEGRADATION AND BIOGENIC SILICA DISSOLUTION IN THE CENTRAL EQUATORIAL PACIFIC

W. R. Martin, M. Bender, M. Leinen, and J. Orchardo

Shipboard whole-core squeezing was used to measure pore water concentration vs. depth profiles of NO₃, O₂ and SiO₂ at twelve stations in the equatorial Pacific along a transect from 15°S to 11°N at 135°W. The NO₃ and SiO₂ profiles

were combined with fine-scale resistivity and porosity measurements to calculate benthic fluxes. After using O₂ profiles, coupled with the NO₃ profiles, to constrain the C:N of the degrading organic matter, the NO₃ fluxes were converted to benthic organic carbon degradation rates. The range in benthic organic carbon degradation rates is 7-30 μ mol/cm²/yr, with maximum values at the equator and minimum values at the southern end of the transect. The zonal trend of benthic degradation rates, with its equatorial maximum and with elevated values skewed to the north of the equator, is similar to the pattern of primary production observed in the region. Benthic organic carbon degradation is 1-2% of primary production. The range of benthic biogenic silica dissolution rates is $6.9-20 \mu \text{mol/cm}^2/\text{yr}$, representing 2.5-5%of silicon fixation in the surface ocean of the region. Its zonal pattern is distinctly different from that of organic carbon degradation: the range in the ratio of silica dissolution to carbon degradation along the transect is 0.44-1.7 mol/Si/mol C, with maximum values occurring between 12°S and 2°S, and with fairly constant values of 0.5-0.7 north of the equator. A box model calculation of the average lifetime of the organic carbon in the upper 1 cm of the sediments, where $80 \pm 11\%$ of benthic organic carbon degradation occurs, indicates that it is short: from 3.1 years at high flux stations to 11 years at low flux stations. The reactive component of the organic matter must have a shorter lifetime than this average value. In contrast, the average lifetime of biogenic silica in the upper centimeter of these sediments is 55 ± 28 years, and shows no systematic variations with benthic flux.

Published in: Deep-Sea Research, 38(12):1481-1516, 1991.

Supported by: NSF Grant OCE87-11962.

WHOI Contribution No. 7614.

VARIABILITY OF THE δ¹³C OF DISSOLVED INORGANIC CARBON AT A SITE IN THE NORTH PACIFIC OCEAN

Ann P. McNichol and Ellen R. M. Druffel

We present a depth profile of δ^{13} C-DIC (dissolved inorganic carbon) and a time-series of surface water δ^{13} C-DIC from seawater samples collected at a single site during the Eve cruise in the North Pacific in June of 1987. Our deep water results confirm those reported by Kroopnick (1985) for GEOSECS Station 213 (10° west of Eve site). We observe a small but significant decrease in the δ^{13} C of DIC in the upper 500 m of the water column over 14 years since the GEOSECS survey.

This is likely due, at least in part, to the input of additional fossil fuel-derived CO₂ to the upper ocean. Spatial variability was observed in surface water results, emphasizing the need for caution when conducting seasonal studies.

Submitted to: Geochimica et Cosmochimica Acta.

Supported by: NSF Grants OCE84-16632 and OCE87-16590.

WHOI Contribution No. 7903.

INFLOW OF CHERNOBYL 90SR TO THE BLACK SEA FROM THE DNEPR RIVER

Gennady G. Polikarpov, Hugh D. Livingston, Ludmilla G. Kulebakina, Ken O. Buesseler, Nikolai A. Stokozov, and Susan A. Casso

Following the Chernobyl reactor accident in April 1986, studies of radionuclides in aquatic systems in general, and in the Black Sea in particular, have focused primarily on the fate and behavior of direct fallout deposition (Buesseler et al., in press; Livingston et al., 1988; Polikarpov et al., 1991). In this paper we present an evaluation of riverine 90Sr input and its use as a tracer for circulation studies of Chernobyl labelled shelf waters. We describe how 90Sr measurements in the Dnepr River in the period 1986 to 1989 can be used to determine the amount and timing of the subsequent 90Sr inflow to the northwest Black Sea. Comparison of these data with measurements made in the Danube River in 1988 demonstrates that the Dnepr 90Sr flux to the Black Sea is about one order of magnitude higher than that of the Danube.

Published in: Estuarine, Coastal and Shelf Science, 34:315-320, 1992.

Supported by: NSF Grant OCE89-17465 and EPA Grant R817047-01-0.

WHOI Contribution No. 7812.

THE GEOCHEMISTRY OF RE AND OS IN RECENT SEDIMENTS FROM THE BLACK SEA

G. Ravizza, K. K. Turekian, and B. J. Hay

The Os isotopic composition of recent sediments from the Black Sea is reported with the concentrations of Re, Os and major and minor elements. Os concentrations range from 0.23 to 0.69 ppb and Re concentrations range from 21 to 85 ppb. Concentrations of both elements are large relative to average crustal material and are positively correlated with organic carbon. 187 Os/186 Os ratios range from 5.7 to 7.1; all of

these values are less radiogenic than the estimated ¹⁸⁷Os/¹⁸⁶Os ratio of seawater and average continental crust material. Variations in the Os isotopic composition of these sediments are attributed to mixing of a hydrogenous component (¹⁸⁷Os/¹⁸⁶Os ratio between 1 and 4). A mixing model is used to determine the fraction of Os in the sediment associated with each component and the burial fluxes of Re and Os in the Black Sea are calculated. In addition, the data are used to estimate the magnitude of systematic error which such initial Os isotopic heterogeneity may introduce into Re-Os age determinations of ancient organic-rich sediments.

In Press: Geochimica et Cosmochimica Acta.

Supported by: NSF Grants OCE84-14753 and OCE86-14363.

WHOI Contribution No. 7786.

THE GEOCHEMISTRY OF RARE EARTH ELEMENTS IN THE SEASONALLY ANOXIC WATER COLUMN AND PORE WATERS OF CHESAPEAKE BAY

E. R. Sholkovitz, T. J. Shaw, and D. L. Schneider

A twelve-cruise time-series study of a seasonally anoxic basin in Chesapeake Bay was carried out between February 1988 and February 1989. Data from filtered bottom water and upper (0-1 cm) pore water samples are presented.

The time-series results demonstrate that rare earth elements (REE) have large seasonal cycles in both the water column and pore waters in response to the development of anoxia in the spring and reoxygenation in the fall. The transition from oxic to sub-oxic to anoxic conditions results in the release of REE into the upper pore waters and bottom waters. The release of REE and Fe are coincident in the bottom waters, while the release of REE lags Fe by approximately 50 days in the upper pore waters. This decoupling is explained in terms of a REDOX front which moves upward from the sediments to bottom waters during the development of seasonal anoxia. The release of REE to the upper pore waters and bottom water are accompanied by (1) fractionation across the trivalent REE series and (2) the preferential input of Ce relative to its trivalent-only REE neighbors. Fractionation within the REE(III) is such that there is preferential release in going from La to Lu (i.e., from the light REE (LREE) to the middle REE (MREE) to the heavy REE (HREE). During reoxygenation, removal of REE occurs from both the water column and upper pore waters and follows the order LRRR>MREE>HREE. Ce removal occurs faster than its neighbor REE(III), indicating a rapid oxidation of CE(III) to Ce(IV).

Submitted to: Geochimica et Cosmochimica Acta.

Supported by: NSF Grant OCE87-11032.

WHOI Contribution No. 7849.

METAMORPHIC AND HYDROTHERMAL PROCESSES: BASALT-SEAWATER INTERACTIONS

Geoffrey Thompson

The volcanic seafloor, once formed, undergoes changes in its physical, chemical and mineralogical properties as a result of interactions with seawater. Part II of this book discusses the importance of many of these initial basalt properties and how their measurement can be interpreted to infer the source, melting history, magmatic evolution and volcanic processes which formed the oceanic basalts. This chapter discusses how these properties can be changed, and the resulting metamorphosis and evolution of the oceanic crust as it ages and passes from its place of origin at the accreting plate margin to its eventual return to the mantle at subduction zones.

Published in: Oceanic Basalts, P. A. Floyd, ed., Blackie & Sons, Ltd., 8:148-173, 1991.

Supported by: NSF Grant OCE90-17352.

WHOI Contribution No. 7753.

MARINE CHEMISTRY

RAPID BIOGEOCHEMICAL COUPLING BETWEEN SURFACE AND DEEP OCEAN WATERS VIA PARTICLES

V. L. Asper, W. G. Deuser, G. A. Knauer, and S. E. Lohrenz

Settling particles are thought to provide the currency for transport of much of the mass and energy from the surface ocean to the seafloor. The primary source of these particles, which are largely biogenic, is photosynthetic production by marine phytoplankton. Various mechanisms may contribute to sinking of particles, including sinking of phytoplankton biomass directly and transformation of the organic matter produced by phytoplankton into rapidly sinking forms such as fecal material of zooplankton or aggregates.

Because a variety of processes may act on particles during their downward transport, it is not known to what extent the supply of organic matter to the deep sea via sinking particles is directly coupled to overlying surface ocean processes. Although various lines of evidence suggest a direct

coupling, a large number of studies have observed transformation processes and advective inputs which have the potential for modifying or diminishing the transmission of surface signals to the deep sea. If these mechanisms were to overwhelm surface productivity signals, then seasonal and annual variations in deep ocean geochemistry and biology could not be strongly correlated with variations occurring in the overlying surface ocean, but would instead be a function of lateral processes associated with deep-ocean circulation.

We present here the first direct comparisons of seasonal variations in upper ocean primary production and particle flux with underlying deep ocean particle flux. These data show that the productivity signal produced in the surface can be rapidly transferred to the deep sea via the settling of particles, producing close temporal coupling between the surface and deep oceans.

Submitted to: Nature.

Supported by: NSF Grants OCE87-16589 and OCE90-17114.

WHOI Contribution No. 7862.

SEASONAL CYCLES OF MANGANESE AND CADMIUM IN GALAPAGOS CORAL

M. L. Delaney, L. J. Linn, and E. R. M. Druffel

Comparison of manganese-to-calcium ratios from corals in the eastern and western Galapagos demonstrates regional differences in seasonal trace metal cycling. The variability of trace metal-tocalcium ratios within the Galapagos Islands is indicative of the geographic importance of the various currents influencing the region (e.g., South Equatorial Current, Equatorial Under- current, and El Niño Current) and of the relative intensity of upwelling at these locations. Manganese-to-calcium ratios in a banded coral Pavona clavus from Isabela Island, the western-most island in the Galapagos, have distinct seasonal cycles for the non-El Niño Southern Oscillation (ENSO) years 1946-50, with lower ratios following intensified seasonal upwelling. Cd/Ca ratios show less distinct seasonal cycles. By comparison to non-ENSO year patterns, the near-moderate ENSO event in 1951 is marked by the disruption of seasonal cycles in Mn/Ca ratios, while Cd/Ca ratios are relatively constant. In contrast, corals from islands further east in the Galapagos (Hood Island, 1964-73, Linn et al., 1990; San Cristobal, 1965-79, Shen and Sanford, 1990), have stronger seasonal Cd/Ca signals, with higher ratios following seasonal upwelling, and less distinct seasonal cycles in Mn/Ca ratios one-half

year out of phase with Cd/Ca variations. Average Mn/Ca ratios are lower for these corals from locations further east, indicating that Urvina Bay appears to have an additional localized source of Mn (Shen and Sanford, 1990). In general, these regional variations in seasonal trace metal cycling are consistent with coral stable isotope signals and geographic locations. These variations are important to consider in using coral records to reconstruct and interpret oceanographic events occurring prior to historical records.

Submitted to: Geochimica et Cosmochimica Acta.

Supported by: NSF Grants RII86-20256, OCE86-08263 and OCE89-16117.

WHOI Contribution No. 7914.

PHOTOCHEMICAL FREE RADICAL PRODUCTION RATES IN THE EASTERN CARIBBEAN

Brian Dister and Oliver C. Zafiriou

Total (NO-scavengeable) free radical production rates have been measured underway on surface waters illuminated by a "1-sun" solar simulator over large areas of the eastern Caribbean in Spring and Fall 1988. A semi-automated computer-controlled system coupled to the ship's clean surface water system yielded more than 900 determinations, extensively documenting large-scale regional and seasonal trends.

Photochemically generated radical production was detectable even in the most oligotrophic waters encountered, and were reasonably well quantified in all waters more reactive than ~ 0.25 nmol L^{-1} min⁻¹ sun⁻¹. Radical production rates varied from ~ 0.1 –0.25 nmol L^{-1} min⁻¹ of full-sun illumination of "blue water" to $> \sim 60$ nmol L^{-1} min⁻¹ in Orinoco River water freshwater and waters of its estuarine region in the high-flow season. Such rates are large enough to support significant geochemical transformations, through the ultimate impacts of the radical chemistries (other than HOOH generation) are not yet known.

The spatiotemporal distribution of free radical production rates clearly shows that the Orinoco riverine input accounts for most or all of the greatly enhanced photoreactivity found over the entire eastern Caribbean basin in Fall. However, the data do not permit us to differentiate any additional contributions due to Amazon inputs or riverine nutrient-stimulated photoreactivity vs that due directly to terrestrial chromophore inputs. Although humic acids may be lost by flocculation, the major part of the photoreactive colored organic matter involved in radical formation clearly mixes quasiconservatively out into high-salinity waters.

Although the Orinoco inputs clearly dominate in this region, paradoxically eastern Caribbean waters are not markedly more reactive at comparable salinities and insolations than those found in the Gulf of Maine and in the North Atlantic Bight, despite their receiving large inputs of highly colored water from two of the largest tropical rivers, each with substantial "black water" tributary components. Three possible resolutions of this apparent paradox are: (1) temperate freshwater inputs might be even more photoreactive on a mass basin than "black water"; (2) marine sources (grazing, benthic and pelagic decomposition) of photoreactive chromophoric material may also be important chromophore sources; or (3) chromophore sinks may be the master control on photoreactive chromophore concentrations over large regions, with more intense sinks being situated in the tropics. More intense tropical "photobleaching" due to higher daily total and UV insolation, longer seasons, and shallower mean mixed layers is one economical but untested explanation.

Submitted to: Journal of Geophysical Research (Oceans).

Supported by: NSF Grants OCE84-17770 and OCE87-00576.

WHOI Contribution No. 7806

PHOTOCHEMICAL OXYGEN ACTIVATION: SUPEROXIDE RADICAL DETECTION AND PRODUCTION RATES IN THE EASTERN CARIBBEAN

Edward Micinski, Lary A. Ball, and Oliver C. Zafiriou

Superoxide ion-radical (O_2^-) , the one-electron reduction product of molecular oxygen, is a long-suspected first intermediate in chemical reactions using oxygen as the ultimate electron acceptor. We have detected photochemical production of O_2^- in a variety of eastern Caribbean waters studied in Spring and Fall by using a chemically direct O_2^- trapping reaction combined with ¹⁵N and/or ¹⁸O isotopic labelling of reactants to provide sensitivity and specificity.

Photochemical superoxide production rates ranged from 0.1-6.0 nmole/ ℓ /min of full-sun irradiation in Spring and from 0.2-8.0 nmole/ ℓ /min in Fall. Thermal O_2^- fluxes were undetectable, though sensitivity for dark production is relatively limited. These superoxide fluxes correlate well with independently measured total (NO-scavengeable) radical fluxes in both seasons and account for \sim one-third of the total radical production. Hence, we confirm that O_2^- is a quantitatively important, perhaps dominant.

reactive transient species in the photochemical radical array. Semi-quantitative estimates suggest that O_2^- dismutation of HOOH and O_2 can account for most or all of the photochemical HOOH production in surface waters.

In Press: Journal of Geophysical Research (Oceans).

Supported by: ONR Contracts N00014-85-C-0001, N0001-14-87-K-0007, and N00014-89-J-1258.

WHOI Contribution No. 7807.

SOME PRACTICAL ASPECTS OF MEASURING DOC—SAMPLING ARTIFACTS AND ANALYTICAL PROBLEMS WITH MARINE SAMPLES

Edward T. Peltzer and Peter G. Brewer

Efforts to reproduce the high-temperature catalytic oxidation technique for the determination of dissolved organic carbon in marine samples are described and details of the construction of a home-made DOC analyzer are presented. Calibration of this instrument is compared with that of a commercial unit from Ionics, Inc. Various problems relating to the determination of the instrument blank, instrument calibration, sample collection, preservation and processing are presented. Several hypotheses explaining the observed analytical artifacts are proposed and possible implications of tese artifacts are discussed.

In Press: Marine Chemistry.

Supported by: NSF Grants OCE87-01461, OCE87-16954, and OCE88-14393.

WHOI Contribution No. 7775.

INSTRUMENTS AND METHODS

RECOVERY OF SUB-MILLIGRAM QUANTITIES OF CARBON DIOXIDE FROM GAS STREAMS BY MOLECULAR SIEVE FOR SUBSEQUENT DETERMINATION OF ISOTOPIC NATURAL ABUNDANCES (13C AND 14C)

James E. Bauer, Peter M. Williams, and Ellen R. M. Druffel

Numerous analyses in the natural sciences depend on the production of CO₂ gas from inorganic and organic carbon samples. The extraction of CO₂ from carrier gas streams for subsequent quantification and characterization is, however, often problematic. A simple and convenient method was therefore developed which

employs Type 13X molecular sieve for the rapid and quantitative recovery of CO_2 from gas streams. The sieve trap method was evaluated for its ability to quantitatively recover CO_2 over a wide range of concentrations $(0.5\text{--}50~\mu\mathrm{moles})$ and carrier flow conditions $(100\text{--}2000~\mathrm{cc} \cdot \mathrm{min}^{-1})$. Recoveries in all cases were 100%. In addition, the method allows accurate and precise determinations of $\delta^{13}\mathrm{C}$ and $\Delta^{14}\mathrm{C}$ to be made on samples at natural abundance levels subsequent to collection by the sieve trap. The simplicity and both the low cost and maintenance of the sieve trap system described here should find numerous applications where quantitative collection and characterization of CO_2 from natural samples is required.

In Press: Analytical Chemistry.

Supported by: NSF Grant OCE87-16590.

WHOI Contribution No. 7847.

DETERMINATION OF THORIUM ISOTOPES IN SEAWATER BY NON-DESTRUCTIVE AND RADIOCHEMICAL PROCEDURES

Ken O. Buesseler, J. Kirk Cochran, Michael P. Bacon, Hugh D. Livingston, Susan A. Casso, David Hirschberg, Mary C. Hartman, and Alan P. Fleer

Procedures have been developed for the analyses of dissolved and particulate ²³⁴Th, ²²⁸Th, ²³⁰Th and ²³²Th in seawater. large volume samples (>1000 liter) are collected using *in-situ* pumps. Seawater is pumped sequentially through a filter cartridge and two MnO₂ adsorbers for the collection of particulate and dissolved Th, respectively. Both filters and adsorbers are analyzed for ²³⁴Th using a simple gamma-counting technique. This newly developed ²³⁴Th procedure can be conducted at sea, and thus provides an easy and efficient method for ²³⁴Th analyses on large volume samples. Subsequent radiochemical purification procedures and low-level alphacounting techniques are used in the lab for the analyses of ²²⁸Th, ²³⁰Th, and ²³²Th on these same samples.

In Press: Deep-Sea Research.

Supported by: NSF Grants OCE88-17836 and OCE90-16494.

WHOI Contribution No. 7896.

PROCEDURE FOR CALIBRATION OF A COULOMETRIC SYSTEM USED FOR TOTAL INORGANIC CARBON MEASUREMENTS IN SEAWATER

Catherine Goyet and Sally D. Hacker

This paper describes a calibration procedure for measurements of total inorganic carbon (C_T) in seawater using a coulometric system. In contrast to a previously published protocol which is based on pure CO_2 gas as a calibration standard, the present procedure is based on measurements of standard solutions treated similarly to seawater samples.

We show that standard solutions for C_T measurements can be easily prepared both in the laboratory and at sea from distilled water and preweighed sodium carbonate salt. With reasonable care, one liter of standard solution can be used regularly over a period of a week. The precision of this calibration procedure ranges from ±0.02% to 0.06%, allowing measurements of seawater samples to within $\pm 0.3 \mu \text{mol C/kg to } 1.3$ µmol C/kg. A preliminary comparison to assess the accuracy of these measurements when compared to an established manometric method performed on the same seawater shows close agreement with a mean \pm S.D. of 1978.4 \pm 1.3 μ mol C/kg for the manometric method and 1978.8 ± 0.9 umol C/kg for the manometric analysis. The difference between these measurements (0.4 μ mol C/kg) is within the precision of either method. These standard solutions are simple, practical and inexpensive to prepare and measure, making them ideal for measurements at sea.

In Press: Marine Chemistry.

Supported by: DOE Grant DE-FGO2-ER60980.

WHOI Contribution No. 7672.

DEVELOPMENT OF A FIBER OPTIC SENSOR FOR MEASUREMENTS OF PCO₂ IN SEA WATER: DESIGN CRITERIA AND SEA TRIALS

Catherine Goyet, David R. Walt, and Peter G. Brewer

Measurements of the partial pressure of CO₂ gas in sea water (pCO₂) is a fundamental ocean chemical need, usually accomplished by gas chromatography of infrared spectrometry. Both these techniques require large, complex and power demanding apparatus. In this paper we explore the possibility of developing and using small low power sensors.

We have developed and tested a prototype pCO₂ sensor for sea water based upon the

fluorescence of a combination of dyes encapsulated within a gas permeable silicone membrane at the tip of a single optical fiber. The optical module (Douglas Instruments) delivers 30 Hz chopped white light to a filter and is passed through a dichroic mirror. This light is then focused on to a 220 µm optical fiber. The fiber, approximately 2 m long, was terminated with a standard coupler equipped with a small silicone nipple. The internal volume of the sensor tip (about 10 μ l) was filled with a combination of a fluorescent indicator and two absorbing dyes so as to achieve the required sensitivity. HPTS (hydroxypyrenetrisulfonic acid) was chosen as the fluorescent species; Neutral Red and DNPA (2-(2,4-dinitrophenylazo)-1-naphthol-3.6-disulfonic acid) were selected as absorbers. Illumination at $\lambda_{ex} = 450$ nm yielded fluorescence at $\lambda_{ex} = 530$ nm, and fluoresced light was returned through the same fiber, reflected at 90° by the dichroic mirror, passed through an interference filter and focused on to a sensitive silicon photodiode.

Experiments were carried out both in the laboratory on standard solutions, and at sea. Comparison at sea with gas chromatographic measurements of pCO₂ on recovered samples showed a precision of 3% in the range 400-500 ppm pCO₂ sensor for detecting oceanic signals. This technology is complementary to optical detection of pH and points the way towards full characterization of the CO₂ system within this measurement framework.

In Press: Deep-Sea Research.

Supported by: NSF Grant OCE87-00808.

WHOI Contribution No. 7673.

A FAST AND SENSITIVE ICP-MS ASSAY FOR THE DETERMINATION OF ²³⁰TH IN MARINE SEDIMENTS

Timothy J. Shaw and Roger Francois

Inductively-coupled Plasma-Mass Spectrometry (ICP-MS) with quadrupole mass analysis provides a very fast and sensitive method for the determination of 230 Th in marine sediments. A detection limit of 0.40 DPM (36 femto-moles) was determined for the method with a precision of better than 3% (1 σ). This is comparable to that of α -counting methods, but samples can be analyzed in five minutes, compared to up to two weeks counting time for α -spectrometry. Sample preparation is also significantly simplified, thus providing a relatively quick and easy method for the determination of "excess" 230 Th accumulation histories in deep-sea sediment cores.

Published in: Geochimica et Cosmochimica Acta, 55:2075-2978, 1991.

Supported by: NSF Grant OCE89-22707.

WHOI Contribution No. 7685.

MULTIPLE INDICATOR FIBER OPTIC SENSOR FOR HIGH RESOLUTION PCO₂ MEASUREMENTS IN SEAWATER

David R. Walt, G. Gabor, and Catherine Goyet

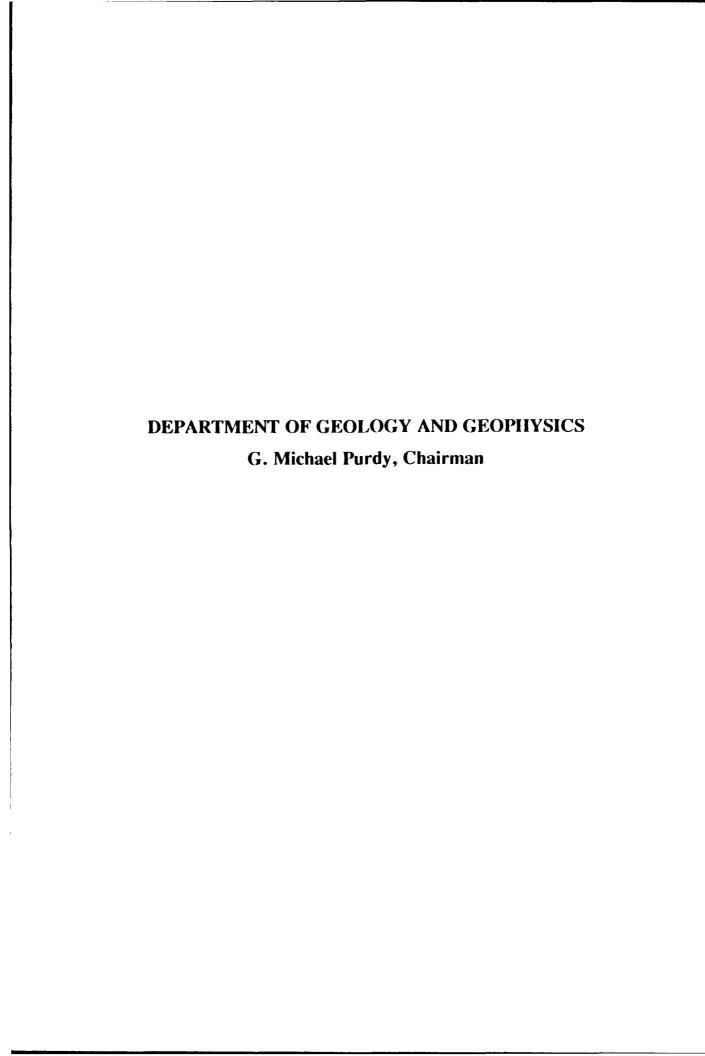
A fiber optic sensor has been developed to measure CO₂ partial pressures in sea water. The sensor is based on indicator combinations to enhance sensitivity. A precision of 7 ppm CO₂ has been demonstrated.

A multiple-indicator fiber-optic sensor was employed to detect low level CO₂ changes in sea water. pKa values of these indicator systems at high ionic strength were determined, and the bicarbonate concentrations were added as calculated by the Henderson Hasselbach equation. The 7-hydroxycoumarin-4-acetic acid (HCA)-metacresolpurple (MCP) indicator system enables detection of changes of 7 ppm CO₂ in the 200-800 ppm CO₂ range—the CO₂ range in sea water.

Submitted to: Analytical Chemistry.

Supported by: NSF Grant OCE87-00808.

WHOI Contribution No. 7868.



ACCELERATOR MASS SPECTROMETRY

ILLUMINATION OF A BLACK BOX: ANALYSIS OF GAS COMPOSITION DURING GRAPHITE TARGET PREPARATION

A. P. McNichol, A. R. Gagnon, G. A. Jones and E. A. Osborne

We conducted a study of relative gas composition changes of CO₂, CO and CH₄ during the formation of graphite targets using different temperatures, catalysts and methods. Reduction with H₂ increases the reaction rate without compromising the quality of the AMS target produced. Methanc is produced at virtually any temperature, and the amount produced is greater at very low temperatures. The reduction of CO to graphite is very slow when H₂ is not included in the reaction.

In Press: Radiocarbon.

Supported by: NSF Grant OCE88-02509.

WHOI Contribution No. 7910.

GEOLOGY

THE GEOLOGIC IMAGE OF BRANSFIELD TROUGH, AN INCIPIENT OCEANIC BASIN ON THE ANTARCTIC CONTINENTAL MARGIN

Juan Acosta, P. Herranz, J. L. Sanz and Elazar Uchupi

The geologic relationships imaged by seismic reflection profiles recorded during the present investigation and data obtained during previous studies indicate that the Bransfield Trough is a continental rift structure in transition to becoming an oceanic one. The asymmetry of the trough suggests that it is a half graben structure whose master fault is on the Antarctic Peninsula side away from the zone of subduction. The fault is opposed by a platform, the South Shetland Islands Ridge (Fig. 9). This tectonic model, however, is in need of verification. Crustal attenuation led to the displacement of a narrow continental fragment away from Antarctica to form the ridge. Sediments on the southeast side of the trough off Antarctica are involved in the faulting which suggests either syn-sedimentary faulting or that sagging and deposition preceded rifting. The tectonic style displayed by Bransfield Trough is morphologically

comparable to that of Arctic Eurasia, where the narrow continental Lomonosov Ridge was broken away from the Barents Shelf by the Nansen Ridge spreading axis. However, extension in the Bransfield Trough is taking place in a back-arc setting behind the South Shetland Trench.

The cross-section geometry of the spreading-axis probably is controlled by the dimensions of the Bransfield Trough which is only 30 km wide. If extension is the result of the cooling and sinking of a subducted oceanic slab, then spreading should cease in the trough in the geologic near future as such mechanism is incapable of sustaining sea-floor spreading for very long. If spreading is the result of active subduction, then sea-floor spreading should persist for some time with the spreading axis becoming more organized with time. At present the spreading axis in the Bransfield Trough consists of discrete igneous centers separated by gaps that may have allowed sediments from Antarctica to reach the northwest side of the trough. Continuity of the axis also is interrupted by structures transverse to the trough's axis. The intersection of these cross-structures with features parallel to the axis of the trough appear to be sites of pronounced magmatic activity. Sediment contribution from the South Shetland Islands Ridge to Bransfield Trough was probably less than that from Antarctica with some of the detritus being trapped by structural lows perched along the southeast flank of the ridge.

If the 30-km-wide Bransfield Trough is representative of the conditions that existed when deposition changes from synrift to drift (postrift) deposition then some inferences can be made regarding the analogous Jurassic/Cretaceous in the North and South Atlantic. For example, the change from syn-rift to drift (postrift) deposition was not coeval along the strike, and the mid-ocean ridge during its initial phases may have consisted of discrete segments with the gaps serving as portals for sediment transport across the floor of the trough. Above all our data show that the transition from rift to drift may have been marked by a complex distribution of synrift and postrift facies.

In Press: The Evolution of Atlantic Continental Rises, Dowden, Hutchinson and Rose, Inc., Stroudsburg.

WHOI Contribution No. 7647.

CALCAREOUS NANNOFOSSIL STRATIGRAPHY OF THE NEOGENE FORMATIONS OF EASTERN JAMAICA

Marie Pierre Aubry

While numerous studies have been devoted to the planktonic and benthic foraminifera in the Neogene of Jamaica, little attention has been paid to the calcareous nannofossils. This contribution is thus a documentation of the calcareous nannofossils in the lower Miocene to upper Pliocene deposits of Jamaica. The Buff Bay section, the most extensive Neogene section in eastern Jamaica, is studied in greater detail, but eight other sections including the San San Bay and Bowden type sections are discussed as well. Current correlations between the zonal schemes established from calcareous nannofossils and planktonic foraminifera are discussed based upon direct correlation between calcareous nannofossil and planktonic foraminiferal zones in these sections. Integration between calcareous planktonic microfossil stratigraphies, and magnetostratigraphy when available, leads to the delineation of regional unconformities and to the interpretation of the Neogene stratigraphic record of eastern Jamaica in terms of sequence stratigraphy. It is shown that the Buff Bay Formation, the San San Clay and the Bowden Formation correspond to separate unconformable stratigraphic sequences. As a result, it is suggested that the San San Clay be regarded as a distinct formation rather than part of the Buff Bay or the Bowden Formation as currently admitted. Several of the holotype and paratype localities that Blow (1969) designated for his Neogene planktonic foraminiferal zones (N-Zones) are located in Jamaica. Direct correlation between these and the calcareous nannofossil schemes of Martini (1971) and Okada and Bukry (1980) are established and the implications are discussed.

In Press: Biostratigraphy of Jamaica Geological Society of America sp. Mem.

Supported by: A consortium of oil companies. WHOI Contribution No. 7797.

TOWARD A REVISED PALEOGENE GEOCHRONOLOGY

William A. Berggren, Dennis V. Kent, John D. Obradovich and Carl C. Swisher III

New information has become available that requires a revision of Paleogene chronology incorporated in most current Cenozoic time-scales (e.g. Berggren et al., 1985 a,b). Age estimates for the limits of the Paleogene (the Oligocene/Miocene and Cretaceous/Paleogene boundaries) have not changed appreciably and remain at about 24 Ma and about 66 Ma, respectively. However, new radioisotope data indicate that boundaries of subdivisions within the Paleogene are generally younger than previously estimated, for example, the Paleocene/Eocene and Eocene/Oligocene by about 2 to 3 m.y. We review the current status of

magnetobioctratigraphic correlations and new radioisotope data, with particular reference to late Eocene-early Oligocene geochronology and provide a reassessment of the age of the Eocene/Oligocene boundary as 34 Ma. We anticipate that with concurrent work on a fundamental revision of the geomagnetic polarity sequence, a comprehensive and detailed new time scale for the Cenozoic will soon be developed.

In Press: Late Eocene-Early Oligocene Climate and Biotic Evolution, Prothero, D. and Berggren, W.A., eds. Geological Society of America Special Paper.

Supported by: NSF Grant OCE91-01463. WHO! Contribution No. 7777.

MAPPING THE SEISMIC STRUCTURE OF THE UPPER OCEANIC CRUST: IMPLICATIONS FROM DSDP SITE 504B, PANAMA BASIN

John A. Collins, Thomas M. Brocher and G. Michael Purdy

We investigate the seismic structure of the upper oceanic crust by comparing both reflection and refraction data collected at Deep Sea Drilling Project (DSDP) Site 504B to the results of downhole logging. Extensive processing of the multichannel seismic reflection data, designed to remove high-amplitude side-scattered arrivals. revealed no conclusive evidence for laterally coherent reflection events generated within the upper 1-2 km of the crust. This observation was initially surprising because drilling shows a well-defined change in physical properties at depths within the basement of about 0.5-0.6 km, corresponding to the transition from volcanic rocks to dikes. To better understand the lack of reflectivity from the volcanic/dike boundary at Hole 504B, we calculated synthetic reflection seismograms for a series of velocity-depth profiles constructed from the logged physical properties. Vertical-incidence synthetic seismograms suggest that the volcanic/dike boundary at Hole 504B has a relatively low effective seismic impedance; in these seismograms, reflections from the modeled geological boundary are obscured by source reverberation and sediment-column multiple reflections. The low impedance contrasts within the upper crust at Hole 504B clearly contrast with those areas where high-amplitude shallow reflections have been observed. The contrasting reflection responses, nonetheless, do not necessarily imply significant differences in the geologic structure The reflection events observed in other areas may be generated at lithological/porosity transitions similar to that sampled at Hole 50B,

the differences in reflection response may be primarily controlled by the thickness of the transition zone. Synthetic seismograms calculated for wide-angles of offset and observed wide-angle data acquired at Hole 504B indicate that the volcanic/dike boundary is readily identified in such data. These observations suggests that for Hole 504B, lateral variations in shallow seismic structure may be better mapped by the wide-angle reflection/refraction technique.

In Press: Journal of Geophysical Research.

Supported by: NSF Grants OCE84-10658 and OCE87-00806.

WHOI Contribution No. 7069.

HYPSOMETRY OF DIVERGENT AND TRANSLATIONAL CONTINENTAL MARGINS OF SOUTHERN AFRICA

K. O. Emery, J. M. Bremner and J. Rogers

Flattenings that may be shelves formed by marine erosion/deposition or by slump masses are present on continental margins of southern Africa that border both the Atlantic and Indian oceans. Breaks in slope, indicated along sounding lines, suggest that a shallow terrace of the Atlantic margin has been warped downward from depths of about -130m southward to about -200m, and a deeper terrace lies between depths of about -150m to about -440m. Examination of contours and hypsometry (areas measured between depth contours) show widespread flattenings at about -65 and -95m on the Indian Ocean margin and -25-155 and -190m along the Atlantic margin. Seismic profiles indicate that some of these and other more local flattenings are on slump blocks and thus are not correlatable for long distances. An additional complication is that sediment introduced by rivers is transported alongshore by wave-induced and oceanic bottom currents, and deltas are ephemeral.

In Press: Marine Geology.

WHOI Contribution No. 7805.

DEGLACIAL MELTWATER DISCHARGE, NORTH ATLANTIC DEEP CIRCULATION AND ABRUPT CLIMATE CHANGE

Lloyd D. Keigwin, Glenn A. Jones, Scott J. Lehman and Edward A. Boyle

High-resolution paleo-geochemical data from the North Atlantic Ocean indicate that in the interval 15,000 to 10,000 ¹⁴C yrs before present (BP) North Atlantic Deep Water (NADW) production was decreased or eliminated four times: at about 14,500 (and probably older), 13,500, 12,000 and 10,500 yrs BP. Each of these events occurred at the same time as abrupt events of meltwater discharge to the surface ocean (inferred from oxygen isotope studies of planktonic foraminifera and from glacial geological studies on land). In addition, each of these times may be associated with brief episodes of cooler climate in the North Atlantic region, the best example of which is the Younger Dryas cooling of 10,500 yrs ago. These results support models linking meltwater discharge, decreased NADW production, and decreased North Atlantic heat flux.

Published in: Journal of Geophysical Research, 96(C9):16,811-16,826, 1991.

Supported by: NSF Grants ATM87-16617, OCE87-10168, DPP88-13875 and DPP90-1468.

WHOI Contribution No. 7681.

HUNDREDS OF SMALL VOLCANOES ON THE MEDIAN VALLEY FLOOR OF THE MID-ATLANTIC RIDGE AT 24-30°N

Deborah K. Smith and Johnson R. Cann

We have identified 481 seamounts from ~6,000km² of Sea Beam swaths of the median valley floor of the Mid-Atlantic Ridge (MAR) between 24 and 30°N. We find that seamount abundances are an order of magnitude larger (on average, 80 per 1,000 km² with relief above 50m) than estimated in previous studies along mid-ocean ridges in the Pacific and South Atlantic, suggesting that at this section of the MAR, seamount volcanism plays an important part in the formation of new oceanic lithosphere. The neovolcanic ridge, often observed on the inner valley floor, appears to be constructed totally of individual coalesced seamounts so that our counts represent a minimum estimate. The frequency distribution of summit heights of the MAR seamounts is consistent with the exponential model describing the heights of off-axis seamounts in the eastern Pacific, but with different parameters. Such a distribution of heights may be a fundamental aspect of seamount volcanism, related to lithospheric properties and/or magmatic plumbing. Seamount-dominated axial volcanism must create a crustal structure very different from classic fissure-fed models.

Published in: Nature, 348:152-155, 1990.

Supported by: NSF Grant OCE88-00497.

WHOI Contribution No. 7678.

SEAMOUNT ABUNDANCES AND SIZE DISTRIBUTIONS, AND THEIR GEOGRAPHIC VARIATIONS

Deborah K. Smith

Submarine volcanoes (seamounts) far out number their subaerial counterparts on Earth. Estimates indicate that there may be as many as a million volcanoes of all sizes in the Pacific Ocean alone, occupying up to 13% of the seafloor area, and corresponding to a uniform layer over 50 m thick or almost 1% of the volume of the oceanic crust. It is obvious that the formation of seamounts is an important part of the evolution of the oceanic lithosphere.

From random crossings of the oceans, and surveys of individual seamounts several basic observations of seamount distributions have been made. For example: the spatial distribution is non-random, seamounts cluster in groups and form linear chains; abundances vary geographically within and between oceans; seamounts originate both on and near to mid-ocean ridges as well as in the middle of lithospheric plates; small size seamounts greatly outnumber large size seamounts. The controls for many of these observations are unknown, and several first-order scientific questions remain to be answered.

A large literature exists on oceanic islands (the largest size seamounts), because of their relative accessibility for studies. This review does not address these studies, but instead focuses primarily on seamounts with heights of less than 3 km, a population that is imperfectly known because of incomplete bathymetric sampling of the oceans. The data and methods used to estimate the abundances, size distributions, and geographical variations of such a population are examined. Because of our incomplete knowledge of the seafloor, obtaining population parameters that describe these smaller size seamounts necessitates the use of statistical techniques. Application of statistics to seafloor bathymetry data is a rapidly growing field of study stimulated by the hope that mapping variations in population parameters will provide more quantitative constraints on the fundamental processes controlling seamount formation.

Published in: CRC: Reviews in Aquatic Sciences, 5:197-210, 1991.

Supported by: NSF Grant OCE88-00497.

WHOI Contribution No. 7679.

MASSIVE SUBMARINE ROCKSLIDE IN THE RIFT VALLEY WALL OF THE MID-ATLANTIC RIDGE

Brian E. Tucholke

Within the past 450,000 yrs a ~4km by 5 km section of ocean crust on the eastern wall of the Mid-Atlantic rift valley was removed in a massive rockslide that disintegrated to form a debris avalanche. Slope failure probably occurred along pre-existing west-dipping faults where hydrothermal metamorphism is inferred to have weakened the crust. The debris avalanche flowed more than 11 km into the rift valley and deposited a debris wedge with a volume of $\sim 19 \times 10^9 \text{ m}^3$. Run-up and rebound features occur where the leading edge of the avalanche encountered a basement ridge, and they suggest rapid transport in an event that lasted only a few minutes. This is the first known occurrence of such large-scale mass wasting along the tectonically active rift valley of a mid-ocean ridge.

Published in: Geology, 20:129-132, 1992.

Supported by: ONR Contract N00014-90-J-1621.

WHOI Contribution No. 7873.

THE RENAVIGATION OF SEA BEAM BATHYMETRIC DATA BETWEEN 9°N AND 10°N ON THE EAST PACIFIC RISE

W. S. D. Wilcock, Douglas R. Toomey, G. M. Purdy and Sean C. Solomon

We present a gridded Sea Beam bathymetric map of a 5100 km² area between 9° and 10° N on the East Pacific Rise (included as a color separate accompanying this issue). The raw bathymetric data are renavigated using a technique for calculating smooth adjustments to navigation that incorporates absolute constraints from satellite fixes and acoustically-located explosive shots and relative constraints from the misfit of bathymetric data at ship track crossovers. We describe a back-projection technique for gridding the bathymetric data that incorporates an approximation for the power distribution within a narrow-beam echo sounding system and accounts for the variable uncertainties associated with multi-beam data. The nodal separation of the resulting map is ~80 m in both latitude and longitude and the sampling of grid points within a 60 x 85 km² region is in excess of 99%. A formal analysis of variance is applied to the gridded bathymetric data. For each grid point, the difference between the variance of data from within a track versus data from between tracks provides

an upper bound on the magnitude of bathymetric misfits arising from navigational errors. The renavigation results in an 88% reduction in this quantity. We also examine the effects of renavigation on the misfit of magnetic and gravity data at crossovers. A striking feature of the final bathymetric map is the sinuous regional shape of the rise axis. In plan view, the local trend of morphology sometimes varies by up to 15° and the distance separating changes in morphological trend are about 10-20 km. In cross section the slope of the rise flanks are notably asymmetric, showing some correlation with the offset of the axial magmatic system as detected by seismic methods. In Press: Marine Geophysical Researches. Supported by: NSF Grants OCE86-15797 and OCE90-00458.

WHOI Contribution No. 7694.

GEOPHYSICS

VERTICAL SEISMIC PROFILE AT SITE 765 AND SEISMIC REFLECTORS IN THE ARGO ABYSSAL PLAIN

S. T. Bolmer, R. T. Buffler, H. Hoskins, R. A. Stephen and S. A. Swift

The first Ocean Drilling Program (ODP) vertical seismic profile (VSP) experiment in a thick sedimentary section was conducted at Site 765 to measure compressional wave velocities and to correlate drilling results with seismic data. Measurements were performed through the cased portion of the hole between 186 and 915 mbsf using both air-gun and water-gun sources. Average velocities for the air-gun source were 1.967 km/s (284-915 mbsf), 1.815 km/s (186-284 mbsf), and 1.633 km/s (seafloor to 186 mbsf, extrapolated). Separation of the wavefield into upgoing and downgoing components by f-k filtering plus deconvolution of the upgoing wavefield produced good VSP records and revealed reflectors that correlate well with seismic profiles. These data were used to correlate the drilling results (lithologic units) with the seismic sequences at the drill site, which will be used to extrapolate the drilling results regionally. A weak sub-basement reflection at approximately 600 m into basement may correspond to the contact between pillow basalts and sheet flows. A comparison between VSP velocities, laboratory measurements, and sonic logs shows generally good agreement below about 420 mbsf.

In Press: ODP, Vol. 123.

Supported by: Purchase orders from NSF, ODP and Texas A&M (nos. 20218, 500 and 2034.

WHOI Contribution No. 7860.

SCIENTIFIC USE OF SUBMARINE TELECOMMUNICATIONS CABLES

R. Butler, A. D. Chave, C. S. Cox, C. E. Helsley, J. A. Hildebrand, L. J. Lanzerotti, G. M. Purdy, T. E. Pyle and A. Schultz

In the coming decades, the earth and ocean science communities will address global problems using new, large-scale, long-term monitoring systems distributed around the planet. These types of measurements will be needed to better understand geophysical processes which vary on time scales of months to decades and to "ground truth" observations derived from satellites. However, achieving broad spatial coverage within the oceans using conventional instrumentation deployed from ships will be very costly, and real-time data telemetry from seafloor-based instrumentation poses many technical challenges. A complementary approach might utilize portions of the worldwide system of transoceanic analog telecommunications cables which are due to retire from commercial service over the next decade as they are replaced by fiber optic technology. For example, Walker (1991) discussion submarine cable usage in the context of global change research.

Realizing that improved observational systems will be required for upcoming, vastly expanded programs to study climate, global change, and the solid earth, several US funding agencies sponsored a Workshop on Scientific Uses of Undersea Cables, convened by the Joint Oceanographic Institutions (JOI) and the Incorporated Research Institutions for Seismology (IRIS), which was held in Honolulu at the end of January, 1990. The meeting was attended by a representative group of scientists from US and Japanese universities, program managers from several US funding agencies, and delegates from the telecommunications industry. A report summarizing the proceedings has been published by JOI [Chave, Butler, and Pyle, 1990]. The focus of the meeting was the impending transfer of the Guam-Japan segment of Trans-Pacific Cable-1 (TPC-1) jointly to the Earthquake Research Institute (ERI) of the University of Tokyo and IRIS.

Subsequent to the Honolulu workshop, IRIS appointed a formal steering group as a subcommittee of the Standing Committee for the Global Seismographic Network to coordinate further US actions on submarine cable use and to plan implementation of the recommendations made at the meeting. In January 1991 a complementary workshop for the Japanese scientific community was held at the Ocean Research Institute, Tokyo, and the Japanese steering committee was restructured. This paper provides a progress report on their activities.

Published in: EOS, 73(97):100-101 1992. Supported by: NSF Grant EAR-9121278.

WHOI Contribution No. 7888.

GEOPHYSICAL CONSTRAINTS ON THE STATE OF STRESS ALONG THE MARQUESAS FRACTURE ZONE

Gail L. Christeson and Marcia K. McNutt

We examine bathymetry and gravity observations acquired by surface ships and deflection-of-the-vertical data derived from the Geosat radar altimeter for the purpose of determining whether the bathymetric relief along the Marquesas Fracture zone, in the central Pacific Ocean, is caused by differential thermal subsidence across a locked fault (high stress case) or volcanism along a zone of relative weakness (low stress case). If the fracture zone can maintain 30 MPa or more of deviatoric stress, we would predict that a ridge and a parallel trough would develop to the south and north respectively, of the fracture zone on account of flexural modification of the step in bathymetry locked into the plate along the fracture zone at the ridge-transform intersection. We find that only 2 out of 32 deflection-of-the-vertical profiles from the Geosat altimetric mission are consistent with this model, while none of the 27 bathymetric profiles or 9 shipboard gravity profiles fits the theoretical predictions. In cases where bathymetry and gravity can be modeled simultaneously, it appears that the gravity anomaly is simply not large enough in magnitude to be consistent with the Moho flexing conformably with the observed bathymetry, as required if the relief is produced by deeper thermal variations across the locked fracture zone. Rather, the bathymetric and potential field data are more consistent with a model in which the relief on the Moho is opposite in sign to that of the surface topography, as would be produced by local or regional compensation of surface loads arising from volcanic activity along the fracture zone. Thus we conclude that the Marquesas Fracture Zone, in contrast to those other Pacific fracture zones which appear to fit the predictions of the locked fault (high stress) model, may be unusually weak, perhaps due to the intense volcanic activity in French Polynesia.

In Press: Journal of Geophysical Research.

Supported by: The Ocean Ventures Fund, NSF Graduate Fellowship Grant and NSF Grant OCE89-19140.

WHOI Contribution No. 7693.

STRUCTURE OF THE NORTHERN SYMMETRIC SEGMENT OF THE JUAN DE FUCA RIDGE

G. L. Christeson, G. M. Purdy and K. M. Rohr

A seismic refraction profile along the axis of the Northern Symmetric Segment of the Juan de Fuca Ridge reveals strong evidence for the presence of a low-velocity zone at a depth of approximately 3 km below the seafloor that is continuous along-axis for at least 30 km. There is no evidence to suggest that the low-velocity zone represents a region of high partial melt; more likely it represents a region of elevated temperatures. The low-velocity zone is capped by a 650-700 m thick high-velocity lid, believed to be formed by the cooling of the hot rock by hydrothermal circulation. Two dimensional modelling of travel times to ocean bottom hydrophone instruments shows that the amplitude (a few hundred meters) of along-axis variation in seismic structure within the crust is on the order of the lateral changes in topographic relief.

Submitted to: Marine Geophysical Researches.

Supported by: ONR Contract N00014-89-J-1015.

WHOI Contribution No. 7902.

SEISMO/ACOUSTIC PROPAGATION THROUGH ROUGH SEAFLOORS

Martin E. Dougherty and Ralph A. Stephen

This paper addresses the scattering of seismo/acoustic energy from rough water-solid interfaces. A 2-dimensional elastic finite difference method with a velocity-stress formulation is used for all of these models which includes all phases, multiples, interface, and interference waves. Initial sinusoidal seafloor models at 15 grid points per wavelength (ppw) show that even medium slopes can greatly increase the amount of energy (especially P to S converted energy) which is transmitted into the bottom. Scattering from microroughness (stair-step definition of a sloping seafloor) is significant for 10 meter steps with a pressure pulse source of 10 Hz center frequency. Additional models with much finer grids (30 and 60 ppw) were computed to decrease the microroughness scattering and to check the accuracy of scattering from 10 meter steps. Most of the microroughness scattering disappears for the 60 ppw model. Scattering strength is similar for all models with 10 meter microroughness. Reciprocal models at 15 and 30 ppw (both with 10 meter stair-steps) show very good agreement. An important conclusion of this work is that the

specification of complex seafloors requires a much finer grid than is necessary for numerical stability and accuracy. This will be true for other numerical methods as well.

Published in: Journal of the Acoustical Society of America, 90(5):2637-2651, 1991.

Supported by: ONR Contract N00014-89-J-1012.

WHOI Contribution No. 7838.

A GLOBAL AND REGIONAL STOCHASTIC ANALYSIS OF NEAR-RIDGE ABYSSAL HILL MORPHOLOGY

John A. Goff

This paper presents the results of a global and regional stochastic analysis of near-ridge abyssal hill morphology. The analysis includes the use of Sea Beam data for the estimation of stochastic parameters up to order 4. These parameters provide important quantitative physical information regarding abyssal hills, including their rms height, azimuthal orientation, characteristic width, aspect ratio, Hausdorff dimension, skewness, tilt, and peakiness. The global data set consists of 64 Sea Beam swaths near the Rivera, Cocos, and Nazca spreading sections of the East Pacific Rise, the Mid-Atlantic Ridge, and the Central Indian Ridge.

In one form of analysis, the parameters are averaged among spreading-rate bins. Each of the spreading rate subsets can be identified as unique from the others in at least one aspect. The slowest spreading-rate subset (Mid-Atlantic data) exhibit the largest scales (rms height, characteristic width and length) of abyssal hills. These parameters generally decrease as spreading rate increases up to the fast-spreading rated data (Pacific-Cocos), but increase going from fast to very fast (Pacific-Nazca) spreading rate data. This indicates some complexity in the relationship between spreading rate and abyssal hill morphology. The plan-view aspect ratio is nearly twice as large for the fast-spreading rate data than for any of the other subsets, and is nearly twice as large for the fast-spreading rate data than for any of the other subsets, and is smallest for the very-fast spreading rate data. The fractal dimension is nearly identical for all spreading-rate subsets. The vertical skewness is positive for the slow and medium spreading rate data, indicating larger peaks than troughs, and negative for the fast spreading rate data, indicating larger troughs than peaks. The kurtosis, or peakiness is everywhere larger than the Gaussian value of 3, and tends to be larger in the Atlantic than the Pacific. The tilting parameter provides substantial evidence indicating steeper

inward facing slopes in the medium and fast spreading rate data, but only marginal evidence for it in the slow-spreading rate data.

From an analysis of correlations among parameters it is found that subsets sometimes behave differently from the entire data set. In particular, while over the global data set the characteristic width exhibits a well-resolved positive trend when plotted versus rms height, these parameters exhibit a more gradual positive trend in the Mid-Atlantic data, and a negative trend in the Pacific-Cocos data. In addition, the plan view aspect ratio, while generally uncorrelated with rms height for the global data set, is positively correlated with rms height for the Pacific-Cocos data set. These results emphasize a strong uniqueness of the Pacific-Cocos data relative to the rest of the data set.

The Pacific-Cocos data consists of 27 swaths concentrated between the Siquieros and Orozco fracture zones. These data provide very good abyssal hill coverage of this well-mapped and studied region and form the basis of a regional analysis of the correlation between ridge morphology and stochastic abyssal hill parameters. In this analysis, it is found that abyssal hill parameters are correlated with the depth of the adjacent ridge axis, indicating that the relative abundance in magma supply, which likely controls the ridge axis depth, may also be an important influence on the formation of abyssal hills.

Published in: Journal of Geophysical Research, 96(B13):21,713-21,737, 1991.

Supported by: ONR Contracts N00014-86-K-0325 and N00014-90-J-1584.

WHOI Contribution No. 7644.

QUANTITATIVE COMPARISON OF BATHYMETRIC SURVEY SYSTEMS

John A. Goff and Martin C. Kleinrock

Spatially coincident Deep-Tow, Sea Beam, and SeaMARC II bathymetric data are statistically analyzed to determine the scales at which each system is reliable for mapping seafloor features. The methods we employ, including ruler measures of contours and profiles, and the covariance function and power spectrum of profiles, allow us to investigate the size of features measured as a function of scale. We find that, relative to Deep-Tow, Sea Beam bathymetry begins to degrade at lateral scales of ~500-800 m, while SeaMARC II begins to degrade at lateral scales of ~1.0-1.5 km.

Published in: Geophysical Research Letters, 18(7):1253-1256, 1991.

Supported by: ONR Contracts N00014-90-J-1584 and N00014-90-J-1434.

WHOI Contribution No. 7704.

IMAGE OF THE MOHO ACROSS THE CONTINENT-OCEAN TRANSITION, U.S. EAST COAST

W. S. Holbrook, E. C. Reiter, G. M. Purdy and M. N. Toksöz

Strong wide-angle reflections from the Moho were recorded by ocean bottom seismic instruments during the 1988 Carolina Trough multichannel seismic experiment, in an area where the Moho is difficult to detect with vertical-incidence seismic data. Pre-stack depth migration of these reflections has enabled the construction of an excellent seismic image of the Moho across the continent-ocean transition zone of a sedimented passive margin. At the resolution of our data (±3 km), the Moho is a smooth feature, rising at a slope of 8°-9° from about 35-36 km beneath the continental shelf to 25 km beneath the outer rise. This zone of crustal thinning defines a distinct, 60- to 70-km-wide continent-ocean transition. We interpret the Moho in the Carolina Trough as a young feature, formed by magmatic intrusion and underplating during the Mesozoic rifting of Pangea.

In Press: Geology.

Supported by: NSF Grants OCE89-17599 and EAR-8418120.

WHOI Contribution No. 7841.

DEEP VELOCITY STRUCTURE OF RIFTED CONTINENTAL CRUST, U.S. MID-ATLANTIC MARGIN, FROM EDGE WIDE-ANGLE REFLECTION/REFRACTION DATA

W. S. Holbrook, G. M. Purdy, J. A. Collins, R. E. Sheridan, D. L. Musser, L. Glover III, M. Talwani, J. I. Ewing, R. Hawman and S. Smithson

We present new ocean-bottom, wide-angle seismic data, collected as a complement to the 1990 EDGE Mid-Atlantic multichannel seismic experiment, which provide a measurement of the deep velocity structure of rifted Appalachian continental crust beneath the U.S. East Coast continental margin. The data are of excellent quality, with reflections from the entire crust and Moho visible from offsets of zero to 100 km. One-dimensional forward and inverse traveltime modeling reveals a 34-km-thick crust consisting of

three layers beneath the post-rift sediments, with velocities of 5.9 km/s, 6.4 km/s, and 6.8 km/s in the upper, middle, and lower crust, respectively. This velocity structure is indistinguishable from that found beneath several Appalachian terranes in the northern Appalachians of New England. The boundaries between these crustal units correspond to major reflective horizons on the coincident reflection data, which are interpreted as fault zones separating distinct Appalachian terranes. The average velocity of 6.8 km/s in the lower crust corroborates the interpretation of the high-velocity (7.2-7.4 km/s) lower crust found farther seaward as the result of pervasive magmatic underplating and places a limit on its landward extent.

Submitted to: Geophysical Research Letters.

Supported by: NSF Grant OCE89-17628.

WHOI Contribution No. 7891.

USING THE F-TEST FOR EIGENVALUE DECOMPOSITION PROBLEMS TO FIND THE STATISTICALLY 'OPTIMAL' SOLUTION

R. S. Jacobson and P. R. Shaw

A fundamental problem using linear inverse theory to solve geophysical problems using eigenvalue decomposition algorithms is to determine how many eigenvalues to include in the solution. If very small eigenvalues are included, the solution variance increases rapidly, particularly if zero-values eigenvalues are computed as positive small numbers and are misidentified. F-tests can be applied to a succession of solutions, each containing an incremental number of eigenvalues, to determine the statistical significance of the data variance reduction. This methodology is widely used for multiple variable regression analysis, but has not been applied to eigenvalue problems. The F-test is used as a statistical criterion for choosing an 'optimal' solution along the trade-off curve of model resolution and model variance for a particular model parameterization.

Published in: Geophysical Research Letters, 18:1075-1078, 1991.

Supported by: ONR Contract N00014-80-J-1018. WHOI Contribution No. 7729.

CAPABILITIES OF SOME SYSTEMS USED TO SURVEY THE DEEP-SEA FLOOR

Martin C. Kleinrock

Perhaps the most fundamental type of information needed to understand marine geology

is seafloor shape. Measurements of depth have come a long way from the 19th century lead line methods. As a result of the widespread use of deep-sea sonar profiling since the mid-20th century, generalized bathymetric maps [e.g., GEBCO, 1980, NOAA-NGDC, 1985] and the data bases of the world's oceans have been produced. Such maps and databases are primarily based upon compilations of individual trackline sonar profiles. Significant advances in sonar technology over the past three decades have provided new classes of mapping systems capable of collecting more than just an individual trackline profile: multibeam bathymetry and sidescan sonar mapping systems. Additionally, vast improvements have been made in the ability to photograph and directly observe the seafloor, measure the potential fields (magnetics and gravity) created by the suboceanic rock, and profile through the sedimentary strata. Remote sensing acoustic, optical, and potential field instrumentation thus play a critical role in determining the nature of the seafloor.

The utility of these new instruments for describing seafloor geology hinges upon understanding the resolution and limitations of the different systems; one must know how to interpret the data and which system should be used to answer a specific set of geologic questions. Most evaluations of system capabilities have concentrated on theoretical resolutions based upon engineering specifications and geometrical and physical considerations [e.g., Tyce, 1986; deMoustier, 1988; Johnson and Helferty, 1990]. analysis of data from a given system from crossing tracklines or comparison with other maps with equal or lesser quality [e.g., Renard and Allenou, 1979], and qualitative and descriptive intersystem comparisons based on observations [e.g., Davis et al., 1986].

Recent work [e.g., Kleinrock, 1989; Kleinrock and Goff, 1990; Kleinrock et al., 1991; Goff and Kleinrock, 1991] has sought to quantitatively determine the practical resolution of deep-water seafloor survey systems. What can each tool really tell us about seafloor geology in practice? What are the limits on the scale of different types of features (e.g., seamounts, scarps, and ridges) which can be detected and characterized from each data type? Is it possible to optimize the interpretability of data from a given system by utilizing finer-scale information in areas of coincident data?

This chapter first provides a brief review of many of the systems commonly used by the oceanographic academic community for seafloor mapping in the deep sea. Comparisons of system capabilities are then presented in two classes: theoretical resolutions predicted from physics and engineering design parameters of each system and practical resolutions based on actual observations from coincidentally located data. Implications of

these results for studying geological problems and future directions in seafloor mapping are also discussed.

Published in: CRC Handbook of Geophysical Exploration at Sea, 2nd Edition, Hard Minerals, by Richard A. Geyer. CRC Press, :36-84, 1992.

Supported by: ONR Contract N00014-90-J-1434. WHOI Contribution No. 7854.

DEPTH TO BASEMENT AND GEOID EXPRESSION OF THE KANE FRACTURE ZONE: A COMPARISON

R. Dietmar Müller, David T. Sandwell, Brian E. Tucholke, John G. Sclater and Peter R. Shaw

Geoid data from Geosat and subsatellite profiles of basement depth across the Kane Fracture Zone in the central North Atlantic were used to examine the correlation between the short-wavelength gooid (λ =25-100 km) and the uncompensated basement topography. The processing technique we apply allows the stacking of geoid profiles, although each repeat cycle has an unknown long-wavelength bias. We first formed the derivative of individual profiles, stacked up to 22 repeat cycles, and then integrated the average-slope profile to reconstruct the geoid height. The stacked, filtered geoid profiles have a noise level of about 7 mm in geoid height. The subsatellite basement topography was obtained from a recent compilation of structure contours on basement along the entire length of the Kane Fracture Zone. The ratio of geoid height to topography over the Kane Fracture Zone valley decreases from about 20-25 cm/km over young ocean crust to 5-0 cm/km over ocean crust older than 140 Ma. Both geoid and basement depth profiles were projected perpendicular to the Kane Fracture Zone, resampled at equal intervals and then cross correlated. The cross correlation shows that short-wavelength geoid anomalies are well correlated to the basement topography. For 33 of the 37 examined profiles, the horizontal mismatches are 10 km or less with an average mismatch of about 5 km. This correlation is quite good considering that the average width of the Kane Fracture Zone valley at median depth is 10-15 km. Most of the remaining seven profiles cross the transverse ridge just east of the active Kane transform zone or overlie old crust within the M-anomaly sequence. The mismatch over the transverse ridge probably is related to a crustal density anomaly. The relatively poor correlation of geoid and basement depth in profiles of ocean crust older than 130-140 Ma reflects poor basement-depth control along subsatellite tracks.

Published in: Marine Geophysical Researches, 13:105-129, 1991.

Supported by: ONR Contracts N00014-87-K-0007 and N00014-90-J-1621 and NSF Grants OCE87-16713 and OCE88-12490.

WHOI Contribution No. 7625.

A RELATIONSHIP BETWEEN SPREADING RATE AND THE SEISMIC STRUCTURE OF MID-OCEAN RIDGES

G. M. Purdy, L. S. L. Kong, G. L. Christeson and S. C. Solomon

An apparently systematic relationship exists between depth to zones of elevated temperature and partial melt beneath mid-ocean ridges and their spreading rate. Recent seismic measurements provide robust determinations at five different locations of depth to the lids of low velocity zones (LVZ) that suggest that as full spreading rates decrease from 120 to 20 mm/year the depth below the seafloor to the lid of the LVZ increases from ~1.5 kms to ~4 kms. This trend could be an artifact of temporal variations in the magma injection process, but our preferred explanation is that because major faults extend to greater depths on slower spreading ridges (as is proven by the earthquake record) then vigorous circulation of cooling water extends to greater depths and blocks upward migration of substantial bodies of melt. A natural consequence of this model is that the total thickness of dikes and extrusives is on average greater on slower spreading ridges. Available data do not contradict this prediction.

Published in: Nature, 335:815-817, 1992.

Supported by: NSF Grants EAR-8407798 and OCE86-15797 and ONR Contract N00014-89-J-1015.

WHOI Contribution No. 7840.

ISOLATION OF SOURCE AND RECEIVER STATICS AND SCALE FACTORS IN WAVEFORM INVERSION OF MARINE REFRACTION DATA

Peter R. Shaw

In this paper I present a method that uses multiple ocean bottom instruments to separate variations in seismic amplitudes and travel times caused by near-source topography and variable source amplitudes from similar variations related to the overall one-dimensional seismic structure. The results indicate that the standard correction for topography, sediment thickness, and source size can be improved with this method, reducing uncertainties in the velocity solution.

Published in: Geophysical Research Letters, 18(8):1429-1432, 1991.

Supported by: ONR Contract N00014-80-J-1018.

WHOI Contribution No. 7776.

THE ROLE OF SEAMOUNT VOLCANISM IN CRUSTAL CONSTRUCTION AT THE MID-ATLANTIC RIDGE (24°-30°N)

Deborah K. Smith and Johnson R. Cann

An analysis of approximately 6000 km² of Sea Beam swaths indicates that the floor of the median valley of the Mid-Atlantic Ridge (MAR) between 24°-30°N is strewn with near-circular volcanoes. We have identified 481 seamounts in the height range 50-650 m. Because many of the features which appear to be seamounts do not meet our criteria fully, they have not been counted, and our numbers are likely a minimum estimate of the population. The large abundance of seamounts on the median valley floor indicates that seamount volcanism plays an important role in the accretionary processes at this section of the MAR. The summit height distribution of the MAR seamount population is consistent with the exponential frequency-size distribution model for off-axis eastern Pacific seamounts (Jordan et al., 1983; Smith and Jordan, 1987). The model parameters for the MAR population yield an average of about 195 seamounts per one thousand square kilometers, and a characteristic height of about 60 m. Shape statistics compiled from the 481 seamounts give parameters that are exactly the same, or cover the same range in values as those obtained from a study of Pacific seamounts in the height range 140-3800 m (Smith, 1988) implying a universal control on seamount construction. Based on the volcanic morphology, we identify 18 spreading segments along the ridge. All except two contain a prominent axial volcanic ridge. Many of the seamounts identified are associated with the axial ridges. From the Sea Beam swaths, we infer that the ridges are composed of piled up seamounts and hummocky flows, and interpret them to be the primary sites of crustal construction. This style of volcanism contrasts strongly with that observed at the East Pacific Rise where seamounts are virtually absent at the spreading axis. The construction of seamounts and hummocky flows may be directly related to the fact that the MAR is fed by magma chambers that are limited in size and frequency. We suggest that small magma pockets with slow eruption rates produce seamounts either from pipes or initial fissure eruptions that collapse to construct a single edifice; small magma bodies with somewhat higher

eruption rates produce hummocky fissure fed flows. Using buoyancy arguments, the heights of the MAR seamounts are related to the depth of the magma bodies. We hypothesize that small magma bodies rise buoyantly to the base of the hydrothermally cooled brittle lid where they are trapped, and then erupt. If this hypothesis is correct, the thickness of the brittle lid controls seamount height, and the exponential distribution of seamount summit heights implies that the thickness of the brittle lid follows an exponential distribution in time and space with characteristic thickness 1.4-1.9 km. If seamounts and hummocky flows are fed each from their own discrete magma body trapped at the brittle/ductile transition, then the lower crust of the MAR will be made up of the products of a multitude of small plutons.

Published in: Journal of Geophysical Research, 97(B2):1645-1658, 1992.

Supported by: NSF Grant OCE88-00497 and ONR Contract N00014-89-J-1021.

WHOI Contribution No. 7884.

FINITE DIFFERENCE MODELLING OF SHEAR WAVES

R. A. Stephen

The finite difference synthetic seismogram method provides the capability to study compressional and shear wave interaction in range dependent marine models. A study has been carried out of the pressure, vertical displacement, and horizontal displacement of the sound field at the seafloor for the P-SV problem. Compressional, shear and interface waves can be clearly identified in both snapshot and time series formats of the sound field for soft sediments (shear wave velocity = 450m/s). Key features have been identified. 1) The coupled shear head wave in the bottom can drain energy away from the compressional head wave. 2) The evanescently generated shear wave can be quite energetic and will create precursors to the Stoneley wave when there is sub-bottom structure. 3) Backscattered, secondary Stoneley waves are generated when the direct water wave hits a change in slope at the seafloor. 4) Weak backscattered water waves are generated from slope discontinuities in laterally heterogeneous waveguides. 5) At the seafloor, Stoneley waves are most evident on vertical displacement sensors. 6) Below the seafloor, at non-normal offsets, body wave energy is largest on horizontal component sensors.

Published in: Shear Waves in Marine Sediments, J.M. Hovem et al., eds. Kluwer Academic Publishers, The Netherlands, :471-478, 1991. Supported by: ONR Contract N00014-90-J-1541. WHOI Contribution No. 7631.

CANONICAL SEAFLOOR MODELS AND THE FINITE DIFFERENCE METHOD FOR LOW-ANGLE ACOUSTIC BACKSCATTER

Ralph A. Stephen and Martin E. Dougherty

In order to study the physics of low-angle acoustic backscatter from the seafloor we present a methodology based on the finite difference method for solving the two-way elastic wave equation. The method has many advantages including the ability to handle scattering 1) from surface and volume heterogeneities simultaneously, 2) from media with shear, as well as compressional properties, 3) from heterogeneities with scale lengths on the order of the acoustic wavelengths, and 4) with a two-way formulation including multiple interactions between scatterers. The major problem in applying the finite difference method is to obtain low grazing angle incidence with reasonable grid sizes and without contamination from high angle energy. We discuss two approaches to this problem. In the first, we use the traditional point source in the water column but we attenuate energy in the undesired directions using the 'telegraph equation' around the source. In the second approach, we introduce a pulse-beam at the desired angle directly into the 'numerical scattering chamber'. Examples of the two approaches are given based on canonical representations of seafloor roughness. Interface waves appear to play a significant role in the backscattering process. Backscattering is strongest for unsedimented basaltic bottoms in which the effects of shear are included. Blanketing the rough basalt with flat sediments (either homogeneous or heterogeneous) reduces the backscattering.

In Press: Proceedings of 3rd IMACS Symposium on Computational Acoustics.

Supported by: ONR Contracts N00014-90-J-1541 and N00014-89-J-1947.

WHOI Contribution No. 7872.

ONR SEAFLOOR NATURAL LABORATORIES ON SLOW- AND FAST-SPREADING MID-OCEAN RIDGES

B. E. Tucholke, K. C. Macdonald and P. J. Fox

The Office of Naval Research has established long-term Natural Laboratories for in-depth studies of the sea floor at both a slow-spreading

(<30 mm/yr) and a fast spreading (>60 mm/yr) mid-ocean ridge. The two Natural Laboratories were selected for their representativeness of global mid-ocean ridge (MOR) environments, and for their logistic accessibility. The Natural Laboratory region for the slow-spreading regime is on the Mid-Atlantic Ridge from Kane F.Z. north to about 27°30'N, and the fast-spreading counterpart is on the East Pacific Rise at 8°-10°30'N, from Siqueiros to Clipperton F.Z. Together, the two Natural Laboratories span all of the most significant geologic variables that are thought to control both the shape and structure of the igneous crust and the scatter of acoustic wavefields from the bottom/subbottom (BSB) at low angles of incidence.

The Natural Laboratory concept has evolved over the past half-dozen years as a mechanism efficiently to address the Navy's scientific interests in geological and geophysical variability of seabed properties [Anonymous, 1988], and in acoustic-wavefield BSB interaction and scatter. Many of the geological and geophysical interests are similar to those embodied in the RIDGE (Ridge Interdisciplinary Global Experiments) program, although RIDGE is a more globally ranging effort [Anonymous, 1989]. The ONR Natural Laboratories and RIDGE program effectively complement and reinforce one another, providing broad opportunities for various scientific communities to accelerate their understanding of interrelations among the marine geological, geophysical, and acoustical characteristics of oceanic crust.

The ONR Natural Laboratories specifically will provide test beds to address the following kinds of issues: 1) the origin and evolution of oceanic crust, 2) the mechanisms of BSB scatter of acoustic wavefields, and 3) calibration and intercomparison of bottom-sensing oceanographic instrumentation, models, and analytic techniques. Each of these is discussed briefly below. As long-term Natural Laboratories, the value of the two natural laboratories will be progressively enhanced with time as a wide variety of experiments and surveys are conducted.

Published in: EOS, 72:268-270, 1991.

Supported by: ONR Contract N00014-90-J-1621 and NSF Grant OCE87-16713.

WHOI Contribution No. 7624.

PLIO-PLEISTOCENE SLOPE CONSTRUCTION OFF WESTERN NOVA SCOTIA, CANADA

Elazar Uchupi and Stephen A. Swift

Atlantic continental slopes have an average gradient of 7° and tend to be irregularly incised by

submarine canyons with reliefs of about 1000 m. In contrast the slope off western Nova Scotia (from 61°30'W to 65°W), Canada, is smooth (relief <300 m) and has declivities ranging from 2.6° off Emerald Bank to 1.6° off LaHave Bank. This lack of deep relief is due to a combination of low subsidence and sedimentation rates during Late Cretaceous and Cenozoic. As a result of this low gradient, canyons that formed on the slope during periods of low sea level and high sediment supply rarely survived, being filled during subsequent regressions. High sedimentation rates by subglacial sediment plumes during late Wisconsin did lead, however, to extensive sediment failure that produced low relief slump and debris flow structures.

In Press: Cuadernos de Geologia Iberica.
Supported by: NSF Grant OCE89-22762.

WHOI Contribution No. 7656.

GEOHISTORY OF THE ANGOLA BASIN REGION AND CONSTRUCTION OF THE CONTINENTAL RISE

Elazar Uchupi

The Angola Basin off western equatorial Africa extending from the Guinea Ridge/Cameroon Volcanic Ridge near the Equator to the Walvis Ridge at 18°S forms a geologic link between the North and South Atlantic (Fig. 1). This basin is the deepest depression in the eastern South Atlantic, and is nearly isolated from the other basins in the South Atlantic; its bottom-water mass is significantly warmer than the other basins and the CCD (Carbonate Compensation Depth) is much deeper (Bolli, Ryan et al., 1978). Congo Canyon (Fig. 2), the only active canyon in the Atlantic, serves as a pathway for turbidity currents to the distal parts of the basin. Antarctic Bottom Water (AABW) reaches the region from west of the Mid-Atlantic Ridge via the west-east trending Romanche Fracture zone at loS (Fig. 2); it enters the Guinea Basin (Fig. 1) east of the ridge, and thence southward across a 4,800 m deep sill on the Guinea Ridge (Figs 1 and 2; Bolli, Ryan et al., 1978). Once in the Angola Basin the bottom water circulates in a clockwise gyre within its central part. Some AABW also reaches the southwest corner of the Angola Basin from the Cape Basin (Fig. 1) via a 3,900 m deep gap at 36°S, 7°W west of the Walvis Ridge. A barrier or barriers located north of 32°S prevent much of this minor flow from spreading onto the main part of the basin north of 20°S (Connary, 1972). The bottom water flow that does reach the basin is very weak as evidenced by the Miocene and younger sediments at Deep Sea Drilling Project Site 364 which are indicative of

partially anoxic bottom conditions (The Shipboard Scientific Party, 1978b). Deep and intermediate water masses reach the Angola Basin from the south via sills at 36.5°S, 5°W and 30°S, 1°E, and a deeply eroded saddle (3,200 m deep) across the Walvis Ridge (Figs. 1 and 2; Bolli, Ryan et al., 1978). The cold northerly flowing Benguela surface Current (Fig. 2) is deflected westward away from the Angola Basin by the Walvis Ridge. It is these conditions, weak bottom current activity, isolation from cold northerly flowing surface currents, and the presence of the Congo Canyon that make the Angola Basin so significant to our understanding of the depositional history of the Atlantic. Unfortunately data that can be used to reconstruct its geology is limited. Because of their petroleum preserves the Cuanza, Congo-Cabinda, and Gabon coastal basins (Fig. 3) and adjacent inner shelves are relatively well known (Belmonte, Hirtz, and Wenger, 1965; Brognon and Verrier, 1966; Reyre, 1966; Hedberg, 1968; Franks and Nairn, 1973; Brink, 1974; Brice et al., 1982; Dailly, 1982; Sieglie and Baker, 1982). However, the other non-petroliferous coastal basins (Douala and Mo medes; Fig. 3) are not well documented. Knowledge beyond the inner continental shelf also is based mainly on single and multi-channel seismic reflection profiles and oblique reflection and refraction measurements obtained through the use of sonobuoys (Baumgartner and van Andel, 1971; Leyden, Bryan, and Ewing, 1972; Uchupi and Emery, 1972, 1974; Von Herzen, Hoskins and van Andel, 1972; Pautot et al., 1973; Beck and Lehner, 1974; Emery et. al., 1975b; Leyden et al., 1976; Lehner and de Ruiter, 1977). The Deep Sea Drilling Project has occupied three sites in Angola Basin, two near the Angola Escarpment (Sites 364 and 365; Bolli, Ryan, et. al., 1978; The Shipboard Scientific Party, 1978b) and one (Site 530; Hay, Sibuet, et al., 1984) at the southern end of the Angola Basin immediately, north of the Walvis Ridge (Fig. 1).

In Press: The Evolution of Atlantic Continental Rises, Dowden, Hutchinson and Ross, Inc., Stroudsburg.

WHOI Contribution No. 7632.

ELECTROMAGNETIC INDUCTION BY A FINITE ELECTRIC DIPOLE SOURCE OVER A TWO-DIMENSIONAL EARTH

Martyn J. Unsworth, Bryan J. Travis and Alan D. Chave

A 2 1/2-D finite element algorithm has been developed to model the response of a 2-dimensional earth to excitation by an arbitrary electric current source. The singularity in the the electromagnetic fields produced by the source is

first removed by separating them into primary and secondary parts. The Maxwell equations are then used to obtain a variational integral in terms of the secondary electric and magnetic fields parallel to the invariant axis. An iterative procedure is then applied to minimize the integral with respect to these two field components. The fields are allowed to decay to zero at infinite range from the source by using a set of infinite boundary elements to implement a radiation condition at the perimeter of the mesh. These features considerably reduce the computational overhead. The numerical solutions for an HED are computed and shown to agree with other calculations and to converge with respect to the parameterization. Finally some simple examples of the electromagnetic fields produced by an HED source at the seafloor are presented to illustrate the utility of the code.

Submitted to: Gcophysics.

Supported by: IGPP/Los Alamos.

WHOI Contribution No. 7886.

THE RAYLEIGH-TAYLOR INSTABILITY OF AN EMBEDDED LAYER OF LOW-VISCOSITY FLUID

William S. D. Wilcock and J. A. Whitehead

The properties of gravitational instabilities formed within two-layer fluid systems are well known and have been applied to a variety of geophysical problems. We present theoretical and experimental results for the gravitational instability developed by a three-layer system, comprising a thin low-viscosity low-density fluid layer sandwiched between two thick layers of equal properties. Linearized equations can be used to solve for the initial growth rates as a function of perturbation wavelength. As is the case for two-layer systems, the results yield a fastest growing wavelength, termed the characteristic wavelength, whose value is much greater than the thickness of the low-viscosity layer. The experimental results confirm the ability of the linearized equations to predict the dominant wavelength of the instability. However, for very thin layers or smaller viscosity ratios a second instability is also observed at a scale much greater than the characteristic wavelength. Numerical solutions show that the wavelength of this stability matches that of a fast growing but short lived mode arising from perturbations which predominantly involve thickening rather than translation of the buoyant layer. The analytical solution also shows that at the characteristic wavelength, the displacement of the lower interface will be initially a factor 2- $\sqrt{3}$ =0.268 (CHECK THIS SYMBOL) that of the upper interface. As

the instability develops the characteristic diapir structures, the experiments show that the relative magnitude of these displacements increase, with underlying fluid being drawn up into the head of the diapir.

Published in: Journal of Geophysical Research, 96(E7):12193-12200, 1991.

Supported by: Ocean Ventures Fund, EAR87-08033. WHOI Contribution No. 7612.

HYDRODYNAMICS

NONLINEAR DIFFUSION OF THE TIDAL SIGNAL IN FRICTIONALLY-DOMINATED EMBAYMENTS

Carl T. Friedrichs and Ole S. Madsen

The dynamics of many shallow tidal embayments may be usefully represented by a single "zero-inertia" equation for tidal elevation which has the form of a nonlinear diffusion equation. The zero-inertia equation clarifies the lowest-order dynamics, namely a balance between pressure gradient and friction. It also provides insight into the properties of higher-order harmonic components via the identification of compact approximate solutions and governing non-dimensional parameters. Approximate analytic solutions which assume a constant diffusion coefficient are governed by the non-dimensional parameters x/L and $||k_0||L$, where L is the length of the embayment, and $||k_0||^$ scales both the length of frictional dissipation and the physical length of the diffusive wave-form. As $||k_0||L$ increases, the speed at which the tidal signal diffuses decreases and the rate of decay of tidal amplitude with distance increases. $||k_0||L$ increases as depth is reduced, friction is increased, forcing amplitude or frequency is increased, or total embayment width is increased relative to the width of the channel. Approximate analytic solutions which assume a time-varying diffusion coefficient result in additional components at the zeroth, second and third harmonic frequencies. The zeroth and second harmonics are governed by the parameter γ , as well as x/L and $||k_0||L$. γ measures the relative importance of time-variations of channel depth $(\gamma > 0)$ versus time-variations in embayment width ($\gamma < 0$). If $\gamma > 0$, the diffusion coefficient is larger near the crest of the tidal wave-form, causing the rising tide to be of shorter duration and mean elevation to be set-up. If γ < 0, the diffusion coefficient is larger near the trough, causing the falling tide to be shorter and elevation to be set-down. The third harmonic is

produced by fluctuations in the diffusion coefficient associated with times of greatest surface gradient. The third harmonic is governed only by the parameters x/L and $||k_0||L$, which indicates the third harmonic is insensitive to time-variations in cross-sectional geometry. Comparisons to field observations and to numerical solutions of the full equations including inertia terms indicate that the zero-inertia equation (1) reproduces the results of the more general 1-D equations to within the accuracy predicted by scaling arguments and (2) reproduces the main features of the nonlinear tidal signal observed in many shallow tidal embayments.

In Press: Journal of Geophysical Research.

Supported by: Ocean Ventures Fund and NSF Grant OCE91-02420.

WHOI Contribution No. 7885.

PALEOCEANOGRAPHY

LATE PALEOGENE CALCAREOUS NANNOPLANKTON EVOLUTION: A TALE OF CLIMATIC DETERIORATION

M. P. Aubry

Diversity changes and patterns of diachrony and provincialism exhibited by the late Paleogene calcareous nannoplankton are analyzed. The latest Eccene (~37 to 36.3 Ma), often regarded as a time of major extinctions, witnessed only a weak change in diversity compared with the profound turnover that occurred near the middle/late Eocene boundary (~40 Ma) and the global extinctions in the early Oligocene (~ 35.2 to 34.5 Ma). The intensity of changes in the calcareous nannoplankton varied with latitude, the major change at high latitudes occurring near the early/middle Eocene boundary (~52 Ma). There is an excellent correlation between the timing of changes in the calcareous nannoplankton and the timing of cooling events as inferred from isotopic studies. There is also a remarkable parallelism in the middle Eocene to early Oligocene evolution of the calcareous nannoplankton and planktonic foraminifera. This is used to show that in addition to decreasing temperatures, eutrophication was a determinant agent in evolutionary turnovers and extinctions in the calcareous nannoplankton whose late Paleogene evolution reflects expansions and contractions of the TRC (trophic resources continuum).

In Press: Middle Eocene-Early Oligocene Climatic and Biotic Evolution D. Prothero and W.A. Berggren, eds. Princeton University Press, Princeton.

Supported by: A Consortium of Oil Companies. WHOI Contribution No. 7792.

RECONSTRUCTION OF CARIBBEAN CLIMATE CHANGE OVER THE PAST 10,500 YEARS

David A. Hodell, Jason H. Curtis, Glenn A. Jones, Antonia Higuera-Gundy, Mark Brenner, Michael W. Binford and Kathleen T. Dorsey

Sediment cores from low-latitude lakes provide some of the best records of tropical climate change since the late Pleistocene. Here we report a high-resolution reconstruction of Caribbean climate based on ¹⁸O/¹⁶O in ostracod shells from Lake Miragoane, Haiti. Climate was dry and lake level was low during the latter part of the Younger Dryas Chronozone (10.5 to 10 kyr BP). Water level in the lake rose at the end of the last deglaciation (~10 to 7 kyr BP reflecting wetter conditions of the early Holocene that persisted for nearly 4 millennia. Lake level declined at ~3.2 kyr BP with the onset of drier climate that generally prevailed throughout the late Holocene. These long-term changes in Caribbean climate are well explained by orbitally-induced (Milankovitch) variations in seasonal insolation that modified the intensity of the annual cycle. Stable isotope and pollen data from this island locality provide a climatic context in which to interpret Antillean biogeography and the development of Caribbean and Mesoamerican cultures.

Published in: Nature, 352:790-793, 1991.

Supported by: NSF Grants OCE88-58012 and BSR85-00548, NASA Space Assistantship Enhancement Program and a Whitehall

Foundation Grant.

WHOI Contribution No. 7791.

HIGH RESOLUTION RECORD OF THE NORTH ATLANTIC DRIFT 14 -8 KYR BP: IMPLICATIONS FOR CLIMATE, CIRCULATION AND ICE SHEET MELTING

Scott J. Lehman and Lloyd D. Keigwin

Atlantic surface circulation shifted toward glacial-like conditions four times during the last deglaciation, often at rates leading to 1°C of SST change per decade. These oscillations correspond closely with evidence for atmospheric T changes in ice cores and with evidence for sudden shifts in Atlantic deep circulation, suggesting that thermohaline mechanisms controlled climate in the N. Atlantic region.

Submitted to: Nature.

Supported by: NSF Grant OCE91-19660.

WHOI Contribution No. 7867.

INCREASED SEASONAL UPWELLING IN THE SUBTROPICAL SOUTH ATLANTIC OVER THE PAST 700,000 YRS: EVIDENCE FROM DEEP-LIVING PLANKTONIC FORAMINIFERA

G. P. Lohmann

The distribution and character of deep-living planktonic foraminifera (such as Globorotalia truncatulinoides and G. hirsuta) are particularly sensitive to the structure of the upper ocean because of the wide range of water depths over which their life cycles extend. Like other planktonic foraminifera, the deep-living species begin growing in shallow surface waters, but unlike the other species they continue growing while sinking into much deeper water. Their reproduction is synchronized with the seasonal deep-mixing and upwelling of nutrient-rich waters that precedes spring bloom. Where deep-mixing is curtailed the abundances of the deeper-dwelling species (G. hirsuta), the deeper-dwelling varieties (eg., left-coiling G. truncatulinoides), and the larger (presumably faster-sinking) shells are reduced (leading to an apparent acceleration in shell development). These changes are observed today in transects from the seasonally deep-mixed subtropical gyres to the seasonally-stable surface waters equatorward of the subtropical convergen s.

Pas, changes in the abundance and character of these deep-living planktonic foraminifera have been measured in a Late Pleistocene record from the subtropical western South Atlantic Ocean. Over the past 700 kyrs, abundances of these species have increased, G. truncatulinoides has changed from the predominantly shallower-dwelling right-coiling to the deeper-dwelling left-coiling variety, and the accelerated shell development characteristic of shallow mixing has shifted toward the rates normally associated with deep mixing. All this indicates that the structure of the upper ocean in the subtropical South Atlantic before 700 kyrs ago was more like that nearer the equator today where mixing is limited to the upper 100-200 m. Since that time the scale of mixing has gradually increased to more than 400 m. This implies a gradual increase through the Late Pleistocene in the seasonal upwelling of nutrients in the subtropical South Atlantic and, consequently, in the intensity of the seasonal maximum in organic productivity.

In Press: Marine Micropaleontology.

Supported by: NSF Grant OCE91-1553.

WHOI Contribution No. 7931.

THE EOCENE-OLIGOCENE TRANSITION: AN OVERVIEW

Donald R. Prothero and William A. Berggren

The middle Eocene to early Oligocene witnessed major changes in global climate and ocean circulation which are reflected in significant turnovers in marine and terrestrial biota. The change from a thermospheric to thermohaline (psychrospheric) circulation is thought to reflect the establishment (and continued, if intermittent, presence) of ice on Antarctica, although a precise chronology of this conjunct evolution remains elusive owing to conflicting interpretations of the stable (O, C) isotope record. Paleoclimatic evidence clearly indicates global cooling and increased aridity during the late middle Eocene and again across the Eocene/Oligocene boundary and earliest Oligocene. The cooling during the middle Eocene has not been satisfactorily explained, although ice may have existed on the Antarctic continent by this time. The most significant cooling event and change in land floras occurred in the earliest Oligocene at about 33.5 Ma (in the revised chronology developed here). By the early Oligocene there were significant ice sheets on Antarctica, probably caused by the thermal isolation, and insulation, of the south polar region as cold currents flowed between the newly separated Antarctica and Australia.

The late middle Eocene - early Oligocene interval was the most significant episode of climatic change and extinction since the end of the Cretaceous, with the exception of the Paleocene/Eocene boundary event. However the latter involved an abrupt (<0.5 m.y.) collapse in global productivity and change from thermohaline to thermospheric circulation and associated major extinction of deep water benthic foraminifera superimposed on a longer term trend towards increasing temperatures. Climatic changes at the Eocene-Oligocene transition is seen to have been the antithesis of those at the Paleocene/Eocene boundary with sequential global extinctions superimposed on a gradually cooling (primarily at high latitudes) earth and increased eutrophication associated with increased biosiliceous productivity at high southern latitudes. In groups ranging from marine plankton to whales, and terrestrial pollen to land mammals, the major wave of extinctions took place at the end of the middle Eocene (Bartonian/Priabonian boundary); the highly diversified, warm-adapted special were the primary victims. Lesser extinctions took place during the late Eocene (mid-Priabonian), at the Eocene/Oligocene boundary (about 34 Ma; chronology developed here), and in the early Oligocene (Rupelien). Extraterrestrial impacts

occurred during the late Eocene (mid Priabonian) but are not associated with any extinctions of consequence. Global biotic changes associated with the mid-late Paleogene climatic deterioration should be interpreted in the framework of endogenic (long-term changes in global circulation and associated restructuring of global environment and trophic resources) rather than exogenic (extraterrestrial) causes.

In Press: Middle Eocene-Early Oligocene Climatic and Biotic Evolution D. Prothero and W.A. Berggren, eds. Princeton University Press, Princeton.

Supported by: NSF Grant OCE91-01463. WHOI Contribution No. 7793.

USING ²³⁰TH IN MARINE SEDIMENTS TO RECONSTRUCT THE LATE QUATERNARY HISTORY OF SEA LEVEL

Niall C. Slowey and William B. Curry

We propose a method to determine past sea levels based on the record of ²³⁰Th accumulating in seafloor sediments. The decay of uranium in seawater produces this nuclide, which then adsorbs rapidly onto particles settling to the seafloor. Since the concentration of uranium is similar at all depths in the water column, the flux of ²³⁰Th to the seafloor at any location are proportional to water column height. Consequently changes in sea level must cause changes in these fluxes. At shallow depths (<1000 m), fluctuations of sea level cause changes in the expected ²³⁰Th flux that are large enough to produce measurable changes in the ²³⁰Th content of the sediment.

We have developed two approaches to determine past sea levels from the content of ²³⁰Th in sediments (1) in a single core, the ratio of the past and present fluxes of ²³⁰Th to a site on the seafloor is a measure of the ratio of the past and present depths of the site below sea level, and (2) in two or more cores from a region where the vertical input of sediment is similar at all depths in the water column, the concentrations of ²³⁰Th in synchronous sediment samples are linearly related to depth and indicate past sea level as the depth where the concentrations extrapolate to zero. The latter approach requires fewer assumptions and allows sea level to be estimated at discrete points in time. The methodology, assumptions, advantages and disadvantages of the first approach is illustrated using preliminary data from a core recovered from the margin of Little Bahama Bank.

Published in: Paleoceanography, 6:609-619, 1991.

Supported by: NSF Grants OCE85-11014 and OCE88-13307.

PALEONTOLOGY

NEOGENE PLANKTONIC FORAMINIFERAL BIOSTRATIGRAPHY OF EASTERN JAMAICA

W. A. Berggren

The Neogene deep water carbonate section exposed at Buff Bay, north coast of Jamaica, is about 300 m thick and spans the interval from early middle Miocene to mid-Pliocene (ca. 16-3 Ma). It has come to serve as a standard reference section for upper Neogene biostratigraphy because several of the N-zones of Blow (1969) are typified here. a diverse tropical planktonic foraminiferal fauna characterizes this section and enables a detailed biostratigraphic subdivision. One obvious hiatus in the upper part of the Bowden Formation spans about 4 my of late Miocene - early Pliocene time; a shorter more subtle, ca. 1 my intra-late Miocene hiatus is thought to exist separating beds of Zone N17 from Zone N16/15.

Faunal analysis reveals general agreement with mid-late Neogene biostratigraphy of Bolli, Blow, and Robinson. A distinct stratigraphic separation between the LO of Paragloborotalia mayeri and the FO of Neogloboquadrina acostaensis suggests that "restoration" of Zone N15 to the planktonic foraminiferal hagiography may be required and that its apparent absence at North Atlantic DSDP Sites 558 and 563 may be due to a widespread early late Miocene hiatus. A new type level in the Buff Bay Formation is chosen for the Globorotalia menardii Zone (Bolli, 1966) = Globorotalia (Turborotalia) continuosa Consecutive Range-Zone (Blow, 1969) because the type sample in Trinidad for these zones (which is the same for both zones) has been found to be correlative with a level within the Globorotalia (Turborotalia) acostaensis -G. (T.) merotumida (N16) Zone of Blow (1969).

Analysis of type level samples used to denote some classic late Neogene zones has shown that the type level of Blow's (1069) Zone N17 is in calcareous nannoplankton Zone NN10 (rather than NN11 as previously thought), the type level of Zone N18 is biostratigraphically equivalent to Zone PL2 (~3.7 Ma, lower Pliocene; i.e. within Zone N19), and the type level of Zone N19 is equivalent to Zone PL3 - PL4 (ca. 3+ Ma). Use of Blow's Pliocene N18 - N21 zones is discouraged.

The taxonomy and stratigraphy of over 40 taxa are discussed and most are illustrated by SEM micrographs.

In Press: Geological Society of America Special Papers.

Supported by: A consortium of oil companies. WHOI Contribution No. 7882.

NEPHROLITHUS FREQUENS GORKA (1957) AND ITS MORPHOTYPES

Thomas Ehrendorfer

A complete morphologic intergradation from biperforate to multiperforate specimens of Nephrolithus frequens Gorka (1957) occurs in the uppermost Maestrichtian chalk at southern high-latitude ODP-Holes 750A (Kerguelen Plateau, Southern Indian Ocean) and 690C (Maud Rise, Weddell Sea). Previous workers have assigned taxonomic importance to the number of performations of the central area. Two subspecies, N. frequens frequens and N. frequens miniporus were recently erected (Pospichal and Wise, 1990), based on the number of performations (four or more and two, respectively). The observation of specimens of Nephrolithus frequens with three perforations in the central area indicates that this represents an artificial division between multiperforate and biperforate types in a morphologic continuum. In addition, some observations on the construction of the central area and the margin of N. frequens are reported.

Submitted to: Journal of Paleontology.

Supported by: AAPG 4643 (Code 31), Ocean
Ventures Fund and in part by a
Research-Grant-in-Aid from the Paleontological
Society.

WHOI Contribution No. 7892.

GROWTH AND CHEMISTRY OF GLOBOROTALIA TRUNCATULINOIDES— PROBES OF THE PAST THERMOCLINE: PART III. SHELL CRUST

G. P. Lohmann

Part III measures the size and developmental stage at which populations of G. truncatulinoides encrust their shells and finds that the size at which shells add a crust is related to thermocline depth. The shallower the main thermocline, the smaller the size at which G. truncatulinoides adds a crust. For the same thermocline depth, left-coiling shells crust at a smaller size than do right-coiling ones.

The criteria for gauging degree of shell crusting permit the crust's mass and chemistry to be calculated from the difference between crusted and non-crusted shells.

In Press: Paleoceanography.

Supported by: NSF Grants OCE84-17040 and BSR86-06701.

WHOI Contribution No. 7043.

PALEOGENE BENTHIC FORAMINIFERS FROM THE SOUTHERN INDIAN OCEAN (KERGUELEN PLATEAU): BIOSTRATIGRAPHY AND PALEOECOLOGY

Andreas Mackensen and William A. Berggren

Benthic foraminifers were studied from lower Paleocene through upper Oligocene sections from Sites 747 and 748. The composition of the benthic foraminifer species suggests a middle to lower bathyal (600-2000 m) paleodepth during the Neogene and a probable upper abyssal (2000-3000 m) paleodepth during the Paleocene at Site 747. Site 748 is thought to have remained at middle to lower bathyal paleodepths throughout the Cenozoic. Principal component analysis distinguished four major benthic foraminifer assemblages: (1) a Paleocene Stensioina beccariiformis assemblage at Sites 747 and 748, (2) an early Eocene Nattallides truempyi assemblage at lower bathyal Site 747, (3) an early through middle Eocene Stilostomella-Lenticulina assemblage at middle bathyal Site 748, and (4) a latest Eocene through Oligocene Cibicidoides-Astrononion pusillum assemblage at both sites. Major benthic foraminifer changes, as indicated by the principal components and first and last appearances, occurred at or close to the Paleocene/Eocene boundary, and in the late Eocene close to the middle/late Eocene boundary.

In Press: Proceedings of the Ocean Drilling Program, Scientific Results, Vol. 120.

WHOI Contribution No. 7784.

BIOSTRATIGRAPHY AND ISOTOPE STRATIGRAPHY OF UPPER EOCENE MICROTEKTITES AT SITE 612: HOW MANY IMPACTS?

Kenneth G. Miller, W. A. Berggren, Jijun Zhang and Amanda A. Palmer-Julson

In view of recent controversy over the number and timing of late Eocene impact events, we evaluated biostratigraphic correlations at Deep Sea Drilling Project (DSDP) Site 612, New Jersey continental slope. Site 612, Core 21, Section 5 contains a tektite horizon which includes distinct microkrystite and microtektite layers (Glass, 1989). Ranges of magnetostratigraphically

calibrated marker taxa firmly constrain the biostratigraphic position of these layers, although planktonic foraminiferal zonal criteria are equivocal for the upper Eocene at Site 612. Radiolarian and foraminiferal biostratigraphy indicate that the tektite layer at Site 612 is biostratigraphically older than a microtektite layer in Barbados that has been correlated with the North American strewn field. The Site 612 tektites are approximately 0.5-1.0 m.y. older than the Barbados microtektites. This conclusion is supported by compositional and isotope differences between the Site 612 tektites and the Barbados microtektites (Koeberl, 1988; Glass, 1989; Stecher et al., 1989), and requires that there were 3 or 4 separate late Eocene impact events. An alternative interpretation correlates the Barbados microtektites with the Site 612 tektites using ⁴⁰Ar-³⁹Ar age measurements and some compositional similarities; this requires that biostratigraphic first and last occurrences were diachronous by ~0.7 m.y. or extremely high sedimentation rates at Site 612. Strontium and oxygen isotope stratigraphies are consistent with magnetobiostratigraphic correlations. The late Eocene impact events do not correlate with climate changes inferred from the marine isotope record.

Published in: Palaios, 16:17-38, 1991.

Supported by: A consortium of oil companies.

WHOI Contribution No. 7680.

CENOZOIC DEEP-SEA BENTHIC FORAMINIFERA: A TALE OF THREE TURNOVERS

Kenneth G. Miller, Miriam E. Katz and W. A. Berggren

We review recent advances in the taxonomy, biostratigraphy, and paleoceanography of Cenozoic bathyal (200-2000 m) and abyssal (>2000 m) benthic foraminifera. Recently published syntheses of the taxonomy and biostratigraphy (van Morkhoven et al., 1986; Berggren and Miller, 1989) provide a framework for evaluating benthic foraminiferal faunal abundance changes and taxonomic turnovers. Several periods of taxonomic stability occurred in the deep sea during the Cenozoic. There were few global first and last occurrences across the Cretaceous/Paleogene boundary and during the Paleocene in the deep sea, and there were few global first or last occurrences in the late Neogene abyssal realm. There were at least three intervals of increased taxonomic turnover and faunal abundance changes in deep-water benthic foraminifera: 1) latest Paleocene (late Zone P6a), followed by an early Eocene period of rapid recolonization; 2) late

middle Eocene to earliest Oligocene (Zones P14 to P 18); and 3) early middle Miocene (Zones N6-7 to N12). We briefly review the nature and possible causes for these three faunal changes and provide new data on the middle Eocene-earliest Oligocene event. These faunal changes were triggered by different mechanisms. We attribute the latest Paleocene "crisis" to an abrupt, transient warming and change in deep-water source regions. The late middle Eocene-early Oligocene taxonomic turnover was relatively minor. However, a dramatic decrease in the abundance of Nuttallides truempyi occurred throughout the deep sea in the late middle Eocene (Zone P14). We directly link this abundance change to a cooling of deep water inferred from the δ^{18} O record. The middle Miocene faunal turnover and abundance changes were not related directly to temperature history, although they may have been related to changes in deep-water sources and/or surface open productivity.

In Press: Proceedings 4th International Symposium on Benthic Foraminifera, University of Tohoku, Sendai, Japan.

Supported by: A consortium of oil companies. WHOI Contribution No. 7692.

EXTINCTION SELECTIVITY AND ECOLOGY IN PLANKTONIC FORAMINIFERA

Richard D. Norris

Planktonic foraminifera have radiated three times since the mid-Cretaceous and independently evolved similar morphological groups and patterns of species longevity in each diversification. All morphological groups include substantial numbers of short-ranging species, but only some groups include large numbers of long-ranging taxa. The long ranges of these 'extinction-resistant' taxa are unlikely to be due to systematic differences in geographic range, b. dy size, or taxonomic practice. Instead, life history traits such as trophic ecology and factors influencing population structure are closely correlated with species longevity during each of the radiations. Generation time and reproductive output are correlated with longevity in living species but the significance of these factors for extinct taxa is unknown. Other variables such as depth distribution are inversely correlated with longevity in Neogene and Cretaceous biotas, but not in Paleogene foraminifera. Perhaps the maintenance of a diverse trophic resource base and large populations contribute to extinction resistance. It is also likely that these traits are correlated with life in geologically persistent watermasses. Indeed, long-ranging species are concentrated in

geologically old, stable environments in the oligotrophic gyres and waters below the thermocline. In contrast, species that live in ephemeral boundary layers are frequently short-ranging. It may be the stability and trophic conditions in water-masses that have been the ultimate arbitrators of species longevity.

In Press: Paleogeography, Palaeoecology, Paleoclimatology.

Supported by: NSF Grant EAR91-06108. WHOI Contribution No. 7911.

WALL TEXTURE CLASSIFICATION OF PLANKTONIC FORAMINIFERA GENERA IN THE LOWER DANIAN

Richard K. Olsson, Christoph Hemleben, William A. Berggren and Chengjie Liu

The early Danian planktonic foraminifera from Zones PO, P α , and P1a can be classified into four groups based on surface wall texture: microperforate, normal perforate smooth-walled, normal perforate cancellate nonspinose, and normal perforate cancellate spinose. A new genus, Praemurica is erected for the cancellate nonspinose group and another new genus, Parasubbotina, is erected for species in the pseudobulloides lineage within the cancellate spinose group. Only two Cretaceous genera, Guembelitria s.l. and Hedbergella, are believed to have given rise to the early Danian planktonic foraminifera, Guembelitria to the microperforate group and Hedbergella to the smooth-walled and cancellate groups. No other Cretaceous planktonic foraminifera are involved in the phylogeny of the Danian planktonic foraminifera. The microperforate are the most diverse group in the Danian and include the genera Parvularugoglobigerina, Guembelitria, Woodringina, Chiloguembelina, and Globoconusa and are included in the Heterohelicacea. This group rapidly declined and most species became extinct before the end of the Danian. The great radiations of planktonic foraminifera of the Paleogene and Neogene are linked to the three other groups. The genera (with at least fifteen species) recognized in these groups include Globanomalina (smooth-walled), Praemurica (cancellate nonspinose), and Eoglobigerina, Parasubbotina and Subbotina (cancellate Spinose) which are placed in the Superfamily Globigerinacea. The absence or rarity of cancellate wall species in lowermost Danian sections such as El Kef is most probably due to their lack of preservation.

In Press: Journal of Foraminiferal Research.
Supported by: NSF Grant OCE91-146300.
WHOI Contribution No. 7874.

PETROLOGY

OPEN SYSTEM MELTING AND THE TEMPORAL AND SPATIAL VARIATION OF PERIDOTITE AND BASALT COMPOSITIONS AT THE ATLANTIS II FRACTURE ZONE

Kevin T. M. Johnson and Henry J. B. Dick

In-situ ion-microprobe analysis of trace and rare earth elements in discrete diopsides in abyssal peridotites from 9 transform dredge hauls from the Atlantis II Fracture Zone (AII F.Z.) shows that these samples have a wide range of trace element contents close to the total range found for the entire SW Indian Ridge. Though the spread in analyses is large, the average composition of the peridotites is close to that reported for the AII FZ by Johnson et al. [1990] and lies at the relatively undepleted end of the spectrum for SW Indian Ridge residual mantle peridotites. A sharp break in peridotite diopside composition and modal mineralogy occurs across the transform, suggesting that it acts as a boundary for different melting regimes and initial mantle compositions. The difference in peridotite compositions is mirrored in spatially associated basalts, which lie on separate parallel liquidus trends in the normative ternary px-ol-pg. Basalts from the east side of the transform have higher normative plagioclase contents, indicating that they may be products of lower degrees of mantle melting than basalts from the western side, consistent with composition. Basalts from the eastern wall also have consistently lower Fe_{8.0} and higher Na_{8.0} than basalts from the western wall, and lie parallel to the global along-ridge FE_{8.0} - Na_{8.0} trend [Klein and Langmuir, 1987] and orthogonal to the local melting paths of Klein and Langmuir [1989].

Our data provide strong evidence for segmentation of the melting regime, with major mantle discontinuities occurring at transform offsets at slow-spreading ridges. Peridotites analyzed along the eastern wall of the fracture zone also show a systematic change in composition with latitude, and with the older peridotites from the median tectonic ridge, define a systematic change in the degree of melting of the mantle occurring beneath the paleoridge axis over the last 11 My. Emplacement of mantle showing the lowest degree of melting, or the least depleted parental mantle composition, corresponds roughly to the time of crystallization of ODP Site 735B gabbros. Melting is modeled as a non steady-state, discontinuous process with 0.1-0.5 volume% aggregated melt retained in the porous residue. The range in degree of it open system melting for the combined suite of AII F.Z. peridotites is

8-20%. Such a large systematic variation would appear to require a dynamically significant change with time, either in the initial temperature and/or a large compositional difference of the mantle beneath the paleoridge axis. This in turn suggests that in the relative reference frame of the ridge axis, mantle flow was non steady-state. This could reflect episodic mantle diapirism beneath the ridge axis, or, alternatively, that the ridge axis has moved over a zone of enhanced upflow in the underlying mantle that was fixed in the absolute hotspot mantle reference frame.

In Press: Journal of Geophysical Research.

Supported by: NSF Grant DPP87-20002, OCE86-08143, and OCE82-18905.

WHOI Contribution No. 7905.

SEDIMENTOLOGY

SEDIMENT TRAP INTERCOMPARISON EXPERIMENT IN THE PANAMA BASIN, 1979

Susumu Honjo, Derek W. Spencer and Wilford D. Gardner

In order to compare the collection efficiency of settling particles among sediment traps in a variety of design concepts, 28 sediment traps of 11 different designs were deployed at 6 depths ranging from 665 m to 3.769 m along 5 rigid moorings anchored in a sill-protected marginal basin about 3,865 m deep for about 4 months from August to November 1979. The traps represented three basic designs: (1) cylinders with the aspect ratio between 2 and 3, (2) funnels with a large opening covered by a baffle with a small grid, and (3) open boxes whose opening was covered by a baffle. All but two of these types of participating traps had a mechanism to isolate the collected sample. Monitoring instruments indicate that all moorings provided a stable platform throughout the duration of Sediment Trap Intercomparison Experiment (STIE) with relatively low current velocity at the middle layers and very low velocity at the deep layers. Total mass flux, fluxes of three size fractions after water sieving, carbonate, combustible and noncombustible fractions, organic carbon, nitrogen and other sedimentary constituents in the individual samples were determined and evaluated with regard to the relative consistency in terms of depth and statistical tests on the similarity of the constituents.

Under the conditions tested, the trapping efficiency of settling particles between a large

funnel trap with baffle and an intermediate-sized cylinder trap was nearly identical considering the laboratory analytical errors. This conclusion might be extended to cylinder traps with diameters as small as 7 cm and a large aspect ratio when deployed rigidly in a low energy ocean environment. A funnel-type trap with a more effective baffle had a higher collecting efficiency than the other traps. Because of mechanical problems, comparison of the box-type traps to the other types was inconclusive.

Published in: Deep-Sea Research, 39(2):333-358, 1992.

Supported by: NSF Grants OCE77-14363 and OCE79-16687.

WHOI Contribution No. 7630.

DEPARTMENT OF PHYSICAL OCEANOGRAPHY

James Luyten, Chairman

OCEAN CIRCULATION & LOW FREQUENCY VARIABILITY

FORMATION OF TAYLOR CAPS OVER A TALL ISOLATED SEAMOUNT IN A STRATIFIED OCEAN

David C. Chapman and Dale B. Haidvogel

A primitive-equation numerical model is used to examine various aspects of the formation of Taylor caps over a tall isolated seamount in a steady, rotating, frictionless, stratified flow. The flow is characterized by three nondimensional parameters: the Rossby number, Ro = U/fL; the Burger number, S = NH/fL; and the fractional seamount height, $\delta = h_m/H$. Here U is the uniform inflow velocity, f the Core lis parameter, L the horizontal length scale of the seamount, N the initial buoyancy frequency, H the deep-ocean depth away from the seamount, and h_m the maximum height of the seamount above the otherwise flat bottom.

For both unstratified (S=0) and stratified (S=1) flows over a tall seamount which ultimately form a Taylor cap, the initial response is similar to that found in previous studies which considered short seamounts δ ll1) in weakly nonlinear flows $(Ro \ll 1)$. Two eddies form over the seamount and co-rotate clockwise around the seamount until one is swept away with the imposed inflow, leaving the other eddy trapped over the seamount to form a Taylor cap. The resulting steady flow is asymmetric with substantially enhanced velocities on the left side of the seamount (looking downstream).

For steady, unstratified flows (S=0) over tall seamounts, Taylor caps occur only for weaker inflows (smaller Rossby numbers) than would be predicted from quasi-geostrophic (QC) theory. This is consistent with the generation of large vertical velocities by the compression and stretching of fluid columns passing over the tall seamounts, in clear violation of the assumption of QC theory.

Taylor caps in steady, stratified flows (S=1) are bottom-trapped with size and shape which are sensitive to the strength of the inflow as well as the stratification. The vertical excursions of water parcels are greatly reduced compared with unstratified flows. Over short seamounts $(\delta < 0.4)$, the transition from a flow with a Taylor cap to one without a Taylor cap occurs at slightly smaller Rossby numbers than would be predicted by QC theory. Over taller seamounts $(\delta > 0.4)$, internal lee waves are generated which largely destroy the fluid trapping of the Taylor cap, producing some flows in which water parcels are temporarily trapped over the seamount before being swept

away by the imposed inflow. This temporary trapping occurs only over mid-size seamounts $(0.4 < \delta < 0.7)$ within a range of moderately strong inflows (0.1 < Ro < 0.2) and does not occur at all over tall seamounts $(\delta > 0.7)$. For seamounts which are taller than $\delta \approx 0.4$, true Taylor caps (i.e. permanent trapping of water parcels) occur only with rather weak inflows (Ro < 0.15).

In Press: Geophysical & Astrophysical Fluid Dynamics.

Supported by: ONR Contract N00014-89-J-1106. WHOI Contribution No. 7761.

VARIATION OF THE WESTERN EQUATORIAL PACIFIC OCEAN, 1986-1988

Thierry Delcroix, Gérard Eldin, Marie-Hélène Radenac, John Toole and Eric Firing

Twenty-one oceanographic sections made along 165°E during 1984-1988 provide a unique picture of the 1986-1987 El Niño and the subsequent La Niña in the western equatorial Pacific. The mean of 6 cruises from January 1984 through June 1986, a relatively normal period, provides a reference with which the later sections are compared. The net warm water transport across 165°E within 10° of the equator was small in this mean reference section: $7 \times 10^6 m^3 s^{-1}$, and the 1986-1987 El Niño was underway. During the following two years the net transport varied widely and rapidly; the extreme were $56 \times 10^6 m^3 s^{-1}$ to the east and $58 \times 10^6 m^3 s^{-1}$ to the west. Changes in the stratification along 165°E were correspondingly large, reflecting both the geostropic balance of the strong zonal currents and the changes in the volume of warm water in the western equatorial Pacific. The anomaly of warm water volume corresponded closely to the time-integral of the warm water transport across 165°E. Local wind forcing and remotely forced waves were both important causes of the transport fluctuations. Winds, precipitation, and currents were all important factors determining the depth of the surface mixed layer and the thickness of the underlying barrier layer. The way in which these factors interact is a strong function of latitude, however.

In Press: Journal of Geophysical Research.

Supported by: NOAA Grant NA85AA-D-AC117.

WHOI Contribution No. 7747.

ADVECTION AND DIFFUSION ESTIMATES IN A THERMOHALINE STAIRCASE REGION

Joyce M. Federiuk and Raymond W. Schmitt

A thermohaline staircase consisting of a series of well mixed layers approximately 30 m thick is found at depths of 300-500 m in a region of the tropical North Atlantic spanning 48° to 58° W, 8° to 17°N. Density ratios $(R\rho \equiv \alpha T_z \beta S_z)$ of 1.6 and below and horizontal property changes within the layers indicate a double diffusive origin for the structure (Schmitt et al., 1987). In this study, property changes on isopycnal surfaces are mapped from two hydrographic surveys of the area. The general north-south gradients in temperature and salinity are modulated by considerable mesoscale variability. The geostrophic velocity field is dominated by the eddies. An inverse model was constructed in density coordinates in order to seek bounds on the cross-isopycnal mixing in the region. However, the eddy variability prevents a significant determination of the vertical mixing rate, indicating that the steady state assumption is violated. There is clearly a need to develop an understanding of how the stairc se layers maintain coherence in the presence of cach variability.

Submitted to: Deep-S a ' search.

Supported by: NSF Grants OCE84-09323 and OCE88-13060.

WHOI Contribution No. 7627.

DOWNSTREAM DEVELOPMENT OF THE GULF STREAM FROM 68° TO 55°W

Melinda M. Hall and Nicholas P. Fofonoff

Two CTD sections across the Gulf Stream at 68° and 55° W were acquired in late March of 1988 within 11 days of one another as part of an effort to look at downstream changes in the current. Using complementary current meter measurements, we construct sections of total (geostrophic + barotropic) velocity, and use them to calculate transport in potential density classes. Potential vorticity sections are presented for both locations, including the effects of planetary, stretching and relative vorticity. The data are also used to examine the core properties of recently formed 18° Water at the two sections. We find that: 1) water parcels in the exposed surface layers experience downstream density and potential vorticity changes consistent with surface forcing; 2) thermocline Gulf Stream transport is conserved downstream, and below the exposed layers is

conserved within individual density classes; 3) sub-thermocline Gulf Stream transport increases modestly at levels above the sill depth of the New England Seamounts but quadruples at levels below that; 4) the calculated potential vorticity structure is consistent with the transport distribution and historical observations, and displays several distinct layers; and 5) transport and potential vorticity distributions together suggest that five active layers and steep bottom topography are required to fully describe downstream evolution of the Gulf Stream as an open ocean eastward jet.

Submitted to: Journal of Physical Oceanography.

Supported by: ONR Contracts N00014-87-K-0001, NR083-004, N00014-88-K-0612 and N00014-89-J-1056.

WHOI Contribution No. 7789.

ON THE TRANSPORT OF THE GULF STREAM BETWEEN CAPE HATTERAS AND THE GRAND BANKS

Nelson G. Hogg

Direct velocity observations from four locations in the Gulf Stream between Cape Hatteras and the Grand Banks are analyzed to determine the baroclinic and barotropic transport of the Stream. Three of the sites are moored arrays where a method similar to that proposed by Hall and Bryden (1985) and Hall (1986) is used; the fourth is the Pegasus site of Halkin and Rossby (1985). The baroclinic transport is found to change little from site to site while the barotropic changes substantially. Total transport reaches 150 Sv at 60°W and remains at that strength to 55°W, the furthest east that we have moored information. These results, augmented by additional information, are used to deduce a scheme for the total transport streamfunction in the western North Atlantic.

In Press: Deep-Sea Research.

Supported by: NSF Grant OCE86-08258; ONR Contracts NR083-004 and N00014-85-C-0001.

WHOI Contribution No. 7663.

A TWO-LAYER MODEL FOR THE WIND AND BUOYANCY FORCED CIRCULATION

Rui Xin Huang

The classic theory of deep circulation by Stommel and Arons (1960) is extended to a two-moving layer model. Instead of specifying the upwelling velocity, the model shows very strong upwelling along the southern and eastern boundaries, while the upwelling in the interior ocean is much smaller. With a medium size of Ekman pumping, the basin is separated into different regions by critical characteristics originated from the Rossby repellor. It is shown that across this boundary temperature and velocity are continuous, but this boundary is a vorticity (or some higher-order discontinuity) front.

Submitted to: Journal of Physical Oceanography.

Supported by: NSF Grant OCE90-17158; and ONR Contract N00014-90-J-1518.

WHOI Contribution No. 7771.

INTERMEDIATE WATER FORMATION IN A 5 × 3 BOX MODEL

Rui Xin Huang

A 5 x 3 box pole-pole ocean model is formulated to illustrate the dynamic importance of fresh water flux in the thermohaline circulation. The model is forced with symmetric thermal forcing and fresh water forcing. Two canonical patterns of fresh water flux have been studied. In case A, strong evaporation at low latitude balances precipitation at high latitude. For medium precipitation/evaporation, the system appears in an asymmetric mode with the meridional circulation totally reversed in one hemisphere and slightly intensified in the other hemisphere. This case mimics the familiar thermohaline catastrophe discussed in many previous numerical experiments based on OGCM. In case B, a fresh water flux pattern based on observations (Schmitt et al., 1989) is used, which is characterized by strong evaporation at mid-latitude and precipitation at poles and the equator. For medium precipitation and evaporation, the system appears in an intermediate mode characterized by intensive intermediate water formation at mid-latitude and extremely slow abyssal circulation in one hemisphere. As a partial compensation, the thermohaline circulation in the other hemisphere is slightly intensified. The intensification of intermediate water formation resembles the glacial circulation pattern in the North Atlantic, as inferred from paleocirculation studies.

Submitted to: Journal of Physical Oceanography.

Supported by: ONR Contract N00014-90-J-1518; and NSF Grant OCE90-17158.

WHOI Contribution No. 7820.

MULTIPLE STATES IN A BOX MODEL OF AN ICE-COVERED OCEAN

Rui Xin Huang

A two-box ocean with ice is formulated in order to understand the dynamic role of sea ice in ocean circulation and climate. In a steady state, there is a balance between radiation and heat transfer. There are three possible states, ice-free, partially ice-covered, and completely ice-covered. All these states are stable to small perturbations. The most important result of the model is that the partially ice-covered state is associated with large meridional temperature gradient and strong meridional circulation and poleward heat flux.

Submitted to: Journal of Physical Oceanography.

Supported by: ONR Contract N00014-90-J-1518; and NSF Grant OCE90-17158.

WHOI Contribution No. 7628.

SUBDUCTION RATE DEFINED AS AN INTEGRAL QUANTITY

Rui Xin Huang

In the oceans, seasonal cycles have important effects on the subduction rate. The subduction rate is a non-local property of the circulation; its proper definition involves averaging over one year of time and trajectory. Subduction rate can be defined by the Eulerian mean or the Lagrangian mean. Two simple examples, one for the northern half of a subtropical gyre and one for a front, show the application of these two definitions of the subduction rate.

Submitted to: Journal of Physical Oceanography.

Supported by: ONR Contract N00014-90-J-1518; and NSF Grant OCE88-08076.

WHOI Contribution No. 7629.

TEMPORAL AND SPATIAL VARIABILITY OF VOLUME TRANSPORT OF THE IN KUROSHIO IN THE EAST CHINA SEA

Hiroshi Ichikawa and Robert C. Beardsley

The temporal and spatial variability of absolute geostrophic volume transport of the Kuroshio in the East China Sea are examined using hydrographic and surface current data collected by the Japan Meteorological Agency on several cross-stream transects during the three-year period 1986-1988. The discrete surface

currents reported are used as the reference velocity in the computation of absolute geostrophic velocity. The volume transport of the Kuroshio (KVT) is then estimated by integration of the downstream (positive) part of the absolute geostrophic velocity through each transect. To further describe the structure of the transport, KVT is decomposed into barotropic (BTKVT) and baroclinic (BCKVT) components, and the contribution of each to KVT is examined. The accuracy of the individual velocity and transport computation is most dependent on the horizontal spacing between consecutive hydrographic and surface current stations in the Kuroshio strong current region. A detailed examination of one well-sampled transect allows classification of the different sampling patterns into three categories: good (with hydrographic and surface current station spacing less than 30 km and 15 km, respectively), intermediate, and poor with corresponding uncertainties of 3, 7, and 10-15 Sv $(1 \text{ Sv} = 10^6 \text{ m}^3 \text{s}^{-2})$. Of the 39 transport sections obtained, 23 were classified good, no intermediate, and 16 poor.

Our analysis of these transport sections made at six transects in the East China Sea and one transect just outside the East China Sea over 1986-1988 indicate that the barotropic contribution to the mean and fluctuating KVT is much larger than the baroclinic contribution in the East China Sea. On average, about 75% of KVT is due to BTKVT inside the East China Sea. While KVT exhibits significant small space and time scale variability with periods of 8-32 days and wavelengths of 150-375 km, presumably associated with the downstream propagation of frontal eddies and meanders at 8-19 km day⁻¹, the mean KVT within the East China Sea is spatially uniform but varies seasonally (KVT large in summer having positive correlation with local downstream wind stress similar to the Florida Current) and on longer time scales (KVT large during large meander events of the Kuroshio south of Japan). Our best estimate of the mean KVT in the East China Sea during 1986-1988 is 23.3 Sv \pm 1.9 Sv. This represents about one half of the mean interior Sverdrup transport at this latitude. The Kuroshio quickly absorbs most of the remaining interior Sverdrup transport as it exists the East China Sea through the Tokara Strait.

In Press: Deep-Sea Research.

Supported by: NSF Grants OCE87-16937 and OCE87-13988.

WHOI Contribution No. 7636.

THERMOHALINE CATASTROPHE IN A SIMPLE FOUR BOX MODEL OF THE OCEAN CLIMATE

Terrence M. Joyce

A four box model of the ocean is examined in which a surface and deep layer of equal thickness and large volume are connected to two polar reservoirs of smaller volume. While the four reservoirs are thoroughly mixed, there is no significant mixing between them; exchange is due to flow between reservoirs with the flow out of or into the polar reservoirs driven by pressure gradients. Newtonian boundary conditions are imposed on the temperature and salinity of the surface layer and the two polar reservoirs; the deep water is forced only by flows into it from other boxes. The temperature and salinity forcing is applied with a different time scale for each variable. When the time scales are nearly equal, the system responds as a simple component fluid with a single solution for each forcing. When the salinity time scale is long compared with temperature, up to four multiple equilibria can be present for a given forcing. These equilibria are unstable to finite amplitude perturbations and numerical solutions exhibit catastrophic transitions from one mode to another. When the deep water formation is totally inhibited as a result of a transition, the system can go into a long-term climatic oscillation, quasi-periodic in nature. The system possesses four "attractors" corresponding to deepwater formation in either, both, or neither of the two polar reservoirs.

Published in: Journal of Geophysical Research, 96(C11):20,393-20,402, 1991.

Supported by: NSF Grant OCE89-9908.

WHOI Contribution No. 7724.

LAGRANGIAN FLOW OBSERVATIONS IN THE EAST CHINA, YELLOW AND JAPAN SEAS

Richard Limeburner, Kuh Kim, Robert C. Beardsley and Julio Candela

Satellite-tracked drifters with drogues centered at 10 and 40 m were deployed in the Yellow and East China Seas in January and July 1986. Two drifters launched in January returned useful data for about 60 days. Both drifters exhibited weak mean velocities of 2-3 cm/s but larger subtidal variability (eddy kinetic energy 31-35 cm²/s²). All ten drifters launched in July returned useful data for at least 90 days. The resulting trajectories of five drifters deployed in the Yellow Sea describe a

weak basin-scale cyclonic gyre in the surface waters of the Yellow Sea in late summer. The center of the gyre was located near 35.6°N, 123.8°E, and the mean velocities along the Korean and Chinese coasts varied from 2 to 6 cm/s. Within the Yellow Sea, the distribution of eddy kinetic energy was relatively uniform spatially at 30-50 cm²/s² except with an increase to about 80 cm²/s² near the Korean coast and higher near the southeast entrance of the Yellow Sea. Drifter trajectories in the East China Sea describe a strong inflow of Kuroshio and shelf water in late summer into the Tsushima Strait through both western and eastern channels. While two drifters continued to move slowly southeastward along the Chinese coast, no drifters entered the Yellow Sea, suggesting that the Yellow Sea Warm Current may not be a coherent and continuous current in summer. The mean eddy kinetic energy in the East China Sea was 112 \pm 43 cm²/s². Three drifters entered the Japan Sea and followed quite different paths, suggesting that the Tsushima Current may not simply split into several semi-permanent branches as it leaves the Tsushima Strait. One drifter entered a cyclonic mesoscale eddy near 37°N, 133°E and made three complete loops with a mean speed and radius of 26 ± 14 cm/s and 35 ± 14 km before exiting. The mean eddy kinetic energy in the Japan Sea west of 138° E was 415 ± 91 cm²/s². One drifter was deployed in the Oshumi branch of the Kuroshio and carried eastward in the Kuroshio and Kuroshio Extension to about 160°E before drifting to the south in the recirculation. While in the Kuroshio and Kuroshio Extension, the drifter had a mean and eddy kinetic energy of 0.29 and 0.38 m^2/s^2 .

Submitted to: Proceedings of IV JECSS Workshop.

Supported by: NSF Grants OCE85-01366, OCE86-16937, OCE87-13988, OCE91-01034; and the Korean Science and Engineering Foundation.

WHOI Contribution No. 7908.

A NOTE ON THE INTER-GYRE MASS **EXCHANGE DUE TO MIGRATING** WIND

Zhengyu Liu

The effect of the meridional migration of the wind field on the interior Sverdrup flow is examined near the boundary between a subtropic gyre and a subpolar gyre. An idealized model ocean is used which has a flat bottom. For annual wind variation with realistic magnitude, the cross-gyre Lagrangian mass flux in the model ocean can reach more than one-tenth of the total Sverdrup transport. The maximum northward penetration occurs for those particles that leave the western boundary at the autumnal equinox while the opposite occurs at the spring equinox.

Submitted to: Dynamics of Atmospheres and Oceans.

Supported by: NSF Grant ATM84-13515.

WHOI Contribution No. 7883.

A NOTE ON THE FEEDBACK OF THE RHINES-YOUNG POOL ON THE VENTILATED THERMOCLINE

Zhengyu Liu, Joseph Pedlosky, David Marshall and Torsten Warncke

The model developed by Pedlosky and Young (1983) is used to investigate the feedback of a Rhines-Young pool on a ventilated thermocline. It is found that the potential vorticity gradient in a ventilated layer is reduced due to the nonlinear coupling with a deep Rhine-Young pool. Physically, this occurs because part of the Sverdrup transport is carried by the deep pool. As a result, the subduction velocity and in turn the potential vorticity gradient of the subducted water is decreased.

Submitted to: Journal of Physical Oceanography.

NSF Grant ATM 89-03890. Supported by:

WHOI Contribution No. 7816.

VARIETY OF CONVECTIVE FLOW PATTERNS INDUCED BY THE SURFACE THERMAL FORCING OF A BOX MODEL

James R. Luyten and Henry M. Stommel

Natural large scale thermal and wind-driven convective patterns in the ocean exhibit a wide range of patterns, partly controlled by the form of surface forcing and partly the nonlinearity of the dynamical and heat advection equations. By stripping down the dynamics to hydrostatic laminar linear body friction and eliminating rotation a model is obtained whose only remaining nonlinearity is in the advection of buoyancy. It is thus possible to see how much of the family of bifurcating solutions obtained is understandable in terms of this one form of nonlinearity.

Submitted to: Proceedings of the Royal Society of London.

Supported by: NSF Grant OCE89-13128; ONR Contracts N00014-90-J-1508 and N00014-90-J-1425.

WHOI Contribution No. 7824.

RECIRCULATING COMPONENTS TO THE DEEP BOUNDARY CURRENT OF THE NORTHERN NORTH ATLANTIC

Michael S. McCartney

The meridional overturning system of the North Atlantic transports warm water ($\geq 4^{\circ}$ C) to subpolar latitudes and returns cold water to subtropical latitudes. The main sources of this cold water are the dense overflows from the subpolar seas and the less dense Labrador Sea Water (LSW) from the subpolar basin. The subpolar seas and the subpolar basin are separated by a system of islands and submarine ridges, south of which a deep northern boundary current (DNBC) is found flowing from east to west and conveying the dense overflows to the Labrador Basin. Joined there by the LSW, the DNBC continues as a deep western boundary current (DWBC) carrying the cold waters to low latitude. Entrainment of warm waters into the overflows warms them and increases the transport of the DNBC. Published transport estimates are larger than can be explained by warm entrainment alone and water mass considerations suggest that cold entrainment components are also involved. This paper discusses three such components, all of which can be thought of as recirculating components of the cold water system, since they involve eastward and northward transport in the subpolar basin interior in opposition to the DNBC and DWBC. LSW participates in the subpolar gyre and conflows to the DNBC in the central and eastern parts of the basin. Along the westward flow of the DNBC some of the LSW is entrained into the denser overflows, while some returns to the Labrador Basin relatively unaltered. Either way, both are recirculations because the deep western boundary current transports are larger by the amount of northward transport of LSW in the interior of the basin. The other two cold entrainment components begin with the northward transport of cold bottom water and lower deep water at mid-latitudes with relatively low oxygen and high silicate. In the eastern basin an eastern intensified flow conveys these waters from the Madeira Basin through the Iberian Basin to the West European Basin. There, northern intensified westward flow past the Rockall Trough and Rockall Plateau marks the true beginning of the DNBC, which loops north into the Iceland Basin to be joined by the Faroe Bank Channel and Iceland Faroe Ridge overflows, and thence passes through the Charlie-Gibbs Fracture Zone (CGFZ) to the Labrador and Irminger Basins. The flow from mid-latitudes in the western basin is difficult to isolate due to the presence of strong deep recirculating gyres in the Newfoundland and Labrador Basins. The

northward throughput of the mid-latitude waters here is recognized extending northwards by a deep silicate maximum extending northwards through these gyres. This higher silicate influence is seen recirculating southward in the DWBC in the Newfoundland and Labrador Basins. This presence and the regional distribution of shear imply a recirculating component to the transport. The northward extending high-silicate influence reaches the Irminger Basin, to influence the evolution of the DNBC. Here an ambiguity exists for this layer could come either from continued northward flow from the mid-latitude western basin, or from the westward flow through the CGFZ (and thus ultimately from to the mid-latitude eastern basin). Either way these are the only sources for low oxygen and high-silicate water for the DNBC. Estimates of the volume transports of the various recirculating components suggest they carry to the deep boundary current a transport roughly equal to that of the northern cold water sources.

Submitted to: Progress in Oceanography.

Supported by: NSF Grants OCE80-15789, OCE78-22223 and OCE86-14486.

WHOI Contribution No. 7818.

DIURNAL TIDES NEAR THE YERMAK PLATEAU

Laurie Padman, Albert J. Plueddemann, Robin D. Muench and Rob Pinkel

A review of moored and drifting current measurements made over the last decade in the vicinity of the Yermak Plateau confirms the early impression that the plateau is a region of enhanced tidal-band variability. Of particular interest are observations from two recent oceanographic programs where drifting platforms have traversed the plateau slope. The increase in tidal current amplitudes is clearly related to the topography of the plateau, but temporal variability due to spring/neap cycling complicates interpretation of short data records from these drifting platforms. Previous studies have modelled the diurnal tide as a near-resonant barotropic shelf wave forced at the perimeter of an axisymmetric submarine plateau. Despite the fact that these models predict reasonable tidal current amplification, we show that the variability of topography around the actual plateau leads to large variations in the dispersion characteristics of diurnally-forced topographic waves, invalidating the assumption of axisymmetry. In particular, there are regions where a free diurnal topographic wave cannot exist at all, blocking the flux of energy around the plateau. An alternate model is one were the tide is considered to have the characteristics of a

barotropic shelf wave on a long, straight escarpment. Certain predictions of this model, such as the cross-shelf variation of tidal ellipse magnitude, orientation, and ellipticity, are found to be in agreement with the available data. The topographic enhancement of the diurnal tide near the plateau is an important process which effects the hydrography and general circulation of the region. For example, the stress divergence applied by the tidal currents to the ice base greatly exceeds the typical contribution from the surface wind, the tide appears to be responsible for the generation of high-frequency internal wave packets which result in energetic mixing patches in the thermocline, and rectification of the tidal currents may result in a mean current transporting Atlantic water along the plateau slope.

Submitted to: Journal of Geophysical Research.

Supported by: ONR Contracts N00014-90-J-1359 and N00014-84-C-0134.

WHOI Contribution No. 7732.

ON THE BAROCLINIC STRUCTURE OF THE ABYSSAL CIRCULATION

Joseph Pedlosky

A simple baroclinic model of the abyssal ocean circulation is formulated in which the reversals of the meridional velocity with depth and hence the layering of the abyss is explained by the longitudinal variation of upwelling into the main thermocline.

Since the barotropic meridional velocity is connected to the local upwelling velocity by the Sverdrup relation, regions of weak upwelling have meridional velocity fields which are essentially baroclinic. The baroclinic velocities are driven by thermal anomalies which propagate westward by stationary diffusive Rossby waves from regions of relatively strong upwelling in the eastern portion of the basin. These dynamically driven, internally generated vertical velocities produce the layered baroclinic structure in the western interior of the basin. A simple linear model, continuous in the vertical, is developed to illustrate these elements of the conceptual picture.

In Press: Journal of Physical Oceanography.

Supported by: NSF Grant ATM89-03890.

WHOI Contribution No. 7795.

GULF STREAM MEANDERS OVER STEEP TOPOGRAPHY AT CAPE HATTERAS

Robert S. Pickart and D. Randolph Watts

Observations of the Gulf Stream thermocline as it meanders over the continental slope off Cape Hatteras are presented. Daily vertical sections of temperature and geostrophic velocity to 1500 m are calculated from an array of inverted echo sounders aligned across the Gulf Stream. These accompany time series of deep currents from a corresponding array of bottom current meters. The vertical sections are computed using a previously derived technique which assumes the Gulf Stream variability is primarily first baroclinic mode. The sections reveal that the Gulf Stream front systematically shoals when it meanders offshore, an effect which is not observed farther downstream. This is accompanied by a compression of the main thermocline which in turn increases the core velocity of the jet but has little effect on overall transport. To explain the shoaling the Gulf Stream is treated as a two-layer system; the lower layer vorticity balance suggests that the shoaling is caused by deep water columns preserving their layer thickness in the presence of the steep topography.

Submitted to: Journal of Geophysical Research.

Supported by: ONR Contract N00014-87-K-0235.

WHOI Contribution No. 7677.

INTERNAL WAVE OBSERVATIONS FROM THE ARCTIC ENVIRONMENTAL DRIFTING BUOY

Albert J. Plueddemann

A free-drifting buoy serving as an ice anchor and flotation sphere for a 125 m instrumented mooring line was deployed in the Arctic pack ice by the R.V. Polarstern in August of 1987 at the northernmost point achieved by the Arktis IV expedition. Current measurements were made from this Arctic Environmental Drifting Buoy (AEDB) using a 150 kHz Acoustic Doppler Current Meter (ADCM) attached to the mooring line at a depth of 16 m below the floatation sphere with the transducers facing downwards. Velocity profiles spanning depths between 36 and 348 m with 16 m resolution were collected at half-hour intervals over a period of 216 days while the buoy drifted from its starting point near 86°N, 22°E to 70°N, 16°W. The full experimental record was separated into three sections corresponding to periods of the drift spent in the Nansen Basin.

over the Yermak Plateau, and in the Greenland Sea. Velocity time series and spectra were computed and results for the three analysis sections were compared. Spectra in the Nansen Basin were found to have energy levels significantly less than those typical for mid-latitudes, roughly a factor of 1/5 less than the canonical Garrett-Munk (GM) level, and a spectral slope between f and 2.5 f that was significantly flatter than that expected from the GM model. Between 83°N and 81°N, as the buoy passed over the Yermak Plateau, internal wave energy increased to levels comparable to GM. Isolated, energetic near-inertial wave packets with upward group velocity were observed in this portion of the record, presumably generated by interaction of the barotropic tide with the bottom topography of the plateau.

Submitted to: Journal of Geophysical Research.

Supported by: ONR Contracts N00014-90-J-1359 and N00014-84-C-0134.

WHOI Contribution No. 7819.

INTERANNUAL VARIABILITY IN THE MID- AND LOW-LATITUDE WESTERN NORTH PACIFIC

Bo Qiu and Terrence M. Joyce

Twenty-two years (1967-88) of hydrographic data collected by the Japan Meteorological Agency along the meridian 137°E and surface wind data compiled by FSU were analyzed to study the interannual variability in the western North Pacific.

In the mid-latitude region north of 22°N, the dominant signal in the dynamic height field was the interannual path variations of the Kuroshio. Analysis of the 39 cruises revealed that whereas the eastward transport of the Kuroshio itself had no significant changes between the straight path and meander path years, the net transport of the Kuroshio system including the recirculation showed a 30% increase during the meander path years. In the straight path years when the net upstream Kuroshio transport was small, intensification of the Kuroshio recirculation south of Japan tended to inflate the eastward transport of the Kuroshio there. The interannual path variations of the Kuroshio strongly influence the water mass movement in the mid-latitude. During the Kuroshio meander years, we found that a significant portion of the North Pacific Intermediate Water east of the Kuroshio meander was blocked from subducting further westward. In the mid-depth layer of 1500-2500 m, analysis of the $\theta - S$ relation revealed a water mass movement negatively correlated to the upper layer Kuroshio path changes, implying a possible compensating

flow in the mid-depth layer for the cold-core eddy emerging north of the Kuroshio.

In the low-latitude region along the 137°E, fluctuations in the surface height anomaly field had a meridionally-coherent structure and large surface height drops concurred with the ENSO events in the tropical Pacific. Accompanying the surface height drops in the ENSO years was an increase in the transport of both the North Equatorial Current (NEC) the North Equatorial Countercurrent (NECC) and a southward shift in the boundary of the NEC and NECC. Based on the FSU surface wind data, these interannual fluctuations of the NEC and NECC were well correlated to the Sverdrup transport fluctuations estimated from the basin-scale wind stress curl field. Using a reduced gravity model and simplified patterns of wind forcing, we showed that this good correlation was because the center of the interannual signal of the wind stress curl field is close to the western Pacific (near the date line) and because the thermocline tilt in the NEC region attenuates the strong latitude-dependency of the long baroclinic Rossby wave.

In Press: Journal of Physical Oceanography.

Supported by: NSF Grants OCE89-07815 and OCE89-9908.

WHOI Contribution No. 7829.

MEAN FLOW AND VARIABILITY IN THE KUROSHIO EXTENSION FROM GEOSAT ALTIMETRY DATA

Bo Qiu, Kathryn A. Kelly and Terrence M. Joyce

Using altimeter data from the Geosat Exact Repeat Mission (ERM), we investigated the mean flow and temporal and spatial variations of the Kuroshio Extension in the region of 140°-180°E and 30°-40°N. Mean surface height profiles were estimated along individual tracks by assuming the velocity profile of the Kuroshio Extension to be Gaussian-shaped and by successively fitting this synthetic current's height profile to the residual height data. Using the mean profiles from ascending and descending tracks, we derived the mean surface height field by an inverse method and obtained the absolute surface height fields for the first 2.5 years of Geosat ERM. Both the mean and the instantaneous height fields thus derived compared well with the available hydrographic data and the SST patterns from the NOAA satellites. The mean surface height difference across the Kuroshio Extension attains its maximum around 146°E between the two quasi-stationary meanders, and its decrease thereafter is mainly due to large-scale recirculations on the southern side of the Kuroshio Extension. The ratio of the eddy kinetic energy over the mean kinetic energy has a nearly constant value of 1.5-2.0 along the Kuroshio Extension path. Propagation of mesoscale fluctuations in the height fields is generally westward except for the upstream region of the Kuroshio Extension. Effects of deep mean flow and baroclinic shear are found to be important in explaining the observed propagation speeds. In the upstream region of 141°E and 154°E, annual variations in the surface height difference across the Kuroshio Extension (δh) have a September maximum with an average amplitude of 0.2 m. For large-scale interannual fluctuations, anomalies in δh are found to be significantly correlated with those of the current axis positions: a larger surface height difference corresponds to a more northerly position of the Kuroshio Extension. The interannual changes in δh are possibly related to the 86/87 ENSO event in the low-latitude Pacific Ocean.

Published in: Journal of Geophysical Research, 96(C10):18,491-18,507, 1991.

Supported by: NASA Contract NAGW-1666; and NSF Grant OCE89-9908.

WHOI Contribution No. 7649.

VELOCITY AND EDDY KINETIC ENERGY OF THE GULF STREAM SYSTEM FROM 700 M SOFAR FLOATS SUBSAMPLED TO SIMULATE POP-UP FLOATS

Philip L. Richardson

Velocity and eddy kinetic energy were calculated from SOFAR float trajectories using original daily values and values subsampled at intervals of 15, 30, and 60 days to simulate pop-up floats that surface for position-fixing at these time intervals. The mean velocity is well reproduced by the 15-day subsampled data. With the 30-day data the peak velocity in the Gulf Stream is reduced and its width increased substantially. With the 60-day data the Stream is highly modified and its southern flanking countercurrent is no longer resolved. Calculated eddy kinetic energy is strongly diminished by subsampling; peak energy in the Stream of 710 cm²/sec² using daily values is reduced to 64 cm²/sec² using 60-day data. Calculated energy in the Sargasso Sea near 25N 60W is reduced from 20 cm²/sec² to 8 cm²/sec² The larger percent decrease of calculated energy in the vicinity of the Stream, 30N-40N, is due to energetic higher-frequency eddy motion in this area.

In Press: Journal of Atmospheric and Oceanic Technology.

Supported by: NSF Grant OCE89-16082. WHOI Contribution No. 7748.

DIRECT OBSERVATIONS OF NUTRIENT FLUXES AT 24°N IN THE PACIFIC OCEAN

Paul E. Robbins and Harry L. Bryden

Large scale biogeochemical cycles are investigated by calculating nutrient transports across a transpacific hydrographic section at 24°N. The net advective flux of inorganic phosphate, nitrate and silicate is indistinguishable from zero but examining the horizontal and vertical structure of the transport yields conclusive results. Southward nutrient transport carried by the zonally averaged vertically overturning meridional circulation balances northward transport by the horizontal anticyclonic gyre in the upper water. Measurements of the silicate cycle are sensitively dependent upon estimates of the wind-driven Ekman transport. The divergence of the measured flux below 3800 dbar provides estimates of organic respiration in the deep ocean. Lack of deep water ventilations allows average Oxygen Utilization Rate (OUR) below 3800 dbar to be determined as $1.4 \pm 0.5 \mu/1/yr$. Downward carbon flux at 3800 dbar is estimated to be 0.10 ± 0.02 mol C/m²/yr. Redfield ratios calculated from observed nutrient flux ratios at depth are in good agreement with those determined by other methods.

Submitted to: Deep-Sea Research.

Supported by: NSF Grant OCE87-16910.

WHOI Contribution No. 7825.

CORRECTION TO "EVIDENCE FOR WIND-DRIVEN CURRENT FLUCTUATIONS IN THE EASTERN NORTH ATLANTIC" BY R. M. SAMELSON

Roger M. Samelson

In the paper "Evidence for wind-driven current fluctuations in the eastern North Atlantic" (Journal of Geophysical Research, 95(C7), 11,359-11,368, 1990) (hereinafter referred to as Samelson 1990) it was found that remote and local observed coherences at 3000 m at a location in the eastern North Atlantic corresponded well in both magnitude and location to the predictions of a simple model. During the course of the work described in Samelson and Shrayer (1991), it was discovered that the theoretical predictions presented by Samelson (1990, Figures 8-13) had

been inadvertently calculated using, for the parameters σ and s, estimates of the inverse e-folding scales for the coherence-squared, rather than coherence, of the wind stress curl. These values were twice (with round-off error) the correct values, corresponding to the e-folding scales that were too short by half. The correct values are given here.

The corrections affect the numerical results, but do not alter the qualitative conclusions of Samelson (1990) in any substantial way. The corrections improve the energy level prediction but degrade the maximum coherence prediction in the 3.7- to 8-day band, where the agreement between theory and observation remains sufficient to provide support for the hypothesis that deep kinetic energy in the eastern basin is primarily wind-driven. In the 8- to 22-day and 23- to 82-day bands, the corrected energy level predictions suggest only that wind driving is strong enough to force observed currents, while little agreement between observed and predicted coherences is found, as before.

Published in: Journal of Geophysical Research, 97(C1):821-822, 1992.

Supported by: NSF Grant OCE89-16463. WHOI Contribution No. 7894.

FLUID EXCHANGE ACROSS A MEANDERING JET

Roger M. Samelson

The motion of fluid parcels in a two-dimensional kinematic model of a meandering jet is investigated using Melnikov's method. The study is motivated by a recent analysis of float trajectories in the Gulf Stream. The results indicate that the efficiency of cross-jet exchange induced by fluctuating meander amplitudes depends strongly on the frequency of the fluctuations. For high frequencies (≥ 0.04 cpd), exchange between the core of the jet and regions of 'trapped' fluid moving with the meander is preferred, while for low frequencies (< 0.04 cpd), exchange between the 'trapped' fluid and the slow-moving fluid surrounding the jet is preferred. Propagating waves superimposed on the meandering jet can efficiently cause exchange between regimes when their phase speeds roughly match the basic flow velocities along the regime boundaries. Numerical results suggest that exchange across the center of the jet is less efficient than exchange between adjacent regimes so that the meandering jet will tend to mix fluid along each of its sides but preserve gradients across the jet core.

In Press: Journal of Physical Oceanography.

Supported by: ONR Contract N00014-91-J-1570. WHOI Contribution No. 7759.

EFFECTS OF HORIZONTAL RESOLUTION ON A LIMITED-AREA MODEL OF THE GULF STREAM SYSTEM

William J. Schmitz, Jr. and J. Dana Thompson

A primitive-equation, n-layer, eddy-resolving circulation model has been applied to the Gulf Stream System from Cape Hatteras to east of the Grand Banks (78-45W, 30-48N). A two-layer version of the model was driven both by direct wind forcing and by transport prescribed at inflow ports south of Cape Hatteras for the Gulf Stream and near the Grand Banks of Newfoundland for the Deep Western Boundary Current. Outflow was determined by a radiation boundary condition and fixed net transport in each layer. Realistic coastlines, bottom topography, and forcing functions have been used, within the limitations of the model. Numerical experiments previously run at 0.2° horizontal resolution (~ 20 km) were found to have some realistic features, but a key unresolved deficiency was that the highest abyssal eddy kinetic energies obtained near the Gulf Stream were too low relative to data by a factor of about 2, with inadequate eastward penetration.

New numerical experiments have extended previous results to higher horizontal resolution, all other conditions being held fixed. At 0.1° horizontal resolution, deep eddy kinetic energies in the vicinity of the Gulf Stream increase by a factor of roughly 2 relative to 0.2°, with possibly excessive eastward penetration. Higher eddy kinetic energy with increasing horizontal resolution is an established result for atmospheric models, and recently a high priority consideration for ocean models. The increase in eddy activity is probably at least partly due to enhanced energy conversion from mean flow to fluctuations due to baroclinic/barotropic instabilities. One special experiment at 0.05 degree horizontal resolution (~ 5 km) yielded kinetic energies nearly the same as the equivalent 0.1° case, suggesting that convergence of the numerical solutions has nearly been reached.

Submitted to: Journal of Marine Research.

Supported by: ONR32-05-3F.

WHOI Contribution No. 7730.

MESOSCALE OCEAN CURRENTS

William J. Schmitz, Jr.

Time-dependent current and temperature patterns with horizontal dimensions of 100-500 km, typically called mesoscale eddies, are ubiquitous features in the world's oceans. The boundary currents and mid-latitude jets that occur in all ocean basins are mesoscale features in their cross-stream dimension, as are their recirculations. Since mesoscale ocean currents are a primary source of eddies via instability mechanisms, the eddy field is as geographical and regional as are strong mean flows. Direct wind forcing of eddies is a minor energy source near strong currents and recirculations, but may be dominant in the interior of subtropical gyres. The linkage between the intensity of mesoscale eddies and energetic ocean currents at mid-latitudes has been a topic of interest in physical oceanography for about twenty years. This review contains an account of the state of the art of this subject, where it is pointed out that numerical experiments may tend toward the observed geography, with of course many observational features yet to be explained. We are probably doing a better job accounting for eddies than for their effects (feedback) on the mean circulation, the latter also being harder to observe, as is climatic scale variability. The similarities and differences between the structure of the eddy fields in various ocean basins have only partially been accounted for, as is also true for mesoscale currents.

It has recently been suggested that a major fraction of the cross-equatorial transport of North Atlantic Deep Water is at least partially compensated for by a cross-equatorial transport of upper-ocean water that flows through the Straits of Florida. This discovery points to a resolution of the Sverdrup Transport dilemma for the North Atlantic. A new, speculative and hopefully provocative, scheme for the general circulation in the North Atlantic is also set forth. Fluctuations in the relative strengths of the diverse components of deep water formed in the North Atlantic may be an important oceanic contribution to climatic scale variability.

Submitted to: Reviews of Geophysics.

Supported by: ONR Contracts N00014-76-C-0197, NR083-400, N00014-84C-0134, NR083-400, N00014-89-J-1039; and NSF Grant OCE85-21082.

WHOI Contribution No. 7889.

ON THE SVERDRUP CIRCULATION FOR THE ATLANTIC ALONG 24N

William J. Schmitz, Jr., J. Dana Thompson and James R. Luyten

The 30 Sv. transported by the Florida Current through the Straits of Florida off Miami may consist of a wind-driven contribution of 17 Sv., along with a thermohaline component of 13 Sv. The latter could flow through the South Atlantic as upper ocean compensation for a net abyssal cross-equatorial flow southward. The Sverdrup transport along 24N in the interior North Atlantic east of 55-60W is about 17 Sv., matching the wind-driven component of the Florida Current. The circulation in the vicinity of 24N and west of 55-60W up to the Bahama Banks contains energetic, shorter spatial scale flows, where there is a similarity between the scales and structure of the C-shaped pattern of dynamic height and the regional pattern of the Sverdrup Transport Contours.

Submitted to: Journal of Geophysical Research.

Supported by: NSF Grant OCE 8521082; ONR Contracts N00014-84-C-0134 and NR 083-400.

WHOI Contribution No. 7859.

A DIAGNOSTIC STUDY OF THE WIND-AND BUOYANCY-DRIVEN NORTH ATLANTIC CIRCULATION

Michael A. Spall

A two-moving-layer diagnostic model with a variable depth mixed layer on top is applied to the annual mean climatology of the North Atlantic. Estimates of the annual mean mass flux from the mixed layer into the upper thermocline (called mixed layer pumping) and subsurface heating rates are obtained on the basin scale from hydrographic data alone. No independent measures of wind stress or other surface forcings are required. In addition, it is shown that the nonlinear terms in the vorticity equation are critical to balance the subsurface heat flux in the Gulf Stream and over most of the subtropical gyre. Evidence is presented for the existence of interior, southeastern, northeastern, and recirculation regimes in the North Atlantic. These regimes are distinguished by the behavior of the characteristic trajectories of the system and by whether the flow is a direct cell (interfacial flux and vertical velocity have the same sign) or indirect cell (interfacial flux and vertical velocity have the opposite sign). It is demonstrated here that one can make use of analytic approaches in the analysis of historical

data sets to yield relatively simple solutions that give a direct link between theory and observations.

Published in: Journal of Geophysical Research, 96(C10):18,509-18,518, 1991.

Supported by: ONR Contract N00014-84-C-0134. WHOI Contribution No. 7689.

COOLING SPIRALS AND RECIRCULATION IN THE SUBTROPICAL GYRES

Michael A. Spall

The influence of cooling in a western boundary current on the recirculation of parcels in the subtropical gyre and their eventual transfer into the subpolar gyre is investigated. It is shown that heat loss to the atmosphere and the resulting vertical convection of dense water in the Gulf Stream of a general circulation primitive equation model forces a counterclockwise spiral of the velocity vector with depth (a cooling spiral). Parcels which pass through this region of cooling are forced to cross under the upper level trajectories from south to north, in opposite sense to the beta spiral experienced in the interior of the subtropical gyre. This crossing of trajectories is an important consequence of the cooling in the western boundary current as it influences both the scale and structure of the subtropical gyre recirculation. A simple expression is derived which relates the spatial scale of the recirculation to the cooling rate in the western boundary current and the wind forcing in the subtropical gyre.

In Press: Journal of Physical Oceanography.

Supported by: Woods Hole Oceanographic Institution.

WHOI Contribution No. 7604.

ROSSBY WAVE RADIATION IN THE CAPE VERDE FRONTAL ZONE

Michael A. Spall

Radiating baroclinic Rossby waves excited through instability of the Cape Verde Frontal Zone are proposed as a mechanism for the generation of mesoscale variability in the mid-ocean (1000 m) eastern basin. Linear quasigeostrophic theory is applied to an idealized front representative of the Cape Verde Frontal Zone to demonstrate that the front is unstable to modes which may radiate away from the frontal region as baroclinic Rossby waves. Evidence for the existence of these waves is obtained from a general circulation primitive equation model. In addition, the model fields are

used to identify characteristic signatures of the waves in terms of quantities which may be directly observed in the ocean. Lagrangian trajectories, Reynolds stress, eddy kinetic energy, and frequency spectra taken from SOFAR float and current meter records are all in good agreement with the amplitude and distribution implied by the wave radiation in both the linear theory and the full primitive equation model. We conclude that the Cape Verde Frontal Zone is a source of radiating baroclinic Rossby waves and that these waves are a non-trivial contribution to the eddy energy at the mid-depth ocean in the eastern basin.

In Press: Journal of Physical Oceanography.
Supported by: NSF Grant OCE90-09463.
WHOI Contribution No. 7709.

A CONJECTURAL REGULATING MECHANISM FOR DETERMINING THE THERMOHALINE STRUCTURE OF THE OCEANIC MIXED LAYER

Henry M. Stommel

It is a well known fact that in the surface mixed layer of the ocean there is a remarkable relation T(S) between annual mean temperature T and salinity S in the range of latitude between about 20 and 50 degrees. An estimate of the mean ratio R = dT/dS in density units in the mixed layer in the range $7 \le T \le 17^{\circ}\mathrm{C}$ can be obtained by scaling off the salinity difference ΔS between the two isotherms 7° and 17° on climatological charts, at several longitudes.

Submitted to: Journal of Physical Oceanography.

Supported by: NSF Grant OCE89-13128.

WHOI Contribution No. 7813.

THE AVERAGE T-S RELATION OF A STOCHASTICALLY FORCED BOX MODEL

Henry M. Stommel and William R. Young

The large scale T-S relation in the ocean mixed layer has a density ratio which, in the mean, is close to 2. There are large fluctuations around this average, perhaps due to stochastic forcing such as rain storms. In this note we study a two box model of the T-S relation in which the mass exchange between the boxes is a function of the density difference, and the effect of rain storms is modeled as random precipitation and evaporation. If the random forcing has a decorrelation time which is much less than the deterministic

evolution, then a Fokker-Planck equation can be used to describe the evolution of an ensemble of box models. We find the equilibrium solution of the Fokker-Planck equation, and then use it to compute the average density ratio of the ensemble. This average is close to 2 provided that random fluctuations are large, and that the mass exchange is proportional to the absolute value of the density difference between the two boxes. (Other models of the mass exchange lead to different average density ratios.) The effect of forcing with a non-zero time average (e.g. large scale persistent gradients in precipitation) is assessed and we conclude that provided the stochastic component of the forcing is sufficiently large the average density ratio remains near 2.

The vision of the mixed layer T-S relation which emerges from this very idealized model is that enormously variable forcing creates salinity anomalies which are eliminated by some mechanism whose efficacy increases with the density gradient. The combination of large fluctuations and nonlinear mass exchange creates at T-S regulator which holds the average density ratio to values around 2.

Submitted to: Journal of Physical Oceanography.

Supported by: NSF Grant OCE89-13128.

WHOI Contribution No. 7912.

THE DOUBLE SILICA MAXIMUM IN THE NORTH PACIFIC

Lynne D. Talley and Terrence M. Joyce

The North Pacific has two vertical silica maxima. The well-known intermediate maximum occurs between 2000 and 2500 meters, with a density relative to 2000 dbar of 36.90 in the northeastern Pacific. The deep maximum, which has not been observed extensively before, is found at or near the ocean bottom in the northern North Pacific in a narrow latitude range. Both maxima have highest silica in the northeast. Maps of silica on isopycnals which intersect the intermediate and bottom maxima show that the lowest silica is found in the western tropical North Pacific, suggesting a route for the spread of South Pacific water into the deep North Pacific. Low silica water is found along the western boundary of the North Pacific, with a separate broad tongue south of Hawaii. The highest silica on both isopycnals is in the northeast Pacific.

Hydrothermal vents seem to be contributors to the maxima, given current estimates of silica concentration in vent waters, heat flux from vents in the northeast Pacific, and the rate of dissolution of silica from opaline bottom sediments and from falling particles. Neither the individual hypothesized sources nor their sum accounts for the entire excess of silica in the maxima, indicating additional sources or an underestimate of vent population or dissolution rates.

Submitted to: Journal of Geophysical Research.

Supported by: NSF Grants OCE84-16211, OCE87-40379, OCE86-58120, OCE84-16197, OCE89-908, OCE83-16930; and ONR Contract N00014-84-C-0218.

WHOI Contribution No. 7706.

AN EASTERN ATLANTIC SECTION FROM ICELAND SOUTHWARD ACROSS THE EQUATOR

Mizuki Tsuchiya, Lynne D. Talley and Michael S. McCartney

A long CTD/hydrographic section with closely spaced stations was occupied in July-August 1988 from Iceland southward to 3°S along a nominal longitude of 20°W. The section extends from the surface down to the bottom and spans the entire mid-ocean circulation regime of the North Atlantic from the subpolar gyre through the subtropical gyre and the equatorial currents. Vertical sections of potential temperature, salinity, and potential density from CTD measurements and of oxygen, silica, phosphate, and nitrate based on distrete water-sample measurements are presented and discussed in the context of the large-scale circulation of the North Atlantic Ocean. The close spacing of high-quality stations revelas some features that have not been described previously. These include: 1) possible recirculation of the lightest Subpolar Mode Water into the tropics, 2) a thermostad at temperatures of 8-9°C lying below that of the Equatorial 13°C Water, 3) an abrupt southern boundary of the Labrador Sea Water at the Azores-Biscay Rise and a vertically well-mixed region to its south, 4) a sharp demarcation in the central Iceland Basin between the newest Iceland-Scotland Overflow water and older bottom water, which has a significant component of southern water, 5) an isolated core of the high-salinity, low-silica Upper North Atlantic Deep Water at the equator, 6) a core of the high-oxygen, low-nutrient Lower North Atlantic Deep Water pressed against the southern flank of the Mid-Atlantic Ridge just south of the equator, 7) a large body of nearly homogeneous water beneath the Middle North Atlantic Deep Water between 20°N and the Azores-Biscay Rise, and 8) a deep westward boundary undercurrent on the southern slope of the Rockall Plateau.

In Press: Deep-Sea Research.

Supported by: NSF Grant OCE86-14486.

WHOI Contribution No. 7723.

DEEP CURRENTS IN THE ARABIAN SEA IN 1987

Bruce A. Warren and Gregory C. Johnson

New features of the deep circulation in the Arabian Sea were revealed by four sections of deep CTD-O₂ stations occupied by the R.R.S. Charles Darwin late in 1986 and early in 1987, during the northeast monsoon, the repeated during the succeeding southwest monsoon. The most prominent elements in the bottom-water layer were (a) a northward flowing, western-boundary current of volume transport about 4×10^6 m³ s⁻¹ in the southern Somali Basin, which appeared to turn eastward at the equator and supply water to the northern Somali Basin from along the equator; and (b) a southeastward flowing boundary current along the northeastern flank of the Calsberg Ridge in the Arabian Basin, which demonstrated that the bottom water of the Arabian Basin enters mainly from the Central Indian Basin. The strength of the boundary current in the Somali Basin implies an unusually large upward velocity at the top of the bottom water, about $12 \times 10^{-5} cms^{-1}$.

Mapping of water properties in the deep-water layer above the bottom water during successive monsoons was undertaken because three earlier surveys had shown differing horizontal distributions there, and had thus raised the possibility of a monsoonal reversal of the circulation, paralleling that in the near-surface water. However, the patterns of variation in the salinity and oxygen fields were essentially the same on the two Darwin cruises, suggesting a broad southwestward flow in the deep-water layer of the Somali Basin during both monsoons. We propose that this pattern was not forced by the monsoons but reflected mainly the mean circulation of the deep water as driven by the upwelling of the bottom water from below; that that pattern might be enhanced during the northeast monsoon if the wind-forcing penetrates into the deep water; and that a moderately strong southwest monsoon (in contrast to the extraordinarily weak monsoon of 1987) would be required to disrupt this distribution of water properties.

In Press: Marine Geology.

Supported by: ONR Contracts N00014-89-J-1076, N00014-87-C-0001; NSF Grant OCE86-14497; and Graduate Fellowship.

WHOI Contribution No. 7607.

CIRCULATION AND WATER MASS BALANCE IN THE BRAZIL BASIN

Huai-Min Zhang and Nelson G. Hogg

Analysis of data from the Levitus (1982) atlas shows that the application of the Montgomery streamfunction to the potential density surfaces induces an error which cannot be ignored in some regions in the ocean. The error arises from the variation of the specific volume anomaly along isopycnal surfaces. By including the major part of this effect, new streamfunctions, named the "pressure anomaly" and "mean pressure streamfunctions", are suggested for use in potential density coordinates.

By including the variations of specific volume anomaly and pressure along isopycnal surfaces, the inverse model proposed by Hogg (1987) is modified for increased accuracy and it is applied to the Brazil Basin to study the circulation, diffusion and water mass balances. The system of equations with constraints of positive diffusivities and oxygen consumption rates is solved by the inverse method. The results indicate that the circulation in the upper ocean is consistent with previous work, but that in the deep ocean differs from some previous analyses. In the NADW depth, we find a coincidence of flow with tongues of water properties. The diffusivities and diapycnal velocities seem stronger in the region near the equator than in the south, with reasonable values. Diffusion plays an important role in the water property balances. Examples show that similar property patterns may result from different processes.

Submitted to: Journal of Marine Research.

Supported by: ONR Contract N00014-90-J-1465; and NSF Grant OCE90-4396.

WHOI Contribution No. 7909.

THEORETICAL AND LABORATORY MODELS

SOME GLOBAL CONSERVATION LAWS IN QUASIGEOSTROPHIC FLOWS WITH PIECEWISE CONSTANT POTENTIAL VORTICITY

George I. Bell and Larry J. Pratt

In the context of quasigeostropic flow, identifies are derived expressing the global conservation of pseudo-momentum and the acceleration of the mean flow at a given latitude. The results are stated for continuously stratified

and n-layer models under a variety of boundary conditions. When the potential vorticity in each horizontal slice is piecewise constant (contour dynamics), these identities may be further simplified and have simple interpretations. In the evolution of a finite amplitude perturbation to a linearly stable jet, it is shown that any increase in the jet perturbations must be balanced by the meridional drift of isolated eddies. It is also demonstrated that no acceleration of the mean flow is possible at latitudes across which there is no potential vorticity gradient. An example of a linearly stable, equivalent barotropic jet is given. According to the momentum conservation law derived, eddies which pinch off from such a jet cannot drift beyond a certain distance from the jet axis and instead eddies tend to be reabsorbed by the jet.

Submitted to: Dynamics of Atmospheres and Oceans.

Supported by: NSF Grant OCE89-16446; and ONR Contract N00014-89-J-1182.

WHOI Contribution No. 7701.

CONDUIT SOLITARY WAVES IN A VISCO-ELASTIC MEDIUM

Roger H. J. Grimshaw, Karl R. Helfrich and Jack A. Whitehead

The theory for waves on a buoyant fluid conduit in a more viscous outer fluid is extended to include a visco-elastic outer fluid. The external fluid is treated as a linear Kelvin-type visco-elastic medium and a wave evolution equation is derived. This equation is identical to the purely viscous case with the exception of a new term representing the elastic effects. A conservation law is derived and used in an analytic treatment for a slowly-varying solitary wave (given initially by the exact solution to the purely viscous case) for the case of small, but non-zero, elasticity. The theory shows that the wave amplitude will decay and a shelf, required for the conservation of mass, will develop behind the wave. Numerical solutions of the evolution equation support the analytic approximation. Laboratory experiments show qualitative agreement with the analytic and numerical development. Geophysical applications suggest that these effects may be most important for melt migration in the asthenosphere.

In Press: Geophysical Astrophysical Fluid Dynamics.

Supported by: NSF Grant EAR-8916857.

WHOI Contribution No. 7676.

INTERNAL SOLITARY WAVE BREAKING AND RUN-UP ON A UNIFORM SLOPE

Karl R. Helfrich

Laboratory experiments have been conducted to study the shoaling of internal solitary waves of depression in a two-layer system on a uniform slope. The shoaling of a single solitary wave results in wave breaking and the production of multiple turbulent surges, or buluses, which propagate up the slope. Significant vertical mixing occurs everywhere inshore of the breaking location. The kinematics of the breaking and bolus run-up are described and a breaking criterion is found. The energetics of the breaking is investigated. Over the range of parameters examined, $15(\pm 5)\%$ of the energy lost from first-mode wave motion inshore of the break-point goes into vertical mixing (i.e., changes in potential energy).

In Press: Journal of Fluid Mechanics.

Supported by: NSF Grant OCE-8902671.

WHOI Contribution No. 7830.

ON THE ABSOLUTE VELOCITY OF THE GEOSTROPHIC CIRCULATION

Grigory Isayev

The explicit expression for the absolute velocity of the adiabatic geostrophic hydrostatic circulation as the function of the streamline directions is found. The angle of the three-dimensional streamline to the horizontal plane is expressed through the density field and the angle of the streamline to the longitude axis which is measurable on the published isopycnic potential vorticity maps. The obtained expression for the absolute velocity holds valid also for the nonadiabatic geostrophic circulation although in this case the streamline directions are not measurable on the isopycnic potential vorticity maps. For the arbitrary smooth velocity field the kinematic equation is derived which provides the expression for the absolute velocity as the function of shears of its horizontal components, absolute value and direction.

Submitted to: Journal of Fluid Mechanics.

WHOI Contribution No. 7635.

THE ROLE OF DISSIPATION MECHANISMS IN THE NONLINEAR DYNAMICS OF UNSTABLE BAROCLINIC WAVES

Patrice Klein and Joseph Pedlosky

The effect of three different parameterizations of dissipation on the nonlinear dynamics of unstable baroclinic waves is studied. The model is the two-layer f-plane model and the dynamics is quasigeostrophic. The dissipation mechanisms are (1) dissipation due to Ekman layers at the horizontal boundary surfaces, (2) the addition of interfacial Ekman friction, or (3) dissipation proportional to the perturbation potential vorticity.

We find, as anticipated by weakly nonlinear theory, a strong effect on the nonlinear amplitude dynamics for supercriticalities as large as four times the threshold value for instability. The use of interfacial friction or potential vorticity damping expunges the vacillating behavior common to the system with type (1) dissipation.

At high supercriticality a barotropic vacillation involving the mean flow and harmonics of the fundamental is superimposed on the basic baroclinic wave dynamics. Examination of the critical transition for the emergence of the barotropic oscillation reveals that the enhanced linear instability of the higher harmonics is responsible for the self-sustained vacillation.

Published in: Journal of the Atmospheric Sciences, 49(1):29-48, 1992.

Supported by: NSF Grant ATM89-03890.

WHOI Contribution No. 7675.

BAROCLINIC INSTABILITY LOCALIZED BY DISSIPATION

Joseph Pedlosky

A two-layer baroclinic flow on an f-plane is rendered locally stable by sufficiently strong Ekman layer friction except in an interval of length 2a in the downstream direction in which the friction is reduced. The localized marginally stable modes are found by matching the solutions found separately in each region where the friction is uniform.

It is shown that localized baroclinic instabilities, anchored to the local unstal are ne are possible as long as the interval length exceeds a critical value on the order of the Rossby deformation radius. The most unstable perturbation modes consist of two coupled vortices in each layer squeezed towards the downstream

edge of the unstable zone. Slightly supercritical states will lead to growth. The growth rate remains substantial until the interval length becomes small with respect to a deformation radius.

In Press: Journal of the Atmospheric Sciences.

Supported by: NSF Grant ATM89-03890.

WHOI Contribution No. 7746.

COASTAL CIRCULATION & DYNAMICS

COLLIDING WATER MASSES OVER THE CONTINENTAL SLOPE EAST OF VIRGINIA

James Churchill, Edward R. Levine, Donald N. Connors and Peter C. Cornillon

A combination of water masses was observed over the continental slope between Cape Hatteras and Hudson Canyon following the passage of a Gulf Stream meander. It was largely made up of fluid discharged form the Gulf Stream and also contained bands of Middle Atlantic Bight (MAB) shelf water and intrusions of slope water. The shelf water bands were entrained into the circulation of a double vortex consisting of a large anticyclonic eddy and a much smaller cyclonic Gulf Stream frontal eddy. Transport of shelf water at the edge of the anticyclonic eddy was estimated to be $1.3 \times 10^5 \text{m}^3 \text{s}^{-1}$, which is comparable with the estimated alongshore transport of water over the MAB shelf. Vigorous mixing of the entrained shelf water with surrounding discharged Gulf Stream water is indicated by the large differences of the latter's T/S properties from the T/S relationship found within the Gulf Stream. These differences were used to estimate the salt fluxes into the shelf water band at the edge of the anticyclonic eddy, with results in the rage of $1.9-6.6 \times 10^{-6}$ gm salt cm⁻²s⁻¹. Analysis of hydrographic data suggests that the salt flux into this band was primarily the result of mixing produced by double diffusive processes. Hydrographic evidence also indicates that turbulence, generated by the surface wind stress and by velocity shear below the wind-mixed layer, significantly contributed to vertical mixing at some locations within the water mass combination.

Submitted to: Deep-Sea Research.

Supported by: NSF Grant OCE88-12778; and ONR Contract N00014-87-K-0235.

WHOI Contribution No. 7731.

THE ROLE OF STRATIFICATION IN THE FORMATION AND MAINTENANCE OF SHELFBREAK FRONTS

Glen Gawarkiewicz and David C. Chapman

We describe a mechanism for the formation of a front at the edge of a continental shelf in an initially linearly stratified fluid lacking horizontal density gradients. We use a primitive-equation numerical model with a specified vertically-uniform inflow imposed at the upstream boundary and allow the flow to evolve alongshelf under the influence of bottom friction. As the flow progresses downstream, the shelf water moves steadily offshore due to the Ekman flux concentrated in the bottom boundary layer. This offshore flow transports light water under heavier water which leads to convective overturning and ultimately a vertically well-mixed density field over the shelf. Large cross-shelf density gradients appear along the bottom at the shelfbreak, where the vertically well-mixed shelf water abuts the linearly stratified water on the upper slope. At the shelfbreak, the bottom boundary layer detaches and continues offshore along upward sloping isopycnals. Neutrally buoyant particles in the bottom boundary layer over the shelf move offshore until reaching the shelfbreak, where they ascent along isopycnal surfaces. Near-surface particles over the outer shelf move alongshelf rapidly with small offshore velocities, while near-surface particles over the inner shelf are drawn shoreward and downwell at the coastal boundary to feed the bottom boundary layer. The basic frontogenesis process is quite robust over a wide range of values of model parameters. The frontogenesis mechanism has important implications for observations of shelfbreak fronts as well as for the biology and chemistry of these fronts.

In Press: Journal of Physical Oceanography.

Supported by: NSF Grant OCE88-16015.

WHOI Contribution No. 7837.

LARGE SCALE PENETRATION OF GULF STREAM WATER ONTO THE CONTINENTAL SHELF NORTH OF CAPE HATTERAS

Glen Gawarkiewicz, Thomas M. Church, George W. Luther, III, Timothy G. Ferdelman and Michael Caruso

A hydrographic cruise on the continental shelf between Chesapeake Bay and Cape Hatteras on the east coast of the United States during the

summer of 1990 revealed a large scale penetration of Gulf Stream water onto the continental shelf north of Cape Hatteras. Gulf Stream water occupied the shelf between the depths of 10 m to 30 m. The layer of Gulf Stream water on the shelf extended 60 km north of Cape Hatteras, and reached at least as far shoreward as the 25 m isobath. Velocities of Gulf Stream water in the upper 110 m of the water column along the 1000 m isobath indicated a flow of 18 to 25 cm/s directed toward the northwest. The Gulf Stream water on the shelf was associated with low values of fluorescence, transmissivity, and nutrients. The presence of the seasonal stratification during the summer may allow enhanced baroclinic penetration of Gulf Stream water onto the continental shelf north of Cape Hatteras.

In Press: Geophysical Research Letters.

Supported by: NSF Grants OCE 916893, OCE 89-16804; and NASA Contract NAGW-1666.

WHOI Contribution No. 7864.

CONTINENTAL SHELF RESPONSE TO FORCING BY DEEP-SEA INTERNAL WAVES

Roger H. J. Grimshaw and David C. Chapman

A two-dimensional, linear, hydrostatic model is used to investigate the response over a continental shelf due to forcing by deep-sea internal waves with nearly arbitrary form. A flat-bottom deep-sea is assumed to have an upper layer with uniform density which extends deeper than the shelf-break depth. The stratification below this layer is continuous and arbitrary. For this stratification, it is shown that the influence of the deep-sea can be entirely represented by a simple boundary condition for the shelf flow imposed at the shelf-break. Solutions over the shelf are obtained for particular cross-shelf depth profiles and consist of an image of the incident wave form which propagates back and forth across the shelf being perfectly reflected at the coast but only partially reflected at the shelf-break. The amplitude of the shelf response generally increases with stronger stratification and/or a shallower shelf-break and can be quite large for some oceanic conditions. Shoaling topography leads to an amplified sea-level response near the coast and may produce an irregular pattern of oscillations.

In Press: Dynamics of Atmospheres and Oceans.
Supported by: NSF Grant OCE89-23065.

WHOI Contribution No. 7733.

COMPARISON OF VELOCITY ESTIMATES FROM AVHRR IN THE COASTAL TRANSITION ZONE

Kathryn A. Kelly and P. Ted Strub

Two methods of estimating surface velocity vectors from AVHRR data were applied to the same set of images and the results were compared with in situ and altimetric measurements. The first method used an automated feature-tracking algorithm and the second method used an inversion of the heat equation. The 11 images were from three days in July 1988 during the Coastal Transition Zone field program and the in situ data included ADCP vectors and velocities from near-surface drifters. The two methods were comparable in their accuracies, relative to the velocity data, underestimating the magnitudes of the velocities by 30-50%, with rms directional differences of about 60°. These differences compared favorably with a baseline difference estimate between interpolated ADCP vectors and drifter data within a well-sampled region, which gave an underestimate by ADCP of 32% and directional differences of 59°. High correlations between the AVHRR estimates and the coincident Geosat geostrophic velocity profiles suggested that the AVHRR resolved the important flow features. Based on this finding of qualitative accuracy the flow field was determined to consist primarily of a meandering southward-flowing current, interacting with several eddies. A strong anticyclonic eddy north of the jet was a robust feature of all the AVHRR-derived solutions; its existence is consistent with nearby observations, although it was in a region which was not adequately surveyed. Incorporation of sparse altimeter data into the AVHRR solutions showed a slight improvement for the inverse method, but not for the feature-tracking solution. The relative advantages of each AVHRR method are discussed, along with the solution characteristics.

Submitted to: Journal of Geophysical Research.

Supported by: ONR Contracts N00014-90-J-1808, N00014-86-K-0751; and NASA Contract NAGW-1251.

WHOI Contribution No. 7851.

THE SURFACE BOUNDARY LAYER IN COASTAL UPWELLING REGIONS

Steven J. Lentz

Observations for the Oregon, Peru, and northern California shelves are used to examine the characteristics of the surface boundary layer in coastal regions during the upwelling season. Both CTD and moored observations reveal the presence of surface mixed layers that are typically 5-10 m thick. Within the surface mixed layer the cross-shelf (cross-wind) current is vertically uniform. While, below the surface mixed layer there is a subsurface maximum in the vertical shear of the cross-shelf velocity. The along-shelf (along-wind) current contains a strong, near-surface, vertical shear. Within the surface mixed layer the vertical shear is linearly related to the shear velocity $u_* = (\tau^*/\rho o)^{\frac{1}{2}}$, where τ^* is the magnitude of the wind stress, and is consistent with a near-surface, wind-driven, log-layer, though the magnitude of the shear is typically larger than expected. When the near-surface water is stratified and there is a significant wind stress, the along-shelf current is usually strongly sheared and the Richardson number (Ri) is near critical $(Ri \sim 0.25)$. Farther down in the water column the flow tends to be more stable ($Ri \geq 0.25$), though near critical Richardson numbers do occur.

The surface mixed-layer depth variability in all three regions is predominantly at diurnal and subtidal frequencies. The diurnal variation in surface mixed-layer depth is due primarily to the diurnal surface heat flux variation rather than the diurnal wind stress. The diurnal current response to the diurnal wind stress over the Peru shelf (latitude 15°S) is different from the response over the mid-latitude Oregon and Peru shelf and superinertial over the mid-latitude shelves. The subtital surface mixed-layer depth variability scales as $u_*/(Nf)^{\frac{1}{2}}$, where N is the buoyancy frequency below the surface mixed layer and f is the Coriolis frequency. Surprisingly, this relationship indicates that the subtidal variability of the surface mixed-layer depth does not depend strongly on either the surface heat flux or advection of heat, both of which are large in coastal upwelling regions. The cross-shelf transport in the surface mixed layer is smaller than the Ekman transport τ^s / ρof and decreases toward the coast, suggesting that upwelling occurs over the entire shelf.

Submitted to: Journal of Physical Oceanography.

Supported by: NSF Grant OCE87-16937.

WHOI Contribution No. 7749.

WIND-FORCED VARIABILITY OF THE DEEP EASTERN NORTH PACIFIC: THEORY AND RELATIONSHIP TO SEAFLOOR PRESSURE AND ABYSSAL CURRENTS

P. P. Niiler, J. Filloux, W. T. Liu, Roger M. Samelson, J. D. Paduan and C. A. Paulson

Data from an array of bottom pressure gauges

and a string of current meters in the vicinity of 47°N, 139°W is used to examine the deep ocean variability forced by ocean surface wind stress curl from August 1987 to June 1988. Bottom geostrophic currents are computed from the pressure gauge array and these correspond well to the long period directly measured currents at 3000 m. The supra-tidal period bottom pressure variations are coherent at 95% confidence with the wind stress curl in period bands of 3-4 days and 15-60 days, but removed in distances of 400 km to 700 km to the northwest and the southeast, respectively. A linear, two-layer hydrodynamic model is used to examine the theoretical forcing produced by random-phased surface wind fields for the conditions of the eastern north Pacific and the 15-60 day period observed response is reproduced credibly. To model 3-15 day variations, more realistic models are required.

Submitted to: Journal of Geophysical Research.

Supported by: ONR Contract N00014-90-J-1153; and NSF Grant OCE89-016463.

WHOI Contribution No. 7836.

SUPERCRITICAL MARINE LAYER FLOW ALONG A SMOOTHLY-VARYING COASTLINE

Roger M. Samelson

A model for hydraulically supercritical atmospheric marine layer flow along a smoothly varying coastline is formulated and solved numerically. The model is motivated by a recent comparison of CODE observations to a simple hydraulic theory, which suggested the presence of an expansion fan and a compression jump downstream of topographic features. The marine layer is modeled as a homogeneous rotating fluid layer decelerated by surface friction and forced by imposed upper-level pressure gradients. The equations are solved by a characteristic-based grid-point scheme. The results indicate that the expansion fan is a robust feature that persists under most conditions in the present, more realistic model, but is dramatically altered in structure by the presence of friction, while the jump may weaken rapidly offshore, due mainly to offshore variations of the layer height upstream of the jump. The supercritical flow features cause variations in wind stress of 10-50% over tens of kilometers.

Submitted to: Journal of the Atmospheric Sciences.

Supported by: NSF Grant OCE89-16463.

WHOI Contribution No. 7634.

INSTRUMENTATION & EXPERIMENTAL METHODOLOGY

SEPARATION OF TIDAL AND SUBTIDAL CUPRENTS IN SHIP-MOUNTED ACOUSTIC DOPPLER CURRENT PROFILER (ADCP) OBSERVATIONS

Julio Candela. Robert C. Beardsley and Richard Limeburner

A simple method is developed to analyze current measurements obtained from a moving platform. The need for this is motivated by the now common use of the ship-mounted acoustic Doppler current profiler (ADCP) to acquire absolute velocity data during an oceanographic survey of a given region. The full potential of this new measurement technique is severely hindered when the presence of high-frequency phenomena (e.g., tidal or inertial motions) prevents a clear visualization of the lower-frequency current structure of interest. Our analysis method is based on a spatial interpolation scheme, using arbitrary functions, that allows for the tidal current time variability, which then permits the tide-induced motions to be subtracted from the ADCP data to yield the subtidal current field. The method also allows nearby moored and drifter current measurements (if available) to be combined with the shipboard ADCP observations in a single analysis to obtain the best description of the tidal and subtidal currents.

To illustrate this method, we present results from the analysis of ADCP data taken during oceanographic surveys in two different continental shelf regions, the East China Sea and the Amazon shelf. A 5-day (CTD) and ADCP survey was made in the East China Sea near the mouth of the Yellow Sea during January 1986. There the currents were essentially barotropic and dominated by the semidiurnal tide. The ADCP-derived cotidal chart for the M_2 (12.42 hours) component agrees well with existing charts derived empirically from sea level observations or from regional numerical models. The ADCP-derived steady flow is also consistent with the observed density field and indicates little flow in or out of the Yellow Sea and a transport of about 1 Sv towards the Tsushima Strait.

Two CTD-ADCP surveys lasting 21 and 23 days were conducted over the Amazon shelf during March and May, 1990. Simultaneously moored current observations were also obtained at three locations along a cross-shelf array 200 km north of the Amazon River mouth, for a common period of at least 2 months (12 February-13 April). Over the shelf tidal and subtidal currents were comparable

in magnitude. Our analysis indicates that the tidal currents were essentially barotropic, semidiurnal, and polarized in the cross-shelf direction, increasing in magnitude towards the inner shelf where current values of more than 2 m/s are common. The ADCP-derived steady currents were aligned in the along-shelf direction and strongly influenced by the North Brazil Current (NBC). During both ADCP surveys, the northwestward flowing NBC was transporting more than 2 Sv over the shelf at depths shallower than 100 m.

Published in: Journal of Geophysical Research, 97(C1):769-788, 1992.

Supported by: NSF Grants OCE85-01366, OCE88-12917, OCE90-17540 and OCE87-16937.

WHOI Contribution No. 7780.

RECENT DEVELOPMENTS IN OCEAN DATA TELEMETRY AT WOODS HOLE OCEANOGRAPHIC INSTITUTION

Daniel E. Frye and W. Brechner Owens

Woods Hole Oceanographic Institution is developing techniques for telemetering oceanographic data from the deep ocean to the laboratory in near real time. Three general approaches which provide a link between subsurface instruments and surface buoys equipped with satellite transmitters are being pursued. These approaches are cabled systems that use electromechanical cables to connect subsurface instruments to a central controller; high data rate acoustic modems to transfer information between multiple remote units and a central controller; and inductive modems that use standard mechanical mooring lines as the transmission medium between instruments deployed on the mooring and a central controller.

These telemetry systems are targeted for general use by the oceanographic community and are designed to be power efficient, low in cost, and capable of integration with most oceanographic data collection systems.

Published in: IEEE Journal of Oceanic Engineering, 16(4):350-359, 1991.

Supported by: ONR contract N00014-86-K-0751. WHOI Contribution No. 7700.

SEA WATER BATTERY FOR LONG LIVED UPPER OCEAN SYSTEMS

D. S. Hosom, R. A. Weller, A. A. Hinton and B. M. L. Rao

The Upper Ocean Processes Group (UOP) at the Woods Hole Oceanographic Institution

(WHOI) has programs directed at understanding and forecasting the time evolution of upper ocean and marine atmospheric boundary layer structures. Many of the regions where forecast capabilities are desired are those characterized by severe weather that are beyond present measurement capabilities. One of the critical requirements to be able to achieve this capability is to supply sufficient energy (electrical power) to operate the instrumentation and instrument protective systems such as heaters. active aspirators, de-icing devices, and powered samplers, in the absence of solar energy. The most promising approach has been the development of a sea water battery for use under surface buoys. WHOI has worked with Alupower, Inc. (Warren, New Jersey) to design, fabricate a prototype battery, and test that battery in a oceanographic surface buoy configuration. The system test using the prototype sea water battery (2 watts for 3 months) with a lead acid buffer battery in the presence of varying loads was successful. The 4.3 kwh design energy was delivered by the end of the test. The tests conducted provide the basis for the design by Alupower Inc. of a family of sea water surface buoy battery (10 watts for one year or 100 kilowatt hours) to a small battery that is also a drogue anchor for use on a drifting float.

Published in: *IEEE Oceans 1991 Proceedings*, 3:1673-1676, 1991.

Supported by: ONR Contract N00014-90-C-0098. WHOI Contribution No. 7707.

A THREE METER DISCUS BUOY WITH IMET METEOROLOGICAL SENSORS

D. S. Hosom, R. A. Weller, K. E. Prada and R. P. Trask

Programs directed at understanding and forecasting the time evolution of upper ocean and marine atmospheric boundary layer structures are ongoing at the Woods Hole Oceanographic Institution. This paper describes five surface moorings that have been deployed in the eastern Atlantic for making meteorological and upper ocean current measurements. These moorings include a variety of current meters and temperature instruments in the ocean and two separate meteorological measurement systems on the buoy. Of interest is a description of the newly developed system called IMET (Improved METeorological Measurements). This system includes sensors that are incorporated into intelligent modules developed as part of the WOCE (World Ocean Circulation Experiment) long lead time program.

Published in: "MTS '91 an Ocean Cooperative: Industry, Government and Academia."

Proceedings MTS '91, New Orleans, November 10-14, 1991. Sponsored by Marine Technology Society. Marine Technology Society, Washington, DC., 1:206-210, 1991.

Supported by: ONR Contract N00014-89-C-1490; and NSF Grant OCE-8709614.

WHOI Contribution No. 7817.

IMPLEMENTATION OF A TITANIUM STRAIN GAUGE PRESSURE TRANSDUCER FOR CTD APPLICATIONS

Robert Millard, Gary Bond and John Toole

The installation and operational characteristics of a titanium element strain gauge pressure sensor in Conductivity-Temperature-Depth (CTD) instruments is described. The behavior of the sensor is examined in both steady state and transient conditions, the latter consisting of thermal shocks achieved in laboratory plunge tests. The titanium pressure sensor has superior linearity and reduced hysteresis as compared with strain gauges which utilize a stainless steel element. However, significant transient pressure errors are noted for certain gauge installations. A model of the pressure sensor's thermal transient is developed from heat transfer theory which is solved for an idealization of the Mark III CTD configuration. This, in turn, motivates a numerical procedure for reducing the thermally induced static and transient pressure error in the titanium strain gauge pressure sensor data, and an installation procedure which thermally isolates the gauge. Residual pressure error in calibrated data from the titanium strain gauge is an acceptably small fraction of a decibar.

Submitted to: Journal of Atmospheric & Oceanic Technology.

Supported by: NSF Grants OCE91-05218 and OCE90-09430.

WHOI Contribution No. 7865.

A NOTE ON THE RESPONSE CHARACTERISTICS OF THE VACM COMPASS

Sarah K. Patch, Edward P. Dever, Robert C. Beardsley and Steven J. Lentz

Several simple laboratory experiments have been conducted to study the dynamic behavior of the VACM compass. While rather crude, these experiments demonstrate that the combined eddy current and bearing friction torque on the compass magnet is proportional to the angular velocity

difference between the compass magnet and housing, and that this combined frictional torque does tend to "critically" damp the free oscillation of the compass. Static experiments on six compasses (with good bearings) indicate a mean (undamped) resonant period of 3-5 secs at 41°N.

The combined frictional torque allows an angular oscillation of the compass housing to drive an oscillation of the compass magnet, and at resonant forcing, the compass magnet oscillates exactly in phase and with equal amplitude with the housing. For small amplitude forcing, the behavior of the compass can be modelled with a linear constant coefficient equation of motion, which suggests that an asymmetric angular forcing of the compass housing (which may occur in the field due to mooring motion) should not cause any error in the mean compass heading, however, forced compass oscillations could cause an error in the magnitude of the vector-averaged velocity.

In Press: Journal of Atmospheric and Oceanic Technology.

Supported by: NSF Grant OCE88-16937. WHOI Contribution No. 7708.

AIR-SEA INTERACTION

ANALYSIS OF SURFACE FLUXES IN THE MARINE ATMOSPHERIC BOUNDARY LAYER IN THE VICINITY OF RAPIDLY INTENSIFYING CYCLONES

Gennaro H. Crescenti and Robert A. Weller

A mooring with a surface buoy was deployed about 300 km southeast of Nova Scotia during the Experiment on Rapidly Intensifying Cyclones over the Atlantic (ERICA) in an attempt to obtain long-term, high quality measurements of meteorological and near surface oceanographic data. The acquired surface data included sea surface temperature, air temperature, relative humidity, barometric pressure, wind velocity, incident solar radiation and downward longwave radiation. A limited time series of sea temperature and current velocity was gathered from current meters at 20 and 50 m beneath the sea surface.

The surface meteorology was described before, during and after the passage of three rapidly intensifying cyclones. Estimates of the surface air-sea heat fluxes, computed from bulk aerodynamic formulae, were also examined for these same storms. A simple heat budget woused to estimate the heat loss/gain of the upper ocean against the air-sea heat transfer at the ocean surface. While the total surface heat heat flux may

sometimes exceed 1000 W m⁻², the data suggests that the main mechanism for cooling the upper ocean water was principally advective. An examination of the air-sea momentum transfer shows that the atmosphere exerted a significant influence on the upper ocean; persistent westerly winds coming off the North American continent transported surface waters to the south.

Submitted to: Journal of Applied Meteorology.

Supported by: ONR Contracts N00014-90-J-1423, N00014-84-C-0134 and NR083-400.

WHOI Contribution No. 7779.

THE HEAT BUDGET IN THE NORTH ATLANTIC SUBTROPICAL FRONTAL ZONE

Daniel L. Rudnick and Robert A. Weller

The heat budget in the North Atlantic subtropical frontal zone is examined using moored measurements of horizontal velocity, temperature, and surface heat flux obtained during the Frontal Air-Sea Interaction Experiment (FASINEX). The three moorings used in this calculation defined a triangle of base 19 km and height 28 km, and were densely instrumented from the surface to 160 m depth. Empirical orthogonal functions (EOFs) are employed to identify components of current and temperature variability with scales that are resolved by the observations. A least-squares fit to the EOF-filtered data is used to derive maps of velocity and temperature. The temperature field is dominated by the passage of fronts, with the highest variability at 160 m. Temperature gradients at 160 m peak at values approaching 0.001°C/m and are indicative of a tilting of the seasonal thermocline. Velocities are directed primarily along isotherms, and are swifter at the surface than at depth. The heat budget, for periods longer than 48 hours, of the upper 160 m is essentially a balance between rate of change of heat and horizontal advection; the correlation between these terms is 0.7. The effect of surface heating becomes apparent in the upper 40 m, notably at the diurnal frequency and its first harmonic. An imbalance in the mean heat budget can be rectified by a mean downwelling velocity of 5×10^{-5} m/s at 160 m.

Submitted to: Journal of Geophysical Research.

Supported by: ONR Contract N00014-84-C-0134.

WHOI Contribution No. 7828.

TECHNICAL REPORTS

CRUISE SUMMARIES OF OCEANUS CRUISES 205, LEG 8 AND 216

Terrence M. Joyce, Marvel C. Stalcup, R. Lorraine Barbour, Jane A. Dunworth and David M. Schubert

A study of the upper ocean thermal and density structure in the northwestern Atlantic in 1989 compared temperature and density measurements made with Expendable Bathythermograph and Conductivity-Temperature-Depth instruments with current data from an acoustic Doppler current profiler and satellite infrared imagery and altimetry. Two cruises were made in the spring and winter of 1989 with the goal of directly measuring the upper ocean currents and variability of the Gulf Stream. The XBT observations were used to extend the measured velocities geostrophically from the near-surface region to depths of 750 meters, thereby allowing transport estimates to be made for the upper ocean. In April the measurements were compared and used with the GEOSAT altimeter which, unfortunately, was not operating during the December cruise.

WHOI Technical Report 91-07.

Supported by: NSF Grant OCE88-17698.

MARINE POLICY CENTER

James M. Broadus III, Director

SOVIET ARCTIC MARINE TRANSPORTATION 1990

Lawson W. Brigham

During 1990, there was no letup in the tempo of operations and the development of Soviet Arctic marine transportation along the Northern Sea Route (NSR). The remarkable polar voyages and high level of Arctic shipping represent a significant, yet little known, component of Soviet maritime power.

Published in: Naval Institute Proceedings, 117(10):109-110, 1991.

Supported by: The John D. and Catherine T. MacArthur Foundation.

WHOI Contribution No. 7852.

THE INFLUENCE OF JAPANESE INDUSTRIAL TARGETING AND TRADE POLICY ON THE MARKETS FOR MARINE ELECTRONIC INSTRUMENTS

James M. Broadus

In the 1988 WHOI report, "Determining the Structure of the U.S. Marine Instrumentation Industry and its Position in the World Industry," we present a broad overview of the organization of firms and industrial networks through which products in the field of marine electronic instrumentation (MEI) are marketed. The research that went into the preparation of that report has been continued with, among other things, an emphasis on technological histories. These histories (or "case studies") have been directed at determining the origins of research and development (R&D) activities, identifying the sources of research sponsorship, and understanding the means by which funding for technological development has crossed the boundaries of end user sectors.

In addition to technology histories, we have begun to analyze technology transfer among private, nonprofit, and public sectors in the MEI field and the role of foreign governments in the promotion of their own MEI industries. Although we were unable to visit Japan, we outline in this paper some of the technological developments that currently are taking place in the MEI field in Japan and to identify some of the major issues facing U.S. industry there.

Japanese government involvement in the MEI field, as in other advanced technology fields, can be divided into two elements: government involvement in the research endeavor, especially through its "intertwined," but coordinated relationship with the industrial establishment, the

"targeting" of broad-scale research opportunities, and the direct sponsorship of R&D, product development, and marketing and trade policy.

Published in: Developing a National Marine
Electronics Agenda: Proceedings of the Marine
Instrumentation Panel Meeting, September
12-14, 1989, A.G. Gaines and K. Lindborg, eds.,
WHOI Technical Report 90-52, :6-12, 1990.

Supported by: NOAA/National Ocean Service through a grant to the Massachusetts Centers of Excellence Corporation, grant No. NA87-AA-D-M00037.

MARINE ELECTRONIC INSTRUMENTATION: AN INDUSTRIAL PERSPECTIVE

James M. Broadus

Marine electronic instrumentation (MEI) is an important subset of ocean technology. It spans a wide range of products including communication and navigation instruments (such as marine radios, global positioning satellite or GPS receivers, and electronic charts), sensors (such as hydrophones, current meters, bathythermographs, and video imaging systems), and data management instruments (such as "marinized" computer hardware and software).

Through research results and the construction of a prescriptive "national agenda," we hope to improve our understanding of international marine electronics markets, to inform constructive policy initiatives, and to demonstrate how increased interaction across sectors can contribute to national scientific progress and economic growth.

Published in: Oceanus, 34(1):102-103, 1991.

Supported by: Marine Policy Center and NOAA/National Ocean Service through a grant to the Massachusetts Centers of Excellence Corporation, grant No. NA87-AA-D-M00037.

THE SEA ENVIRONMENT: GOOD NEWS, BAD NEWS

James M. Broadus

This article provides an overview of the current status of the ocean environment, identifies the outstanding issues to be addressed in coming years, and suggests some possible connections with future naval activities. Growing problems with coastal pollution, continued pressure on living resources, heightened political concern for the environment, and a reorganization of national priorities following relaxation of Cold War tensions imply changes that will affect the sea services for

years to come. The Coast Guard will see a major expansion of its environmental enforcement mission over the coming decade. More emphasis on fisheries enforcement and on the formulation and enforcement of environmental regulations for both domestic and international navigation are likely. Navy involvement will probably focus on support of ocean science and research and development as well as enhanced environmental practice in its own operations and demonstration of innovative technology.

Published in: Naval Institute Proceedings, 117(10):50-55, 1991.

Supported by: The John D. and Catherine T.

MacArthur Foundation and the U.S. Naval
Institute.

WHOI Contribution No. 7669.

WORLD TRENDS IN OCEAN INDUSTRY

James M. Broadus

As an indicator of economic trends in the ocean sector, estimated revenues or expenditures in the major component activities of the ocean sector are aggregated. These include world naval expenditures, ocean freight charges, marine fish landings, and offshore oil and gas revenues. These are the major components, but the set is incomplete and is intended only as a rough guide to trends. We conclude that the ocean sector grew from just under \$800 billion (constant 1989) in 1978 to nearly \$1 trillion in the early 1980s, then contracted back to about \$800 billion by 1988. Meanwhile, world aggregate real GNP was climbing steadily from about \$15 trillion to nearly \$20 trillion. Ocean industry is thus an important part of the world economy. In relative terms it is comparable to or larger than such important sectors as mining, communications, or transportation. Whether its relative economic importance will grow or shrink in the intermediate future (10 years or so) is hard to say, but it seems reasonable to expect relative growth over the longer term (25-50 years). The comparative importance of various components of ocean industry is likely to continue changing over time. There is some reason to expect the naval sector to contract, but the value of shipping, fishing, oil and gas, and recreation all should increase.

Published in: Marine Policies Toward the 21st Century: World Trends and Korean Perspectives, S-Y Hong, ed., Occasional Paper No. 1:247-268, 1991.

Supported by: Department of Commerce, NOAA, National Sea Grant Program under Grant No. NA90-AA-D-SG480(R/S-20), Korea Ocean Research and Development Institute, and the Marine Policy Center. WHOI Contribution No. 7835.

INDUSTRIAL ORGANIZATION AND COMPETITIVE DYNAMICS IN MARINE ELECTRONIC INSTRUMENTATION

James M. Broadus, Porter Hoagland and Hauke L. Kite-Powell

Marine electronic instrumentation is a small but critically important area of high technology. Annual production of marine electronic instrumentation in the U.S. in on the order of \$3 to \$5 billion, with perhaps 20 to 30 percent of this being exported, and a smaller amount being imported. The world market for these products is estimated at about \$10 billion annually. Some general observations apply to the "industry" as a whole. With some variations across industry groups and sectors served, it is generally very competitive both in its structure and its behavior. Firms tend to seek out differentiated niches or specialties in product lines, but there are only modest barriers to mobility across product lines. A relatively few firms dominate the supply of large-scale systems development for military applications, but sales to most end-use sectors are fairly broadly-distributed across a number of small and medium-sized firms. Minimum efficient scale of operations in the industry appears to be low (though there may be unrealized economies of scale in both R&D and manufacture), and barriers to entry and exit are minimal for most product lines.

R&D intensity and the rate of inventiveness and innovation are particularly important to the success of firms in the marine electronic instrumentation industry. In the United States, the Navy is the most important factor in both R&D funding and procurement. Navy procurement of marine electronics products (estimated at 98 percent of federal total) is substantial, representing between 50 and 75 percent of U.S. domestic sales.

Published in: Oceans '91, 1:361-362, 1991.

Supported by: Marine Policy Center and NOAA/National Ocean Service through a grant to the Massachusetts Centers of Excellence Corporation, grant No. NA87-AA-D-M00037.

THE OCEANS AND ENVIRONMENTAL SECURITY

James M. Broadus and Raphael V. Vartanov

Environmental affairs have taken on geopolitical importance and the concept of environmental security is gaining currency as a way of thinking about international environmental management. It draws on the widely understood

notion of international, strategic interdependence (in facing threats of nuclear war or economic collapse) to focus attention on the similarly shared exposure to threats from global environmental degradation. Implicit in the concept is a direct link to a conventional understanding of international security arising from the potential for conflict over resource use and environmental practices.

The article describes joint research on environmental security and the world ocean involving the Woods Hole Oceanographic Institution (WHOI) and the Institute for World Economy and International Relations (IMEMO) of the Russian Academy of Sciences. Early in the collaboration a working definition was formulated: "Environmental security is the reasonable assurance of protection against threats to national well-being or the common interests of the international community associated with environmental damage." Critical problems of international environmental security were determined to be those that are likely to destabilize normal relations between nations and provoke international countermeasures. Eight cases are discussed: hazardous materials transport, nuclear contamination, sea-level rise, North Pacific fisheries depletion, Arctic Ocean sensitivities, the Southern Ocean, land- based marine pollution, and international law of the sea.

Published in: Oceanus, 34(2):14-19, 1991.

Supported by: The John D. and Catherine T.

MacArthur Foundation and the Soviet Peace
Research Institute.

MOULT STAGGERING IN THE AMERICAN LOBSTER: A STATISTICAL ANALYSIS

Diane F. Cowan, Jelle Atema and Andrew R. Solow

Hazlett (1991) correctly pointed out that our claim that female lobsters, Homarus americanus, stagger their moults was not based on statistical analysis (Cowan & Atema 1990). However, subsequent analysis supports our original conclusions. Here, in response to Hazlett's comments, we discuss the biological relevance of moult staggering, correct Hazlett's errors, and apply proper statistical methods to analyze our data.

Published in: Animal Behavior, 42:863-864, 1991.

Supported by: Marine Policy Center.

INTEGRATED ENVIRONMENTAL MANAGEMENT AND LAND-BASED POLLUTION IN THE EAST ASIAN SEAS

Mark E. Eiswerth

This article presents general observations from the intersection of two areas of research: one dealing with land-based pollution in Southeast Asia and the other, with cross-media pollutant transfers and integrated environmental management. Research on land-based marine pollution is one component of the ongoing collaborative research project, "Environmental Security and the World Ocean: Analytical Approaches and Shared Solutions," conducted jointly by the Institute of World Economy and International Relations, Academy of Sciences, USSR, and the Marine Policy Center, Woods Hole Oceanographic Institution (WHOI). The project focuses on principles of and threats to international environmental security; economic and legal analysis of their causes and possible prevention and control; comparisons of management approaches; and prospects for US-Soviet bilateral, as well as multilateral, cooperative actions.

Published in: Tropical Coastal Area Management, 5(3):6-9, 1990.

Supported by: The John D. and Catherine T.
MacArthur Foundation, the Soviet Peace
Research Institute, The Pew Charitable Trusts
and the Marine Policy Center.

WHOI Contribution No. 7637.

ELECTRONIC INSTRUMENTATION AND COASTAL RESOURCES MANAGEMENT IN THE 1990'S

Arthur G. Gaines, Jr.

This paper deals with the growing need for electronic instruments designed for use in monitoring and managing coastal resources. Increased activity in monitoring U.S. coastal waters is evident at many levels of government as well as in private organizations. For example, the EPA "bays program" beginning with Chesapeake Bay is a monitoring/management concept that has spread to regional water bodies around the country, such as Puget Sound, Narragansett Bay, Buzzards Bay, Massachusetts Bay and others. The very strong social context of environmental issues around the world, including eastern Europe and the former Soviet Union, suggest a more vigorous monitoring and management effort will be forthcoming, as governments respond to citizen based priorities. In this article, we focus on smaller local programs which will be needed in large numbers in the years to come.

Published in: Developing a National Marine Electronics Agenda: Proceedings of the Marine Instrumentation Panel Meeting, September 12-14, 1989, A.G. Gaines and K. Lindborg, eds., WHOI Technical Report 90-52, :87-96, 1990.

Supported by: NOAA/National Ocean Service through a grant to the Massachusetts Centers of Excellence Corporation, grant No. NA87-AA-D-M00037.

ELECTRONIC INSTRUMENTATION AND ENVIRONMENTAL SECURITY

Arthur G. Gaines, Jr.

"Environmental security" is a recent term drawing attention to the idea that some of the cold war connotations of "national security" have environmental or public health analogs-when actions by one nation have an inadvertent, adverse impact on another's environment. The definition of environmental security is still debated, but it generally implies significant, large scale environmental impacts bearing on a second nation's (or shared) public health, agriculture, natural resources, and/or other market and non-market assets. Impacts of large oil spills, large accidental releases of radioactivity, and voluminous industrial effluents could be examples of such activities; resulting diminished quality of life, loss of economic activity or natural resources, and disease could be examples of impacts. Recent discussions have gone so far as to include the topic of international mechanisms for legal and monetary remediation for breaches of environmental security.

Advances in electronic instrumentation for sensing, signaling, control, and integration hold many implications for detecting and preventing undesired environmental impacts surrounding human activities. This short discussion focuses on two areas in which we have ongoing programs.

Published in: Oceans '91, 1:369-370, 1991.

Supported by: Marine Policy Center and NOAA/National Ocean Service through a grant to the Massachusetts Centers of Excellence Corporation, grant No. NA87-AA-D-M00037.

THE NARROW RIVER: LABORATORY FOR SCIENCE AND MANAGEMENT

Arthur G. Gaines, Jr.

The Narrow River displays most of the post-glacial history of southern New England. A 10-mile trip from its tidal inlet at Narragansett

Beach in the south, to beyond its headwaters in the north, represents a trip backward in time; from the marshes, flats, and estuarine lakes of the souther area ("recently" flooded by the sea) to the ponds of the central portion that are still freshwater, to the dry kettle holes in the north, yet to be filled either by rising groundwater, or the rising ocean.

Published in: Maritimes, :1-2, May 1991. Supported by: Marine Policy Center.

SCIENTIFIC RESEARCH AND THE GALÁPAGOS MARINE RESOURCES RESERVE: SYNOPSIS OF A WORKSHOP APRIL 20-24, 1987, GUAYAQUIL, ECUADOR

Arthur G. Gaines, Jr. and Hernán Moreano Andrade

In 1986 the government of Ecuador established the Galápagos Marine Resources Reserve encompassing the entire Galápagos Archipelago, an area embracing 55,000 square kilometers of the Pacific Ocean and its underlying seabed. A workshop, sponsored by the National Science Foundation, was held on April 20-24, 1987, in Guayaquil, Ecuador, to address the role of scientific information in planning for the management of this new Marine Reserve. The "Scientific Research and the Galápagos Marine Resources Reserve Workshop" was jointly coordinated by the Marine Policy Center of the Woods Hole Oceanographic Institution, and the Oceanographic Institute of the Navy of Ecuador (Instituto Oceanográfico de la Armada).

Ten North American scholars and about thirty scholars from Ecuadorian governmental and non-governmental scientific organizations, concerned with issues related to the Galápagos, met to discuss the status of scientific information on marine areas surrounding these islands. The workshop also focused on the role this information should play inc rafting a management plan that will, a) recognize and mesh with environmental realities of this complex oceanic setting, b) incorporate new scientific information as it becomes available, and c) accommodate the needs of scientists working in the remote, typically harsh and often unique setting the A hipelago provides the international academic community.

Despite some important gaps, considerable scientific information is available to Reserve managers, and examples of the use of scientific information in other marine reserves is also available. Important areas of innovation are needed in order to gather and use information effectively for the management of this vast ocean area. Remote sensing technology and international cooperation offer promise in this regard.

Supported by: Marine Policy Center and the Oceanographic Institute of the Navy (Ecuador) with partial support from the National Science Foundation.

WHOI Technical Report 91-41.

AUKS AT SEA [REVIEW]

J. Christopher Haney

In this book review, I consider research results from a monograph entitled, "Auks at Sea." This volume presents the proceedings of a symposium sponsored by the Pacific Seabird Group in 1987 and is contribution number 14 to the series "Studies in Avian Biology" published by the Cooper Ornithological Society. "Auks at Sea" is the first attempt ever to address the marine biology of the only taxon of wing-propelled diving seabirds in the northern hemisphere. It contains 17 papers originating from work on 12 alcid species in the Bering Sea, Pacific coast of North America, and eastern and western North Atlantic Ocean. I evaluate the findings in the context of recent theories and paradigms concerning population regulation in seabirds, the influences of patch dynamics, and temporal/spatial scaling in resource availability.

Published in: The Auk, 108(4):996-999, 1991.

Supported by: Marine Policy Center and The Pew Charitable Trusts.

WHOI Contribution No. 7668.

THE PLIGHT OF CRANES: A CASE STUDY FOR CONSERVING BIODIVERSITY

J. Christopher Haney and Mark E. Eiswerth

Cranes provide an exemplary case for evaluating conservation policy because: 1) they are a charismatic group with high public visibility, 2) as migratory vertebrates they provide an umbrella for the protection of aquatic habitats and a wider set of species, 3) they are a widely-distributed avian family, consequently protection efforts have favored international cooperation, 4) genetic and taxonomic relationships have been studied, and 5) populations of at least seven crane species are threatened, endangered, or otherwise considered at direct risk. We use comparisons among the world's cranes to show how biogeographic, taxonomic, and genetic data bases can be linked for conservation decisions. We show that decisions typically faced by a conservation planner are themselves diverse (e.g., choosing species for captive propagation, or

identifying priority habitats for maintaining taxonomic distinctiveness), thereby obviating the utility of any single, all-purpose measure of diversity. Conservation priorities are shown to change with successive informational input regarding phylogenetic relationships, extinction risks, and population trends, and to differ greatly from priorities based on species richness alone.

Published in: Proceedings of the 1991 International Crane Workshop, 6:13-20, 1992.

Supported by: Marine Policy Center and The Pew Charitable Trusts.

WHOI Contribution No. 7727.

TESTING FOR RESOURCE USE AND SELECTION BY MARINE BIRDS

J. Christopher Haney and Andrew R. Solow

We describe an unfamiliar yet easily computed statistical procedure for determining dietary, habitat or other resource preferences of marine birds. The technique tests for significant differences between individual categories of observed and expected frequency data. We illustrate the procedure by examining marine habitat preferences of Short-tailed Shearwaters (Puffinus tenuirostris) and dietary preferences of Crested Auklets (Aethia cristatella) in the northwestern Bering Sea, Alaska. Compared to other analytical approaches typically used during field investigations of marine birds, this technique has both practical and statistical qualities that favor its application, including: 1) robust and easily-met assumptions, 2) control of the experiment-wise error rate, 3) flexible response to unforeseen logistical and sampling problems that frequently arise at sea, 4) greater specificity for determining resource preferences and 5) results based directly on counts of birds rather than samples of line transects or some other arbitrary observation interval.

Published in: Journal of Field Ornithology, 63(1):43-52, 1992.

Supported by: Minerals Management Service and U.S. Fish and Wildlife Service through Intraagency Agreement No. 14-12-0001-30391, the Marine Policy Center, and The Pew Charitable Trusts.

WHOI Contribution No. 7683.

RARE, LOCAL, LITTLE KNOWN AND DECLINING BREEDERS. A CLOSER LOOK: ALEUTIAN TERN

J. Christopher Haney, Jon M. Andrew, and David S. Lee

The Aleutian Tern (Sterna aleutica) is a rare and little-studied seabird confined to the Bering, Chukchi, and Okhotsk seas, with the world population probably numbering fewer than 25,000 individuals. We review the known breeding range, nesting biology, foraging and feeding habits for this species within the U.S. and U.S.S.R. Populations have low reproductive success due to subsistence hunting, inclement weather during the breeding season, and heavy predation on eggs and chicks. Aleutian Terns are vulnerable to environmental degradation within both their breeding (North Pacific) and suspected wintering grounds (southeast Asia). For conservation and management purposes, we recommend future research that can determine the sizes and stabilities of breeding populations, the degree and reasons for nest site tenacity, the age at which first breeding occurs, and the locations of non-breeding populations during summer.

Published in: Birding, 23(6):346-351, 1991.

Supported by: U.S. Fish and Wildlife Service, the Marine Policy Center, the John D. and Catherine T. MacArthur Foundation, and The Pew Charitable Trusts.

WHOI Contribution No. 7643.

AN OBSERVATION OF FEA'S PETREL

PTERODROMA FEAE

(PROCELLARIIFORMES:
PROCELLARIIDAE) OFF THE
SOUTHEASTERN UNITED STATES,
WITH COMMENTS ON THE
TAXONOMY AND CONSERVATION OF
SOFT-PLUMAGED AND RELATED
PETRELS IN THE ATLANTIC OCEAN

J. Christopher Haney, Craig A. Faanes, and W. R. P. Bourne

The soft-plumaged petrel and related species (Pterodroma spp.) remain one of the most poorly-known seabird taxa in the Atlantic Ocean, and there is cause for serious concern over the continued survival of two North Atlantic forms. Originally, soft-plumaged petrels were considered to be a single albeit morphologically-variable complex of a single species. however, taxonomists now generally consider the complex to contain at least three species including the nominate. We report a marine occurrence of a North Atlantic

species, probably Fea's petrel *P. feae*, from the South Atlantic Bight off the coast of the southeastern United States. We describe morphological characteristics for separating the various forms, and consider the recent at-sea sightings in relation to dispersal factors such as seasonal wind regimes and co-association with other seabird species that regularly migrate from eastern to western sectors of the North Atlantic Ocean.

In Press: Brimleyana.

Supported by: Marine Policy Center and The Pew Charitable Trusts.

WHOI Contribution No. 7763.

GEOMETRY OF VISUAL RECRUITMENT BY SEABIRDS TO EPHEMERAL FORAGING FLOCKS

J. Christopher Haney, Kurt M. Fristrup, and David S. Lee

Using geometric arguments, we calculate theoretical upper (20-30 km) and lower (0.7-6.2 km) limits to maximum horizontal distances over which volant seabirds can be visually recruited to joint Type I flocks in the open ocean. These are compared to empirical estimates for recruitment distances obtained from chumming experiments conducted in the western Atlantic Ocean off the southeastern United States. The product of arrival times and flight speeds for individuals (n = 164)joining 10 flocks indicated that potential recruitment distances were closer to the lower theoretical limits, with a mean distance of 4.5 km when flight time and ground speed were adjusted for detection lags, wind speed, and zigzag flight. Distances and time spans for mutual attraction among seabirds have important consequences for evaluating intra- and inter-specific interactions at the community level, as well as direct implications for sampling independence during distributional surveys that employ consecutive line transects or other sequential counting methods.

In Press: Ornis Scandinavica, 23(2), 1992.

Supported by: University of Georgia, Skidaway
Institute of Oceanography, South Carolina
Wildlife and Marine Resources Department,
NOAA/National Marine Fisheries Service,
Burleigh- Stoddard Fund, Sheldon Fund, NSF
grants OCE81-10707 and OCE81-17761, the
Marine Policy Center, and The Pew Charitable
Trusts.

WHOI Contribution No. 7712.

PROBLEMS IN THE MESO-SCALE INTERPRETATION OF SATELLITE CHLOROPHYLL DATA

Eric W. Henderson and John H. Steele

The satellite data for the North Sea show significant differences from in situ measurements when analyzed in terms of variance as a function of spatial scale. It seems likely that various factors in the instrument and in the data processing could produce changes in this variance distribution particularly at small scales (large wave numbers) of the order of 1 to 10 km.

For these reasons, it appears inappropriate to use the satellite data to infer conclusions about plankton dynamics in the meso-scale range.

In Press: Continental Shelf Research.

Supported by: The Vetlesen Foundation and the Marine Policy Center.

WHOI Contribution No. 7934.

ADVANCED MARINE TECHNOLOGIES AND HISTORIC SHIPWRECK MANAGEMENT

Porter Hoagland

Rapid technological advances recently have increased access to submerged cultural resources, such as historic shipwrecks. As access to the resource becomes less costly and as more people become aware of its existence and potential value, demand for the resource expands and the potential for conflicts over resource use may increase. The presence of actual or potential conflicts may give rise to political forces that reshape the ethical rules of professional societies or existing legal institutions, such as U.S. federal and state laws.

The study of problems in the management of historic shipwrecks affords a better understanding of the relationship between technological advance and public policy formulation. We often think of the formulation of public policy as a reaction to technological advance. Discoveries are made and innovations are created, shifts occur in the distribution of wealth among individuals in society, and government policies are developed to rectify perceived inequities or to resolve conflicts. It should be recognized, however, that the relationship between technology and public policy involves feedback effects: public policy can influence both the rate and scope of technological advance.

If public policies are established that restrict activities associated with commercial salvage, combined underwater archaeology and commercial salvage, or even the practice of underwater archaeology itself, then we can expect to see adverse effects on the development of technologies useful specifically for these applications. But this expectation does not suggest that laissez faire management of historic shipwrecks is appropriate. In many cases, very strong arguments can be put forward to preserve specific historic shipwrecks. It is important to recognize that, as public policy is formulated, if its effects on the pace and scope of research and development of marine technologies are ignored, then the benefits to society of technological developments could be lost.

Submitted to: Sea History.

Supported by: NOAA, National Sea Grant Program
Office, Grant No. NA90-AA-D-SG480 (E/L3-PD

WHOI Contribution No. 7823.

THE ADVANCED MARINE ELECTRONICS INSTRUMENTATION INDUSTRY AND THE EUROPEAN MARKET: GOVERNMENT POLICIES AND INTERNATIONAL COMPETITIVES

Porter Hoagland and Hauke L. Kite-Powell

We present the preliminary results of a series of 39 interviews with government officials and industry representatives in seven European countries concerning the influence of national and international government policies on the nature and development of the European marine electronic instrumentation (MEI) markets. We describe the importance of the marine sector to European countries producing MEI technologies. Using some very restrictive assumptions, we estimate the size of the MEI market in European (about \$1.2 billion in 1987) to be roughly half the size of the U.S. market. European institutions are undergoing rapid changes, including recent increased emphasis on collaborative "technology transfer" type research efforts across sectors (following the U.S. lead) and across national borders. We expect broadly defined marine markets to grow in Europe, thereby having a positive effect on the markets for marine electronics. But the extent to which U.S. firms can continue to participate and maintain their position in the markets for MEI products and services in Europe remains uncertain. The best policy for U.S. firms may well be one of cautious optimism and close attention to the potential for strategic alliances with established and emerging European

Published in: Developing a National Marine Electronics Agenda, A.G. Gaines and K. Lindborg, eds., WHOI Technical Report 90-52, :13-32, 1990. Supported by: Marine Policy Center and NOAA/National Ocean Service through a grant to the Massachusetts Centers of Excellence Corporation, grant No. NA87-AA-D-M00037.

EUROPEAN ADVANCED MARINE ELECTRONIC INSTRUMENTATION: A U.S. PERSPECTIVE

Porter Hoagland and Hauke L. Kite-Powell

This article presents a U.S. perspective on the influence of government policies on the nature and development of advanced marine electronic instrumentation (MEI) technologies in Europe. U.S. firms traditionally have enjoyed a strong international competitive advantage in the MEI field, but European institutions are undergoing rapid changes that may affect the competitive position of firms in advanced technology industries. These include the consolidation of firms in specific markets and the increased emphasis on centralized. collaborative 'technology transfer' research efforts across sectors and across national borders. We expect broadly defined marine markets to grow in Europe. The best policy for U.S. firms may well be one of cautious optimism and close attention to the potential for business relationships with established and emerging European firms.

Published in: Marine Policy, 15(6):431-454, 1991.

Supported by: Marine Policy Center and NOAA/National Ocean Service through a grant to the Massachusetts Centers of Excellence Corporation, grant No. NA87-AA-D-M00037.

WHOI Contribution No. 7785.

LEGAL AND POLITICAL ISSUES OF THE ANTARCTIC LEGAL REGIME

Christopher C. Joyner

Three major issues of political and legal significance have challenged Antarctic diplomacy in recent years. First, despite success in 1988 by the Antarctic Treaty Consultative Parties (ATCPs) to negotiate a special convention to regulate Antarctic mineral activities, that effort was rendered politically stillborn when two critical claimant ATCP members, Australia and France, decided in 1989 to oppose the agreement and advocated instead establishment of an international wilderness preserve status for the Antarctic, under which any mining activities would be permanently banned. This decision touched off diplomatic tensions between ATCP states which favored creation of a minerals regime and those which sided with the Australian-French position.

Emerging from the minerals debate came a second prominent issue for the ATCPs, namely how best to fashion a special legal regime to ensure comprehensive environmental protection for the Antarctic. Convening in a special meeting at Vina del Mar, Chile in late 1990 and at Madrid, Spain in April 1991, the ATCPs produced the draft text for a Protocol to the Antarctic Treaty on Environmental Protection. This protocol obligates parties to consider the Antarctic as a natural preserve devoted to science, and commits them to comprehensive environmental protection of the region's environment. Four annexes to the protocol dealing with waste disposal and waste management, conservation of Antarctic flora and fauna, marine pollution, and environmental impact assessment were also negotiated. Regarding minerals and mining, the protocol prohibits any activity other than scientific research.

A third major issue turns on how best to conserve and manage living resources in the circumpolar oceans. Since 1982, the Convention for the Conservation of Antarctic Living Resources (CCAMLR) has operated towards this end. It has, however, enjoyed only mixed success. The CCAMLR has facilitated scientific assessments concerning biomass and distribution of living marine resources in the Antarctic, but the accuracy of those data remains uncertain, largely due to reporting problems and unstandardized data collection formats. The CCAMLR Commission has successfully attained agreement to close specific sectors of the Southern Ocean for times when fishery stocks are depleted, to impose minimum mesh sizes for nets, and to implement an inspection system of fishing vessels within the area. Even so, certain distant water fishing states have forestalled the adoption of stricter conservation policies for the region in the Commission's deliberations.

The lesson gleaned from these issues is clear: While the Antarctic Treaty System may not be threatened, only good faith, diplomatic negotiations and political compromise can produce mutually beneficial solutions to serve the best interests of both ATCPs states and all mankind.

In Press: Proceedings, Conference on Maritime Issues in the 1990's.

Supported by: The George Washington University and the Marine Policy Center.

WHOI Contribution No. 7787.

DIFFERENTIATING USE AND NONUSE VALUES FOR COASTAL POND WATER QUALITY IMPROVEMENT

Yoshiaki Kaoru

Evaluation of benefits from water quality improvement is an important part of cost-benefit analyses for achieving efficient management of marine resources. This paper measures benefits of water quality improvement at three coastal ponds on Martha's Vineyard in Massachusetts. Use, option and existence values are elicited from owners of properties on Martha's Vineyard. A statistical test for comparing existence values between users and nonusers of the ponds rejects the assumption of weak complementarity. Results from a selection bias model indicate exclusion of protest as well as missing bids does not cause significant biases for estimating respondents' willingness to pay. Individual socioeconomic characteristics are found to have distinctively different effects for explaining use, option and existence values. These findings emphasize importance of nonuse value from water quality improvement and socioeconomic characteristics for explaining different categories of values.

Submitted to: Environmental and Resource Economics.

Supported by: The Pew Charitable Trusts, the Marine Policy Center and the Edgartown Harbor Association, Inc.

WHOI Contribution No. 7752.

VALUING MARINE RECREATION BY THE NESTED RANDOM UTILITY MODEL: FUNCTIONAL STRUCTURE, PARTY COMPOSITION AND HETEROGENEITY

Yoshiaki Kaoru

As increased attention on marine pollution problems calls for improvements of marine environmental quality, evaluation of benefits from water quality improvements provides important information for cost-benefit analyses. Random utility models (RUM) have been frequently used to evaluate recreation benefits. This paper discusses and evaluates four issues on which the analyst has not paid much attention in describing recreational site choices and implementing the RUM for benefit measurement: (1) implications of estimating a nested RUM on functional structure of the underlying indirect utility function, (2) effects of party composition on recreational decisions and benefit estimates, (3) heterogeneity in individual characteristics and benefit estimates, and (4)

variation in benefit estimates across quality improvement scenarios about how and where in the model quality variables are improved. A three-level nested RUM is estimated and benefits of water quality improvements are measured for marine recreational fishing in the Albemarle-Pamlico Estuary of North Carolina. These four issues are found to be important for describing recreational behavior and measuring benefits of water quality improvements.

Submitted to: Journal of Environmental Economics and Management.

Supported by: North Carolina Sea Grant Program, Woods Hole Independent Study Award, The Pew Charitable Trusts and the Marine Policy Center.

WHOI Contribution No. 7809.

AN OVERVIEW OF TECHNOLOGY TRANSFER AND INTELLECTUAL PROPERTY MANAGEMENT BETWEEN MARINE SCIENCE RESEARCH INSTITUTIONS AND THE COMMERCIAL SECTOR

Hauke L. Kite-Powell and Porter Hoagland

In this paper, we examine nonprofit/commercial interactions in the field of oceanography, using the Woods Hole Oceanographic Institution (WHOI) as an example. The technology transfer and intellectual property management policies and practices of WHOI are examined and compared to those of universities, federally funded R&D centers, and nonprofit scientific organizations in other fields of research endeavor.

By way of introduction, we outline a number of issues that face nonprofit research institutions when they consider ways to enhance technology transfer. These issues are not necessarily novel, but they may be receiving renewed attention as a result of changing national trends in research sponsorship (a growing share of private vs. public funding for R&D) or modifications of government policies (patent law changes, tax code amendments, and federal technology transfer policy changes). The pursuit of private funding in the present time of tight public budgets is leading many nonprofit research institutions to look more closely at technology transfer as a potential source of revenue.

Published in: Developing a National Marine Electronics Agenda: Proceedings of the Marine Instrumentation Panel Meeting, September 12-14, 1989, A.G. Gaines and K. Lindborg, eds., WHOI Technical Report 90-52, :40-51, 1990.

Supported by: Marine Policy Center and NOAA/National Ocean Service through a grant

to the Massachusetts Centers of Excellence Corporation, grant No. NA87-AA-D-M00037.

IS THERE A GLOBAL WARMING PROBLEM?

Andrew R. Solow

Although the global warming issue has been raised periodically over the past fifty years, it has now caught the public's eye and promises to be the premier environmental issue of the 1990s and beyond. To those who follow this issue, it seems that there is some debate within the scientific community over whether it is a serious one. In many ways the broad outline of this debate has remained unchanged over the past fifty years. Atmospheric science and climatology have advanced quite a lot over that period, however, and the details of the debate are somewhat clearer. The purpose of this chapter is to outline current scientific understanding of the global warming issue as a means of providing background to the debate.

Published in: Global Warming: Economic Policy Responses, R. Dornbusch and J.M. Poterba, eds., The MIT Press, Cambridge, :7-28, 1991.

Supported by: Instituto Bancario San Paolo di Torino.

MODEL-CHECKING IN NON-STATIONARY POISSON PROCESSES

Andrew R. Solow

An approach to assessing the fit of a parametric non-stationary Poisson process model to data is presented. The approach uses kernel estimation in conjunction with a parametric bootstrap. An example is given.

In Press: Applied Stochastic Models and Data Analysis.

Supported by: Marine Policy Center.

WHOI Contribution No. 7844.

DECISION-MAKING AND THE VALUE OF INFORMATION UNDER UNCERTAINTY

Andrew R. Solow and James M. Broadus

An approach to decisionmaking and the value of information under uncertainty is presented. This approach is based on Bayesian decision theory. The approach is developed in the context of an actual case study concerning responding to uncertain future sea level at Long Beach Island, New Jersey.

In Press: Environment and Emerging Development Issues, P. Dasgupta and K-G. Maler (eds.), Oxford University Press, 1992.

Supported by: World Institute for Development
Economics Research, United Nations University
and The Pew Charitable Trusts.

WHOI Contribution No. 7650.

MAPPING WATER QUALITY BY LOCAL SCORING

Andrew R. Solow and Arthur G. Gaines

The mean density of bacteria in a water body is commonly monitored using quanta assay. This paper describes the use of local scoring in estimating the spatial distribution of mean density from quantal assay results at a set of point locations. An application to estimating the mean density of fecal coliform bacteria in a coastal pond is presented. Model diagnostics based on a parametric bootstrap are also presented.

In Press: Canadian Journal of Statistics.

Supported by: Marine Policy Center and the Edgartown Harbor Association, Inc.

WHOI Contribution No. 7906.

ON THE MEASUREMENT OF BIOLOGICAL DIVERSITY

Andrew R. Solow, Stephen Polasky and James M. Broadus

In optimizing strategies aimed at the conservation of biological diversity, it is necessary to compare the consequences of competing strategies for biological diversity. This paper presents a general approach to this problem. An example concerning the conservation of crane species is given.

In Press: Journal of Environmental Economics and Management.

Supported by: The Pew Charitable Trusts and the Marine Policy Center.

WHOI Contribution No. 7875.

THE STATISTICAL ANALYSIS OF WHISTLE EXCHANGES IN DOLPHINS

Andrew R. Solow, Peter Tyack, and Laela Sayigh

A method for analyzing whistle exchanges in dolphins is described. The goal of the analysis is to detect and describe dependence between the timing of whistles in two whistle sequences. The method is based on modelling the whistle exchange as a stationary bivariate point process and estimating the cross-intensity function using kernel methods. An application to two whistle exchanges between a mother and her calf reveals a strong asymmetry, with the mother responding to the calf's whistles out the calf not responding to the mother's whistles.

In Press: App. od Statistics.

Supported by: Marine Policy Center and NIH under Grant No. R29BC00429-03.

WHOI Contribution No. 7764.

CAN ECOLOGICAL THEORY CROSS THE LAND-SEA BOUNDARY?

John H. Steele

Terrestrial and marine ecological research are usually carried out in different institutions, published in different journals and funded from different sources. There are obvious disparities in space and time scales of processes; for example, trees compared with phytoplankton as primary producers; and the structure of their physical and chemical environments are quite distinct. Yet many common problems exist-patch dynamics, food web topology, density dependance. Especially there are questions about the nature of the biotic/abiotic relations in the two environments.

These comparisons are discussed across sectors particularly in the context of space and time scale interactions between biological processes and the physical milieu. It is proposed that theories developed in one sector can be tested most critically in the other, with potential for greater generality. These extensions are often peripheral to research but the present focus on "global ecosystem dynamics" makes integration of these components a central and pressing issue.

Published in: Journal of Theoretical Biology, 153:425-436, 1991.

Supported by: Woods Hole Oceanographic Institution, National Science Foundation Grant No. OCE-9024396 and the Marine Policy Center.

WHOI Contribution No. 7811.

MARINE ECOSYSTEM DYNAMICS: COMPARISON OF SCALES

John H. Steele

When marine and terrestrial ecological systems are compared at the same time scales, there are very great differences in their relations with their physical environments. Similarities arise

when comparisons are made at different time scales. There are significant consequences for management.

Published in: Ecological Research, 6:175-183, 1991.

Supported by: Woods Hole Oceanographic Institution, National Science Foundation Grant No. OCE-9024396 and the Marine Policy Center.

MARINE FUNCTIONAL DIVERSITY

John H. Steele

The practical implication of land-sea functional diversity is that it would be inappropriate to apply terrestrial perspectives to marine communities, particularly in the context of management or conservation. Although marine systems may be much more sensitive to alterations in their environments, they may also be much more adaptable.

Published in: BioScience, 41(7):470-474.

Supported by: Woods Hole Oceanographic Institution, National Science Foundation Grant No. OCE-9024396 and the Marine Policy Center.

WHOI Contribution No. 7684.

THE ROLE OF PREDATION IN PLANKTON MODELS

John H. Steele and Eric W. Henderson

Models of carbon and nitrogen cycles in the ocean are a major tool in elucidating short- and long-term patterns of chemical fluxes. Variability in space and time are usually attributed to changes in ocean physics at different scales. This paper stresses the significance of the upper (predatory) closure in these simple nutrient-plant-herbivore models. The mathematical form used to close the system and the values given to the parameters have very marked effects on the overall response. In particular the major differences between North Atlantic and Pacific patterns may depend on this aspect as much as on the physical cycles. It is shown that the selection of different closure forms in five recent modelling studies corresponds to differences in the nutrient dynamics and plankton cycles. Thus, the general character of the results from these models will depend on both the form of the mortality closure and the parameter values used. Our ignorance in both areas is considerable.

Published in: Journal of Plankton Research, 14(1):157-172, 1991.

Supported by: Woods Hole Oceanographic Institution, National Science Foundation Grant No. OCE-9024396 and the Marine Policy Center.

WHOI Contribution No. 7815.

INNOVATION IN ENVIRONMENTAL POLICY

T. H. Tietenberg, Ed.

This important new book is an indispensable guide to the development and implementation of environmental policy. It presents authoritative analyses and state of the art summaries which will be essential both to scholars and practitioners trying to keep abreast of the most recent developments in this fast changing field.

The book sheds new light on two areas of environmental policy-liability law and enforcement-which are experiencing dramatic change. It shows how economic analysis can provide useful and meaningful insights about subjects such as criminal penalties, private enforcement, liability for oil spills, tort remedies and lender liability which have hitherto only been considered by lawyers. Drawing on the latest advances in both economics and law, it critically assesses how the most recent innovations in liability law and enforcement are actually working in practice.

Published in: Innovation in Environmental Policy, Edward Elgar Publishing, Ltd., United Kingdom, 269 pgs., 1992.

Supported by: Marine Policy Center, The Pew Charitable Trusts, and Resources for the Future, Inc.

PALEOSHORELINES AND THE PREHISTORY OF BARBUDA, WEST INDIES

David R. Watters, Jack Donahue and Robert Stuckenrath

The recognition of the position of ancient shorelines can be a critically important portion of the environmental interpretation of archaeological sites. Of equal importance is the determination of the cause as well as rate of change for a shoreline position. It is essential to know whether either the sea level or a land area adjacent to the ocean has been undergoing progressive change (and how rapidly) during the course of prehistoric occupation in a region. This can vary from a situation as in the Shumagin Islands, where tectonic uplift is extreme, to the case of Barbuda, where both sea level change and land movement are relatively small.

Published in: Paleoshorelines and Prehistory: An Investigation of Method, Lucille L. Johnson, ed. CRC Press, Boca Raton, :15-52, 1992.

Supported by: Marine Policy Center, the Anne L. and George H. Clapp Charitable and Education

Trust, the M. Graham Netting Research Fund, and the Edward O'Neil Research Fund of the Carnegie Museum of Natural History.

RECENT DEVELOPMENT IN LEGAL PROTECTION OF HISTORIC SHIPWRECKS IN P.R. CHINA

Hongye Zhao

Historic shipwrecks represent significant elements of human history and have become integral parts of the cultural heritage of mankind. China has a long maritime history and is very rich in historic shipwrecks. Facing a recent increase in treasure hunting for historic shipwrecks under China's seas, the Chinese government has become more concerned about the protection of marine cultural resources. In 1989, China enacted her Regulation on Protection and Administration of Underwater Cultural Relics, which provides a legal framework for the protection and management of historic shipwrecks in China. Under this Regulation, China asserts jurisdiction over historic shipwrecks not only in her internal waters and territorial sea but also in other sea areas under China's jurisdiction. Furthermore, China reclaims the ownership of historic shipwrecks originating from China found within these waters. The issues of jurisdiction over and title to historic shipwrecks beyond the territorial sea are matters not only of municipal law but also international law, which determines the jurisdictional limit of coastal States. From the approaches of international and comparative law, this article analyzes China's assertions and claims regarding historic shipwrecks in different maritime zones. In addition, it addresses some relevant issues such as Chinese authority for the protection of historic shipwrecks, procedures for archaeological exploration and excavation of historic shipwrecks, and recent marine archaeological discoveries in China.

In Press: Ocean Development and International Law, 23(4), 1992.

Supported by: Marine Policy Center.

WHOI Contribution No. 7808.

GRADUATE STUDENTS

Abstracts of papers of theses submitted in 1991 by graduate students of the Woods Hole Oceanographic Institution Doctoral Degree Program and the Woods Hole Oceanographic Institution/Massachusetts Institute of Technology Joint Program in Oceanography/Oceanographic Engineering. Other papers authored or coauthored by graduate students are included in the departmental sections.

GEOTHERMAL HEAT FLUX FROM HYDROTHERMAL PLUMES ON THE JUAN DE FUCA RIDGE

Karen G. Bemis

Estimates of the heat output of hydrothermal vents, identified along the Endeavor and Southern Segments of the Juan de Fuca Ridge, are used to evaluate the total heat flux associated with hydrothermal circulation for the ridge segment. An array carried by D/V ALVIN samples the temperature and velocity structure of hydrothermal plumes from individual vents. The maximum heat flux calculated for a single vent is 50 MW, but the average vent output is only 13 MW per vent for 31 vents. The estimates for any given vent may very over an order of magnitude. This uncertainty is due mainly to the difficulty of locating the centerline of the plume relative to the point of measurement, although the uncertainty in determining the constants from the appropriate equations based on laboratory experiments contributes a significant share to the net error. For the Endeavor Segment, the minimum total geothermal heat flux due to hydrothermal circulation exceeds 70 MW. The minimum estimate for the Southern Segment is 16 MW. The maximum estimate is probably closer to the total heat flux (236 MW and 66 MW respectively). The estimated heat flux density is 3300 W/m² for the Endeavor vent field and 39 W/m² for the Southern vent field. Focused hydrothermal venting accounts for only a small fraction of the heat available according to steady-state predictions of conductive heat flux; however, other hydrothermal phenomena (e.g. diffuse flow) account for the greater share of the total hydrothermal heat flux.

Supported by: NSF Grant No. OCE87-14511 and WHOI Education Office.

OBSERVATIONS OF WAVE-MEAN FLOW INTERACTION IN THE PACIFIC EQUATORIAL UNDERCURRENT

Esther C. Brady

The contribution of tropical instability waves to the momentum and energy balances of the Pacific Equatorial Undercurrent is investigated using velocity and temperature time series from the three-dimensional Equatorial Pacific Ocean Climate Study mooring array at 110°W. Tropical instability waves are an energetic band of variability typically with periods between 14 and 36 days which are thought to be generated by instability of the equatorial currents. They are frequently observed as meanders of the equatorial

front in satellite sea surface temperature maps. Here, they are observed as large oscillations in the meridional velocity records at 110° W with an energy peak at 21 days. Westward phase propagation is observed in this band with a phase speed of $-0.9~(\pm 0.3)~{\rm m~s^{-1}}$ and a wavelength of $1660~{\rm km}$. Upward phase propagation is observed which is consistent with downward energy propagation. The observed propagation characteristics are compared with those of the mixed Rossby-gravity wave.

The variability in this band produces large northward fluxes of eastward momentum and southward fluxes of temperature which affect the dynamics of the mean Undercurrent through the Reynolds stress divergence, and the Eliassen-Palm flux divergence. The waves produce a northward flux of eastward momentum, uv, which is largest at the northern mooring in the upper part of the array. The meridional divergence of eastward momentum, $-\partial(uv)/\partial y$, decelerates the Undercurrent core down to 150m. This implies a coupling between the Undercurrent and the South Equatorial current with the eastward momentum of the Undercurrent transferred to the westward flowing South Equatorial Current. To estimate the vertical momentum flux divergence, the vertical eddy flux of eastward momentum, uw, is inferred using the eddy temperature equation. The vertical eddy momentum flux is positive and largest at the core and a deceleration below. The Eliassen-Palm flux divergence is small above the core of the Undercurrent at 75 m, but below the core, is sufficient to balance the deeply penetrating eastward pressure gradient force.

The instability waves are important to the energetics of the mean Undercurrent. An exchange of kinetic energy from the mean Undercurrent to the waves through shear production is estimated. A local exchange is suggested since the rate at which the mean undercurrent loses kinetic energy through instability is comparable to the rate at which the waves gain energy through shear production. The conversion from mean to eddy potential energy is an order of magnitude smaller with the waves gaining potential energy through conversion of mean available potential energy. The observations of upward phase propagation and downward Eliassen-Palm flux suggest that the waves propagate energy downward into the deep ocean.

The energetics and momentum balance of the mean Undercurrent is investigated further by analyzing the downstream change in the Bernoulli function on the equator along isentropes or potential denisty surfaces using mean hydrographic sections at 150°W and 110°W. A downstream decrease in the Bernoulli funcation is observed which is due to a decrease in the Acceleration Potential since the mean kinetic energy of the

Undercurrent changes little from 150°W to 110°W. The lateral divergence of eddy momentum fluxes calculated on isotherms is sufficient to balance the observed decrease in the Acceleration Potential. The downstream decrease in the Acceleration potential has further implications for the mean energetics since this "downhill" flow releases mean available potential energy stored in the east-west sloping thermocline. The rate at which the Undercurrent releases available potential energy, is shown to be comparable to the rate at which the mean flow loses kinetic energy by interaction with the waves, with the waves gaining kinetic energy in the process. Thus, it is hypothesized that in the eastern Pacific this downstream release of available potential energy is ultimately converted into a downstream increase in the kinetic energy of the waves rather than the kinetic energy of the mean flow as occurs in the western Pacific. To maintain an equilibrium, the waves radiate energy into the deep ocean as is suggested by the upward phase propagation and the downward Eliassen-Palm flux.

Supported by: National Science Foundation.

IMPLEMENTATION AND EVALUATION OF A DUAL-SENSOR TIME-ADAPTIVE EM ALGORITHM FOR SIGNAL ENHANCEMENT

John R. Buck

This thesis describes the implementation and evaluation of an adaptive time-domain algorithm for signal enhancement from multiple-sensor observations. The algorithm is first derived as a noncasual time-domain algorithm, then converted into a casual, recursive form. A more computationally efficient gradient-based parameter estimation step is also presented. The results of several experiments using synthetic data are shown. These experiments first illustrate that the algorithm works on data meeting all the assumptions made by the algorithm, then provide a basis for comparing the performance of the algorithm against the performance of a noncasual frequency-domain algorithm solving the same problem. Finally, an evaluation is made of the performance of the simpler gradient-based parameter estimation step.

Supported by: Massachusetts Institute of Technology.

THE MARINE GEOCHEMISTRY OF RHENIUM, IRIDIUM AND PLATINUM

Debra Colodner

The platinum group elements occur in low concentrations in most crustal materials.

Sedimentary enrichments above these low background levels are thought to arise only from very specific processes, and thus are relatively easy to interpret. The thesis describes aspects of the marine geochemistry of two of these elements, iridium and platinum, as well as a neighbor in the periodic table, rhenium. Because Pt and Ir are highly enriched in meteorites compared to the Earth's crust, variations in their concentrations have been interpreted as reflecting changes in the amount of cosmic material in sediments. Re is also scarce (<0.1 ppb) in most crustal materials, but is highly enriched in anoxic sediments, making it a very sensitive indicator of anoxic conditions. Our ability to interpret the sedimentary concentrations of these elements has been hampered by our lack of knowledge about their marine geochemistry and their behavior during sediment diagenesis. The thesis therefore attempts to answer two general questions: 1. Can Re, Ir and Pt be redistributed by the geochemical changes associated with early diagenesis of marine sediments? 2. What are the processes controlling Re enrichment in anoxic sediments?

Techniques were developed to measure Re, Ir and Pt in seawater, sediments and sediment pore waters. For all of these elements, this involves separation and preconcentration by anion exchange (Hodge et al., 1986 and Koide et al., 1987) and analysis by isotope-dilution, inductively-coupled plasma mass spectrometry, with flow injection to introduce the sample.

The distribution of Pt in the water column has been the subject of two recent studies with conflicting results (Goldberg et al., 1986 and Jacinto et al., 1989). In an attempt to resolve their differences, and to gain insight into the forms in which Pt arrives at the sediment-water interface, Pt was determined in two Atlantic and one Pacific profile. The results agree with neither of the former studies and reveal invariant concentrations with depth of 270±60 fM. The observed profiles indicate that Pt is relatively unreactive in the water column.

The post-depositional mobility of Re, Ir and Pt was investigated in North Atlantic abyssal sediments, where pelagic sediments are interspersed with relatively organic-rich turbidites. The emplacement of turbidite units leads to the reduction and partial dissolution of hydrogenous minerals in the pelagic sediments directly underlying them. Pt and Ir are cycled with manganese and cobalt, during this process, indicating a hydrogenous, relatively mobile form of these elements. Following emplacement, an oxidation front gradually penetrates through the turbidites, leading to the redistribution of many transition metals. In these sediments, Pt exhibits a peak at the redox boundary similar to that found for Cu and V, suggesting an association with

organic matter. These early-diagentic processes lead to variations in the concentrations of Pt and Ir that should not be confused with changes in cosmic flux when interpreting the geologic record.

In order to constrain the oceanic Re budget, Re was determined in seawater, river waters, sediment pore waters and the Black Sea. Two detailed open ocean profiles confirm predictions of conservative behavior for the element with a concentration of 44± pmol/kg. A survey of Re in rivers of the Orinoco Basin indicates a strong black shale source for the element. A transect through the Amazon Estuary suggests a possible desorptive flux of the element near the river mouth. The Orinoco and Amazon values, combined with several measurements in the Ganges-Brahmaputra Basin, allows calculation of a residence time for Re in seawater of approximately 750 ky.

Re concentrations in pore waters were determined at one oxic (Pacific) and one anoxic (Chesapeake Bay) site. The results are consistent with previous work which suggested that Re can only be enriched in sediments under reducing conditions. Additionally, Re does not appear to cycle with manganese oxides in the upper portion of sediments. Compared to Mo, Re is removed from pore waters deeper in the sediment column. Re was also compared to Mo and U in the Black Sea. Its distribution is similar to the other elements, with enrichment in surface relative to deep waters, and removal to sediments at or below the sediment-water interface. The residence time of Re in the Black Sea appears to be intermediate between that of Mo (100 y) and U (1000y).

Supported by: Woods Hole Oceanographic Institution through the Ocean Ventures Fund. Through the Massachusetts Institute of Technology, funding was provided by the Office of Naval Research, the National Science Foundation, a National Science Foundation Graduate Fellowship and an Ida Green Fellowship.

MANTLE CONVECTION, MELT MIGRATION AND THE GENERATION OF BASALTS AT MID-OCEAN RIDGES

Matthew J. Cordery

In this thesis I develop a thermodynamically self-consistent numerical model of melting, melt migration and mantle flow beneath a mid-ocean ridge. The models I explore consider sub-ridge mantle upwelling to have two components. The plate-spreading divergence of the lithosphere results in an upwelling beneath the ridge axis. Melting-induced density changes also result in a component of upwelling flow. The rate of plate spreading and the nature of the flow field determine the first order temperature structure of

the mantle. At some depth, the adiabatically rising mantle crosses its solidus and begins to melt. Loss of latent heat upon melting keeps the mantle temperature on its solidus throughout the melting regime. Melt separates from its host rock and rises to the surface under the influence of buoyancy forces and mantle flow-derived pressure gradients. Advection of heat by the melt carries heat to shallower depths and can result in further melting. Extraction of a basaltic melt from the mantle results in a reduction in the mantle density due to the finite size of the melting regime result in enhance upwelling near the ridge axis. This enhanced upwelling results in further melting due to the enhanced advection of thermal energy above the mantle solidus.

The mantle solidus used in this thesis is unique in that it depends not only upon pressure but upon the mantle model mineralogy and oxide composition as well. I assume explicitly that the mantle model mineralogy and oxide composition as well. I assume explicitly that the mantle mineralogy corresponds to that of a slightly depleted spinel lherzolite defined by the assemblage olivine, orthopyroxene, clinopyroxene, and aluminous spinel. Mantle composition is defined by concentrations of the following oxides: K₂O, Na₂O, CaO, FeO, MgO, TiO₂, SiO₂, Al₂O₃. Melt compositions are also defined by these same oxides. Melting is assumed to occur via a fractional mechanism. Melting begins at the pressure where the mantle temperature intersects the solidus and melting ends at the pressure where conductive cooling becomes important or clinopyroxene is lost as a mineral phase. Mantle density is calculated from the proportions of the minerals present and their Fe/Mg ratio.

The effects of heat transport by the melt and of varying the latent heat of melting are isolated by fixing the mantle velocity field to be that due to solely to the spreading of the lithospheric plates. The latent heat of melting causes the mantle temperature to lie along the solidus in accordance with the requirements of thermodynamics. A zero latent heat of melting would result in all of the manlte melting when it reaches a certain depth. A small (250 J kg⁻¹⁰C⁻¹) but finite latent heat of melting results in large melt production rates and a melting regime with a finite thickness and melting continues until clinopyroxene is lost as a phase. A more reasonable latent heat (450 J Kg⁻¹°C⁻¹) yields much smaller latent heats of melting because less melting is required for a given amount of energy. As a result, crustal thickness are lower for a small latent heat (3.0 vs. 4.7 km) and melting ceases at the pressure where conductive cooling becomes important. Advection of heat by the melt causes melting rates to increase, perhaps substantially depending upon melting rates and the degree to which melt is

focussed towards the ridge.

The effects of varying the mantle viscosity. spreading rates and melting-induced buoyancy forces are investigated. Increasing the half-spreading rate from 1 cm yr-1 to 8 cm yr-1 results in a widening of the melt regime because the depth to which conductive cooling is important becomes shallower. The width over which signficant melting occurs, however, is limited by the horizontal distance over which significant vertical mantle flow occurs (100 km). The flow field places an physical limit upon the crustal thickness as the spreading rate increases. Again, the minimum depth of melting is defined by the depth at which clinopyroxene is lost as a phase. Melt production rates are determined not only by the advection of heat by the mantle and melt, but by changes in the solidus temperature and its pressure derivative as well.

Melting-induced density changes in the mantle drive convection beneath the ridge. This effect is not important when the half-spreading rate is faster than 4 cm yr⁻¹ because viscous stresses dominate the small lateral variations in mantle density. At slow spreading rates (1 cm yr⁻¹), lateral density variations are larger due to the smaller dimensions of the melting regime. For a viscosity of 10¹⁹ Pa s, the density driven convection is weak resulting in a marked dependence of crustal thickness upon spreading rate. For a viscosity of 1019 Pa s, the density driven convection is weak resulting in a marked dependence of crustal thickness upon spreading rate. For viscosity of 10¹⁸ Pas, convection is more vigorous at the slowest spreading rate resulting in higher melting rates. Convection narrows the melting regime at the slow spreading rates but this does not prove an effective mechanis. 1 for focussing the melt to the ridge axis, especially at the faster spreading rates where convection is limited. Downwelling in the mantle is extremely limited due to the positive buoyancy of the residual mantle. At this viscosity, the crustal thickness is a constant function of spreading rate. For both iscosities, mantle flow-derived pressure gradients are nominal compared to melt buoyancy forces and the melt rises vertically resulting in broad crustal accretion zones at the surface.

If the mantle viscosity depends upon temperative and pressure then mantle viscosities are high (x10²⁰Pa s) in the conductive lid overlying the melting regime and low (10¹⁸Pa s) within the melting regime itself. The low viscosities in the melting regime allows convection to significantly reduce the spreading rate dependence of crustal thickness. The high viscosity in the conductive lid magnifies pressure gradients in the mantle. It is shown, however, that these enhanced pressure gradients are still an ineffective mechanism for focussing melt to the ridge.

Several geophysical observables (thermal topography, gravity anomalies, seismic travel time) are calculated for each model. For a fixed spreading rate, no detectable differences exist between models with different mantle viscosity parameters. The mantle model mineralogy is equally homogeneous as is the oxide composition of the aggregate primary melts. This indicates that some parameter other than spreading rate or mantle viscosity structure is responsible for the observed variation in mid-ocean ridge basalt chemistry.

Finally, a model is presented where in the permability of the mantle is allowed to be anisotropic. The argument is made that finite strain in the mantle affects the directional permeability of the mantle. If this anisotropy tensor is proportional to the square of the finite strain, then melt can be focussed to the ridge axis regardless of spreading rate.

Supported by: Massachusetts Institute of Technology.

A STUDY OF NORTH ATLANTIC VENTILATION USING TRANSIENT TRACERS

Scott C. Doney

The oceanic distributions of tritium (³H), ³He, and the chlorofluorocarbons (CFCs) can be used to contrain the time-scales of the major ventilation pathways for an ocean basin such as the North Atlantic. I present a new global model funcation, developed from a factor analysis of the WMO/LAEA data set, for predicting the spatial and temporal variability of bomb-tritium in precipitation. Model estimates for the atmospheric ³H delivery to the North Atlantic are recomputed and combined with advective ³H input estimates in a budget for the North Atlantic Basin. Key features of the model budget include refined estimates of the ³H vapor flux and southward advection of ³H in the low salinity, surface flow from the Arctic. Arctic tririum sources contribute about half of the observed increase (40%) in the decay corrected tritium inventory from the 1972 GEOSECS program and the 1981 TTO/NAS

The ³H concentration in the intermediate and deep waters for the sub-polar North Atlantic increased substantially between 1972 and 1981. A time dependent model for the ³H and ³He inflow to the abyssal Atlantic from the Nordic Seas is developed. The ³H and ³He distributions in the abyssal North Atlantic and Deep Western Current (DWBC) are also presented. A simple model of abyssal circulation is constructed using the model Nordic Seas overflow curves, the observed tracer gradients in the DWBC, and the GEOSECS and

TTO tracer inventories for the deep basins. Although the tracer concentrations in the boundary current are rather insensitive to the velocity of the boundary current, they do place bounds on the magnitude of recirculation between the boundary current and the interior. On average, a volume equal to the boundary current transport is entrained/detrained over a length scale of about 5000 km. About half of the overflow water entering the western basin of North Atlantic since the mid-1960's has been mixed into the deep Labrador Sea and subpolar gyre.

The effects of tracer boundary conditions on thermocline ventilation and oxygen utilization rate estimates are discussed. Tracers that equilibrate rapidly with the atmosphere, such as ³He and the CFCs, have lower apparent ventilation time scales than tracers, such as tritium and radiocarbon, that are reset slowly in the surface layer. The results of a simple box mixing model are compared with tritium and ³He data from a 1979 survey of the eastern subtropical North Atlantic. On shallow density surfaces, the computed tritium ventilation rates are 'wo to three times slower than those for ³He; deeper in the thermocline, the two tracer ventilation rates converge. This trend may be related to the decreasing effectiveness of ³He gas exchange in equilibrating the deeper winter mixed layers of the more northerly isopycnal outcrops. Box models using limited surface exchange tracers (e.g. tritium and ¹⁴C) can under predict oxygen utilization rates (OUR) by up to 3 times due to differences between tracer and oxygen boundary conditions while ³He may overestimate OUR by 10-20%.

I present and discuss the distributions of two chlorfluorocarbons (CFCs) in the eastern North Atlantic measured on a 1988 hydrographic cruise between Iceland and the equator. CFC tages seawater fills the entire sub-polar water column and subtropical thermocline. Measurable CFC levels are found at the ocean bottom as far south as 35°N; the CFC penetration depth shoals to about 750 meters in the tropics. The CFC data are used to illustrate the ventilation time-scales for the water masses in the eastern basin and to calculate OUR values in the subtropical thermocline. The CFC data in the tropical oxygen minimum off of Africa are significantly lower than the values on similar density surfaces in the subtropics, providing support for the idea that the tropical oxygen minima are controlled primarily by physical rather than biological mechanisms. The evolution of the tropical and subtropical CFC distributions between the 1972-73 TTO/TAS program and the 1988 cruise are also examined. Other features of the CFC data include a clear signal of Labrador Sea Water mid-depth ventilation, a CFC-enriched overflow water boundary current along the Iceland slope, a northward flowing deep boundary current

along the eastern margin of the basin, and a mid-depth equatorial plume of upper North Atlantic Deep Water.

Supported by: National Science Foundation under Grant No. OCE-8615289 and Grant No. OCE-8800957.

ACOUSTIC SCATTERING FROM ELASTIC ICE: A FINITE DIFFERENCE SOLUTION

J. Robert Fricke

In this thesis I consider acoustic scattering from rough Arctic ice. Many scattering studies using the method of small perturbations (MSP) have been done; none are able to explain the low frequency scattering loss observed in long-range propagation experiments. Neither the magnitude nor the frequency dependence of the loss are properly modeled. Roughness and slope are required to be small if the MSP is to yeild solutions. While the average roughness of the ice in the Arctic satisfies the smallness criterion, both of the restrictions are violated by discrete, large pressure ridges for the important frequency band of 10-100 Hz. An empirical fit to the observed loss has been derived and may be written $L_e = 3f \frac{3}{2} dB/Km$, where f is frequency in

Reasoning that a full-wave solution holds the key to the scattering phenomenon, I use the finite difference method to solve the elastodynamic equations numerically. In contrast to the MSP, this technique allows arbitrary roughness. unrestricted in slope, displacement, or radius of curvature. Because of this feature, finite difference solutions provide direct, physical insight into the scattering mechanism of rough sea ice. The underlying analytic formulation treats the air-ice-water complex as a heterogeneous continuum in three dimensions. A place strain approximation reduces the formulation of two dimensions. This, in turn, limits the computational burden when computing the finite difference solution, while permitting the salient features of the scattering process to be studied.

Numerical experiments involving scatter from individual roughness elements are conducted. A broadband source excites the numerical grid and the interplay of acoustic and elastic energy is observed during the course of the experiment. Two classes of roughness elements are considered: pressure ridge formations, of various shapes and sizes, and an ice edge. The specular loss from an ice edge is too low to explain the observed scattering loss in the central Arctic. Newly formed pressure ridges in the Arctic are loose aggregations of ice blocks with free flooding interstitial voids.

These ridges cannot support shear strain and are modeled as fluid structures connected to elastic ice plates. Multi-year ridges, in contrast, are completely frozen and are better modeled as elastic structures.

Specular energy loss is affected by three identified phenomena: mass loading, excitation of place waves, and a material dependent power law. The first two phenomena affect the magnitude of the specular loss, while the last affects the frequency dependence.

- Specular energy loss is proportional to ridge cross sectional area for both fluid and elastic ridges, and for a fixed ice density, area is proportional to mass per unit length.
- For a 3 m ice place surrounding an elastic ridge, the excitation of place waves roughly doubles the specular loss relative to the loss of an identical ridge floating free. Loss from fluid ridges is unaffected by the presence or absence of a surrounding ice plate.
- Fluid ridges produce a dipolar diffraction pattern with a specular loss power law of $f\frac{3}{2}$, while elastic ridges produce a quadrupolar pattern and a power law of $f\frac{9}{2}$.

These results are used to argue the scatter from relatively young, large pressure ridges is the dominant scattering mechanism in long-range acoustic propagation. Future work with scale models at ultrasonic frequencies and full-scale experiments are required before this hypothesis can be fully tested.

Supported by: Office of Naval Research.

HUMAN FACTORS ENGINEERING IN SONAR VISUAL DISPLAYS

Lawrence Francis Galvin

Undersea technology is on the verge of equipping remotely operated vehicle (ROV) pilots with a three-dimensional (3-D), real-time display incorporating data from a wide variety of sensors including sonar (sound navigation and ranging), cameras, and lasers. Effective collection, computation, and presentation of this data to the pilot in a single display presents hardware, software and human factors problems. This thesis focuses on human factors issues associated with the display of information which could enhance the pilot's effeciency of performance. Background information on human factors engineering, 3-D computer graphics displays, and application of the 3-D perspective display precede the details of the experiment.

Five specific contains an amount and a second secon include altering the displayed field of view, providing a screen grid, displaying the current range to the target of interest, using a vertical color scheme, and controlling the display update rate. Seven tests measure the effects of these display enhancements on the simulated piloting of an ROV. The effects of the ROV simulation and operator learning curves are removed to compare perfomance changes due to the various enhancements directly. Operator comments during and after testing as well as test monitor/author observations provide insight into the experiment. Test result implications for system design trade-offs are discussed in detail. Recommendations for future research and the proposed construction of a fully equipped ROV simulator complete the work.

Supported by: U.S. Navy.

NEAR-EQUATORIAL DEEP CIRCULATION IN THE INDIAN AND PACIFIC OCEANS

Gregory C. Johnson

Theory and observations of deep circulation in the near-equatorial Atlantic, Indian and Pacific Oceans are reviewed. Flow of deep and bottom water in the near-equatorial Indian and Pacific oceans, the two oceans with only a southern source of bottom water, is described through analysis of recent CTD data. Zero-velocity surfaces are chosen through use of water-mass properties and transports are estimated. Effects of basin geometry, bottom bathymetry and vertical diffusivity as well as a model meridional inertial current on a sloping bottom near the equator are all discussed in conjunction with the flow patterns inferred from observations.

In the western equatorial Indian Ocean, repeat CTD surveys in the Somali Basin at the height of subsequent northeast and southwest monsoons show only small differences in the strength of the circulation of the bottom water (potential temperature $O < 1.2^{\circ}C$). A deep western boundary current (DWBC) carrying about $4x10^6m^3s^{-1}$ of this water is observed moving north along the continental rise of Africa at 3°S. The cross-equatorial section suggest that the current turns eastward at the equator. The northern section show a large mass of the coldest water in the interior east of the Chain Ridge, augmenting the evidence that the DWBC observed south of the equator turns east at the equator rather than remaining on the boundary, and feeds the interior circulation in the northern part of the basin from the equator. The circulation of deep water $(1.2^{\circ}C < O \le 1.7^{\circ}C)$ in the Somali and Arabian Basins is also analyzed. A DWBC flowing

southward along the Carlsberg ridge in the Arabian Basin is described.

In the central equatorial Pacific Ocean a recent zonal CTD section at 10°N, allows estimation that $5.0x10^6m^3s^{-1}$ of Lower Circumpolar Water (LCPW, $O < 1.2^{\circ}C$) moves northward as a DWBC along the Caroline Seamounts in the East Mariana Basin. In the Central Pacific Basin, 8.1x10⁶m³s⁻¹ of LCPW is estimated to move northward along the Marshal Seamounts as a DWBC at this latitude. An estimated $4.7x10^6m^3s^{-1}$ of the LCPW moves back southward across 10°N in the Northeast Pacific Basin along the western flank of the East Pacific Rise an dan equatorial jet is observed to flow westward from 138°W to 148°W shifting south of the Line Islands at 2.5°S, 159°W. The net northward flow of LCPW across 10°N in the Pacific Ocean is estimated at $8.4x10^6 m^3 s^{-1}$. The net southward flow of the silica-rich North Pacific Deep Water $(NPDW, 1.2 < O \le 2.0^{\circ}C)$ in the central Pacific Ocean estimated at $2.7x10^6m^3s^{-1}$ is also discussed.

In the Indian Ocean, the eastward equatorial flow in the bottom water of the Somali Basin differs from the prediction of a flat-bottom uniform-upwelling Stommel-Arons calculation with realistic basin geometry and source location. The behavior of a uniform potential vorticity meridional jet on a sloping bottom is examined in an attempt to explain the observed behavior at the equator. The inertial jet dows not cross the equator in a physically plausible fashion dowing to the constraint of conservation of potential vorticity. Mass and heat budgets for the bottom water of the Somali Basin are of interst with respect to the equatorial feature. Upwelling through the $O = 1.2^{\circ}C$ surface is estimated at $12 \pm 4x10^{-5}cms^{-1}$ and a rough heat budget for the deep Somali Basin results in an estimate of vertical diffusivity of $9 \pm 5cm^2s^{-1}at3800m$. Numerical model results indicate that large vertical diffusivities result in eastward jets in the bottom water at the equator.

In the Pacific ocean the DWBC observed flowing northward south of the equator crosses the equator with transport nearly intact, albeit split into two at 10° N by the tortuous bathymetry. However the southward flow along the East Pacific Rise in the Northeast Pacific Basin and the westward equatorial jet this flow feeds are puzzling. The basin depth decreases equatorward and eastward, which may allow some southeastward flow in the Stommel-Arons framework. However, the equatorial jet is still unexplained. The estimated vertical velocity and diffusivity at 3600 db of $2 \pm 2x10^{-5}cms^{-1}$ and $4 \pm 3cm^2s^{-1}$ for the area between 12° S and 10° N are much smaller than estimates in the Somali Basin.

Thus the two oceans, similar in their single southern source of bottom water, have DWBC's

which behave remarkably differently near the equator. In the Somali Basin of the Indian Ocean the DWBC appears to turn eastward at the equator, with large vertical upwelling velocity and large vertical diffusivity estimates for the bottom water of the basin. In the Pacific Ocean and DWBC appears to cross the equator, but there is a puzzling westward flowing equatorial jet in the bottom water of the Northeast Pacific Basin.

Supported by: Office of Naval Research and a Secretary of the Navy Graduate Fellowship in Oceanography.

PREDICTIONS AND OBSERVATIONS OF SEAFLOOR INFRASONIC NOISE GENERATED BY SEA SURFACE ORBITAL MOTION

Timothy E. Lindstrom

A model is developed for the prediction of the seismo-acoustic noise spectrum in the microseism peak region (0.1 to 0.7 Hz). The model uses a theory developed by Cato J. Acoust. Soc. Am., 89:1096-1112 (1991)] for an infinite depth ocean in which the surface orbital motion caused by gravity waves may produce acoustic waves at twice the gravity wave frequency. Using directional wave spectra as inputs, acoustic source levels are computed and incorporated into a more realistic environment consisting of a horizontally stratified ocean with an elastic bottom. Noise predictions are made using directional wave spectra obtained from the SWADE surface buovs moored off the coast of Virginia and the SAFARI sound propagation code, with a bottom model derived using wave speeds measured in the EDGE deep seismic reflection survey. The predictions are analyzed for noise level variations with frequency, wave height, wind direction, and receiver depth. These predictions are compared to noise measurements made in ECONOMEX using near-bottom receivers located close to the surface buoys. Good agreement is found between the predictions and observations under a variety of environmental conditions.

Supported by: U.S. Navy.

MASS, HEAT, OXYGEN AND NUTRIENT FLUXES AT 30°S AND THEIR IMPLICATIONS FOR THE PACIFIC-INDIAN THROUGH FLOW AND THE GLOBAL HEAT BUDGET

Alison M. MacDonald

Six hydrographic basinwide sections, two in each of the three major ocean basins, are employed

in a set of inverse calculations to determine the extent of exchange between the Pacific and Indian Oceans through the Indonesian Archipelago and the net global oceanic heat flux at 30°S.

Using a model which combines the data for the South Pacific and South Indian Oceans, it is found that even the largest existing estimates of Indonesian Passage through flow (20 Sv) are consistent with the data. However, the available information cannot limit the extent of the exchange, i.e. both smaller and larger through flows produce physically reasonable circulation patterns. The seasonal and interannual variations which have been found by other investigators and which we are incapable of resolving, lead us to conclude that in the long term mean an estimate of 10 Sv for the through flow is most reasonable.

Globally, at 30°S, we find a net oceanic heat flux of -1.1±1.7 PW, which is not significantly different from zero. It is dominated by a large (>1 PW) southward heat flux in the Indian Ocean. Large equatorward (0.8 PW) heat flux values in the South Atlantic Basin are not consistent with our data. We therefore conclude that although our data are consistent with some water following the warm water return path for NADW (Gordon 1986), the cold water path must play the dominant role in the maintenance of the global thermohaline cell associated with the formation process of NADW.

Supported by: Massachusetts Institute of Technology.

VACUOLATION, PROLIFERATION AND NEOPLASIA IN THE LIVER OF BOSTON HARBOR WINTER FLOUNDER

Michael J. Moore

Neoplasia has been found in the livers of bottom-feeding fish taken from heavily contaminated freshwater and marine habitats. This study examined the progressive development and ultimate diversity of liver neoplasia in winter flounder (Pseudopleuronectes americanus) from Deer Island Flats, Boston Harbor, Ma., USA., and encompassed histopathology, ultrastructural pathology, immunohistochemistry and experimental toxicology. It was found that liver neoplasia was most prevalent adjacent to a major sewage outfall, and that the predominant neoplastic cell type was cholangiocellular. Cholangiocellular neoplasms ranged from non-invasive tubular cholangiomas to invasive anaplastic cholangiocellular carcinomas. The latter were solid, tubular, cystic and scirrhous in form. Hepatocellular adenomas and carcinomas were also present, but only infrequently. Abnormally vacuolated hepatic epithelia were intimately associated with neoplasite lesions of all types.

These vacuolated cells were first seen in the center of the hepatic tubule, as vacuolated preductular biliary epithelial cells. Later, cells of the entire hepatic tubule were vacuolated. Foci of vacuolated cells were visible grossly, and often contained or were adjacent to neoplastic lesions. Vacuolation, biliary hyperplasia, aggregation of macrophages and necrosis were first seen in two year old fish. The lesions then appeared to progress, becoming more severe and prevalent as the fish grew. Of the fish for which age data were available, the youngest fish to contain a liver neoplasm was 5 years old. Prevalence of neoplasis did not differ between gender of fish. Liver neoplasia and vacuolation persisted in fish that were maintained in clean water on clean food for five months. However, the prevalence of vacuolation decreased with increasing distance from urban contamination, being absent in fish from Georges Bank.

Ultrastructional examination of winter flounder liver from clean and contaminated sites revealed a loss of hepatic glycogen and lipid stores with increasing environmental contamination, with a concomitant increase of abnormal proliferated endoplasmic reticulum (ER). Fluid accumulation in the cisternal space of the ER, and the perinuclear space and mitochondria led to vesicle formation. These vesicles coalesced, to from large cellular vacuoles that compressed the nucleus and residual cytoplasm to the margins of the cell. Vacuolation appeared to be a process that affected preductular cells, hepatocytes, cholangiocytes, neoplastic cells, and exocrine pancreatic cells. To assess the role of vacuolated cells in the progression to neoplasia, evidence for replicative nuclear DNA synthesis was sought by assaying for the nuclear incorporation of a nucleotide analog, bromodeoxyuridine (BrdU). Tissue sections from fish labelled with BrdU were stained immunohistochemically using an anti-BrdU monoclonal antibody. Constitutive DNA synthesis was observed in basal gill and intestinal epithelia, and renal hemopoietic cells. Increased levels of DNA synthesis were observed in vacuolated cells, hyperplastic biliary epithelia, and most particularly in neoplastic cells, some of which were vacuolated. These observations were taken to suggest that vacuolated cells were capable of DNA synthesis, and that this, along with their intimate spatial relationship with neoplastic cells implied that they may be involved in the progression to neoplasia. To further investigate these observations, attempts were made to recreate the feral disease in the laboratory. Methods were developed for atraumatic capture, transport and year round maintenance of winter flounder. Long term colonies were established and experiments designed to reproduce the situation in wild-caught fish. The long latency between first exposure of larvae to genotoxic carcinogens in the native fish

from Boston, and the actual appearance of neoplasia many years later, leads to the assumption that chronic exposure to epigenetic carcinogens was the rate limiting step in this neoplastic progression. Technical grade chlordane was chosen as representative of the hepatotoxic epigenetic carcinogens present in Boston Harbor sediments. Acute and subacute exposures were conducted, to establish the toxicity of the fish to chlordane, and to examine the resultant histopathology. A chronic feeding study was then conducted for one year, using chlordane and benzo(a)pyrene. Histological alterations induced in treated fish included elevated levels of macrophage aggregations, perisinusiodal edema, necrosis, and a proliferative reaction that involved the formation of structures that were apparently primitive biliary tubules.

These studies have shown that winter flounder exposed to chemical contaminants appear to undergo a set of histopathological changes that precede neoplastic change. Cellular vacuolation is a significant change that may be directly involved in the progression to neoplasia. It is a relatively common lesion and is an excellent marker in winter flounder for the detection of the chronic biological effects of the particular chemical contaminants in the Boston Harbor environment, at a stage long before overt neoplasia is evident.

Supported by: Public Health Service through Grant Nos. 5 RO1 CA 44306, 5 Ro1 ESO4220, the Ocean Ventures Fund, NOAA National Sea Grant College Program Office, Department of Commerce, under Grant No. NA86AA-D-SG090, the Donaldson Charitable Trust and the Massachusetts Water Resources Authority under Contract No. 0045.

GLOBAL POSITIONING SYSTEM MEASUREMENT OF CRUSTAL DEFORMATION IN CENTRAL CALIFORNIA

Mark H. Hunter

In Chapter 2, we develop a conventional terrestrial reference frame-designated SV6-for the analysis of Global Positioning System (GPS) observations. The reference frame adopts the geocentric origin and scale defined by eleven years of satellite laser ranging (SLR) observations. The precise relative locations of 80 sites that primarily realize the SV6 frame are derived from very-long-baseline interferometry (VLBI) observations. The orientation is consistent with the International Earth Rotation Service terrestrial reference system. The coordinates of sixteen sites with well-determined local vector ties between collacted VLBI and SLR reference pointes used to make the VLBI coordinate system commensurate

with the SLR system; the sites are globally distributed, including nine in North America, three in Europe, and one each in China. Australia, Hawaii, and Kwajalein. A scales of the VLBI and SLR systems differ by 4±1 parts in 10⁹. SV6 includes estimates of the temporal evolution and uncertainties of the coordinates from VLBI and geophysical observations and we develop a methodology for systematically combining temporally heterogeneous space-geodetic observations with geophysical and geological information, such a global plate tectonic motion models.

In Chapter 3, we present estimates of crustal deformation in central California from thirteen GPS campaigns, conducted primarily by a consortium of four universities from December 1986 to February 1991. Each major campaign occupied a network of seven to twenty sites in California repeatedly for four to five days, with additional fiduciary control provided by sites distributed across North America, and in Hawaii and Europe. The precision of the estimated baseline vectors, based on the day-to-day scatter over each campaign, is 3-5 mm in the horizontal components with 1-3x10⁻⁸ dependence on baseline length for well-designed experiments. The precision in the vertical is 15-25 mm. Precision is most strongly affected by changes to the fiducial network and ionospheric conditions. Systematic constant error sources may be responsible for a slight increase in long-term scatter over short-term scatter.

We then estimate relative motion between twelve sites in California that have observations spanning 1.5-4.2 years with uncertainties at the 1-1.5 mm/yr level. Confidence in some of the estimated rates is limited by apparent inconsistencies between experiments with poor fiducial control. The estimated relative motions of Owens Valley and Palos Verdes with respect to Vandenberg are consistent with VLBI-derived rates. We estimate north-south convergence across the eastern Santa Barbara channel at 5.2 mm/yr, and our results are consistent with a change to left-lateral shear in the central Santa Barbara channel. The estimated deformation across the Santa Maria fold and thrust belt has less convergence and more right-lateral shear than had been previously estimated from triangulation and trilateration measurements. The relative motion of six sites along the western margin in the vicinity of Vandenberg are consistent with 2-4 mm/yr motion on the Hosgri fault. Relative motion east of the San Andreas suggests that an additional 2-4 mm/yr motion may be accommodated within a shear zone located in Owens Valley and the Mojave Desert.

Supported by: Massachusetts Institute of Technology.

DEVELOPMENTAL CHANGES IN THE STRUCTURE AND FUNCTION OF LOBSTER HHEMOCYANIN

Kirby S. Olson

Respiratory systems function as one of the interfaces between an organism and its environment; the flexibility of this system may therefore constrain the distributional limits of the organism. The respiratory system of a substantial number of marine invertebrate species, particularly amongst the decapod crustaceans, contain hemocyanin as the oxygen binding protein. Previous investigations have revealed a great deal about the structural and functional properties of this respiratory pigment, but a number of important questions remain unanswered. No strong correlation has yet been established between differences in the structure of the oligomer or the diversity of its subunits and the functional properties of the protein. The link between anatomy, habitat, and hemocyanin structure or function is also still unclear in many areas. This thesis was designated to examine aggregate size, subunit composition, and oxygen binding properties of hemocyanin in the larval, juvenile, and adult stages of Homarus americanus. These studies elucidate the relationship between structure and function of hemocyanin, and provide some insights on larval ecology as well.

Hemocyanin occurs in all larval stages of the American lobster in concentrations between 8 and 12 mg/ml; concentration in the adult is about five times that of the larval stages. Calculations of cardiac output based on preliminary measurements of heart rate and heart size for the first three larval stages indicate that the oxygen bound to the hemocyanin may be required for routine

respiration.

The ratio of hexameric and dodecameric forms of hemocyanin were determined for each of the stages under study. Stage I and II larvae possess almost exclusively hexameric hemocyanin, but stage III larvae have almost equal proportions of the two forms. The dodecamer predominates in the fourth stage larvae, and is the only form found in the juvenile lobster. Adult lobster hemolymph appears to contain both forms, but only the dodecameric hemocyanin has an absorption peak characteristic of oxygen binding at the hemocyanin active site.

Oxygen binding curses were constructed for all stages and showed sigmoid oxygen binding curves typical of hemocyanin. Oxygen binding curves for larval stages I, II, and IV and the juvenile were similar to each other and showed no significant change between the two temperatures. Curves for stage III had a position and shape intermediate to

that of the other larval stages and that of the adult. The Bohr shift showed a significant increase at stage III, but no additional significant changes occurred in the slope prior to or subsequent to that stage. Cooperativity showed no trend with pH at any stage, except possibly in stage I.

SDS-PAGE gels of the hexamer and dodecamer of hemocyanin in each of the stages of the lobster provided information on the number of types of monomers in the aggregates. The larvae starts out with a hexameric hemocyanin consisting of a single type of monomer. At the third stage a second type of monomer is added. This type of monomer is present in small amounts in the stage III hexamer, but in the dodecamer of stage III it occurs in the same proportion as the first type of monomer. The presence of the second type of monomer in an equal concentration correlates with the appearance of the substantial proportion of dodecameric hemocyanin. These two structural changes are reflected in a significant increase in the slope of the Bohr shift. In adult lobsters a third type of monomer is present; there is no change in aggregate size or Bohr shift at this point, but the oxygen tension required for saturation of half the sites on the pigment (the P_{50}) is significantly lower. Addition of SDS types of monomer occurs during larval development in the lobster and appears to alter aggregate size, response to pH changes, and the P₅₀, although cooperativity is unaffected.

Supported by: NOAA Saltonstall-Kennedy Project under Grant NA89-EA-D00014, and NOAA Grant No. NA87-AA-D-OMO93.

GLOBAL ISOTOPIC SIGNATURES OF OCEANIC ISLAND BASALTS

Lynn A. Oschmann

Sr, Nd and Pb analyses of 477 samples representing 30 islands or island groups, 3 seamounts or seamount chains, 2 oceanic ridges and 1 oceanic plateau [for a total of 36 geographic features] are compiled to form a comprehensive oceanic island basalt [OIB] data set. These samples are supplemented by 90 selected mid-ocean ridge basalt [MORB] samples to give adequate representation to MORB as an oceanic basalt end-member. This comprehensive data set is used to infer information about the Earth's mantle. Principal component analysis of the OIB+MORB data set shows that the first three principal components account for 97.5components [EMI, EMII, HIMU and DMM] are required to completely encompass the range of known isotopic values. Each sample is expressed in terms of percentages of the four mantle components, assuming linear mixing. There is significant correlation between location and isotopic signature within geographic features, but not between them, so discrimination analysis of the viability of separating the oceanic islands into those lying inside and outside Hart's (1984, 1988) DUPAL belt is performed on the feature level and yields positive results.

A "continuous layer model" is applied to the mantle component percentage data to solve for the spherical harmonic coefficients using approximation methods. Only the degrees 0-5 coefficients can be solved for since there are only 36 features. The EMI and HIMU percentage data sets must be filtered to avoid aliasing. Due to the nature of the data, the coefficients must be solved for using singular value decomposition [SVD], versus the least squares method. The F-test provides an objective way to estimate the number of singular values to retain when solving with SVD. With respect to the behavior of geophysics control data sets, only the degrees 2 spherical harmonic coefficients for the mantle components can be estimated with a reasonable level of confidence with this method.

Applying a "delta-function model" removes the problem of aliasing and simplifies the spherical harmonic coefficient solutions from integration on the globe to summation over the geographic features due to the properties of delta-functions. With respect to the behavior of geophysi... control data sets, at least the degree 2 spherical harmonic coefficients for the mantle components can be estimated with confidence, if not the degrees 3 and 4 as well. Delta-function model solutions are, to some extent, controlled by the nonuniform feature distribution, while the continuous layer model solutions are not.

The mantle component amplitude spectra, for both models, show power at all degrees, with no one degree dominating. The DUPAL components [EMI, EMII and HIMU], for both models, correlate well with the degree 2 geoid, indicating a deep origin for the components since the degrees 2-3 geoid is inferred to result from topography at the core-mantle boundary. The DUPAL and DMM components, for both models, correlate well [and negatively] at degree 3 with the velocity anomalies of the Clayton-Comer seismic tomography model in the 2500-2900 km depth range [immediately above the core-mantle boundary. The EMII component correlates well [and positively] at degree 5 with the velocity anomalies of the Clayton-Comer model in the 700-1200 km depth range, indicating a subduction related origin. Similar positive correlations for the geoid in the upper lower mantle indicate that subducted slabs extend beyond the 670 km se mic discontinuity and support a whole-mantle convection model.

Supported by: U.S. Navy.

SURFACE-REFERENCED CURRENT METER MEASUREMENTS

Markku Junani Santala

A general discussion of possible techniques for observation of near-surface currents indicates that the surface-following frame of reference will provide several advantages over the Eulerian or Lagrangian frames. One problem will surface-following measurements is the biasing effects of the waves. A technique for making unbiased measurements is developed. This technique requires that both the sensor velocity and the fluid velocity be measured. A sensor platform, the Surface Acoustic Shear Sensor (SASS), which makes the required measurements is described.

The processing scheme for interpreting the measurements from the SASS is described at length. The data that SASS has obtained from two deployments in the Shelf Mixed Layer Experiment (SMILE) is presented. This data shows clearly that the biasing effects of waves can not, in general, be ignored. In the summary of the data we find suprisingly little shear in the downwind direction in the top 4 m of the watercolumn. In the crosswind direction observed, observed shear seems to be indicative of an across shelf pressure gradient and intense near-surface mixing.

Supported by: National Science Foundation through Grant No. OCE-87-16937.

UPPER OCEAN DYNAMICS DURING THE LOTUS AND TROPIC HEAT EXPERIMENTS

Rebecca R. Schudlich

This thesis examines the effect of mean large-scale currents on the vertical structure of the upper ocean during two recent observational programs: the Long Term Upper Ocean Study (LOTUS) and the TROPIC HEAT experiments. The LOTUS experiment took place in the northwest Atlantic Ocean, a mid-latitude region away from strong mean currents, and extended over one entire seasonal cycle. The TROPIC HEAT experiments took place in the central equatorial Pacific Ocean during two 12-day periods in 1984 and 1987, at opposite extremes of the seasonal cycle. We use observations from these field experiments as well as one-dimensional numerical models of the upper ocean to analyze the dynamics of the vertical structure of the upper ocean at the equator and in mid-latitudes. Due to the different nature of the observations, we focus on the long term mean structure of the upper ocean in the LOTUS observations (Chapters 2 and 3), and on the diurnal cycle in the equatorial

upper ocean in our analysis of the TROPIC HEAT

observations (Chapters 4 and 5).

In the LOTUS observations, we find that the observed current is coherent with the wind over low frequencies (greater than an inertial period). Using a wind-relative averaging method we find good agreement with Ekman transport throughout the first summer and winter of the LOTUS experiment, with the exception of a downwind component in the wintertime. The mean current spiral is flat compared to the classic Ekman spiral, in that it rotates less with depth than does the Ekman spiral. The mean current has an e-folding depth scale of 12 m in the summer and 25 m in the winter.

Diurnal cycling is the dominant variability in the summer and determines the vertical structure of the spiral. In the winter, diurnal cycling is almost non-existent due to greatly reduced solar insolation. There is a persistent downwind shear in the upper 15 m during the winter which may be partially due to a bias induced by surface wave motion but which is also consistent with a logarithmic boundary layer.

The Price et al. (1986) model is reasonably successful in simulating the current structure during the summer, capturing both the mean and the diurnal variation. The model is less successful in the winter, though it does capture the overall

depth scale of the current spiral.

In our analysis of the TROPIC HEAT observations, we extend the Price et al. (1986) model to the equatorial upper ocean. The model is initialized with the stratification and shear of the Equatorial Undercurrent (EUC), and is driven with heating and wind stress. A surface mixed layer is determined by bulk stability requirements, and a transition layer below the mixed layer is simulated by requiring that the gradient Richardson number be no less than 1/4. A principal result is that the nighttime phase of the diurnal cycle is strongly affected by the EUC, resulting in deep mixing and large dissipation at night consistent with observations of the equatorial upper ocean during TROPIC HEAT. Other features of the equatorial circulation (upwelling and the zonal pressure gradient) are of little direct importance to the diurnal cycle.

The daytime (heating) phase of the simulated diurnal cycle is unaffected by equatorial circulation and is very similar to its mid-latitude counterpart. Solar heating produces a stably stratified surface layer roughly 10 m thick within which there is little, O(3 x 10⁻⁸ W kg⁻¹), turbulent dissipation. The diurnal stratification, though small compared to the EUC, is sufficient to insulate the EUC from wind stress during the day. For the typical range of conditions at the equator, diurnal warming of the sea surface is 0.2-0.5 °C, and the diurnal variation of surface current (diurnal jet) is 0.1-0.2

m s⁻¹, consistent with observations.

The nighttime (cooling) phase of the simulated diurnal cycle is quite different from that seen at mid-latitudes. As cooling removes the warm, stable surface layer, the wind stress can work directly against the shear of the EUC. This produces a transition layer that can reach to 80 m depth, or nearly to the core of the EUC. Within this layer the turbulent dissipation is quite large, O(2 x 10⁻⁷ W kg⁻¹). Thus, the simulated dissipation has a diurnal range of more than a factor of five, as observed in the 1984 TROPIC HEAT experiment, though the diurnal cycle of stratification and current are fairly modest.

Dissipation estimated from the model is due to wind working directly against EUC, and is similar to observed values of dissipation in both magnitude and depth range. Overall dissipation values in the model are set by the strength of the wind stress rather than the structure of the EUC, and rise approximately like $\frac{u}{3}*$ for a given Undercurrent. This suggests that the lower values of dissipation observed in the 1987 TROPIC HEAT experiment were due to the lower wind stress values rather than the relatively weak Undercurrent.

The main findings of this thesis are: 1) When the diurnal cycle in solar heating is strong, it determines the local vertical structure of the upper ocean (in both the LOTUS and TROPIC HEAT observations). The price et al. (1986) model is its extension to the equator simulate the upper ocean fairly well when the diurnal cycle is strong. Under these conditions it is necessary to make measurements very near the surface (10 m depth) to fully resolve the wind-driven flow. 2) When surface waves are strong, surface-moored measurements of current may have a significant wave bias. To accurately estimate this bias, simultaneous measurements of current may have a significant wave bias. To accurately estimate this bias, simultaneous measurements of current, current meter motion, and surface waves are needed. 3) Mean currents strongly amplify the nighttime phase of the diurnal cycle in the equatorial upper ocean, and therefore alter the mean structure of the equatorial upper ocean.

Supported by: Office of Naval Research under Grant No. N00014-89-J-1053.

THE MODERN AND GLACIAL THERMOCLINES ALONG THE BAHAMA BANKS

Niall C. Slowey

As a primary feature of ocean circulation and a key component of the global carbon cycle, changes in the thermocline must be accounted for if we are to understand the processes involved in

Quaternary climatic fluctuation. Toward this goal, this thesis contains studies of the modern and glacial thermoclines at the Bahama Banks and it presents an novel approach to determine sea level based on the flux of ²³⁰Th and ²³¹Pa from thermocline waters to the seafloor.

In the first chapter, the hydrography of the modern thermocline in Northwest and Northwest Providence Channels, Bahamas, is investigated using CTD data. Potential temperature-salinity relationships demonstrate that the deep waters and most of the thermocline waters in these channels originates in the Sargasso Sea. Cross channel sections of water properties suggest the following: (1) water from the shallow core of the Deep Western Boundary Current (Fine and Molinari, 1988) may circulate along the channel margins, and (2) where the western end of Northwest Providence Channel opens to the Florida Straits, shallow flow is toward the straits in the southern portion of the channel and away from the straits in the northern portion.

In the next two chapters, changes in the temperature and nutrient structures of the thermocline from the last glaciation to the recent Holocene are inferred from isotopic variations of the planktonic foraminifera Globigerinoides ruber $(212-250 \ \mu m)$ and G. sacculifer $(300-350 \ \mu m)$ and the benthic foraminifera Planulina wuellerstorfi, P. ariminensis, P. foveolata and Cibicidoides pachyderma (250µm) in a suite of cores from the margins of Little and Great Bahama Banks. During the last glaciation, δ^{18} O values were from 1.4 to 1.9 per mil greater than during the recent Holocene. Based on the δ^{18} O/sea-level model of Fairbanks (1989), we estimate that the upper 1500 m of the water column was cooler by at least 1 °C-the deepest waters were several degrees cooler. The temperature gradient (dT/dz) was steeper and the base of the thermocline appears to have stayed at about the same depth or risen slightly. At all depths in the thermocline, δ^{13} C was greater during the last glaciation than during the recent Holocene by at least 0.1-0.2 per mil and as much as 0.6 per mil in the lower thermocline. While recent Holocene δ^{13} C reaches minimum values in the lower thermocline (the poorly-ventilated oxygen minimum/phosphate maximum layer), this feature was not present during the last glaciation. These data show that the concentrations of nutrients throughout the thermocline were reduced and that there was no oxygen minimum layer, indicating greater, more uniform ventilation of thermocline waters.

These results are consistent with our understanding of the physics of thermocline circulation and evidence for hydrographic conditions at the ocean surface during the last glaciation, indicating a direct response of thermocline circulation to changes in climate.

Cooler thermocline waters reflect cooler surface ocean temperature at mid-latitudes where thermocline isopycnal surfaces outcrop. Increased, more uniform ventilation of the glacial thermocline is consistent with both more vigorous glacial winds leading to increased Ekman pumping and all isopycnal surfaces of the thermocline outcropping in the area of Ekman downwelling. Taken together with previous studies of intermediate-depth waters, these data document that the entire upper water column of the North Atlantic was depleted in nutrients during the last glaciation. A final suggestion of the third study is that Mediterranean and southern source waters contributed little to deeper intermediate-depth waters in the North Atlantic.

The fourth chapter presents two new approaches to reconstruct the sea-level history based on the fluxes of ²³⁰Th and ²³¹Pa to the seafloor. The approaches rely on the fact that fluxes of these nuclides to a site on the seafloor are proportional to the height of the water column above the site. Consequently, a change in sea level causes changes in the ²³⁰Th and ²³¹Pa fluxes which, at shallow sites, are large fractions of the total fluxes. Past sea level can be reconstructed using either the record of nuclide accumulation in a single core of sediment, or nuclide concentrations in synchronously deposited sediment samples from cores collected over a range of water depths. Importantly, this record of sea level is both continuous (not just high stands) and independent of the assumptions of constant seawater temperature or uplift rate required by some other approaches.

Supported by: National Science Foundation.

ACOUSTIC WAVE SCATTERING FROM A RANDOM OCEAN BOTTOM

Dajun Tang

This thesis investigates low frequency acoustic wave scattering from the ocean bottom. It is divided into four parts. The first part models the ocean bottom as a fluid medium where sound speed and density are constants except a layer in which the density is still a constant, but the sound speed is composed of a large constant and superimposed with a small random component. It is assumed that the random sound speed is horizontally well correlated and vertically poorly correlated.

In the second part, an integro-differential equation method is used to calculate the scattering from that random layer. Emphasis is put on the study of the spatial correlation of the scattered field. It is found that the spatial correlation length of the scattered field is related to the correlation length of the scatterer, therefore is is possible to

invert the bottom correlation length by measuring the spatial correlation of the scattered fields using multiple receivers. Also included in this part are an estimation of energy loss in the coherent field, a discussion on the influence of bottom anisotrophy, and a comparison between the integro-differential equation method and the Born approximation.

The third part concerns the influence of the bottom roughness. A small roughness is added to the water/bottom interface and pertubation method is used to calculate the scattering from the roughness. Under the assumption that the roughness and the volume inhomogeneity are uncorrelated, comparisons are made on the scattering strengths between roughness scattering and volume scattering, and the spatial correlation of the total scattered field is evaluated. It is found that at low frequencies, volume scattering cannot be ignored when the seafloor is not very rough, and it is possible to distinguish the two scattering mechanisms by measuring spatial correlations of the scattered field.

In the fourth part, the classical definition of the bottom scattering cross section is questioned, and a new set of parameters, the Scattering Correlation Coefficient, is introduced, which does not have the ambiguites associated with the coventional notion of the scattering cross section.

Supported by: Office of Naval Research under Contract No. N00014-86-C-0338.

DIFFUSE FLOW FROM HYDROTHERMAL VENTS

D. Andrew Trivett

The effluent from a collection of diffuse hydrothermal vents was modelled to determine the fate of this source of flow under typical environmental conditions at seafloor spreading centers. A laboratory simulation was conducted to test an analytic model of diffuse plume rise. The results showed that diffuse plumes are likely to remain near the seafloor, with their maximum rise height scaled with the diameter of the source of diffuse flow. The entrainment of ambient seawater into these plumes is limited by the proximity to the seafloor, thus slowing the rate of dilution.

The model of diffuse plume behaviour was used to guide 'a design and implementation of a scheme for monitoring the flow from diffuse hydrothermal vents in the ocean. A deployment of an array at the Southern Juan de Fuca Ridge yielded measurements of a variety of diffuse plume properties, including total heat output.

Two distinct sources of hydrothermal flow were detected during the field deployment. The larger source was 1-1.5km north of the instrument array, and its energy output was 450±270MW. A smaller

source was located 100m east of one instrument in the array. The energy output of this source was 12±8MW. The rise heights of the centerlines of these plumes were 45m and 10m, respectively.

Supported by: National Science Foundation through Grant OCE-8917448, NOAA National Sea Grant College Program Office, Department of Commerce, under Grant No. NA86-AA-D-SG090, Ocean Ventures Fund, and WHOI Friends of Vents through a Grant from the Mellon Foundation.

PROPULSION OPTIMIZATION FOR ABE, AN AUTONOMOUS UNDERWATER VEHICLE (AUV)

Thomas J. Woodford

The oceanographic community is moving towards unmanned autonomous vehicles to gather data and monitor scientific sites. The mission duration of these vehicles is dependent primarily on the power consumption of the propulsion system, the control system and the sensor packages.

A customized propulsion thruster is designed. This includes a specialized propeller tailored to ABE and a matched motor and transmission. A non-linear lumped parameter model of the thruster is developed and experimentally verified. The model is used to predict thruster performance and compare the design thruster with other variants of propeller and motor/transmission combinations.

The results showed that there is a trade-off between rapid dynamic response and power conservation. For the typical ABE trajectory, the designed thruster provides good dynamic response and the lowest power consumption of all the modelled thruster units.

Supported by: U.S. Navy.

THE STRUCTURE AND TRANSPORT OF THE BRAZIL CURRENT BETWEEN 27° AND 36° SOUTH

Jan C. Zemba

A set of four hydrographic sections through the Brazil Current are analyzed to identify downstream changes in the Brazil Current. The data, from the Thomas Washington Marathon Cruise, Leg 9, are at 27, 31, 34 and 36°S. The region they span details the change of the current from a relatively small near surface feature to a large, deep current. While the Brazil Current does not appear to develop transports as large as those found in the Gulf Stream, the calculated transports greatly exceed previous estimates. At

27°S the current extends down to approximately 700 m and transports 12 Sv southward; this value is consistent with previous estimates farther north. Downstream, surface layer transport increases, the current deepens, and the transport reaches a maximum of 80 Sv at 36°S. Part of the growth comes from the tight recirculation found just offshore of the Brazil Current. The recirculation strengthens and deepens to the south, with a minimum transport of 4 Sv north at 27°S and a maximum of 33 Sv at 36°S.

The change in the current is also reflected in its shear profiles. At 27°S Brazil Current shear is found only in the upper portion of the water column, over the continental slope. Downstream, the current moves off the slope into deeper water and develops top-to-bottom, monotonic shear. To obtain velocity from the shear profiles, zero velocity surfaces are chosed based on conservative use of tracer information.

A simple basin-wide model is used at 31°S to tie limits on the size of Brazil Current and recirculation to various limits on layer-to-layer exchanges south of the section. The multi-layer model - based on changes in depth of several isotherms - is used to extend the interpretation of the current beyond that of an isolated ocean feature. The model is required to conserve mass in each layer, either by applying barotropic transports or by allowing layer-to-layer exchanges south of the section. Solutions are deemed acceptable if the sense, or direction, of the various layer-to-layer conversions are consistent with accepted ideas of water mass formation. Initially, a two layer model is employed. Governed by the conservation of mass in each layer, the two layer model has only one constraint on the resulting solutions: a conversion of cold-to-warm water in the south (or the surface layer flowing north and the deep layer flowing south). Such a meridional flow pattern is consistent with the equatorward heat flux in the South Atlantic. The single constraint, however, is not strong enough to limit the solution region in any significant way. The final model presented has four layers, and acceptable solutions have the net transports of the surface layer and the bottom water northward and form intermediate water from North Atlantic Deep Water in the south. The resulting solution set has a fairly small range of transports for the Brazil Current, with surface layer transports between 20 and 35 Sv; this range is consistent with the value calculated from hydrographic data at 31°S. Given the complex interleavings of the South Atlantic water masses, the four layer model performs remarkably well.

Finally, total protential vorticity is calculated from the hydrographic sections. Centrary to what one might expect, the reference level choice is not a significant problem: where currents are large, most of the signal in relative potential vorticity comes from the measured shear, and where currents are small, the relative potential vorticity is not significant compared to the planetary vorticity. Unfortunately, the process of taking two horizontal derivatives of the density field results in a jittery relative potential vorticity signal. As a result, a clear potential vorticity profile could not be constructed for the current. This variability may be real – the ocean is frequently much noisier than one imagines. It may also be possible, though, to smooth the data sufficiently so that a cleaner picture emerges.

Despite the problems involved in obtaining a quantitative profile of the potential vorticity, qualitative changes are useful in detecting different flow regimes. By comparing the downstream changes in total and planetary potential vorticity, one can deduce frictional and inertial regimes in the different layers. The presence of a frictional regime at the inshore edge suggests that care should be taken in assuming that potential vorticity is conserved in western boundary currents. In addition the potential vorticity is conserved in western boundary currents. In addition the potential vorticity sections trace a pattern of the recirculation feeding into the Brazil Current in the upper layers; other tracers did not provide a clear image.

The final picture which emerges is not of a small, surface-trapped Brazil Current; rather, it is that of a classic western boundary current, increasing in strength and depth before turning east into the interior ocean.

Supported by: Office of Naval Research under Contract No. N00014-82-C-0019 and the National Science Foundation through Grant NO. OCE86-14486.

CIRCULATIONS AND WATER MASS BALANCES IN THE BRAZIL BASIN

Huai-Min Zhang

Based on the Levitus atlas, we find that the application of the Montgomery streamfunction to the isopycnal surfaces induces an error which can not be ignored in some regions in the ocean. The error arises from the sloping effect of the specific volume anomaly along isopycnal surfaces. By including the major part of this effect, new streamfunctions, namely the pressure anomaly and main pressure streamfunctions, are suggested for the use in potential density coordinates.

By using the newly proposed streamfunction and by including the variations of specific volume anomaly along isopycnal surfaces, the inverse model proposed by Hogg (1987) is modified for increasing accuracy and applied to the Brazil Basin to study the circulation, diffusion and water

mass balances. The equations in the model, i.e. the dynamic equation, continuity equation, integrated vorticity equation, and conservation equations for heat, salt and oxygen (in which a consumption sink term is allowed), are written in centered finite difference form with lateral steps of 2 degree latitude and longitude and 8 levels in the vertical. This system of equations with constraints of positive diffusivities and oxygen consumption rates is solved by the inverse method. The results indicate that the circulation in the upper oceans is consistent with previous works, but that in the deep ocean is quite different. In the NADW region, we find a coincidence of the flows with the tongues of water properties. The diffusivities and diapycnal velocities seem stronger in the region near the equator than in the south, with reasonable values. Diffusion plays an important role in the water mass balance. Examples show that similar property fields may result from different processes.

Supported by: Massachusetts Institute of Technology.

FLOW OVER FINITE ISOLATED **TOPOGRAPHY**

LuAnne Thompson

One and two layer models are used to study flow over axisymmetric isolated topography. Inviscid or nearly inviscid flow in which non-linear effects have order one importance is considered. and both the effects of β and finite topography are included.

A one-layer quasi-geostrophic model is used to find the shape of Taylor columns on both the f-plane and the β -plane in the inviscid limit of the frictional problem. In this limit, the boundary of the Taylor column is a streamline, and the velocity in both directions vanishes on the boundary. The fluid within the Taylor column is stagnant, corresponding to the solution that Ingersoll (1969) found for flow over a right circular cylinder on the f-plane. In this case, the Taylor column is circular. An iterative boundary integral technique is used to find the solutions for flow over a cone on the f-plane. In this case the Taylor column has a tear drop shape. Solutions are also found for flow on the β -plane over a cylinder, and the Taylor column is approximately elliptical for westward flow with the major axis in the x direction, while it is slightly elongated in the y direction for eastward flow. The stagnation point of the Taylor column is located on the edge of the topography for all the solutions found. It was not possible to find solutions for smooth topographic shapes.

Steady solutions for flow over a right circular cylinder of finite height are studied when the quasi-geostrophic appoximation no longer applies. The solution consists of two parts, one which is

similar to the quasi-geostrophic solution and is driven by the potential vorticity anomaly over the topography and the other which is similar to the solution of potential flow around an cylinder an dis driven by the matching conditions on the edge of the topography. When the effect of β is large, the transport over the topography is enhanced as the streamlines follow lines of constant background potential vorticity. For eastward flow, the Rossby wave drag can be much larger than predicted from quasi-geostrophic theory.

A two-layer model over finite topography using the quasi-geostrophic approximation is developed. The topography is a right circular cylinder which goes all of the way through the lower layer and an order Rossby number amount into the upper layer, so that the quasi-geostrophic approximation can be applied consistently. This geometry allows description of flow in which an isopycnal intersects the topography. The model is valid for a different regime that existing models of steady flow over finite topography in a continuously stratified fluid in which the bottom boundary is an isopycnal surface. The solutions contain the two components that are found in the barotropic model of flow over finite topography. The model breaks down when the interface goes above the topography which occurs more easily when the stratification is weak. Closed streamlines occur more readily over the topography when the stratification is weak, whereas in traditional quasi-geostrophic theory they occur more readily when the stratification is strong. Near the topography, the interface is depressed to the right and raised to the left (looking downstream).

A hierarchy of time-dependent models is used to examine the initial value problem of flow initiation over topography on the f-plane. A modified contour dynamics method is developed that extends the range of problems to which contour dynamics can be applied. The method allows boundary and matching conditions to be applied on a circular boundary. A one-layer quasi-geostrophic model is used to show that more fluid that originates over the topography remains there when the flow is turned on slowly than when it is turned on quickly. Flow over finite topography in a one-layer model shows a variety of different behaviors depending on the topographic height. When the topography has moderate height, two cyclonic eddies are created; when the topography fills up most of the water column, the fluid oscillates on and off the topography as it moves around the topography in a closkwise direction, and none of the fluid is shed downstream. Two quasi-geostrophic stratified models are considered, one in which the topography is small, and the other in which it is finite. In the small topography model, an eddy is shed which is cyclonic, warm-core, and bottom-trapped. In contrast, the

shed eddy is cyclonic, cold-core, and surface-intensified in the finite depth model using the geometry described above.

Supported by: Office of Naval Research.

Index	
Ackert, Robert P C-8	Buesseler, Ken O
Acosta, Juan	Buffler, R. TGG-5
Alatalo, Philip B-4	Burr, G. S
Altabet, Mark A	Butler, R
Anderson, Donald MB-1,13	Butman, Cheryl Ann AOPE-15,16
Andrade, Hernán MoreanoMPC-4	
Andrew, Jon M	Candela, Julio AOPE-3;PO-4,19
Arenovski, Andrea LB-1	Cann, Johnson R
Arnold, Maurice	Capuzzo, Judith McDowell B-3
Asper, V. L	Caron, David A B-2,3,15,16
Atema, Jelle MPC-3	Caruso, Michael PO-17
Aubry, Marie Pierre	Casso, Susan A
m 1 1	Castro, Belmiro AOPE-3
Bachelet, Guy	Caswell, HalB-3
Bacon, Michael P	Catipovic, Josko AAOPE-7,16
Ball, Lary A	Cavanaugh, Colleen B-3
Ballard, Robert D AOPE-12	Chan, L. H
Banta, G. T	Chapman, David CPO-1,17
Barbour, R. Lorraine	Chave, Alan D
Bauer, James E	Chiu, C. S
Belastock, Rebecca A	Chu, Dezhang
Bell, George IPO-14	Church, Thomas M. PO-17
Bemis, Karen G	Churchill, James PO-16
Bender, M	Clegg, Simon L
Berggren, William A	Cochran, J. Kirk
Bergström, Bo I	Cody, Chris WB-3
Berman, Mark S B-5,23	Cohen, Joel E
Berninger, UGB-2	Collins, John A
Berteaux, H. O AOPE-14	Colodner, Debra GS-2
Binford, Michael WGG-15	Connors, Donald N PO-16
Blanding, Wayne R AOPE-4	Conway, Noellette B-3
Blough, N. V	Cordery, Matthew J
Blusztajn, J	Cormier, Milton J B-18
Bocconcelli, A AOPE-14	Cornillon, Peter C PO-16
Bock, Erik JAOPE-8	Cowan, Diane FMPC-3
Boden, LindaAOPE-9	Cox, C. S
Bolmer, S. T	Crescenti, Gennaro HPO-21
Bond, GaryPO-21	Curry, William B
Bonilla, J	Curtis, Jason H
Bothner, Michael H	D 1 16 1
Bourne, W. R. P MPC-6	Daher, Mary Ann B-24
Bowen, Andrew	Dahl, Peter HAOPE-12
Bowlin, James BAOPE-9,17	Davis, Cabell S
Boyle, Edward A	Delaney, M. L. C-16 Delcroix, Thierry PO-1
Brady, Esther CGS-1	
Bremner, J. M	DeLong, Edward F
Brenner, Mark	Denton, George H
Brewer, Peter G	Deschamps, J. R
Brichet, Evelyne	Deuser, Werner G
Brigham, Lawson W MPC-1	Dever, Edward PPO-21
Broadus, James MMPC-1,2,10	Dick, Henry J. B
Brocher, Thomas M	Diebel, Carol E
Broda, James EAOPE-14	Dister, Brian
Brook, Edward J	Donaghay, Percy B-23
Bryden, Harry LPO-9	Donahue, D. J
Buck, John R GS-2	Donahue, JackMPC-12

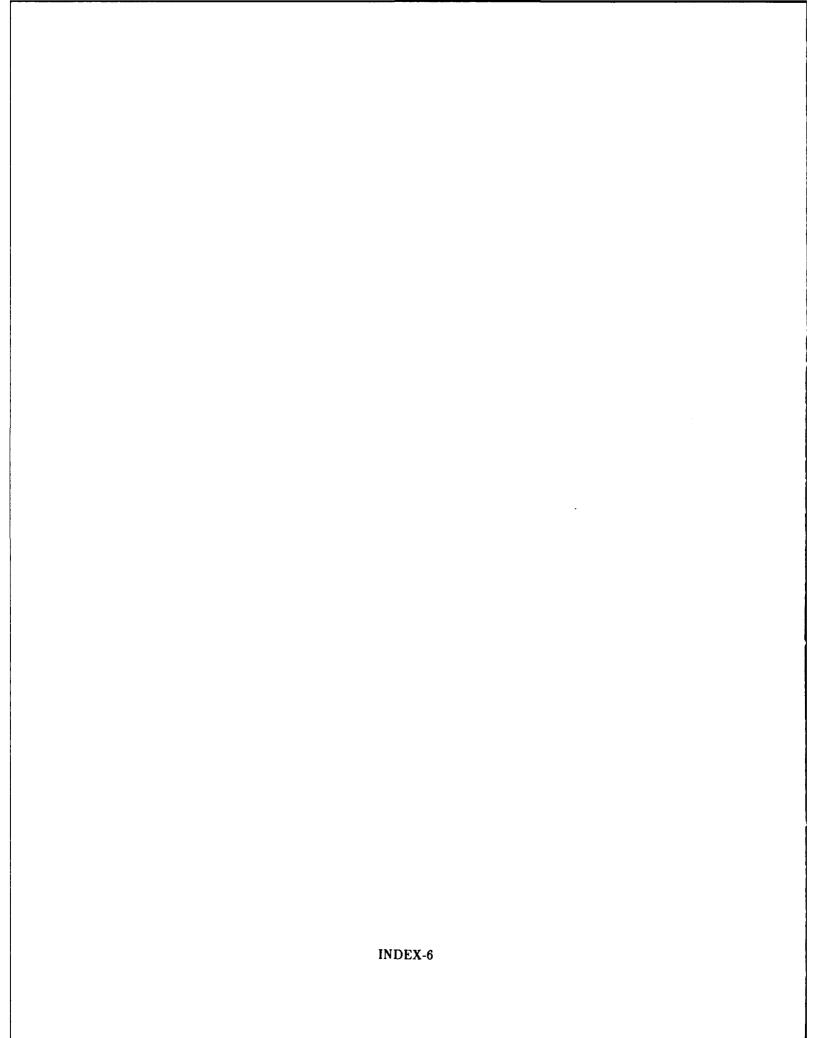
Doney, Scott C	German, C. R
Dorsey, Kathleen T	Geyer, W. Rockwell AOPE-3
Doucette, G. J	Gillis, K
Dougherty, Martin EGG-6,11	Glover, David M
Doutt, James AAOPE-18	Glover, Ed B-12
Druffel, Ellen R. M C-1,3,4,8,10,14,16,18	Glover, L., III
Duester, Alan R AOPE-11	Goericke, Ralf
Duff, John H	Goff, John AGG-7
Dunlap, Paul V	Goldman, Joel CB-11,12
Dunworth, Jane A PO-22	Goyet, Catherine
2 41	Grabher, A
T 1 1 17' ' ' 17' T 10 10	
Eckenrode, Virginia K B-18	Grassle, J. FB-21
Edmond, J. M	Grassle, Judith P AOPE-15
Edwards, R. L	Green, Sarah A
Ehrendorfer, Thomas	Griffin, S. M
Eiswerth, Mark E MPC-3,5	Grimshaw, Roger H.JPO-15,17
Elder, Bob	Grosenbaugh, Mark AAOPE-7
Elderfield, H	Gross, Thomas AOPE-9
Eldin, GérardPO-1	Gulesserian, Armine
,	Guiesserian, Armine
Elskus, Adria AB-9,22	
Emeis, Kay-Christian	Hacker, Sally D
Emery, K. O	Hahn, Mark E B-12,22
Ewing, J. I	Haidvogel, Dale BPO-1
Ewing, J. I	
	Hall, Melinda MPO-2
Faanes, Craig AMPC-6	Haney, J. Christopher MPC-5,6
Fabry, V. J	Haney, James F B-23
Falkowski, P	
	Hannick, L. I
Farrington, John WB-9;C-7	Hannington, Mark D
Federiuk, Joyce MPO-2	Hara, Tetsu
Fent, Karl	Harbison, G. R
Ferdelman, Timothy GPO-17	Harder, W
rerdefinally 1 mothy G	
Filloux, J	Hare, Linda R B-14
Finlay, B. J	Hargraves, Bruce RB-23
Firing, Eric	Harrison, P. JB-7
Fleer, Alan P	Hartman, Mary C
Flierl, Glenn R B-4	Haury, L. RB-5
Fofonoff, Nicholas PPO-2	Hawman, RGG-8
Foote, Kenneth GAOPE-16	Hay, B. J
Fouquet, Yves	Helfrich, Karl RPO-15
Fox, P. J	Helsley, C. EGG-5
Francois, Roger	Hemleben, Christoph
Franks, P. J. S	Henderson, Eric WMPC-7,11
Freitag, Lee EAOPE-7,16	Herranz, P
	Harris Data M
Frew, Nelson M	Herzig, Peter M
Fricke, HansB-14,18	Herzog, M
Fricke, J. RobertGS-5	Higgs, N. C
Friedrichs, Carl TGG-14	Higuera-Gundy, AntoniaGG-15
Frisk, George V	Hildebrand, J. AGG-5
Fristrup, Kurt MB-24;MPC-6	Hinton, A. A
Frye, Daniel E AOPE-7,14;PO-20	Hirschberg, David
	Hoagland, Porter MPC-2,7,8,9
C-1 C	
Gabor, G	Hoaki, Toshihiro B-26
Gagnon, A. RGG-1	Hodell, David AGG-15
Gaines, Arthur G., JrMPC-3,4,10	Hogg, Nelson G
Gallager, Scott M	Holbrook, W. S
Galvin, Lawrence FrancisGS-6	Honjo, Susumu
Gambacorta, Agata B-18	Hoskins, HGG-5
Garabedian, Stephen F D-20	Hosom, D. S
Garabedian, Stephen P	Hosom, D. S. PO-20 Hover Franz S AOPF-6
Gardner, Wilford D	Hosom, D. S. PO-20 Hover, Franz S. AOPE-6 Howald, Terrance J. B-24

Howes, Brian L	Liberatore, Stephen PAOPE-11
Huang, Rui Xin	Lim, Ee Lin
Huber, Robert B-14	Limeburner, Richard AOPE-3;PO-4,19
Hunter, Mark HGS-9	Lindstrom, Timothy EGS-7
	Linn, L. J
Ichikawa, Hiroshi PO-3	Lisa, Teresita AB-8
Isayev, Grigory PO-15	Liu, Chengjie
• , • •	Liu, W. TPO-18
Jacobson, Dean MB-13	Liu, Zhengyu PO-5
Jacobson, R. S	Livingston, Hugh D
Jannasch, Holger W	Lobel, Phillip SB-16
Jenkins, William JĆ-9,10	Lohmann, G. P
Johnson, Carl G	Lohrenz, S. E
Johnson, Gregory CGS-6;PO-14	Lundberg, Kelly S B-8
Johnson, Kevin T. M	Luther, George W., IIIPO-17
Jones, Glenn A	Luyten, James RPO-5,11
Joyce, Terrence M	Lynch, James FAOPE-13
Joyner, Christopher CMPC-8	• ,
Jörg, Daniele B-25	MacDonald, Alison M
	Macdonald, K. C
Kalko, E. K. V	Mackensen, Andreas
Kammer, David P	Madin, Laurence P
Kaoru, Yoshiaki MPC-9	Madsen, Ole SGG-14
Katz, Miriam EGG-18	Maliotis, George
Keafer, Bruce A B-1	Marshall, David PO-5
Keigwin, Lloyd DGG-3,15	Martin, W. R
Keller, William C AOPE-3	Maruyama, Tadashi B-26
Kelly, Kathryn APO-8,18	Matsumoto, G. IB-15
Kent, Dennis VGG-2	McCaffrey, Mark A
Kieber, David J	McCartney, Michael SPO-6,13
Kils, Uwe B-23	McNichol, Ann P
Kim, Kuh PO-4	McNutt, Marcia KGG-6
King, Linda L	Mei, Chiang C
Kite-Powell, Hauke L MPC-2,7,8,9	Meighen, E. A
Klein, PatricePO-16	Merriam, StevenAOPE-16
Kleinrock, Martin C	Metzger, Kurt
Kloepper-Sams, Pamela JB-22	Miceli, Geraldine
Knauer, G. A	Millard, Robert PO-21
Koelsch, Donald E	Miller, Arthur AOPE-4
Kremer, Patricia B-14	Miller, J. H AOPE-13
Kristjansson, Jakob K	Miller, Kenneth R
Kulebakina, Ludmilla G	Mills, R
Kumar, VijayAOPE-1,12	Mindell, David A AOPE-5
Kurr, Margit B-14	Miranda, Luis B AOPE-3
Kurz, Mark D	Molyneaux, Stephen J
König, Helmut B-14	Moore, Karen E
Romg, Hennut	Moore, Michael JGS-8
Lalou, Claude	Moore, Richard B
Lanzerotti, L.JGG-5	Morel, François M. M
Larson, R. J	Mueller, Ulrich B-8
le Roex, Anton	Muench, Robin DPO-6
Lee, David SMPC-6	Musser, D. L
Legeckis, Richard VAOPE-3	Müller, R. Dietmar
Lehman, Scott J	,
Leinen, M	Nelson, Robert K
Lentz, Steven J AOPE-3;PO-18,21	Newhall, A. E AOPE-13
Levine, Edward RPO-16	Niller, P. P
Lewis, L. M	Norris, Richard DGG-19
Lewitus, Alan J	Notarbartolo di Sciara, Giuseppe B-24

	Rona, Peter A
	Rudnick, Daniel LPO-22
O'Kane, Dennis JB-18	
Obradovich, John D	Samelson, Roger M
Olson, Kirby SGS-10	Sancetta, CB-19
Olsson, Richard K	Sanders, Robert WB-2,3
Orchardo, J	Sandwell, David T
Osborne, E. A	Santala, Markku JunaniGS-11
Oschmann, Lynn AGS-10	Sanz, J. L. GG-1
Owens, W. Brechner PO-20	Sayigh, Laela
Ostlund, H. G	Scheltema, Amélie H
Oblana, II. G	Scheltema, Rudolf S
Padman, Laurie PO-6	
Paduan, J. D. PO-18	Schempf, Hagen
Paffenhöfer, Gustav -AB-23	Schipka, JuttaB-18
	Schmitt, Raymond WPO-2
Palmer-Julson, Amanda A	Schmitz, William J., JrPO-10,11
Patch, Sarah KPO-21	Schneider, D. L
Paulson, C. APO-1	Schubert, David MPO-22
Peal, Kenneth R AOPE-6	Schudlich, Rebecca RGS-11
Pedlosky, Joseph	Schuler, Dale L AOPE-3
Peltzer, Edward T	Schultz, A
Petrecca, R. F B-21	Schultz, L. W
Phinney, CurtisB-9	Schulze, Peter CB-23
Pickart, Robert S PO-7	Sclater, John G
Pinkel, RobPO-6	Scott, Steven D
Plant, William J	Sellers, Cynthia JAOPE-18
Pley, UrsulaB-18	Shalvi, Ofir
Plueddemann, Albert JPO-6,7	Shaw, Peter RGG-8,9,10
Poland, AlanB-12	Shaw, Timothy J
Polasky, Stephen MPC-10	
Polikarpov, Gennady, G	Sheridan, R. E
Porta, Dave	Sholkovitz, Edward R
	Shum, K. TAOPE-8
Prada, K. E	Slotine, Jean-Jacques E AOPE-2
Prasher, Douglas C B-3,13,18	Slowey, Niall CGG-16;GS-12
Pratt, Larry J PO-14	Smith, Deborah KGG-3,4,10
Prendergast, Franklyn G	Smith, Richard L5-20
Prindle, B AOPE-14	Smithson, SGG-8
Prothero, Donald RGG-16	Smolowitz, Roxanna M B-22,23
Pruell, R. J	Snelgrove, Paul V. RAOPE-15,16;B-21
Purcell, J. EB-17	Solomon, Sean CGG-4,10
Purdy, G. Michael AOPE-14;GG-2,4,5,6,8,10	Solow, Andrew R
Pyle, T. E	Somers, Tagore AOPE-1
	Soutar, A
Qiu, BoPO-8	Spall, Michael APO-11,12
• '	Spencer, Derek W
Rachel, ReinhardB-18	Spiesberger, John LAOPE-4,8,9,17
Radenac, Marie-Hélène PO-1	Stalcup, Marvel CPO-22
Rajan, Subramaniam D AOPE-10,11,12,13,18	Stanton, Timothy KAOPE-1,10,16
Rao, B. M. L	
Ravizza, G	Starczak, Victoria RAOPE-16;B-25
Read, Andrew J	Steele, John H
	Stegeman, John J B-9,12,21,21,22,23
Reiter, E. C	Stephen, Ralph A
Repeta, Daniel J	Stetter, Karl O
Reyss, Jean Louis	Stewart, W. KennethAOPE-1,2,5,12
Richardson, Philip LPO-9	Stienen, Christian
Richman, Sumner B-23	Stoecker, Diane KB-3,11
Robbins, Paul E PO-9	Stokozov, Nikolai A
Robertson, K. J	Stommel, Henry MPO-5,12
Rogers, J	Strickler, J. Rudi B-5,23
Rohr, K. M	Strub, P.Ted
	,

Stuckenrath, Robert	MPC-12
Swisher, Carl C., III	GG-2
Talley, Lynne D	PO-13
Talwani, M	GG-8
Tang, Dajun	AOPE-17;GS-13
Tarafa, Martha	
Taylor, Craig C	B-14
Taylor, F. W	
Teal, John M	B-9
Terray, Eugene A.	AUPE-3
Thompson, Geoffrey	DO:10.11
Thompson, J. Dana	GS-16
Thomson, J	C-11
Tietenberg, T. H	MPC-12
Toksöz, M. N	GG-8
Toole, John	PO-1,21
Toomey, Douglas R	GG-4
Trask, R. P	PO-20
Travis, Bryan J	
Triantafyllou, George S	AOPE-7
Triantafyllou, Michael S	AOPE-7
Trincone, Antonio	B-14
Tripp, Bruce W	B-9
Trivett, D. Andrew	. AUPE-3;G5-14
Trowbridge, John H	PO_13
Tsuchiya, Mizuki	GG-4 9 11
Turekian, K. K.	C 15
Turner. Ruth	B-3
Turner, Ruth Tyack, Peter	B-3
Turner, Ruth Tyack, Peter Uchupi, Elazar	B-17;MPC-10 GG-1,12
Turner, Ruth	B-17;MPC-10 GG-1,12 AOPE-1,6,12
Turner, Ruth Tyack, Peter Uchupi, Elazar Ulrich, Nathan Unsworth, Martyn J	B-3 B-17;MPC-10 GG-1,12 AOPE-1,6,12 GG-13
Turner, Ruth Tyack, Peter Uchupi, Elazar Ulrich, Nathan Unsworth, Martyn J Valois, Frederica W.	
Turner, Ruth Tyack, Peter Uchupi, Elazar Ulrich, Nathan Unsworth, Martyn J Valois, Frederica W. Vanderploeg, Henry A.	B-17;MPC-10GG-1,12AOPE-1,6,12GG-13B-2B-2
Turner, Ruth Tyack, Peter Uchupi, Elazar Ulrich, Nathan Unsworth, Martyn J Valois, Frederica W Vanderploeg, Henry A Van Veld, P. A	B-17;MPC-10GG-1,12AOPE-1,6,12GG-13B-2B-23B-23
Turner, Ruth Tyack, Peter Uchupi, Elazar Ulrich, Nathan Unsworth, Martyn J Valois, Frederica W Vanderploeg, Henry A Van Veld, P. A. Vartanov, Raphael V	B-17;MPC-10
Turner, Ruth Tyack, Peter Uchupi, Elazar Ulrich, Nathan Unsworth, Martyn J Valois, Frederica W Vanderploeg, Henry A Van Veld, P. A Vartanov, Raphael V Villareal, Tracy A	B-17;MPC-10
Turner, Ruth Tyack, Peter Uchupi, Elazar Ulrich, Nathan Unsworth, Martyn J Valois, Frederica W Vanderploeg, Henry A Van Veld, P. A. Vartanov, Raphael V	B-17;MPC-10
Turner, Ruth Tyack, Peter Uchupi, Elazar Ulrich, Nathan Unsworth, Martyn J Valois, Frederica W Vanderploeg, Henry A Van Veld, P. A Vartanov, Raphael V Villareal, Tracy A Vogelbein, W. K	B-3 B-17;MPC-10 GG-1,12 AOPE-1,6,12 GG-13 B-23 B-23 B-23 MPC-2 B-19,23,24 B-23
Turner, Ruth Tyack, Peter Uchupi, Elazar Ulrich, Nathan Unsworth, Martyn J Valois, Frederica W Vanderploeg, Henry A Van Veld, P. A Vartanov, Raphael V Villareal, Tracy A Vogelbein, W. K. Walt, David R.	B-17;MPC-10
Turner, Ruth Tyack, Peter Uchupi, Elazar Ulrich, Nathan Unsworth, Martyn J Valois, Frederica W Vanderploeg, Henry A Van Veld, P. A Vartanov, Raphael V Villareal, Tracy A Vogelbein, W. K. Walt, David R. Ward, K. B	B-17;MPC-10
Turner, Ruth Tyack, Peter Uchupi, Elazar Ulrich, Nathan Unsworth, Martyn J Valois, Frederica W Vanderploeg, Henry A Van Veld, P. A Vartanov, Raphael V Villareal, Tracy A Vogelbein, W Walt, David R Ward, K Ward, William W Warncke, Torsten	B-3 B-17;MPC-10 GG-1,12 AOPE-1,6,12 GG-13 B-23 B-23 MPC-2 B-19,23,24 B-23 C-19,20 B-13 B-3,18 PO-5
Turner, Ruth Tyack, Peter Uchupi, Elazar Ulrich, Nathan Unsworth, Martyn J Valois, Frederica W Vanderploeg, Henry A Van Veld, P. A Vartanov, Raphael V Villareal, Tracy A Vogelbein, W Walt, David R Ward, K Ward, William W Warncke, Torsten Warren, Bruce A	B-3 B-17;MPC-10 GG-1,12 AOPE-1,6,12 GG-13 B-23 B-23 MPC-2 B-19,23,24 B-23 C-19,20 B-13 B-3,18 PO-5 PO-14
Turner, Ruth Tyack, Peter Uchupi, Elazar Ulrich, Nathan Unsworth, Martyn J Valois, Frederica W Vanderploeg, Henry A Van Veld, P. A Vartanov, Raphael V Villareal, Tracy A Vogelbein, W Walt, David R Ward, K Ward, William W Warncke, Torsten Warren, Bruce A Waterbury, John B	B-3 B-17;MPC-10 GG-1,12 AOPE-1,6,12 GG-13 B-2 B-23 B-23 MPC-2 B-19,23,24 B-23 C-19,20 B-13 B-3,18 PO-5 PO-14 B-2,11,24
Turner, Ruth Tyack, Peter Uchupi, Elazar Ulrich, Nathan Unsworth, Martyn J Valois, Frederica W Vanderploeg, Henry A Van Veld, P. A Vartanov, Raphael V Villareal, Tracy A Vogelbein, W Walt, David R Ward, K Ward, William W Warncke, Torsten Warren, Bruce A Waterbury, John B Watkins, William A	B-3 B-17;MPC-10 GG-1,12 AOPE-1,6,12 GG-13 B-2 B-23 B-23 MPC-2 B-19,23,24 B-23 C-19,20 B-13 B-3,18 PO-5 PO-14 B-2,11,24 B-17,24
Turner, Ruth Tyack, Peter Uchupi, Elazar Ulrich, Nathan Unsworth, Martyn J Valois, Frederica W Vanderploeg, Henry A Van Veld, P. A Vartanov, Raphael V Villareal, Tracy A Vogelbein, W Walt, David R Ward, K Ward, William W Warncke, Torsten Warren, Bruce A Waterbury, John B Watkins, William A Watters, David R.	B-3 B-17;MPC-10 GG-1,12 AOPE-1,6,12 GG-13 B-2 B-23 B-23 MPC-2 B-19,23,24 B-23 C-19,20 B-13 B-3,18 PO-5 PO-14 B-2,11,24 B-17,24 MPC-12
Turner, Ruth Tyack, Peter Uchupi, Elazar Ulrich, Nathan Unsworth, Martyn J Valois, Frederica W Vanderploeg, Henry A Var Veld, P. A Vartanov, Raphael V Villareal, Tracy A Vogelbein, W Ward, K Ward, K Ward, K Ward, William W Warncke, Torsten Warren, Bruce A Watters, David R Watts, D. Randolph	B-3 B-17;MPC-10 GG-1,12 AOPE-1,6,12 GG-13 B-2 B-23 B-23 MPC-2 B-19,23,24 B-23 B-13 B-3,18 PO-5 PO-14 B-2,11,24 B-17,24 MPC-12 PO-7
Turner, Ruth Tyack, Peter Uchupi, Elazar Ulrich, Nathan Unsworth, Martyn J Valois, Frederica W Vanderploeg, Henry A Var Veld, P. A Vartanov, Raphael V Villareal, Tracy A Vogelbein, W Ward, K Ward, K Ward, William W Warncke, Torsten Warren, Bruce A Waterbury, John B Watkins, William A Watters, David R Watts, D Randolph Webb. Christine M	B-3 B-17;MPC-10 GG-1,12 AOPE-1,6,12 GG-13 B-2 B-23 B-23 MPC-2 B-19,23,24 B-23 B-23 C-19,20 B-13 B-3,18 PO-5 PO-14 B-2,11,24 B-17,24 MPC-12 PO-7 AOPE-16
Turner, Ruth Tyack, Peter Uchupi, Elazar Ulrich, Nathan Unsworth, Martyn J Valois, Frederica W Vanderploeg, Henry A Van Veld, P. A Vartanov, Raphael V Villareal, Tracy A Vogelbein, W Ward, K Ward, K Ward, K Ward, William W Warncke, Torsten Warren, Bruce A Waterbury, John B Watkins, William A Watters, David R Watts, D Randolph Webb, Christine M Weiman, Robert	B-3 B-17;MPC-10 GG-1,12 AOPE-1,6,12 GG-13 B-2 B-23 B-23 MPC-2 B-19,23,24 B-3,18 PO-5 PO-14 B-2,11,24 B-17,24 MPC-12 PO-7 AOPE-16 AOPE-16
Turner, Ruth Tyack, Peter Uchupi, Elazar Ulrich, Nathan Unsworth, Martyn J Valois, Frederica W Vanderploeg, Henry A Van Veld, P. A Vartanov, Raphael V Villareal, Tracy A Vogelbein, W Ward, K Ward, K Ward, K Ward, William W Warncke, Torsten Warren, Bruce A Waterbury, John B Watkins, William A Watters, David R Watts, D Randolph Webb, Christine M Weiman, Robert Weinberg, James R	B-3 B-17;MPC-10 GG-1,12 AOPE-1,6,12 GG-13 B-2 B-23 B-23 MPC-2 B-19,23,24 B-23 B-23 C-19,20 B-13 B-3,18 PO-5 PO-14 B-2,11,24 B-17,24 MPC-12 PO-7 AOPE-16 AOPE-16 AOPE-1
Turner, Ruth Tyack, Peter Uchupi, Elazar Ulrich, Nathan Unsworth, Martyn J Valois, Frederica W Vanderploeg, Henry A Van Veld, P. A Vartanov, Raphael V Villareal, Tracy A Vogelbein, W Ward, K Ward, K Ward, K Ward, William W Warncke, Torsten Warren, Bruce A Waterbury, John B Watkins, William A Watters, David R Watts, D Randolph Webb, Christine M Weiman, Robert Weinstein, Ehud Weiskel Weiskel Weiskel Weter	B-3 B-17;MPC-10 GG-1,12 AOPE-1,6,12 GG-13 B-23 B-23 B-23 B-23 B-23 C-19,20 B-13 B-3,18 PO-5 PO-14 B-2,11,24 B-17,24 MPC-12 PO-7 AOPE-16 AOPE-15 B-25 AOPE-15 B-25
Turner, Ruth Tyack, Peter Uchupi, Elazar Ulrich, Nathan Unsworth, Martyn J Valois, Frederica W Vanderploeg, Henry A Van Veld, P. A Vartanov, Raphael V Villareal, Tracy A Vogelbein, W Ward, K Ward, K Ward, K Ward, William W Warncke, Torsten Warren, Bruce A Waterbury, John B Watkins, William A Watters, David R Watts, D Randolph Webb, Christine M Weiman, Robert Weinberg, James R	B-3 B-17;MPC-10 GG-1,12 AOPE-1,6,12 GG-13 B-23 B-23 B-23 B-23 B-23 C-19,20 B-13 B-3,18 PO-5 PO-14 B-2,11,24 B-17,24 MPC-12 PO-7 AOPE-16 AOPE-15 B-25 AOPE-15 B-25

Welsch, Wolfgang	B-23
Westler, William M	R-3
Wother David	
Wethey, David	D-20
Whelan, Jean K	
Whitehead, Jack A	GG-13;PO-15
Whitfield, M	
Wiebe, P. H	AOPE-1;B-4
Wilcock, William S. D	GG-4,13
Williams, Albert J., 3rd	
Williams, Peter M	
Wirsen, Carl O	
Woodford, Thomas J	
Woodin, B. R	B-23
Yen, Jeannette	B-23
Yoerger, Dana R	
Young, William R	
Zafiriou, Oliver C	C-2 17
Zemba, Jan C	
Zhang, Huai-Min	
Zhang, Jijun	GG-18
Zhao, Hongye	
, 	



DOCUMENT LIBRARY

March 11, 1991

Distribution List for Technical Report Exchange

Attn: Stella Sanchez-Wade Documents Section Scripps Institution of Oceanography Library, Mail Code C-075C La Jolla, CA 92093

Hancock Library of Biology & Oceanography
Alan Hancock Laboratory
University of Southern California
University Park
Los Angeles, CA 90089-0371

Gifts & Exchanges Library Bedford Institute of Oceanography P.O. Box 1006 Dartmouth, NS, B2Y 4A2, CANADA

Office of the International
Ice Patrol
c/o Coast Guard R & D Center
Avery Point
Groton, CT 06340

NOAA/EDIS Miami Library Center 4301 Rickenbacker Causeway Miami, FL 33149

Library Skidaway Institute of Oceanography P.O. Box 13687 Savannah, GA 31416

Institute of Geophysics University of Hawaii Library Room 252 2525 Correa Road Honolulu, HI 96822

Marine Resources Information Center Building E38-320 MIT Cambridge, MA 02139

Library
Lamont-Doherty Geological
Observatory
Columbia University
Palisades, NY 10964

Library Serials Department Oregon State University Corvallis, OR 97331 Pell Marine Science Library University of Rhode Island Narragansett Bay Campus Narragansett, RI 02882

Working Collection Texas A&M University Dept. of Oceanography College Station, TX 77843

Library
Virginia Institute of Marine Science
Gloucester Point, VA 23062

Fisheries-Oceanography Library 151 Oceanography Teaching Bldg. University of Washington Seattle, WA 98195

Library R.S.M.A.S. University of Miami 4600 Rickenbacker Causeway Miami, FL 33149

Maury Oceanographic Library Naval Oceanographic Office Stennis Space Center NSTL, MS 39522-5001

Marine Sciences Collection Mayaguez Campus Library University of Puerto Rico Mayaguez, Puerto Rico 00708

Library
Institute of Oceanographic Sciences
Deacon Laboratory
Wormley, Godalming
Surrey GU8 5UB
UNITED KINGDOM

The Librarian CSIRO Marine Laboratories G.P.O. Box 1538 Hobart, Tasmania AUSTRALIA 7001

Library Proudman Oceanographic Laboratory Bidston Observatory Birkenhead Merseyside L43 7 RA UNITED KINGDOM

50272-101

30272-101				
REPORT DOCUMENTATION PAGE	1. REPORT NO. WHO1-92-19	2.	Recipient's Accession No.	
4. Title and Subtitie Abstracts of Manuscripts Submitted in 1991 for Publication		on	5. Report Date May, 1992	
		6.		
7. Author(s) Editor: Alora Paul		8.1	Performing Organization Rept. No. WHOI-92-19	
9. Performing Organization Name and	Address	10.	Project/Task/Work Unit No.	
Woods Hole Oceanographic Ins Woods Hole, Massachusetts 02		11.	Contract(C) or Grant(G) No.	
WOOds Hole, Massachusetts 02		(G)	į	
12. Sponsoring Organization Name an	d Address	13.	. Type of Report & Period Covered	
			Technical Report	
		14	,	
15. Supplementary Notes This general should be sited as:	Woods Hola Ossanos Inst Toch Dom	WHOL02 10		
This report should be cited as:	: Woods Hole Oceanog. Inst. Tech. Rept.,	w nOI-92-19.		
16. Abstract (Limit: 200 words)		······································		
of the Woods Hole Oceanogra published. The volume is inte The abstracts are listed by	abstracts of manuscripts submitted for publicaphic Institution. We identify the journal of unded to be informative, but not a bibliogratitle in the Table of Contents and are group ter, or the student category. An author inde	those manuscripts which a phy. ed into one of our five dep	oartments, Marine Policy	
17. Document Analysis a. Descripto	DIS			
abstracts				
oceanography				
ocean engineering				
b. Identifiers/Open-Ended Terms				
c. COSATI Field/Group				
18. Availability Statement		19. Security Class (This Repo UNCLASSIFIED	rt) 21. No. of Pages 204	
Approved for publication	on; distribution unlimited.	20. Security Class (This Page		